Holocene jökulhlaups, glacier fluctuations and palaeoenvironment, Mýrdalsjökull, South Iceland.

Kate T. Smith

Ph.D.

University of Edinburgh

2003

Declaration

I declare that this thesis has been composed by myself and is wholly my own work, except where other authors' work is explicitly acknowledged within the text.

Kate Taylor Smith

Abstract

This thesis develops a chronology of jökulhlaup (glacier burst flood) activity from Mýrdalsjökull in southern Iceland. Throughout the Holocene, the interaction of the volcano Katla and the overlying ice cap of Mýrdalsjökull have triggered many jökulhlaups. Crucially however, our knowledge of the possible flood routes is incomplete. Flood activity to the south and east of the ice cap has been well constrained from historical and geomorphological studies, but routes to the west of the ice cap have not been fully investigated. This is important for understanding the interaction of Katla and its overlying ice cap as well as from the perspective of hazard assessment.

New geomorphological, sedimentological and tephrochronological data have identified 15 flow events during the Holocene. The majority of these were hyperconcentrated flow events originating from, or close to, the northwest area of the ice cap and are associated with subglacial volcanism. One flood originated in the Veiðivötn area and on 3 occasions flooding from Katla may have been accompanied by floods from Eyjafjallajökull. A further two events relate to re-mobilisation of thick airfall tephra deposits. Silicic pumice found on the sandur and close to the ice margin indicates that the Markarfljót acted as a terrestrial transport route for pumice found along North Atlantic coasts, and was possibly a route for silicic Katla jökulhlaups. Additionally, flood routes and glacial landforms show that Entujökull reached a maximum Holocene extent in the mid-Holocene, extending further downvalley than during the Little Ice Age.

In prehistory, floods were directed to both the south and west of Mýrdalsjökull. Similarly timed jökulhlaups took these paths when floods also flowed from Eyjafjöll into the Markarfljót. This suggests that concurrent routing of floods to the south and west of Mýrdalsjökull is related to synchronous volcanic activity in Katla and Eyjafjallajökull. Since the 10th Century most Katla floods have been routed to the south east, possibly reflecting changes in intra-caldera eruption sites or subglacial topographic change associated with the Eldgjá eruption in c.935 AD, as suggested by Larsen (2000).

The environmental impacts of these floods were significant. Late prehistoric and early historic floods had a major role in shaping the landscape faced by the earliest Norse colonisers of the region. Future flooding could pose a distinct hazard to farmland downvalley and to popular tourist areas in North Þórsmörk.

Table of Contents

Volume 1

Chapter 4: Results: Geomorphology

Chapter 5: Results: Tephras

Chapter 6: Results: Flood Deposits

Chapter 7: Reconstruction and Chronology

Chapter 8: Implications: jökulhlaups, glacier fluctuations and palaeoenvironment

Volume 2

Figures
Appendices 1-5

Appended Illustrations

Geomorphological maps (Figures 4.1.2 and 4.1.3) and key
Correlated tephra logs and key

Acknowledgements

This research has been funded by NERC (UK) research studentship GT04/1999/ES/0077, Icelandair UK and AMG Outdoor Ltd.

Many people have helped with useful and inspiring suggestions, developing ideas and general encouragement. David Sugden and Andy Dugmore have been inspiring and very patient supervisors. Very special thanks go to Guðrún Larsen who has been invaluable. Thanks also to Hreinn Haraldsson (Vegagerðin), Elsa Vilmundardóttir and Ingibjörg Kaldal (both Orkustofnun) in Iceland. In the School of Geosciences, University of Edinburgh, Anthony Newton has helped with most aspects of this thesis and been a good friend and Peter Hill has supervised all Electron Microprobe work. Steve Dowers saved my thesis files at the last minute. Nick Spedding helped with devising some of the original research questions. Hreggviður Norðdahl and Neil Stuart provided encouraging and helpful discussion in my examination.

Numerous people have provided help in the field and cheerfully dug holes in all conceivable weather; Katharina Niederndorfer, Amy Hunt, Fiona Murray, Edward Stevens, Laura Campbell, Andy Chamberlain, Monica Winsborrow, Anthony Newton, Andy Casely and Eleanor Green.

I have received exceptional help from everyone in Iceland; the communities of Fljótshlíð, Seljaland (particularly Sigrún Adolfsdóttir), the Stevens family at Fljótsdalur, wardens at Botn and Þórsmörk, everyone at Fornleifastofnun Íslands. Páll Baldursson helped with translations from Icelandic.

I could not have had a more welcoming or friendly time in Edinburgh and many friends have provided substantial moral support; Chris, Fran, Nick, Jez, Tom, Keith, Ann, Darcey, Steve, Bob, Clare, Sarah, Amin, Jessica and Jenny.

Final thanks go to my parents for supporting me all the way through University and for always managing to believe in me. This thesis would not exist without their combined proof-reading and organisational skills, tolerance and kindness against difficult odds in the final stages.

Katla and Kötlugjá

"At one time in Þykkvabæjar-monastery the abbot had a house-keeper called Katla. She was bewitched and owned a pair of trousers that had natural powers designed to let the one wearing it never tire while running. Katla used the pants when necessary. Everybody, including the abbot himself, feared her magic and temper. A shepherd called Barði stayed there. He often got into clashes with Katla when some sheep were missing after a round-up. One time in autumn the abbot and housekeeper went to a party and they left Barði at home to bring back the sheep. Now, the shepherd didn't quite find all the sheep. He planned, for speed, to use Katla's trousers. He ran and found all the sheep. At once, Katla came home and she was soon sure that Barði had taken her trousers. She therefore secretly took Barði and suffocated him in a vat of sour whey and left him there. Certainly, nobody knew where he was and it remained that way until after the winter when the sour whey became short in the vat and people heard her say *"Soon Barði will be seen"*. But when the time came near that the flaw in her wickedness would be found out and due consequences determined she took her trousers and ran out of the Abbey to the north-west towards the glacier and plunged from above into a crack in the ice. Shortly after this there was a flood from the glacier aimed towards the Abbey and Álftaverið. It is a customary belief that her magic causes such floods. Since then, floods have mainly issued from the gorge in which she sheltered, Kötlugjá, and flowed over Kötlusandur."

Translated from 'Íslenzkar Þjóðsögur og Ævintýri' (Icelandic folktales and fairy-tales),
collated by Jón Árnason (1862)

Chapter 1: Introduction and Background

1.1 Introduction and Overall Aim

The main aim of this thesis is to use geomorphological and sedimentological data combined with tephrochronology to reconstruct Holocene jökulhlaups and associated fluctuations of Mýrdalsjökull, in southern Iceland.

Why Iceland?

The main theme of this thesis is the interaction of glaciers and subglacial volcanoes. The study of ice-volcano interaction is a relatively young and rapidly developing science, since subglacial eruptions are difficult to observe. The eruption of the Gjálp fissure beneath Vatnajökull in 1996 is one of few subglacial eruptions that has been studied in depth (Guðmundsson et al 1997). Research in this field is critically important for understanding the behaviour of ice underlain by volcanically and geothermally active areas, the nature of volcanic systems and eruptions when covered by ice and the resultant hazards associated with the interaction between the two. Iceland is an ideal location for this research.

Iceland's landscape largely reflects the influence of volcanism and glaciation in the environment. The island is mainly volcanic in origin and is the largest volcanic region in Europe (Scarth and Tanguy 2001). The country is built on a 400km long stretch of the Mid-Atlantic Ridge, a spreading axis raised above the level of the sea by the North Atlantic mantle plume, the Icelandic hotspot. High precipitation levels, location just south of the Arctic Circle and the mountain-building of volcanic activity have helped form four main ice caps (Vatnajökull, Mýrdalsjökull, Langjökull and Hofsjökull) as well as numerous small ice caps and glaciers. The interaction of ice caps with underlying volcanoes results in large-scale floods called jökulhlaups.

Why jökulhlaups?

Jökulhlaups (glacier outburst floods) are dominant landscape-forming events in southern Iceland. Despite this, jökulhlaup research in Iceland has predominantly focussed upon recent and historical jökulhlaup activity, lacking investigations into the history and nature of Holocene flooding. However, this line of investigation is important because it provides information about the interaction of icecaps and their underlying volcanoes and has important hazard awareness implications.

It has been shown in numerous studies of hazard management that geomorphological and sedimentological studies of past events can be used as a sound basis for understanding the routing and nature of possible future hazards (Cooke and Doornkamp 1990, Stoiber and Williams 1990). This is particularly the case with lahar and pyroclastic flow management but could be equally well applied to catastrophic flood events. Thus, Björnsson (1992;96) states that *'knowledge of the sources and behaviour of jökulhlaups is essential for advance warnings, preventative measures and civil defence in Iceland'*, a point argued in the 1970s by Nye (1976; 183) who pointed out that *' it is ... practically important as well as scientifically interesting to understand the ... phenomenon fully'*.

Research in to post-glacial floods and lahars from volcanoes in North and South America, Indonesia and New Zealand, has been more active (e.g. Beget and Nye 1994, Kohlbeck et al 1994, Scott et al 1995, Waythomas et al 2000, Manville et al 2000, Lavigne and Thouret 2003). The nature of Icelandic jökulhlaups has been debated by numerous authors and in most discussions they have been considered as different from lahars and volcanigenic floods elsewhere. Further study of Holocene jökulhlaups in Iceland allows comparisons to be made and contrasts to be drawn between Icelandic jökulhlaups and similar events worldwide.

Why glacier fluctuations?

Iceland's climate is influenced strongly by the position of the atmospheric polar front and the cold Arctic and warm North Atlantic Drift ocean currents (Figure 1.1.1). The polar front is formed where cold air from the Arctic meets warm air from the Atlantic in the region of Iceland. The Icelandic climate is highly susceptible to variations in the location and strength of these air masses, which are affected by even minor regional climatic changes. Dugmore (1987) notes that Iceland is situated beneath the upper atmospheric North Atlantic cyclone track such that depressions forming in Newfoundland often become most intense around Iceland. Since these phenomena are part of the wider patterns of North Atlantic Circulation, variations in the global climate are likely to result in changes to the cyclonic activity over Iceland.

Many studies have used glacial extent as a proxy for climatic change, particularly in Iceland where glaciers provide a sensitive record of changes in the climate of the North Atlantic (e.g. Dugmore 1987, Guðmundsson 1997, and Jóhannesson and Sigurðsson 1998). Glacier fluctuations in this study are relevant to the routing of jökulhlaups. However, the trigger for many of these jökulhlaups, subglacial volcanism, may mean that the fluctuations of glaciers underlain by active volcanoes may solely reflect climatic signals. Bradwell (2001) emphasised the need for consideration and further study of the influence of volcanic, geothermal and topographic factors on the fluctuations of Icelandic glaciers and wariness in interpretation of glacier fluctuation studies from glaciers overlying active volcanoes as proxy records of climate change.

Thesis outline

The thesis is divided into eight chapters. This chapter introduces the background to the thesis, considering glacier fluctuations and jökulhlaups in general. Chapter 2 outlines the specific case of Mýrdalsjökull and Katla and identifies questions to answer in this thesis. Chapter 3 focuses upon methodology and outlines the nature of the study area, the Markarfljót valley. Geomorphological evidence for the action of jökulhlaups and glaciers within the Markarfljót valley is presented in Chapter 4 and is accompanied by four fold-out maps. The construction of a chronology of events in the Markarfljót hinges upon the compilation of a sound stratigraphic framework using tephra layers as described in Chapter 5. This stratigraphy is then used to identify sedimentary units across the valley. Those units determined to be possible flood deposits are presented in Chapter 6, along with areas of flood deposition which may lie outside this framework. A chronology of flood events, related to different positions of Entujökull, is composed from this data are discussed in Chapter 7. Reconstruction of flood nature and extent for different flood events is included here, presenting a new Holocene record of the timing, nature and extent of jökulhlaups in the Markarfljót valley. Finally, Chapter 8 reviews the wider implications and limitations of this research, highlighting the main contributions made in this thesis.

1.2 Glacier Fluctuations

This chapter outlines the main Holocene glacier fluctuation records of Iceland and links with glacier records elsewhere. Recent key reviews include those by Guðmundsson (1997), Mackintosh (2000) and Bradwell (2001). Everest (2003) reviews trends in the North Atlantic while Benn and Evans (1998) discuss global patterns of glacial change. Forcing factors for glacier fluctuations are discussed, with particular emphasis on the roles of volcanic and geothermal activity on glacial extent.

Glacier fluctuations during the Holocene

The most recent, Pleistocene glaciation began around 120,000 years ago and reached a maximum (Last Glacial Maximum; LGM) in most parts of the northern Hemisphere around 18,000 B.P.[1] (Andrews 1979). In parts of Europe and North America deglaciation took until 9,000 BP, with periodic readvances and retreats of ice margins. Recent work in Scotland has identified various significant Late Glacial readvances indicating that deglaciation involved active stepped retreat rather than large-scale downwasting of stagnant ice (Brown 1993, Brazier et al 1998). Many of these advances were not synchronous. Dyke and Prest (1987) noted that while some margins of the Laurentide ice sheet were readvancing others were retreating. Two main periods of widespread re-advance occurred between the LGM and deglaciation. Around 14,000 years ago glaciers in Denmark and Scandinavia readvanced during the Older Dryas. Everest (2003) cosmogenically dated glacially transported boulders in the Cairngorms in Scotland to between 16 and 15,500 years ago. The Younger Dryas, 11 – 10,000 BP however was a far more widespread glacial readvance. Evidence of this event has been found throughout the North Atlantic and also possibly in North America, South America and New Zealand although synchronicity between the northern and southern hemispheres is debated (e.g. Ivy-Ochs et al 1999, Hajdas et al 2003, Owen et al 2003, Turney et al 2003). In Britain the Younger Dryas, also known as the Loch Lomond Stadial, saw the redevelopment of an ice sheet in the West Highlands and corrie glaciation in the Cairngorms, Lake District and Snowdonia (Benn 1992, Bennett and Boulton 1993, Everest 2003).

Rapid retreat from the advanced position of the Younger Dryas glacial limits is generally recognized. Between 10,000 and 9,000 BP the Scandinavian ice sheet was reduced to a dome of ice in northern Sweden (Eronen 1983). The Laurentide ice sheet in North America had retreated to a terrestrial position and deposited the Cockburn moraines between 8-9,000 years BP (Falconer et al 1965) and within 1,000 years had been reduced to remnants in Arctic Canada (Benn and Evans 1998, England et al 2000). The offshore records from around Scotland indicate that by around 10,300 B.P., after the advance during the Younger Dryas, the ice cover of Britain had virtually disappeared. Theories on the deglaciation of Iceland have changed over time from the single re-advance during overall deglaciation

[1] Calibrated years unless otherwise indicated by 'B.P.', denoting ^{14}C years before 1950.

to the dual and then multiple readvance theories (Norðdahl 1991). Traditionally there are recognised to be two main advance periods in Iceland; Álftanes stage –about 12,000 BP and Búði stage 10,000 – 9,500 BP.. The Álftanes end-moraine has been linked to the Older Dryas Stage elsewhere in Scandinavia and the Búði moraines to the Younger Dryas event. However, more recent mapping of so-called 'Búði-stage' moraines has produced a new suite of dates primarily of Preboreal age around 9,500 B.P(Ingólfsson and Norðdahl 1994). This indicates that the Búði moraine complex may have been a terminal position for an ice sheet in the early Holocene and that perhaps the Álftanes moraine is not coincident with Older Dryas advances, but rather with the Younger Dryas (Hjartarson and Ingólfsson 1998). It appears likely that a number of readvances occurred in the late Weichselian and early Holocene with greater extent than was once thought (Norðdahl, pers. comm. 2004).

What is certain and most pertinent to this thesis is that by 8,000-7,000 BP the central highland area was ice free (Kaldal and Vikingsson 1991). The Þjórsár lava in south central Iceland has no signs of glaciation and peat immediately underlying it has been radiocarbon dated to 7,800 BP. Lake sediments aged between 9,400 and 7,800 BP have been identified to the northwest of Mýrdalsjökull indicated that there was an subaerial lake here by this time. The earliest dates for soil accumulation on the south coast range from 8,800 to 6,800 BP, around Eyjafjallajökull and Sólheimajökull, indicating that the escarpment slopes in this area were free of ice by at least 8,000 BP (Dugmore 1987).

The ~10,000 years since the Younger Dryas is known as the Holocene period. The global record of Holocene glacier fluctuations is complex and patterns of retreat and advance of glaciers are not necessarily synchronous even over relatively small areas. This may be an artefact of selective preservation of the geomorphological record, comparisons being made between many different glaciers of different sizes and with different local conditions, the use of different dating techniques and different researchers working in slightly different ways. Röthlisberger (1986) tried to reduce these possible variations in data collection by compiling a series of curves of fluctuations around the world using data collected by himself from glaciers of similar size (Figure 1.2.1). These curves show remarkable similarity, particularly between northern and southern hemisphere records. Guðmundsson (1997) compared a composite Icelandic record with Röthlisberger's European Alp size record and a record from northern Scandinavia from Karlen (1988) (Figure 1.2.2). This comparison showed less clear relationships, though possibly the Icelandic record somewhat lags behind advance and retreat patterns elsewhere in Europe.

The start of the Holocene period saw a climatic amelioration, sometimes known as the Holocene Climatic Optimum. By the mid 8th Millenium BP it has been suggested that the Fennoscandian ice sheet had virtually gone (Lundquvist 1986). Glacier fluctuation studies from Hardangrjokulen and Josteldalsbreen in Norway indicate that these glaciers melted in the early to mid Holocene (Nesje and Kramme 1991). However, studies from northern Norway indicate that glaciers did not melt away during the Holocene, rather experiencing numerous fluctuations and at several times reaching

Holocene maximum limits (Karlen 1988, Ballantyne 1990). Various Icelandic studies have similarly suggested that Iceland may have been largely ice free during the early Holocene although, as elsewhere, country-wide evidence is not conclusive (Bjornsson 1979, Kaldal and Vikingsson 1991 and Ingolfsson et al 1997).

The Climatic Optimum with limited ice cover was followed by a mid Holocene period of glacial advances often termed the Neoglacial. Timing of Neoglacial advances varies spatially across the globe, but in many locations appears to be manifest as at least three periods of glacial expansion separated by retreat phases. Alaskan Holocene advances appear to have begun as early as 7,600 BP, at a time when Scandinavian ice cover was still limited (Calkin 1988). Icelandic neoglacial advances seem to have occurred around 7,000-4,500 BP, c.3000 BP and 2,000-1,000 BP. North Iceland neoglacial activity and patterns from Vatnajökull suggest the onset of neoglaciation around 6,000 BP (Guðmundsson 1998 and Bradwell 2001). Limits dated by Dugmore (1989) at Sólheimajökull indicate slightly earlier activity around 7,000 BP.

The most recent widespread glacial expansions occurred during the Little Ice Age (LIA) between the late 16th Century and the early 20th Century (Grove 1988). The timing and extent of glacier advances and retreats during this time was variable. Benn and Evans (1998) note that patterns of LIA glacier fluctuations in Norway are related to varying distance from moisture sources, latitude and altitude. The Mer de Glace in the French Alps advanced to a historical maximum between 1590 and 1645, and again in 1825-26 threatening the village of Les Bois near Chamonix, which had to be evacuated (Goepfert 1993). In 1690 Jean d'Aretha, Bishop of Geneva came to Chamonix to exorcise the glaciers because of the destruction they were causing to fields and farms as they advanced. In Britain the Thames froze over on numerous occasions and permanent snow patches formed in the Scottish Highlands between the 18th and 19th centuries (Manley 1971, Lamb 1979). Glaciers in the Southern Canadian Rockies and in Southern Norway reached their Holocene maximum in the LIA (Luckman and Osborn 1979, Caseldine and Matthews 1987, Matthews 1991).

In the 1930s and 1940s it was suggested that the LIA expansion of glaciers represented the maximum advance of Icelandic glaciers in the Holocene (Eythorsson 1935, Thorarinsson 1936, 1944). However, Thorarinsson (1956, 1964) later identified moraines associated with earlier, more extensive advances of outlets of Vatnajökull, requiring a reconsideration of this theory. Debate still surrounds the issue of the timing of the Holocene glacial maximum in Iceland. Evidence exists for three main theories; a Neoglacial maximum, a mid 18th to early 19th Century maximum or a late 19th Century maximum. The Neoglacial theory is backed up by evidence from Sólheimajökull (Dugmore 1987, 1989), Öræfajökull (Gudmunsson 1998), Lambatungnajökull (Bradwell 2001) and North Iceland (Caseldine 1991, Caseldine and Stotter 1993, Kirkbride and Dugmore 2001a). However, these early maximum dates are sometimes considered anomalous because a significant body of evidence exists for a Little Ice Age (1600- 1900 AD) Holocene maximum that is somewhat synchronous with the wider North West

European patterns (Karlen 1988, Matthews 1991, Bickerton and Matthews 1992, Dahl and Nesje 1994, 1996, Kirkbride and Dugmore 2001b). The role of volcanic and geothermal conditions beneath the catchments of Sólheimajökull and Öræfajökull have cast doubt on whether their behaviour may be related to volcanic activity rather than the wider climatically controlled glacial patterns (Bradwell 2001).

The timing of the advances within the Little Ice Age have been disputed, with various authors favouring either the late 19th Century or mid 18th to early 19th Century maximums. The late 19th Century pattern is considered dubious since it is based on lichenometric dating using the largest-lichen technique which Kirkbride and Dugmore (2001b) suggest does not agree with tephrochronological dating results and may give overly young dates when used alone. Bradwell (2001) notes that most Icelandic LIA limits dated with lichenometry give maximum advance ages of 1850-1900 AD. However, use of population lichenometric studies by Bradwell (2001) at outlets of Vatnajökull, has produced a Little Ice Age glacial advance date of c.1750-1800 AD, which is confirmed by tephrochronology and is comparable with other south Iceland Little Ice Age advance records.

Causes of glacier fluctuations

The main control on most patterns of glacial fluctuation is climatic. Glacier mass balance (the balance between growth by snow and ice accumulation and loss of mass through melting and iceberg calving) responds to climatic change. An increase in snow / ice accumulation in a colder or wetter period will be realised as positive mass balance and cause an advance of the glacier terminus. Similarly, warmer and drier climatic conditions will result in less snow accumulation and increased melting, resulting in glacial retreat. The point on the glacier where accumulation and ablation (melting) balance is termed the equilibrium line and the altitude at which this lies (the ELA) fluctuates in response to mass balance changes and climatic change. A cooling can cause a drop in the ELA producing a larger area for accumulation, whereas a warming will raise the altitude of the equilibrium line and reduce potential for accumulation.

Other environmental evidence confirms this pattern. Periods of warming and cooling during the Holocene have been identified from studies of pollen, marine and ice core records and other proxy data sets, and the main periods of glacial advance and retreat can be tied in with periods of colder/wetter and warmer/drier climate. Many studies of glaciers around the world have shown links between air temperature, precipitation and humidity and fluctuations in glacier mass balance and ice margin positions (eg. Nesje 1989, Chen and Funk 1990, Brazier et al 1992, Hastenrath and Kruss 1992). Guðmundsson (1997) reviews environmental change throughout the Holocene in Iceland, associating climatic proxy data to glacier fluctuations (Figure 1.2.3). He notes that frequent environmental change occurred during the Holocene in Iceland. In particular, he identifies a dramatic though brief period of cooling in the inferred temperature records around 5,000 B.P., which ties in

with the timing of glacial advances in both north, and south Iceland. He also states that in general good correlations exist between the timing of geomorphic change, glacier fluctuations and climatic change, though some lags in response times are apparent and would be expected.

Lags in response to climatic changes vary regionally and also between individual glaciers. In some cases glacier behaviour may be completely decoupled from climatic trends. In Iceland the main factors to consider are hypsometry, topography, surging and subglacial volcanic or geothermal activity.

The different response of glaciers with different hypsometries to variations in ELA (representing climatic change) is shown in Figure 1.2.4. Different topographic settings, whether a glacier expands on to an open, unconfined sandur plain or is located in a narrow valley, also influence the pattern of fluctuations and the geomorphic record left behind (Mackintosh 2000). A glacier in a confined valley situation will fluctuate along the length of the valley, exaggerating climatic variation. However, topographic thresholds can exist, such as breaks in slope, valley wall termination or bedrock barriers, which may provide non-climatic limits to glacial extent. Glaciers of different size, with different hypsometries and topographic settings react differently to the same regional climatic changes, even when located in adjacent valleys. This was shown in a recent study of LIA behaviour of two small outlet glaciers from Mýrdalsjökull (Casely 2001).

Surging can dominate glacial fluctuations and although an uncommon phenomenon, it is known to be concentrated in some parts of North America, in the Pamirs in western Asia, in Svalbard and Iceland and is characterised by major fluctuations or cycles in glacier flow speed (Benn and Evans 1998). Periods of slow flow (quiescent phase) occur when ice builds up in the upper parts of the glacier and the ice front stagnates. These are interspersed by periods of fast flow (active phase) when ice is rapidly transferred down-glacier resulting in a rapid, often significantly large, advance of the ice front and a reduction in the glacier gradient. The causes of surge behaviour are the focus of much research but are not necessarily associated with climatic conditions, rather by the internal dynamics of the glacier system (Meier and Post 1969). Many studies have linked surge behaviour with changes in basal sliding, subglacial water pressures variations and evolution of the glacio-hydraulic system (Kamb 1987, Fowler 1987, Björnsson 1998). Icelandic surging glaciers include Bruarjökull, Eyjabakkajökull and the large south-western outlet glacier of Vatnajökull, Skeiðarárjökull. None of the major outlet glaciers in the study area are known to regularly surge.

Particularly relevant to this thesis is the potential influence of volcanism and geothermal activity on glacier fluctuations as summarised in Figure 1.2.5. The main factor, increased basal melting, results in an increase in subglacial water pressure and enhanced basal sliding and has been linked to glacial advances from Mount Washington (Sturm et al 1991). However, this behaviour is not necessarily universal. During the Gjálp eruption beneath Vatnajökull in 1996 changes in glacier flow patterns and

velocity were only noticed around the cauldrons on the ice surface, which had been caused by increased subglacial melting, with no change elsewhere in the ice sheet (Chapman et al 2000). The implication of this is that subglacial eruptions beneath temperate glaciers may only have localised impacts on glacier flow. When volcanic eruptions breach the ice surface they can remove significant proportions of glacier volume and can significantly change the ice surface topography and the dynamics of a glacial system. Shoestring Glacier lost about 75% of its volume during the Mount St. Helens eruption in 1980 through 'beheading' in the volcanic blast and landslide and through enhanced melting and erosion of the glacier surface by hot ash flows, mudflows and avalanches (Brugman and Meier 1981). The resultant effect was a reduction in glacier sliding attributed to the removal of the accumulation area water source and consequent reduction in subglacial water pressure.

Tephra fall on ice surfaces can also influence fluctuation patterns. Recent studies of this kind have linked tephra cover to alterations in ablation patterns and thus glacier fluctuations (Brugman 1986; Sturm et al 1986, 1991; Driedger 1981, Kirkbride and Dugmore, in press). While thicker tephra cover may insulate the ice surface inhibiting retreat, thin layers of tephra covering a glacier can enhance melt and contribute to glacial retreat.

Conversely, fluctuations of glaciers may also influence patterns of volcanism. Guðmundsson (1998) found close links between eruptions of the Öræfajökull volcano and glacier fluctuations suggesting that crustal loading and unloading association with glacier fluctuations was the driving mechanism for the timing of some volcanic eruptions. This is a long-standing theory that changing stresses associated with glacial expansion and retreat can influence patterns of subglacial volcanism (Rampino et al. 1979, Hall 1982, Sejrup et al 1989).

1.3 Jökulhlaups

Jökulhlaup is Icelandic for an unusually large glacial flood. These are also known as glacier outburst floods in the U.K. and North America, débâcles in mainland Europe and aluviones in South America. 'Jökulhlaup' has been brought into international usage because Iceland was one of the first locations in which this phenomenon was recognised. Jökulhlaups are both powerful geomorphic agents and significant natural hazards, posing a threat to human life and settlement in glaciated regions around the world. Frequent jökulhlaups in Iceland cause loss of life, damage to agricultural land and important communication links. The 1996 eruption of the Gjálp fissure beneath Vatnajökull is perhaps the most famous Icelandic jökulhlaup which was widely reported by the international media and gave scientists a unique opportunity to study the processes involved in subglacial eruptions and the subsequent flood. Nobody was hurt in this event since the flood passed across largely uninhabited sandur plains to the south coast but damage to bridges, roads, power lines and optical telephone lines mounted to $15 million US (Halldórsson 1998).

Jökulhlaups can be caused by a number of events and tend to produce flows of mixed sediment and water, often carrying large ice blocks. The ratio of sediment to water can vary and various authors have debated the most appropriate definition of the term 'jökulhlaup' and the point at which a jökulhlaup transforms from a flood to a mudflow, lahar-like event, slurry flow and hyperconcentrated flow or debris flow (e.g. Jónsson 1982, Maizels 1997, USGS 1998). This thesis however will use the term "jökulhlaup" in its most simple sense to mean all unusually large-scale glacially derived sediment-water flows, of any composition. Particular terms will be used to define specific sediment-water mixes, as sub-classifications of jökulhlaups, referring to their nature and flow and the sediments they deposit.

Mechanisms of generation and flow paths contribute to variations in flood hydrographs, rheology and proglacial flood routing, which subsequently influence the geomorphic and sedimentary legacy of palaeo-events. This section will briefly review the mechanisms of jökulhlaup generation and flow before going on to look at their impact on the landscape and sedimentary records of a region.

Jökulhlaup generation

Multiple mechanisms of jökulhlaup generation exist. These can be sub-divided in to non-volcanic and volcanic causes (Table 1.3.1A and B). Björnsson (1992) gives a good discussion of jökulhlaup mechanisms in Iceland, while Major and Newhall (1989) comprehensively discuss lahar and volcanic flood formation. Röthlisberger and Lang (1987) review extreme floods in particular ablation, rainfall and lake / subglacial water pocket drainage events.

TABLE 1.3.1A: Non-volcanic jökulhlaups

Trigger for jökulhlaup	Characteristics and statistics	Example	Further details
Marginal ice-dammed lake drainage	60-70% floods in Swiss Alps (Haeberli 1983). Tends to involve larger amounts of water than other non-volcanic jökulhlaups. Flow from lake site may be through thin ice following the underlying topography. Where the dam consists of a large area of debris covered stagnant ice drainage maybe gradual as a drainage channel melts a path through the core of ice (Benn pers. Comm. 2003).	Extensive literature.	
Rupture of sub-/en-/supraglacial water bodies	30-40% floods in Swiss Alps (Haeberli 1983). Route from lake site to ice edge may be influenced by glacier surface slope if source is subglacial (Shreve 1972). Many possible different triggers .. see text.	Extensive literature. Mount Rainier, Washington (Hoblitt et al 1995)	• One cause among many debris flows on volcano associated with mixing of water and loose debris.
Moraine-dammed lake drainage	Common wherever sediment availability is high enough for moraine construction. More stable than ice-dammed lakes. If moraines are ice-cored they are less stable and melting of the dam is possible. Usually associated with incision of barrier by draining water rather than	Central Asia has long history of debris and earth flows from failed debris dams (Cunha 1998;43) Pamir Mountains, Tajikistan (Cunha 1998) Karakoram (Hewitt 1964, 1982) Khumu Himalaya (Ives 1986, Watnabe et al 1992)	1966 flood for Lake Yashinkul', SE Pamir: lake formed behind moraine and rockfall. Triggered flood by seismic tremor (Cunha 1998, 43-44).

Trigger for jökulhlaup	Characteristics and statistics	Example	Further details
	over-topping or basal breach, by increasing lake level. Linked to glacial advance, breaching of water body within glacier or wave generation from a calving event or avalanche. Moraine- and stagnant-ice dammed lakes frequently form at the snouts of heavily debris-mantled glaciers. Prone to failure especially if triggered by seismic tremors.	Cordillera Blanca, Peru (Lliboutry et al 1977), British Columbia, Canada (Clague et al 1985), Tibet (Yongjian and Jingshi 1992), European Alps (Tufnell 1984). Moraine dam failure due to an ice avalanche from Langmoche glacier, Nepal in 1985 (Benn and Evans 1988)	
Rockfalls, snow and ice avalanches on to glacier / proglacial lake	When debris, snow or ice from nearby slopes falls on to the slopes of glacier, water from on or within the glacier can be expelled and entrained triggering a debris-laden flow. Similarly if the material falls in to a proglacial lake. More common in areas with extensive unstable slopes or particularly prone to earthquake activity. Large-scale rockfalls / avalanches can erode ice and snow.	Steinsholtsjokull, South Iceland 1967	• rockfall onto glacier, evacuated and destroyed proglacial lake. Compressed air trapped by falling rock and ice launched flow forwards into lake and downvalley Kjartansson 1967)
Glacier surges	Surges can cause temporary blockage of adjacent valleys and thicken pre-existing ice dams, resulting in catastrophic flooding (Rothlisberger	Vernagtferner, Ötztal Alps, Tyrol Skeidararjokull, Iceland 1929 and	• Repeated flooding associated with surges since 1599 (Hoinkes 1969). • Gudmundsson et al (1995)

Trigger for jökulhlaup	Characteristics and statistics	Example	Further details
	and Lang 1987, Bjornsson 1992). Also, flooding is associated with the change in drainage that accompanies surges.	1991	suggest that surges initially lowered the ice surface then gradually built up the elevation may have effected the height of the ice dam at Grimsvotn lake, influencing jökulhlaup frequency.
Extreme ablation and prolonged and heavy rainstorms	Most common cause of floods in glacierized basins. Discharges orders of magnitude lower and generally less catastrophic than lake discharge or volcanic flood events.	Importance of meteorological floods in studies of catastrophic floods viewed differently by different authors.	• Rothlisberger and Lang (1987: 231) state that these should be considered separately from other flood types in studies of catastrophic flood frequency. • Haeberli (1983:85) suggests that the degree of importance assigned to an event should be dependant on the impact on human life. • Maizels and Russell (1992) class flooding from extreme melting and prolonged extreme rainfall as triggers for jökulhlaups. • Hoblitt et al (1995) note jokulhlaups from South Tahoma Glacier, Mt Rainier, Washington due to periods of unusually high temperature or rainfall in summer to early autumn. Walder and Driedger (1993) treated these floods as small-scale but frequent causes of debris flow hazards.

TABLE 1.3.1B: Volcanic jökulhlaups

Trigger for jökulhlaup		Characteristics	Example	Further details
Basal melting	Geothermal activity and lake formation	Frequent and regular flooding where geothermal fields are covered with ice.	Grimsvotn (dates?), Iceland (references) White River Glacier, Mount Hood, location, 1926, 1931, 1946, 1949, 1959, 1968. (Swanson et al 1989)	• Geothermal lake drainage...expand. • Geothermal and fumarole activity beneath the ice has caused jokulhlaups.
	Subglacial eruption	Melts ice rapidly. Beneath thicker ice cover this collects and drains after a threshold is crossed. Basaltic eruptions thought more likely to cause large-scale jokulhlaups because of thermodynamics of the magma-ice interaction.	Katla, Iceland 1918 (referenes) Gjalp, Iceland 1996 (Gudmundsson et al 1997) Deception Island, Antarctica 19?? (Smellie 1999)	
Surficial melting	Pyroclastic flow, hot blast, pyroclastic surge.	Melting from frictional energy and heat transfer. Scouring of the glacier surface and erosion of ice. Entrainment of ice blocks, glacial debris and supraglacial water. ~40% of all lahars and floods.	Drift Glacier, 1989-90, location? Trabant and Meyer (1992). Nevado del Ruiz, Columbia 1985 (Naranjo et al. 1986, Lowe et al. 1986, Major and Newhall 1989)	• Pyroclastic flows and surges entrained snow and large boulders of glacier ice as they passed over a steep icefall. Four eruptive events resulted in four floods up to 20,000m^3s^{-1}. • Small pyroclastic flows and surges resulted in melting on 10% of the ice cap and generated jökulhlaups. Entrainment of sediment downslope increased the debris load, forming hyperconcentrated flows or lahars. The largest 'lahar' was 47.

Trigger for jökulhlaup		Characteristics	Example	Further details
	Lava flow	Heat transfer due to conduction is normally too slow to cause significant melting and thus flooding. More frequently meltwater becomes a steam and a chilled margin forms on the edge of the lava flow. ~5% of all lahars and floods*	Kliuchevskoi, USSR, 1984-85 *	• Lava flows recorded that melted a channel into glacier ice and formed a 'lahar'.
	Ejection of water from crater lakes	~2% of all lahars and floods.	Mount Ruapehu, New Zealand 1969 *	• A large volume of water was ejected from Raupehu's crater lake during an explosive eruption, eroding snow, ice and debris from surrounding glacier ice.
	Ash fall	Rarely produce lahars / floods immediately, though sometimes asociated witrh floods with heavy rainfall post-eruption. Ashfall is known to alter ablation rates but rarely produces much meltwater (Driedger 1981, *)		

* Major and Newhall (1989)

The most common cause of catastrophic flooding is the failure of marginal ice-dammed lakes, accounting for 60-70% of all recorded floods in the Swiss Alps (Haeberli 1983). Similarly the emptying of glacier-dammed lakes is the most frequent cause of Icelandic jökulhlaups (Tufnell 1984). Jökulhlaups can also be caused by rupture of water bodies on, within or beneath glacial ice, generally due to variations in water pressure or ice overburden pressure in the glacial system. Seasonal evolution of the drainage network is often believed to be associated with outburst floods, particularly smaller scale events, as are patterns of surging or other periodic influences such as rockfalls, avalanches, moraine dam failures and extreme weather events. Large jökulhlaups in Iceland have been related to cyclic release of water from subglacial geothermal areas and rapid melting from subglacial volcanic eruptions (Björnsson 1992).

The production of meltwater in a volcanic eruption has been much discussed and the main ideas will be summarised here. Despite this relatively wide range of situations in which jökulhlaup events may occur, the principles behind the water storage and drainage mechanisms are often common to all. Thus, the mechanisms of water storage, jökulhlaup triggers and maintenance or curtailment of flow will be discussed. This discussion will concentrate on the more catastrophic and frequent jökulhlaup events caused by subglacial volcanism and ice-dammed lake drainage.

Water storage

Water may collect and become stored in ice-marginal, supraglacial, englacial and subglacial locations. Marginal lakes dammed by glaciers commonly form at the confluence of two joining valley glaciers, where a tributary stream is dammed by the advance of a main valley glacier or where a main valley stream is dammed by the advance of a tributary valley glacier. Ponding of water along the glacier margin tends to be enhanced if the ice margin is heavily debris mantled. Marginal ice dammed lakes are also particularly common in sub-polar and polar environments where drainage is restricted by glacier ice frozen to its bed, limiting the development of en- and subglacial drainage routeways. Surging glaciers which experience periodic rapid advance may temporarily block adjacent valleys and thicken pre-existing ice dams, thus allowing an increased build up of water and higher potential for catastrophic flooding (Röthlisberger and Lang 1987). Repeated flooding has been associated with surges of the Vernagtferner in the Ötztal Alps, Tyrol since 1599 (Hoinkes 1969). Thus, retreat and advance of glaciers can control the storage capacity of marginal ice-dammed lakes. As glaciers have thinned and retreated since the turn of the century there have been changes in flood characteristics from ice-dammed lakes. Initially the frequency of floods increased as ice dams became destabilised. However, as ice thins less storage of water is possible and the destructive force of floods diminishes (Fisher 1969, Björnsson 1992). Other marginal lakes may form in proglacial areas, dammed by moraine or other topographic highs.

Water storage within the glacial system occurs at a variety of scales, from intersections between individual ice crystals to large subglacial lakes, such as Lake Vostok, beneath the East Antarctic Ice Sheet, as illustrated in Table 1.3.2. Concise and clear summarises of water storage within glaciers are given by Fountain and Walder (1998; 317-318) and Knight (1999, 95-98).

Supraglacial water storage mainly consists of storage in snow and firn and in depressions, potholes and lakes. Water flow on the ice surface is controlled by topographic variations as with a normal subaerial stream. On temperate ice, ponded supraglacial water tends to be a temporary phenomenon, which under normal conditions, drains as efficient englacial and subglacial routeways develop in late spring/early summer. Water is then directed into the main glacial drainage system. However Benn et al. (2001) have described the formation of many supraglacial lakes in the Khumbu Himal (Nepal) that do not appear to be linked to the main glacial drainage system. As these heavily debris-mantled glaciers thin, the lakes increase in size and increasingly become hazardous. Multiple such supraglacial lake systems have already drained catastrophically.

Storage and flow of water within and beneath glacial ice is controlled by the distribution of water pressure potential, a balance between water pressure and ice overburden pressure as defined by Shreve (1972), summarised in Box 1.3.1. Englacial storage mainly occurs between ice crystals (Lliboutry 1971), but large water bodies are also stored in voids and truncated conduits within the main body of the ice.

Water cavities and subglacial lakes dominate subglacial storage. Water may also be stored in a porous substrate. However, the distribution of till layers beneath glaciers and their ability to transmit water from storage on a short time scale are frequently undetermined, due largely to a lack of information from subglacial environments. Fountain and Walder (1998) state that daily discharge variations cannot be explained in relation to basal till storage due to the limited storage capacity in the thicknesses of till observed from borehole studies and the small discharges estimated to be released from a strained saturated till layer. Thus, they refer to the storage capacity of water in cavities, on scales of a few millimetres to metres across, which develop when the glacier bed is rough and in the lee of bedrock highs. Cavity storage has been inferred for surging glaciers, particularly Variegated Glacier where the volume of water stored during the surge of 1982-83 was equivalent to a layer of water across the bed, approximately 1m thick (Fountain and Walder 1998; 318). Further credence is given to this theory when considering the seasonal evolution of Alpine glaciers and the release of water from subglacial cavities in a 'spring event' (Nienow et al 1998).

Subglacial lakes may develop into very large reservoirs. A large subglacial lake, with a surface area of about 10,000 km^2 has been detected by radio-echo sounding beneath the central East Antarctic Ice Sheet (Kapista et al. 1996). Shoemaker (1991) suggests that similar sized lakes existed beneath the Laurentide Ice Sheet during the last glacial period. Björnsson (1977) and Nye (1976) consider the

TABLE 1.3.2: WATER STORAGE IN GLACIERS (grey shaded areas supply significant volumes of water to jökulhlaups, based on their potential for storing water)

Scale	Supraglacial	Englacial	Subglacial
↓ Increasing scale and availability for rapid release of stored water.	Snow and firn accumulation	Between and within ice crystals (veins)	Porous substrate (till)
	Potholes (particularly noted in surging glaciers)	Englacial voids	Cavities in lee of bedrock highs.
	Supraglacial depressions (lakes)	Sections of abandoned channels, moulins and crevasses.	**Subglacial lakes** in bedrock depressions and in areas where ice surfaces directs water into subglacial cupola.

Box 1.3.1: Shreve's (1972) theory of water flow through glaciers

Shreve's theory explains the direction of water flow within a glacier, and the orientation of englacial and subglacial conduits. Basically, the direction of flow is controlled by variations in hydraulic or water pressure potential (Ø):

$$\emptyset = \emptyset_0 + \rho_w.g.z + \rho_i.g.(H-z) + P_m$$

Where $\emptyset$ = *hydraulic potential,* $\emptyset_0$ = *reference potential,* ρ_w = *density of fresh water (~1000kgm^{-3}),* g = *gravitational acceleration (9.81m^{2}s^{-1}),* z = *elevation of conduit above reference datum,* ρ_I = *density of ice (~910kgm^{-3}),* H = *elevation of ice surface above reference datum,*
P_m = *adjustment of hydraulic potential due to decrease in pressure in the vicinity of the conduit.*
(Notation from Benn and Evans, 1998)

But, more simply this equation is basically the sum of the constituent pressures, which result in the total potential energy of water flow within a glacier:

i.e. The potential energy generated by raising the water above sea level plus the additional potential energy gained by pushing down on it with a mass of ice:

Hydraulic potential = a + b + c + d

a – $\emptyset_0$, refers to the **potential energy at the base or reference level**, assuming sea level this term = 0.

b = ρ_w.g.z, refers to the **potential energy associated with raising water to the height of the conduit above the reference datum** (if this is a subglacial conduit, height due to the **elevation of the bed**).

c = ρ_I.g.(H-z), is associated with **pressure from the overlying ice**. Note that (H z) is the ice thickness above the conduit.

Figure 1: Constituent parts of Shreve's (1972) equation:

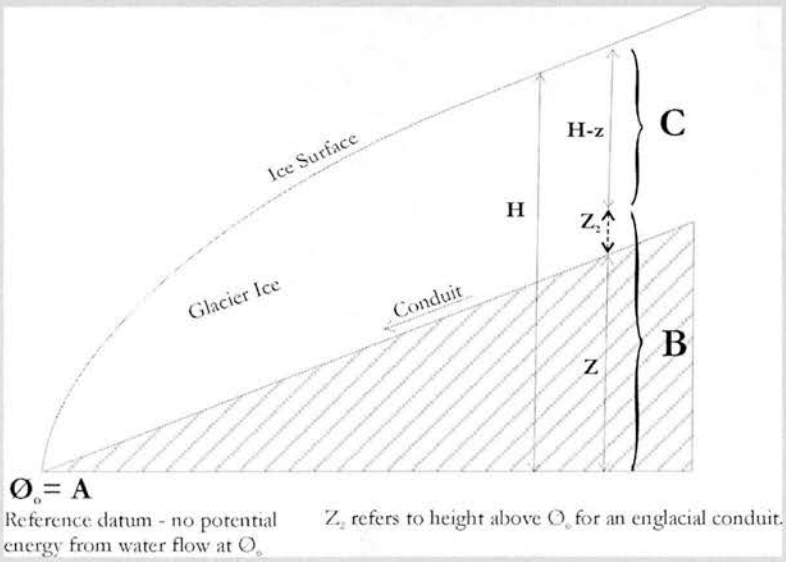

The final term, d = P_m, refers to the pressure reduction in the vicinity of the conduit, a 'dimple' in potential energy of water flow in a conduit:

Figure 2: Pressure reduction in the vicinity of a conduit:

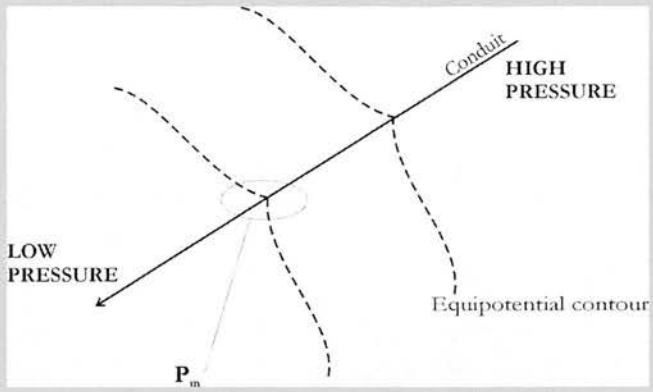

While this equation and theory was developed for flow in full, pressurised conduits, it is often regarded as defining hydraulic potential throughout the glacier (Paterson 1994) and the final term is then left out.

This theory states that equipotential surfaces develop along surfaces where hydraulic potential (**Ø**) is constant. These equipotential surfaces *'will slope downward in the up-glacier direction with a gradient approximately 11 times that of the (ice) surface' (Shreve 1972; 211).* However, with increasing surface slope this factor of 11 tends to decrease. Thus, ice surface slope predominantly controls the positioning of equipotential surfaces, with the orientation of the glacier bed being less significant unless the ice surface is flat, or bed slope is more than 11 times the magnitude of the ice surface slope.

Water flow will be orientated perpendicular to these surfaces, controlled by hydraulic gradient (rate of change of hydraulic potential) from low to high pressure. Since ice surface slope may often be discordant with bed slope, water may traverse a slope or even flow uphill, along a path that would not be possible for a subaerial stream.

Figure 3: Equipotential surfaces and water flow in a glacier (after Paterson 1994; 113; fig.6.4)

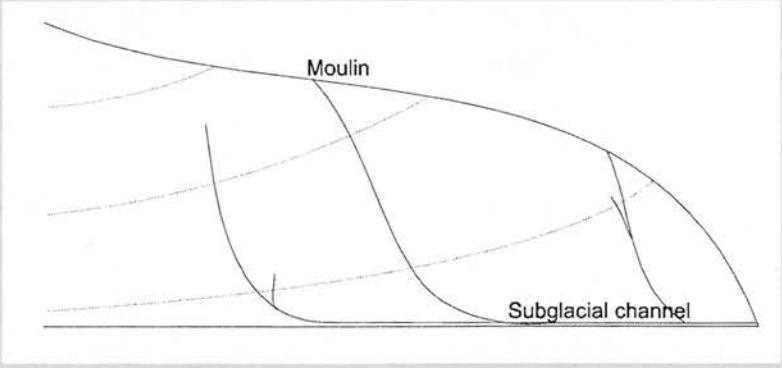

References:

Paterson, 1994 *The Physics of Glaciers 3rd edition,* Chapter 6, pp.103-131, Elsevier Science Ltd, Oxford.

Röthlisberger, H. and H. Lang 1987 Glacier Hydrology *In,* Gurnell, A. M. and M. J. Clark (eds.) *Glacio-fluvial Sediment Transfer,* John Wiley and Sons, pp.207-284.

Shreve, R. L. 1972 Movement of water in glaciers, *Journal of Glaciology,* v.11, no.62, pp.205-214.

TABLE 1.3.3: From Smellie (1999). Volcanic eruptions beneath thin and thick ice.

Glacier thickness and structure	Eruption type	Impact on ice and surface	Meltwater drainage	Examples
THIN GLACIER • Alpine/thin margin of ice sheet/cap. • Composed mainly of snow, fern and fractured ice. • <<100-150m thick • **Permeable**	Explosive to start with. As meltwater drains becomes less violent. Pillow lava not likely to form due to lack of interaction with water. May produce pyroclastic cone and lava.	Extensive melting, cavity formation. Depression of and / or breaking of the ice surface.	Continuous drainage of meltwater in a sheet or in conduits. **Tends not to cause large-scale jokulhlaups because not significant ponding of water.**	• Subglacial eruption on Deception Island (Antarctica), 1969 • Examples from geological record of interbedded tills, volcaniclastics, lava and hyaloclastite breccias I Iceland and Antarctica.
THICK GLACIER • >>150m thick • **Impermeable** • Very thin permeable layer at surface	Eruption largely subaqueous, effusive? (as below)	Extensive melting, vault formation. Surface depression concentrates meltwater flow to 'vault' and hydrostatic pressure acts as a seal until threshold crossed.	Can be sealed in vault by hydrostatic pressure Leakage may occur forming channel. Rapid meltwater production may trigger sheet flow at glacier bed or supraglacial overflow. May ultimately float ice dam. Water level may rise and float ice dam before being high enough to overflow.	• Flotation has at times occurred at Grimsvotn, Iceland.
THICK GLACIER • >>150m thick • Thick **permeable layer** above impermeable ice.	Eruption into lake. Subaqueous unless continues 'till lake drains. May form tuya if eruption becomes subaerial. Effusive because of pressure from overlying ice. Becomes explosive as ice thins and interacts with meltwater.	As above. Overflow possible .. thus erosion of ice surface or disruption of fern surface by jokulhlaup.	Meltwater will accumulate until encounters fern aquifer then drains. If fern thickness >10-25% thickness underlying ice, the water accumulation cannot float the ice dam. May drain though subglacial leakage.	• Gjalp 1996?

TABLE 1.3.4: Comparison between subglacial basaltic and rhyolitic eruptions. From Tuffen (2001; 180; table 2).

Property of eruption	**Subglacial rhyolite**	**Subglacial basalt**	**Implications**
Magma temperature [a]	800-900°C	1100-1200°C	Less energy released as rhyolite is quenched
Melting potential [a]	≤8 times own volume of ice	≤14 times own volume of ice	Positive pressure changes during rhyolite eruption, negative during basalt
Pressure changes during eruption [a]	Positive	Negative	**Rhyolite: meltwater tends to drain away; basalt: meltwater tends to collect at vent**
Magma viscosity [a]	10^6-10^7 Pa s	10^3-10^4 Pa s	Rhyolite eruptions tend to be more explosive, larger aspect ratio lava flows
Effusion rate [a]	10^1-10^2 m^3s^{-1}	10^1-10^4 m^3s^{-1}	Inward ice creep [b] more significant during rhyolitic eruptions because edifice growth is slower [a]
Distribution [c]	Iceland, mostly at central volcanoes	Antarctica, Iceland, British Columbia	Basalt much better studied than rhyolite
Recent eruptions	None observed	Gjálp 1996, Iceland[c]	Insight gained on basaltic eruptions, not on rhyolitic

[a] Hoskuldsson and Sparks (1997); [b] Guðmundsson et al. (1997); [c] Smellie (1999)

formation of subglacial lakes and their drainage, based predominantly on the theory of Shreve (1972). Water may accumulate within a depression beneath an ice dome or where an ice surface depression focuses water flow into a cupola, as illustrated in Figure 1.3.1. In both cases water accumulates in an area of low hydraulic pressure surrounded by a 'seal' of high hydraulic potential.

Subglacial volcanic eruptions

Subglacial geothermal and volcanic activity can increase the rate of water accumulation significantly by enhanced basal melting. Basal melting through either eruptive or geothermal activity has accounted for approximately 35-36% of all historical glacial lahars and jökulhlaups, the majority of which have occurred in Iceland (Major and Newhall 1989).

Continuous melting of ice at the glacier bed by geothermal heat results in the formation of a crevassed depression in the glacier surface, as has been observed on the surface of Mýrdalsjökull during active periods of Katla (Björnsson et al 2000). This was again noticed during the recent upsurge of activity and subsequent small jökulhlaup from Sólheimajökull during the summer of 1999. Similar features are found above geothermal areas on Vatnajökull, and most famously above the geothermal lake Grímsvötn, from which regular jökulhlaups are released (Björnsson et al 2001). Once this depression has formed it will direct ice and water flow towards the geothermal area and allow the formation of a subglacial lake or cupola (Thorarinsson 1953, Björnsson 1974, 1975). Water cavities formed in this way will slowly develop, unless influenced by eruptive activity, increase in size and be released in jökulhlaups, as would occur with a non-volcanic subglacial lake.

Subglacial eruptions have resulted in some of the largest and most destructive jökulhlaups during historic times (Tufnell 1984, Röthlisberger and Lang 1987, Björnsson 1992) and those from Grímsvötn and Katla have been by far the largest in Iceland (Rist 1983). Major and Newhall (1989) also describe eruptions on Deception Island, Antarctica, 1967-69, which caused subglacial heating and subsequent flooding to a depth of 15m, damaging buildings on the island. Little has been directly observed concerning the processes of subglacial eruptions. The recent eruption of the Gjálp fissure in Iceland provided an excellent opportunity to study a subglacial eruption (Guðmundsson et al 1997). Höskuldsson and Sparks (1997) have carried out laboratory-based studies of subglacial eruption processes. These studies have focussed on calculations of ice cavity generation during an eruption and used jökulhlaup hydrographs to infer details of subglacial eruption processes.

Volcanic eruptions cause rapid ice-melt either through effusive lava emplacement and convective transfer of heat energy as pillow lava cools or, from the explosive eruption of pyroclastic material, causing turbulent mixing and thus heat transfer. A subglacial eruption may be silicic or basaltic and also effusive or explosive. Basaltic eruptions are far more common and observations of contemporary subglacial eruptions have all been basaltic in nature. No recent silicic events have been observed and

discussions of their nature are based upon studies of geological sequences, theoretical models and inferences made from observations of basaltic events (Tuffen et al 2001). Whether an eruption is effusive or explosive is a function of the water content of the magma and the ice overburden pressure (Höskuldsson and Sparks 1997).

Smellie (1999) classified subglacial eruptions based on the thickness of overlying ice (Figure 1.3.2 and Table 1.3.3). These divisions are primarily based upon the study of geological sequences interpreted as formed under these conditions. Once ice melt begins a subglacial water cavity develops as occurs with geothermal heating, although at a much faster rate. Smellie (1999) suggests that under thin ice conditions water will be unlikely to accumulate subglacially and drainage will be continuous, limiting the scale and increasing the duration of meltwater discharge. With eruptions beneath thicker ice sheets water will be more likely to pond.

Overburden pressure, magma temperature and processes of heat transfer between magma and the surrounding ice influence meltwater production rate. Particularly rapid rates of melting have been noted with eruptions from Katla and the Gjálp fissure eruption in 1996. In the eruption of Katla in 1918, a total volume of 1-2km^3 was generated and the first flood wave was released within four hours of the eruption commencing. It is believed that this rapid melt rate is enhanced by development of prismatic cooling fractures in the pillow lava and explosive interaction between lava and water causing mechanical stirring (Höskuldsson and Sparks, 1997). Guðmundsson et al. (1997) explain similar rapid ice-melt in the Gjálp fissure eruption by fragmentation of the magma and *'highly turbulent convection of a mixture of meltwater and quenched ash fragments'*.

In geothermal cupolas and normal subglacial lakes, glacier surface and bedrock topography is believed to influence storage capacity and thus theories of hydrostatic and equilibrium conditions are used to explain their patterns of storage and release. However, Höskuldsson and Sparks (1997) suggest that there is a difference between the volume of glacial ice that is melted in an eruption and the extruded lava and generated meltwater that replaces it. They state that basaltic lava can melt more than ten times its own volume of ice and note that water takes around 8-10% less space than ice. This change in volume would result in a change in pressure in the subglacial cavity, which would apparently be much more influential on stability of the stored water body than the pressure relationships in a 'normal' subglacial cavity, drawing water away from or towards the vent. Table 1.3.4 compares subglacial rhyolite and basalt eruptions. Critically for meltwater production, rhyolitic magma only reaches around two thirds of the temperature of basaltic eruptives and thus has less potential for melting ice. Pressure changes associated with this melting are thus different for basaltic and silicic eruptions. Meltwater from a subglacial rhyolite eruption is likely to drain continuously because of positive pressure changes during an eruption, whereas a basaltic eruption causes a negative pressure change around the vent, causing ponding of meltwater, particularly under thick ice.

When a subglacial eruption breaks through the ice cover and becomes subaerial, water storage will be limited. As opposed to basal melting, normal subaerial volcanic phenomena may occur; pyroclastic flows, blasts of hot gas, lava flows, the ejection of heated water from a crater lake and incandescent ash fall causing surficial melting.

Release of stored water and jökulhlaup triggering

Multiple mechanisms exist to trigger jökulhlaup drainage from an ice-dammed lake. Generally the lake level will rise until a threshold is exceeded allowing the lake seal to be broken and for water to drain over, through or under the ice. The basic principles associated with crossing this threshold tend to be the same as those which are essential to understanding the normal and seasonal water flow within glaciers; the interaction between water pressure and ice overburden pressure. Thus, drainage will occur when there is a reversal of hydraulic gradient. Instead of running towards the lake, allowing ponding to occur, it must be reversed to allow drainage from the lake into the rest of the glacier hydraulic system.

One of the first suggestions given for a mechanism of ice-dammed lake drainage was that the lake level rose until it overtopped the dam, cutting a channel into the ice surface (Glen 1954). While this process has been observed on Axel Heiberg Island in Arctic Canada (Maag 1969) under polar conditions, in temperate areas lakes tend to drain sub- or en-glacially and at much lower lake levels. The two main types of mechanism applicable to temperate glacial lake drainage are ice dam flotation and initial tunnel formation either from the lake or towards the lake from the rest of the glacial system.

Ice dam flotation was initially suggested by Thorarinsson (1953), and has been further considered by Nye (1976), Spring and Hutter (1981) and Clarke (1982). This theory is based on drainage occurring when a rise in the lake level increases hydrostatic water pressure such that it reaches or exceeds ice overburden pressure at the ice dam and lifts the ice off the underlying surface. Theoretically this occurs when the lake level rises to or exceeds nine tenths of the height of the ice dam. The exact level of lake water required to float the ice dam depends on glacier ice debris content and crevassing at the ice surface. High debris content within the ice dam could suppress flotation, requiring a higher lake level to trigger drainage (Tweed 2000). Crevassing on the other hand would allow a lower lake level to float the ice dam. If a floating ice tongue were to be raised by a rising lake level it would act as a 'buoyant cantilever', reduce ice overburden pressure at the seal and allow drainage at a lower lake level than otherwise predicted (Nye 1976, Björnsson 1988). Björnsson (1992) reviewed the model of ice dam flotation, comparing theoretical results with actual lake drainage events in Iceland. He found that the model worked well but that drainage often occurred prior to the theoretical critical lake level was reached for ice dam flotation, particularly at the subglacial cupola of Grímsvötn, beneath Vatnajökull.

Therefore it may be that lake drainage is also associated with exploitation of weaknesses in the ice dam either within the structure of the ice or at the ice/bed interface. Triggers such as earthquakes, geothermal melting of the ice dam or sudden rapid sliding may cause drainage to occur at these weak points in the dam. Smellie (1999) suggests that drainage may occur at a junction between 'permeable' and 'impermeable' ice, following the base of a firn layer. If the firn layer is between 10 and 25% as thick as the underlying 'impermeable' ice, drainage will occur along this englacial route before the lake level reaches a depth great enough to cause flotation.

Glacial ice is not impermeable. Capillaries lie along the intersections between ice crystals, allowing a certain degree of permeability, making it possible for seepage of water through the ice mass (Nye and Frank 1973). The discharge of water through this vein network will vary depending on the coarseness of the ice. Estimates of vein capacity vary, expressed in terms of a water layer at the base of the glacier equivalent to 1mm per year to 1m per year for fine to coarse-grained ice (Hooke 1998). The efficiency of this network is low, since ice passages may be prone to blockage by air bubbles (Raymond and Harrison 1975) and closure through ice deformation and recrystallization (Lliboutry 1971). Continuous seepage has been identified from Summit Lake, British Columbia, by dye tracing experiments (Fisher 1969).

When a large quantity of water is introduced to this vein system, usually through crevasses or moulins, the tiny passages expand to become tubes on a mm scale. This process occurs via the melting mechanisms proposed by Shreve (1972) and Röthlisberger (1972) (see Boxes 1.3.1 and 1.3.2). These workers both derived theories of water flow in glaciers, assuming circular, full, pressurised conduits under steady-state conditions. Further work by Hooke et al. (1990) has considered mathematically, the flow of water under non-steady-state conditions with variable discharge, conduit shape and water pressures. Hooke (1998; 121) discusses the propagation of larger crevasses and the intersection with the mm-scale conduit system. This allows a dramatic increase in water supply to this tiny network of passages, which, he suggests, enlarges the tubes *'until they can transmit all of the incoming water downward into the glacier'*. The concept of gradual expansion of veins to allow continuous seepage from a glacial lake and eventual jökulhlaup initiation is similar to the link between crevasses and veins. An increase in water level may increase the available water supply to the vein network thus allowing tunnel formation.

Lake drainage may also be triggered by changes within the rest of the glacial drainage system. Switching of the glacial drainage system from a distributed network of passages to a more discrete system of tunnels is an effective method of draining stored water. This can happen seasonally with spring melting, in response to unusually high ablation rates or heavy rainfall (e.g. Walder and Driedger 1995) and also at the termination of surge conditions. Low-pressure conduits 'capture' drainage from higher-pressure water cavities. This idea could be comparable with the 'capturing' of lake water by a developing discrete conduit network in the rest of the glacier. The pre-existing linked

cavity network, is likely to become unstable with increasing discharge thus allowing preferential capture of drainage by larger, lower pressure cavities and the development of an upward branching arborescent network of conduits. Dye tracing experiments (e.g. Nienow et al 1998) and borehole studies (Gordon et al. 1998) at the Haut Glacier d'Arolla provide evidence for differential meltwater routing through glaciers and preferential development of low pressure conduit networks upglacier as the melt season progresses. Such linkages between lakes and the normal pattern of drainage within a glacier have been proposed in discussions of specific jökulhlaup events (Whalley 1971, Fisher 1969, Clarke 1982, Shakesby 1985).

In the majority of these cases R-channels enlarged by thermal and mechanical erosion propagating through the ice are envisaged as the main routeways for lake water to drain. However, since the expansion of this tunnel network is limited by the rate of tunnel expansion (Box 1.3.2) it has been suggested that jökulhlaups may also flow as a sheet across the glacier bed (Shoemaker 1992) particularly as they burst from the subglacial cupola. Observations of jökulhlaups indicate that water mostly tends to exit the glacier from one or more marginal tunnels. This suggests that even if the initial release of water flows as a sheet, topography and/or hydraulic pressure gradients focus the water flow into large conduits down-glacier, agreeing with most theoretical models.

Roberts et al (2001) describe the flow of water during the jökulhlaups from Skeiðárarjökull in 1996 and Sólheimajökull in 1999. In both of these floods water left the glacier from supraglacial fractures as well as from ice-marginal outlets. They suggest that although initial drainage from Skeiðárarjökull was from a pre-existing discrete conduit outlet at the glacier snout, as the discharge of the jökulhlaup increased the conduit was no-longer able to contain the water and pressure increase forced water to be spread across the glacier bed and upwards through englacial drainage routes into moulins and crevasses. Additionally they suggest that during periods when the drainage system was particularly poorly adjusted to the increased water pressure the distributed drainage would have locally formed a temporary linked cavity network allowing ice overburden (and in places the tensional shear strength of the ice) to be overcome causing fracturing of the overlying ice and supraglacial drainage. This type of routing is particularly likely to occur in a volcanic event since meltwater production continues throughout the duration of the flood.

Jökulhlaup termination occurs as either the lake drains, the ice dam collapses or the conduits close through ice deformation or freezing of water on to the conduit walls. Nye and Clarke's models predict termination of the jökulhlaup later than tends to occur in reality. Grímsvötn floods tend to end when the lake is still 100m deep. Hooke (1984, 1989) discusses water flow through open conduits (at atmospheric pressure) and variations in conduit shape. Hooke's broad, low conduits have closure rates that are much higher than 'R' conduits and thus may be able to help explain 'early' termination of floods.

BOX 1.3.2: Röthlisberger's theory of conduit flow (1972)

Tunnel size is controlled by two main factors, r and m, that reflect the differences between ice overburden pressure, water pressure in the conduit and the ability of flowing water to melt the ice walls at the pressure melting point:

1. r = Closure of the conduit by ice deformation, due to the pressure difference between ice overburden pressure and water pressure within the conduit. Frazil ice growth on the tunnel walls also enhances tunnel closure with loss of heat from the water.

2. m = Opening of the tunnel by melting of the conduit walls, depending on the rate of conversion of potential energy to frictional heat to melt the ice walls.

A constant sized conduit, as defined by Röthlisberger (1972), would exist when the closure of the tunnel was balanced by tunnel opening (Figure A):

When r = m.

FIGURE A: ICE DEFORMATION VS. MELT IN A CONDUIT (*Röthlisberger and Lang 1987; 237)*

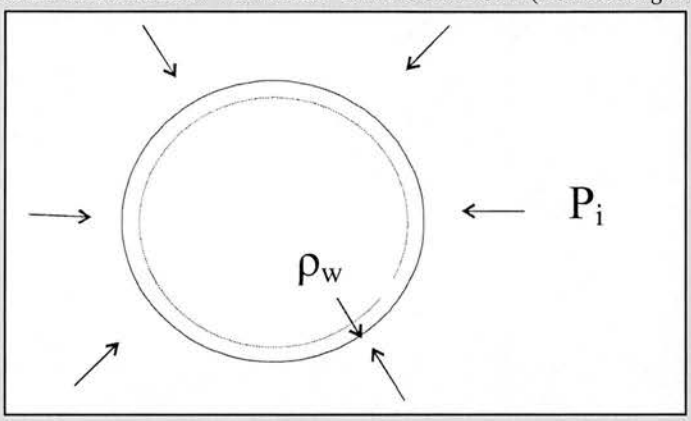

Thus conduits will expand or contract based on the relationship between r and m. Shreve (1972) and Röthlisberger (1972) both state that for two such passages of unequal size, the larger passage will be enlarged at the expense of the small tunnel, thus forming an upward branching arborescent network of passages. This is true for both a tiny vein system and a large conduit network, thus indicating the potential for a whole discrete drainage system to exist with increasingly larger but fewer conduits with proximity the glacier bed and margin.

At the glacier bed conduits were assumed to flow in tunnels with a semicircular cross-section over a perfectly smooth bed (Figure B).

FIGURE B: SEMICIRCULAR SUBGLACIAL RÖTHLISBERGER TUNNEL

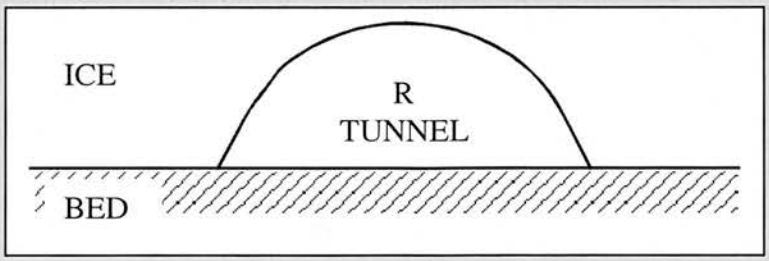

These subglacial tunnels have become known as Röthlisberger or 'R' channels, and are incised upwards into the overlying ice. Abundant field evidence exists for the existence of subglacial tunnels 'carved' into ice. However, the exact shape is known to vary from the theoretical semicircular cross-section (Hooke 1989), as will be considered in discussion of non-steady state flow and the maintenance of flow to the glacier margin.

Proglacial flow: hydrographs and rheology

The impact of a jökulhlaup on the geomorphology and particularly on the sediments of an area is strongly related to the nature of the flow (Maizels 1991, Maizels and Russell 1992, Bennett and Glasser 1996, Russell and Marren 1999). Two key variables are the nature of the hydrograph (progression of discharge over the duration of a flood) and debris concentration in the flow. Additionally, jökulhlaups have an impact on parts of the landscape which are normally relatively free of meltwater flow, since glacier routing can force jökulhlaups to be emitted from the glacier several kilometres from the glacier snout, supraglacially and marginally, as well as into the immediate glacier foreland. Thus, there are three important aspects of jökulhlaup flow beyond the ice margin; hydrograph characteristics, rheology of the flow and route taken. These have implications for the study of palaeo-jökulhlaups since these characteristics determine the nature of their geomorphic and sedimentary legacy.

Discharge and Hydrographs

Discharge varies depending on the nature of flow through the glacial system and on generation process. The largest discharges tend to be associated with volcanic eruptions, although the duration of these floods is often considerably more brief than large-scale lake-emptying floods.

Different generation mechanisms also result in different jökulhlaup hydrographs (Figure 1.3.3). Outburst from glacier-dammed lakes are characterised by an approximately exponential rising limb and a more rapid decline, indicating subglacial drainage through gradually expanding tunnels, closed off by dam collapse or closure of tunnels through ice deformation. Costa (1988) notes a similar hydrograph for drainage of an ice-dammed lake through dam overflow on Baffin Island in 1967. Hydrographs determined for jökulhlaups from Grímsvötn have been recorded (and estimated) since the 1930s and show this general pattern, with larger floods having a shorter duration. Maizels and Russell (1992) note the form of a hydrograph from the drainage of an ice-dammed lake in west Greenland, with this steep rise to peak discharge and more rapid reduction in discharge on the falling limb. Hydrographs from volcanically triggered jökulhlaups tend to be almost a mirror image of this pattern with a rapid rise to peak discharge, followed by a more gradual falloff (Figure 1.3.4).

The shapes of these hydrographs are probably best explained in terms of adjustment of the glacial drainage system to the rate and scale of heightened meltwater input. Ice-dammed lake drainage tends to involve smaller volumes of water than other types of jökulhlaup and normally drains through subglacial tunnels, which gradually expand to meet the drainage requirements of the exiting lake water. This causes a gradual but broadly exponential rise in discharge to a peak. A rapidly decreasing falling limb reflects the emptying of the lake or lowering of the ice dam which very quickly cuts off the supply of water. On the other hand, volcanic and geothermally induced floods tend to involve

larger volumes of water and may rapidly produce more and more water for much of the duration of the flood. In the case of subglacial eruptions the heat from the eruption pile tends to continue to melt glacial ice even after the termination of the eruption. Normal glacial drainage often cannot adapt quickly enough to deal with this vast influx of water. This may force water into supraglacial routes or cause sheet flooding, and thus localised flotation of the ice. Both of these allow a rapid release of water leading to a dramatically rising discharge to a peak early in the flood. Gradually the glacial drainage system will adapt to water input but rapid tunnel closure will be avoided by continued production of meltwater from the eruption site.

Additional to these basic patterns there may be halts or sudden peaks in discharge during the flood. These represent either lulls in meltwater production (in the case of a volcanic jökulhlaup, or more likely, temporary damming within the glacial drainage system caused by blockages of tunnels or the inability of the system to meet the discharge requirements of the released water. Roberts et al (2000, 2001) discuss englacial fracturing and resultant supraglacial routing caused by high water pressure when large volumes of floodwater cannot be transported by the normal glacial drainage system. It has been speculated that in very large floods the vast discharges of water themselves can temporarily dam the floodwaters upstream of a constriction in the proglacial flood path. This is hydraulic damming and may have occurred during the Missoula Floods.

Flow rheology

Jökulhlaup flows can be characterised by different mixtures of water and sediment and resultant differences in flow behaviour, termed rheology (Figure 1.3.4). Flow types range from water-dominated 'water floods' through 'hyper-concentrated' flows to 'debris' flows. Jökulhlaups can be composed of greater than 80% solid material (Jonsson 1982) or be mainly fluidal flows with high water contents (Figure 1.3.5). Variations in flow type result in varying flow behaviour and resultant differential erosion, deposition and sediment types. Different flows caused by different triggering mechanism can have different rheological characteristics. Volcanically triggered floods tend to have higher sediment concentrations. Ice-dammed lake drainage in areas with little unconsolidated sediment tends to produce more water-dominated flows.

Scott (1988, 1989) defined flows as either 'cohesive' or 'non-cohesive' to avoid genetic terminology. Cohesive flows have greater clay content than non-cohesive flows. Cohesive debris flows at Mount Rainier, Washington form when debris avalanches originate from water-rich, hydrothermally altered parts of the volcano. They contain relatively large amounts of clay derived from chemically altered rocks and are thus cohesive. Mount Rainier's non-cohesive debris flows are triggered whenever water mixes with loose rock debris, such as the mixing of pyroclastic flows or pyroclastic surges with snow or ice; small debris avalanches; extremely heavy rain; or rapid release of water from glaciers (Hoblitt, et.al., 1995). These classifications have helped workers to identify genesis and flow processes of

ancient sedimentary deposits, as well as allowing the recognition of transformations in flow processes and thus correlations to be made between non-similar deposits that are stratigraphically coincident (e.g. Palmer et al 1991 and Pringle and Palmer 1992).

However, the nature of the flood route can determine flow characteristics. A single flow event can change nature as it flows downstream either by entraining more sediment (bulking) or by incorporating more water (fluidisation). Downstream transition of flows occurs when sediment is entrained or deposited resulting in bulking or fluidisation of the flow, with distance from the source. Scott (1988) described lahar-runout flows, which result from increasing fluidisation of a lahar downvalley. Similarly, more watery flows following the main hyperconcentrated flow surge of a jökulhlaup have been observed in sediments by Maizels (1991, 1993) and Harrison and Fritz (1982). Periodic 'intersurge' flows may also occur between more sediment-dominant pulses during one flood event (Maizels 1997). There is strong evidence for transition of flow types within one jökulhlaup event, the main sediment-laden stage which is recorded in the sedimentary record to the greatest extent, as well as initial and final stages of much more fluid-dominated flows with large amounts of water. This is certainly the case for recorded and observed volcanically-generated jökulhlaups. However, sedimentary evidence compiled by Maizels (1991) suggests that lake outburst floods (subglacial and marginal) tend to be predominantly water floods, with no major sediment-carrying stage.

Processes of erosion and deposition

The processes that operate during a jökulhlaup to erode both bedrock and unconsolidated material such as moraine or sandur surfaces are the same as those that operate under normal flow. However, the relative importance of their action may be different and their effectiveness increased. In particular, sandur surfaces may remain comparatively stable during 'normal' flow regimes only changing channel patterns significantly at high flood levels when bars and large areas of the floodplain may be inundated by powerful flows.

Processes of abrasion (corrasion), cavitation, fluid stressing (quarrying) and particle entrainment conduct mechanical erosion. Drewry (1986; 63-72) provides a mathematical discussion of abrasion and cavitation by glacial meltwater while Morisawa (1985; 37-70) gives a very clear, comprehensive review of particle entrainment and mechanical fluvial erosion. Additional to these processes in jökulhlaup flows is the erosive action of icebergs. It should be noted that these processes are likely to act together rather than separately.

Abrasive wear is the breakage of rock due to grinding and impact of transported particles within a flow, either in suspension or as bedload. Engineers studying damage to pipelines by sediment-laden flows have carried out much of the research on fluvial abrasion. Small flakes of rock are initially

broken off the bedrock and the resultant pit or groove may then be enlarged through further clast-rock collisions or through the grinding action of particles carried by vortices and eddies in the flow, set up by the initial indentation. Abrasion is controlled by the number of bed / particle collisions and the characteristics of the clasts and bed and is thus most effective in turbulent, rapid flows with <20% sediment concentration by weight. In particular channels composed of soft or unconsolidated rocks will be effectively eroded. Some jökulhlaups are characterised by high sediment concentrations and the associated dampening of turbulence may reduce the effectiveness of abrasion. Very large-scale floods such as occurred from Lakes Missoula and Bonneville in Washington and Idaho respectively, are likely to have resulted in a degree of abrasional wear although Baker (1973) notes that the very deep flows may have dampened turbulence and reduced the effectiveness of abrasion.

Cavitation is associated with the pressure fluctuations generated by high velocity, turbulent flow over rough beds. Localised low-pressure areas may allow water pressure to reach 'vapour' pressure forming gas bubbles. These bubbles may be transported by the flow into regions of slighter higher pressure and thus collapse. When this bubble collapse occurs in contact with the bed localised high impact forces will be produced by the intense pressure and shock waves, against the rock (Barnes 1956, Drewry 1986). This can result in failure of the rock through 'fatigue wear', causing pitting and etching, well-known problems in hydraulic engineering which can cause severe damage to pipeline materials. Cavitation is however, a somewhat controversial concept and its role in normal fluvial and jökulhlaup erosion is questioned. In general flow, Benn and Evans (1998; 124) note that it is unlikely to occur alone, due to high velocities required which are often coupled with suspended sediment suitable for corrasive action, thus making the identification of cavitation in action somewhat difficult. Baker (1973) also doubts its relevance to the deep, swift flows of the Channelled Scablands, due to the dampening of turbulence. However, in a recent review of river incision into bedrock, Whipple et al (2000) state that *'cavitation is more likely to occur in natural systems than previously argued'.* This statement is based on the observation of the natural aeration of turbulent waters in open channel flow and the concentration of fine sediment particles allowing the possibility of bubble nucleation, which they suggest enhances the likelihood of cavitation. Despite this, they note that even though cavitation is plausible, there is *'no direct field evidence'* of cavitation damage. They suggest however, that cavitation is critical in flute and pothole erosion in association with abrasion, which may be responsible for eradication of characteristic cavitation pitting, found in damaged engineering structures. Thus, cavitation is believed to be likely in high velocity, turbulent flows over rough beds, but unlikely if sediment concentration is too high (>20%) or flows are very deep, as with abrasive wear.

'Fluid stressing' is caused by the direct hydraulic action of water on the bed, causing mechanical breakage of bedrock or moulding of unconsolidated beds into ridges *'from which shreds and large masses of mud can be torn'* (Allen 1982 in Benn and Evans 1998; 124). In bedrock channels this process is often called quarrying although in glaciological literature this term may be avoided to limit

confusion with glacial erosion processes. Hydraulic lift and drag on loose plucked pieces of rock will 'quarry' bedrock channels. The action of vortices (or 'kolks' Baker 1973) in the flow can enhance this hydraulic action. Baker (1973) and Baker et al (1987) considered the action of vortices and flow separation to be the principal processes involved in the erosion of the Channelled Scablands (Figure 1.3.6).

Particle entrainment applies to erosion of unconsolidated deposits such as sandur surfaces and morainal material, and takes place according to a range of hydraulic principles discussed in detail by Morisawa (1985). The most important concept is that particle motion will only occur after a certain threshold velocity has been met, 'the threshold of particle motion'. Once the drag forces exceed the resisting forces, holding the clast in place, the particle will be entrained by the flow. Generally, drag forces increase with particle surface area while resisting forces increase with particle mass. This basic pattern is complicated by enhanced drag forces due to turbulent flow and enhanced resistance due to packing of particles or bed armouring, as well as the flow dynamics of different particle shapes which may enhance or reduce drag forces depending on the degree of streamlining.

The main distinctions between depositional flood features, other than variations in scale, is that there are features associated with water / sediment interaction and features associated with ice block deposition and meltout. Additional to these categories are features associated with flood deposition into a proglacial lake and also subglacial deposition by jökulhlaup flows.

Deposition processes also relate to flow rheology. In water-dominated flows deposition occurs as flow competence decreases and clasts can no longer be rolled or carried in suspension by the floodwaters. However, in more sediment-laden flows clasts can float in the slurry and may be supported by other particles in the flow rather than by the action of the flowing water. This means sediment-laden flows can support larger clasts than similarly sized water floods.

Jökulhlaup landforms

Jökulhlaup flows have the potential to be highly erosive, deposit large amounts of sediment and extensively rework or mould pre-existing deposits. However, flow factors such as discharge and sediment load characteristics and routeway factors such as topography and geology will influence the geomorphic impact of any single flood event. Erosional and depositional features characteristic of jökulhlaup flows and the factors relevant to their formation will now be discussed.

Erosional landforms

The highly erosive potential of jökulhlaup flows is famously illustrated in the enormous channels and *'river bottom topography magnified to the proportion of river-valley topography'* (Bretz 1932; 26-28)

of the Channelled Scablands, Washington State, U.S.A. (e.g. Baker 1973). During deglaciation of the late Pleistocene ice sheet, Glacial Lake Missoula ponded up to around 2500km^3 of water, the drainage of which released up to 70 flows, some as large as 2184 km^3 (Benn and Evans 1998). A vast area of the northern Columbia plateau was inundated, and the flood flowed into the Columbia River, incising into extensive basalt lava flows and loess deposits.

A progression of forms caused by vortex action was envisaged by Baker et al (1987) and has been backed up by experiments; initial incision down to the underlying bedrock, followed by 'plucking' of the well-jointed basalt by 'kolks' to form longitudinal grooves and potholes, pothole enlargement and coalescence to bute and basin topography and final inner channel formation and cataract recession (Figure 1.3.7). This incorporates many forms, and it seems likely that other processes as well as fluid stressing and kolk action played a role in the overall Channelled Scabland Formation. However, Baker et al's (1987) model does serve to emphasize the potential power of vortices and catastrophic flood flows.

While representing the potential extremes of terrestrial jökulhlaup erosion, the applicability of such features to modern day analogues has been questioned, certainly without extreme scaling down to such an extent that comparisons may be unreliable (Russell and Marren 1998). However, various workers have used the channelled scablands as an analogue for similar Martian landscapes, while noting the possibility that similarity of form does not necessarily imply similarity of origin (Rossbacher and Rhodes 1987). This has lead to interesting discussions of possible fluvial action on Mars and the impact of liquid methane and nitrogen elsewhere in the solar system.

Longitudinal grooves, potholes and small abandoned cataracts can all be found on smaller scales, along with gorges formed by jökulhlaups. During the flood from the 1967-69 eruption of Deception Island, Antarctica, a steep gully was eroded into unconsolidated volcanic rock (Major and Newhall 1989). A similar origin has been proposed for deep canyons along Jökulsá á Fjöllum, to the north of Vatnajökull (Björnsson 1992).

Potholes are found on a great range of scales from large pools below dry cataracts to centimetre scale erosion marks on bedrock surfaces. Their formation has been associated with the grinding, abrasive action of loose clasts which are often found in their bases. However, small-scale potholes and erosion marks are often related to cavitation. Some small-scale erosion features, described as crescentic cavitation marks by Maizels and Russell (1992) appear similar to so-called glacial 'p-forms'. Hjolstrom (1935) carried out experiments, which found that turbulent flow of water around a bolt resulted in cavitation erosion on the attached metal plate. Similarly, Kor et al (1991) and Shaw (1988, 1994) suggest that glacial p-forms are associated with fluvial vortex action and thus the similarity of form between erosion marks from jökulhlaup flows and glacial processes may reflect similar

processes of formation. This makes genetic interpretation of small-scale erosion marks difficult unless accompanied by other evidence of either jökulhlaup or glacial action.

Traditionally striations on bedrock are also interpreted as indicators of glacial abrasion and ice flow. However, McCarroll et al (1989) studied well-developed 'striations' on rock surfaces in front of Mjølkedalsbreen, Jotunheimen, southern Norway, in an area known to have been subject to catastrophic subglacial discharge of a glacier-dammed lake. Some of these striations or scratches found in the flood path were characterised by crosscutting relationships and low length : width ratios, 'commonly tapering towards the end' (p.195). This they interpret as implying a *'striking blow'*, by saltating debris transported by subglacial jökulhlaup flow. Maizels and Russell (1992) refer to fluted forms or scratches accompanied by cavitation marks and potholes formed by short-lived and sediment-laden pressurised jökulhlaup flow in subglacial tunnels.

While there has been much focus on erosion of bedrock channels, stemming from the Channelled Scabland research, confined jökulhlaup flow erodes river alluvium, valley-side colluvial fans (Clague and Evans 1997) and incises into previous jokulahlaup deposits (Maizels 1991) (Figure 1.3.8). This erosion of routeway material increases the debris load of the flow contributing to transitions in flow type downstream. Flows can significantly alter previous channel patterns and bar morphology. Glacier-outburst flooding from Ape Lake in British Columbia caused widening of the channel zone by up to 200 metres and toe slope failure of valley walls (Deslodges and Church 1992). Streamlined residual hills and bar forms have been noted across the jökulhlaup-dominated sandur plains along Iceland's south coast (Maizels 1989, 1992, Maizels and Russell 1992; Figure 1.3.9) and in the Channelled Scablands (Figure 1.3.10).

Ice-blocks can produce similar erosion features in unconsolidated material to those formed by clast-bed interaction in bedrock channels. While being transported by the flow ice blocks abrade or scour the underlying topography. This action leaves a trail of iceberg tracks, scour (striation) marks and crater features, somewhat akin to the marks left by icebergs on the floors of former glacial lakes.

Depositonal landforms

As with erosional features, depositional landforms often resemble normal fluvial features – bedforms and bars for example. Others, however, distinctly reflect jökulhlaup activity, particularly when combined with studies of the deposits themselves. Depositional landforms vary depending upon the routeway topography and nature and composition of the flow.

The largest depositional feature produced by a jökulhlaup flow is the sandur or outwash plain, such as Mýrdalssandur and parts of Sólheimasandur. Outwash plains may be characterised by normal seasonal runoff regimes. However, in areas of jökulhlaup drainage, even infrequent flooding can dominate the

patterns of sedimentation and overall morphology of the sandur (Maizels 1989, 1991; Figure 1.3.11). If unconfined by valley sides, sandurs tend to be relatively uniform features composed of large coalescing fans, superimposed by erosional channels, bars and ripple forms. Valley-confined sandur may also act as major stores for sediment carried by jökulhlaups (Russell and Marren 1999) but are more likely to be completely inundated or subject to backwater ponding due to flow constriction.

Local and within-channel features of a jökulhlaup sandur environment include streamlined bars, dunes, 'washed' sandur and boulder lags, pitted or kettled outwash, ice-block obstacle marks and lobate or hummocky fans. Boulder deposits, bar forms, lags and erratics are also characteristic of some jökulhlaup flows and reflect high sediment concentrations and sediment transport and subsequent depositon related to peak discharges. The location of these features is influenced strongly by the topography of the flood routeway, with differences distinguishable between unconfined flows (sandur plains), confined proglacial bedrock channels and tributaries (bars, boulder deposits and slackwater deposits), infilled rock basins (valley sandurs) and ice-marginal lakes (deltas and strandlines) (Russell 1991, Maizels and Russell 1992).

Bar formation is reviewed in detail by Maizels (1997), who identifies three main types of bar associated with jökulhlaup deposition.; expansion bars, pendant bars and eddy bars (Figure 1.3.12). Expansion bars, as the name suggests, are formed as flows spread out and decelerate, particularly at the junctions of tributary channels. Downstream accumulation of a large bar may occur associated with the main flood wave, followed by waning stage winnowing and armouring of the bar surface. Pendant bars form in the lee of an obstacle due to local flow deceleration. Large pendant bars, up to 3.2km in length formed in the channeled scablands. Eddy bars are generated where backwater eddies form as main and tributary flows interact, depositing sediments from combined flows. Streamlined boulder bars are also frequently described and are associated with erosion of previously deposited jökulhlaup deposits during waning stage flows

Bedforms such as dunes and ripples formed in jökulhlaup channels resemble large-scale versions of those formed in normal river channels. The terms dune and ripple normally refer to undulating sedimentary structures produced by current or wave action, with dunes being large (>4cm) than ripples. In relation to jökulhlaup deposition solitary undulations tend to be termed dunes and suites of undulations are ripples or megaripples. Scott (1988) refers to whaleback dunes indicating their streamlined form. Gravel dunes and large-scale ripples have been described in relation to the Channelled Scablands (Baker et al 1997) and at Sólheimasandur in Iceland (Dugmore 1987, Maizels 1991; Figure 1.3.13).

Jökulhlaup flows frequently carry large quantities of ice on to the sandur plain and in heavily sediment-dominated flows ice blocks often appear to 'ride' or 'float' on the surface of the flow. Ice blocks may originate from the glacier snout as well as from ice-cored moraines (Olszewski and

Weckwerth 2000). Meltout of the transported ice blocks or division of flow around ice blocks can result in a variety of landforms. Hummocky topography, pitted or kettled outwash and ice-block obstacle marks are all related features, influenced by the density and extent of ice block transport.

Kettle features form when ice blocks remain submerged in the flow once deposited, whereas ice block scour marks, produced through both erosive and depositional processes, develop if the ice block remains on the surface of the deposit or is exhumed by erosive waning flows. Russell and Knudsen (1999) observed that larger ice blocks transported by the 1996 Vatnajökull flood were partly or completely exhumed by waning stage flows. Smaller blocks up to 3m in height remained buried. Maizels (1992) has described and modelled a variety of 'boulder ring structures' or 'kettle' formations (Figure 1.3.14). The resultant morphology of the ring structure depends on the concentration of debris within the ice block and on the depth that the block is submerged in the surrounding flow deposits – a more complex mode of formation than meltout kettles (Olszewski and Weckwerth 2000). Boulder-rich ring structures up to 4m high and 40m in diameter were observed on Mýrdalssandur as a result of the large-scale floods from Katla in 1918 (Maizels 1992, Olszewski and Weckwerth 2000, Wisniewski et al. 2000). Distribution of these features across the sandur showed a marked concentration upstream and in the central area of the sandur reflected the main areas of ice block transport along the main flood path, channel margins and highest bar surfaces. Olszewski and Weckwerth 2000 have identified a more complex form of kettle from Mýrdalssandur, not described by Maizels (1992), which they state was formed during the declining phase of the Katla 1918 flood. This form is described as a rimmed-normal kettle where the rim is not visible on the surface but occurs approximately 1m below the surface.

Ice scour marks form where ice blocks divert the flow of the flood, causing streamlined erosion or obstacle marks. Accumulation of coarser material occurs in a ridge formation downstream of the ice block obstacle (obstacle shadow). Similar scour and deposition patterns develop around large boulders stranded on the sandur surface. The largest ice blocks deposited in 1996 from Vatnajökull formed elongated clusters on the outwash fan in front of the main glacial outlet (Russell and Knudsen 1999).

Hummocky topography is characteristic of this combination of scour marks, kettled surfaces and channel patterns. A jökulhlaup deposit at Fort Augustus, Scotland, is described by Russell and Marren (1998) as having 'hummock and hollow' terrain, with decreasing scale of features downstream, which fits well with the contemporary evidence from the 1996 Vatnajökull flood. Recent work by Fay (2000) suggests that widespread hummocky or 'kettled' topography that has often been interpreted as ice stagnation / ice block meltout features may have been misinterpreted and actually represent *'dynamic'* jökulhlaup activity. Certainly widespread kettled topography has been identified in association with deglaciation sequences and it is possible that jökulhlaup scours and kettles have been grouped together with meltout features in identification. Cutler et al (2000) have found evidence in Wisconsin from a group of tunnel valleys and outwash fans that indicates a period of catastrophic flooding shortly prior

to deglaciation associated with release of subglacial lakes as frozen ice margins melt and provide free drainage. This would suggest that jökulhlaup features and deglaciation topography may be closely related in space and thus classical 'kettled' ice stagnation topography may require re-evaluation. Fay (2000) states that the distribution of kettles can indicate the mode of formation, either jökulhlaup / meltout. Jökulhlaup kettles tend to form on bar surfaces, as clusters and decrease in size with distance from the glacier, whereas no-flood kettles will be located more randomly across the sandur surface. Flood kettles may be more randomly located in backwater areas but will also be characterised by scour forms due to flow separation.

It is clear that a great majority of the landforms associated with jökulhlaup flows are very similar to those formed in a normal braided river environment. It may thus be difficult to differentiate jökulhlaup landforms and thus a jökulhlaup route from 'normal' braided river morphology, based solely on geomorphological criteria. However, as Russell and Marren (1999) note, and is clear from this discussion, features such as ice block obstacle marks, heavily kettled surfaces and boulder-ring structures, all associated with ice block deposition, are indicative of jökulhlaup flow. Similarly widespread erosional scouring of surfaces and anomalously large features, particularly channels are also believed to be diagnostic features. Thus, very extensive or heavily ice-laden flows are more likely to have a persistent geomorphological impact upon an area and thus be identifiable. For clear recognition of jökulhlaup routes therefore, geomorphology alone cannot be sufficient as a diagnostic tool. Consequently it is necessary to combine geomorphological evidence with that gained from analysis of sediments.

Jökulhlaup Sedimentology

Clearly the characteristics of the sediments deposited by jökulhlaups are very much dependent on the flow type and the topography. Most work on jökulhlaup sedimentology in Iceland has been carried out on the southern sandur plains (e.g. Maizels 1989, 1991, 1992, 1993, Russell and Knudsen 1999, Russell et al 2001). Much more extensive research has been carried out on lahar and lahar-runout deposits, particularly in North America (e.g. Harrison and Fritz 1982, Scott 1988, Costa 1988).

Maizels has produced lithofacies models of jökulhlaup sandur formation, comparing them with sandur facies controlled by 'normal' braiding processes (Figure 1.3.15). Type I sandur is composed of repeated cycles of thin, upward-fining gravel, sands and silts from 'normal' ablation flow. Type II sandur, formed by ice-dammed lake drainage, up to ten metres more in depth, is composed of coarsening-upwards, clast-supported cobble gravels, overlain by a fining-upward unit of fine gravels, sands and silts.

Catastrophic volcanic type III sandur up to 8 metres or more in depth, are composed of four units (Figure 1.3.16). The basal unit is crudely bedded, and overlain by the main flow unit of structureless

pumice granules, and capped by trough cross-bedded and horizontally bedded granules. Above this, a lag deposit of boulders and ice-blocks (Figure 1.3.5a) may exist for up to a year (Figure 1.3.17). Such deposits are found in river and gravel-pit sections across Solheimasandur. Maizels' (1991) sandur type III has many similarities with 'Mount St. Helens-type flows', described by Harrison and Fritz (1982), with three main units; a basal massive, graded unit, an overlying finer grained, stratified unit and an upper deposit predominantly composed of matrix-supported very large clasts and log debris. Scott (1988) has also described waning stage flows, with characteristic bedding from Mount St. Helens, particularly showing convoluted laminations near the surface. Other 'lahar' deposits described from activity at Nevado del Ruiz, Columbia, in 1985 (Lowe et al. 1986, Naranjo et al 1986) also involve hyperconcentrated flow deposits with massive coarse-grained thick sequences in proximal zones. These flows travelled a long distance in confined channels before spreading out and depositing their sediment, and thus are dominated by sediment derived from the local valleys rather than much primary eruptive material.

The model of Maizels (1991, 1993) is particularly associated with sandur facies development. However, more complex and more variable deposits seem to be left along channelled jökulhlaup routes and in backwater areas. This explains some of the differences noted by Scott and other workers. In channels, deposits may be less identifiable since they may consist of thin washes of material. However, in areas of the channel that might experience 'backwater effects' there may be two sediment transport peaks throughout one event (Russell 1991).

Slackwater or backwater deposits form in areas of diminished flow power, such as in tributary channels with a high angle to the main routeway, and act as sediment traps. Distinctive sediment assemblages can be formed and in confined areas of a jökulhlaup routeway they may be all that remains in the long term to indicate the occurrence of a jökulhlaup event. Where channel geometry has been established, slackwater deposits have been used in palaeohydrological studies to determine palaeodischarge and hydraulic gradient. Well-sorted sands with occasional gravel clasts, climbing ripple sequences and horizontal laminations are common (Russell and Knudsen 1999). Pulses of flow either during one event or from repeated flood events may form slackwater rhythmites or varves, which because of uncertainty about frequency of their formation are sometimes difficult to interpret (Maizels 1997).

What is most noticeable about comparisons of research in Icelandic sandur environments with studies carried out in more topographically varied environments is that channelling of flows produces more varied deposits, in the sense of predictablitity of facies sequences as well as in the material which makes up the deposit. Sandur deposits are often similar to the models proposed by Maizels and pumaceous granules, sands and silts dominate volcanigenic jökulhlaup deposits (and even ice-dammed lake drainage event, in areas of ample volcaniclastic material). In areas where flows have been channelled for substantial lengths of their flow they have entrained material from their flow path

and tend to form deposits which are rich in both volcaniclastic material and local country rock lithics. As noted in the discussion of flow types, valley confinement can also allow flow transformation to occur which produces a wide range of flow types and thus sediment types. Costa (1988) has summarised the key sedimentary characteristics of water floods, hyperconcentrated flow and debris flows.

Which of these models best fits the deposition from a palaeo-jökulhlaup will depend on the generation mechanisms, sediment sources and flow path. The critical difference appears to be whether the flow is confined within a valley or is emitted directly from the ice onto an open sandur plain. Valley-confined jökulhlaup flows are likely to resemble the Maizels and Russell models within the immediate glacial foreland. However, as the flow travels downstream it is likely to entrain more debris and/or more water and transform to produce deposits that most resemble those described by Scott.

Further complexities may be encountered caused by differential patterns of erosion and deposition. Russell (1991) states that in sandur and delta environments, deposits represent multiple ice-dammed jökulhlaup events, whereas bedrock confined channels and spillways only record low stage deposits from the last event and the high stage deposits of the first jökulhlaup, due to erosional processes. These unconformities will mark erosion of flows into underlying deposits and the time gap in the sedimentary record may be difficult to quantify. Pringle and Scott (2002) discuss the vulnerability of volcanigenic deposits to erosion and burial by subsequent flows and other geological processes, creating an incomplete record of activity at many volcanoes. In particular they suggest that small lahars may not be preserved in the geological record despite probably being more frequent events. These problems of censoring of the sedimentary record by later events applies to most aspects of sedimentology and must be born in mind when using sedimentary records to reconstruct patterns of past events.

Since jökulhlaup and lahar events produce this wide range of deposits it may be very difficult to differentiate jökulhlaup deposits from other diamicts, formed by glacial, mass movement or localised small-scale flood events. Russell and Marren (1999), encountering this problem suggest that extensive deposition as well as relationship to geomorphic evidence must be recorded to positively identify palaeo-jokulhaups.

Chapter 2: Katla and Mýrdalsjökull: Interaction and questions

This chapter focuses on the issues associated with the interaction of Katla and Mýrdalsjökull and aims to pinpoint gaps in the present knowledge about jökulhlaup activity and glacier fluctuations in the region. Questions arising from this discussion are used to form specific objectives for this thesis.

2.1 Katla and Mýrdalsjökull

Katla lies in the eastern volcanic zone and is the largest and most active volcanic system in the area, one of the most active volcanoes in Iceland. The Katla Volcanic System (KVS) consists of a central 70km3 ice-filled caldera and the NE-SW trending fissure swarm of Eldgjá (Figure 2.1). The Holocene eruptive history of the Katla volcanic system began with the major explosive Sólheimar eruption around 12,000 BP that generated the Skógar /Vedde ash found in Iceland and Scandinavia and formed a significant part of the North Atlantic Ash Zone One (NAAZO), (Lacasse et al 1995). Since this major eruption the KVS has been characterised by explosive hydromagmatic basaltic activity from the central caldera, explosive dacitic activity probably from vents within the central caldera and effusive basaltic activity from flank vents and the Eldgjá fissure swarm (Larsen 2000). Explosive basaltic activity is most common and is associated with tephra production and catastrophic laharic floods or jökulhlaups. The exact number of Holocene basaltic Katla eruptions is not know although it is believed to be of the order of 150 or more (Larsen et al 1999). About 17 eruptions are known to have occurred in the Katla system in the last 1000 years, the last big eruption being in 1918. Recently at least 12 silicic tephra layers have been identified from Katla, dating from c. 6600 – c. 1675 BP (SILK tephras, Larsen et al 1999). It is not known whether silicic eruptions of Katla result in large-scale floods. However, silicic ocean-transported pumice has been found along the coasts of the North Atlantic, very similar in composition to the SILK tephras (Newton and Dugmore 1995).

Mýrdalsjökull is the most southerly ice cap in Iceland, covering almost 600km^2 (Figure 2.2). It lies on top of, and within the Katla caldera, where the ice is hundreds of metres thick. Three main outlet glaciers breach the caldera rim and thus drain ice and water from the central volcanically and geothermally active region, Kötlujökull to the south-east, Sólheimajökull to the south and Entujökull to the west. A large piedmont lobe, Sléttjökull flows to the north into the high interior plateau. The ice cap is asymmetrical in shape, thickest on the southern side and over the central caldera and becoming much thinner and spread out in a lobe to the north (Figure 2.3). Small glaciers flow over the edge of the caldera and terminate as small valley glaciers, some of which are truncated and feed their snouts by avalanching.

Glacier fluctuations

The Holocene glacial records of Mýrdalsjökull outlets have been well studied (Figure 2.4) and two clear patterns of behaviour have been identified:

- Glaciers that have Holocene maximum extent in the Little Ice Age, and
- Glaciers that experience Holocene maximum extent in the neoglacial, prior to the Little Ice Age.

Small outlet glaciers, which do not breach the caldera wall, exhibit the first type of response with no evidence of pre-LIA moraines outside ridges that date from the mid to late 19th Century. Casely (2001) determined that the Goðaland glaciers of Krossárjökull and Tungnakvíslarjökull reached a LIA (and Holocene) maximum extent between 1820 and 1870 AD, dating ridges using both tephrochronology and population lichenometry. He also noted that while both glaciers appear to respond to climatic signals the response times for the two outlets differ. This he attributed to differences in topography and hypsometry.

The eastern outlets, Sandfellsjokull and Oldufellsjokull have similar records with their outermost moraines dated to the late 19th Century by lichenometry (Evans et al 1999). The validity of these dates has been questioned (Kirkbride and Dugmore 2001a, Bradwell 2001). Comparative studies using both lichenometry and tephrochronology suggest that the largest lichen method of lichenometry employed by Evans et al produces dates that are overly young. However, it is certainly clear that although the exact timing of this advance is doubted, these limits mark a Holocene maximum during the LIA rather than earlier in the Neoglacial.

Kruger and Humlum (1981) studied the margins of Sléttjökull, noting three main geomorphological regions; a glaciofluvial area outside the moraine ridges, a marginal moraine complex composed on a number of parallel ridges and between these moraines and the ice front, an area of till with flutes, drumlins, small ridges, basins and meltwater channels. They attributed the main parallel ridges to an advance around 1890.

Sólheimajökull and Kötlujökull both breach the caldera wall and show evidence of Holocene advances which extend beyond the moraines formed during the LIA. Kötlujökull passes through a breach in the Katla caldera to the southeast and flows as a large broad lobe onto the relatively flat plain of Mýrdalssandur. During historic times jökulhlaups have been routed over and beneath Kötlujökull and across the sandur plain. Heim (1983) recorded LIA moraines in the foreland of Kötlujökull, dating to c.1900 AD 1.2 km from the ice front. Until recently, no further evidence had been published for earlier advances, possibly due to the destructive censorship of past jökulhlaups

which have removed or buried any significant relief on the sandur plain. However, a till sheet found above the SILK YN tephra dated to 1676±12BP has been mapped at the margins of the sandur by Schomaker et al (2003). No end moraine has been found but this dated till shows that Kötlujökull extended far across the foreland from the LIA moraine limit between c.1610BP and the late 19th Century, possibly soon after the deposition of SILK YN.

Sólheimajökull in stark contrast has the longest and most complex record of Holocene advances in Iceland. Dugmore (1987, 1989) identified three main glacial stages in the Holocene; the 'Drangagil' stage (7000-4500 BP), the 'Holsargil' stage (>3100 BP) and the 'Ytzagil' (1200 – 1400 BP) stage (Figure 2.5). Historical readvances or stillstands also occurred in the 10th Century, possibly in the 14th Century and c.1700 – 1900 AD (the Little Ice Age) (Dugmore 1987, 1989). This record indicates that in the mid Holocene Sólheimajökull was far more extensive than many other Icelandic glaciers and also than most of the other, small outlets of Mýrdalsjökull.

Dugmore and Sugden (1991) suggest that the apparently anomalous fluctuations of Sólheimajökull are best explained by ice-divide migration. This theory suggests that during the mid Holocene Sólheimajökull drained a larger proportion of the ice cap than it does today, due to changes in the ice cap surface shape over time associated with uneven precipitation patterns over the ice from the maritime location of Mýrdalsjökull (Figure 2.6). However, modelling work by Mackintosh (2000) indicates that the behaviour of Sólheimajökull can be explained entirely by climatic forcing when topography is incorporated in to models of glacial response. Mackintosh sub-divides Icelandic glaciers in to five categories based on their topographic situation, relating this to their response to climatic fluctuations. He suggests that Sólheimajökull has a short response time to climatic change (<50 years) while confined within a valley with no pinning point. Such glaciers, he claims, have a high mass balance sensitivity and hypsometric sensitivity and their valley location is favourable to moraine preservation (at least where jökulhlaups are not highly destructive). The results of Mackintosh's modelling suggest that valley width can influence glacial response, emphasizing the importance of topography. For example, he notes that a topographic threshold occurs at Sólheimajökull where the glacier widens on to the sandur plain at which point glacier response becomes decoupled from climatic change. Other explanation may include the influence of volcanic or geothermal activity within the catchment of Sólheimajökull.

Jökulhlaup record

The jökulhlaup record from the Mýrdalsjökull / Katla area extends as far back as the deglaciation of the area, from when the Younger Dryas ice melted, through the Holocene to the present day. However, the length and level of detail of the record varies for the different outlets. In some cases it is possible to attribute floods to volcanic or lake emptying origins and in other cases the triggers for flooding are unknown. No glacial floods are known to have occurred from any of the small outlets,

with records of flooding restricted to those glaciers which breach the caldera wall, and possibly from Sléttjökull to the north. Records available through historical documents and geomorphological and sedimentological studies suggest that the routing of jökulhlaups from Mýrdalsjökull may have switched between different outlets over time; from Kötlujökull in the south-east most recently, Sólheimajökull in the south in late prehistoric and early historical time and possibly to the west in prehistory (Figure 2.7). The records and evidence from each of these routes will be considered in turn.

Since the late 12th century jökulhlaups have primarily flowed from or over Kötlujökull and across the expansive Mýrdalssandur to the south-east (Larsen 2000) (Figure 2.8). Since the last major eruption and flood in October 1918, which inundated Mýrdalssandur, there have been several small-scale floods. In 1955 and 1956 floods were associated with a possible minor subglacial eruption and drainage of an ice-dammed lake respectively (Rist 1967, Thorarinsson 1957).

Floods during the Holocene and until the 14th Century issued from Sólheimajökull, building up and flowing over the large Skogassandur and Sólheimasandur fans (Dugmore 1987, Dugmore et al 2001). Dugmore (1987) found geomorphological and sedimentological evidence for four floods from Sólheimajökull during prehistory (Figure 2.9); "Layer K" hlaup (3480+60 14C BP) below the SILK UN tephra, "Layer L" hlaup (2260+60 14C BP) between the SILK YN and SILK UN tephras, "Skógasandur" hlaup (1480+75 14C BP, Jonsson 1982) between the Landnám tephra and SILK YN, "Eystriheidi" hlaup between the Landnám layer and the Skógasandur hlaup. A further two floods were identified in the 10th century ("Lodmundar" flood, possibly around 934 AD) and in the 14th Century (c. 1357). Drainage of an ice-dammed lake occurred to the west of Sólheimajökull during the Late Little Ice Age. Maizels and others have studied these jökulhlaup deposits in great detail providing much of the information now known about jökulhlaup sedimentation in Iceland (e.g. Maizels 1993).

A small flood occurred in July 1999 from Sólheimajökull. It is thought that this event may have been related to enhanced geothermal activity and a series of small earthquakes and cauldron formations that developed at the ice surface between July-October 1999. It is possible that the enhanced activity beneath Mýrdalsjökull in the summer of 1999 may be a precursor of an eruption in the Katla system.

The record of activity from the west (and north west) of Mýrdalsjökull extends much farther back into the Holocene and to the time of deglaciation but the causes, extent, timing and impacts of these events is poorly constrained. Lacasse et al (1995, 1996) identified volcaniclastic sediment gravity flows rich in material from the EVZ in cores from the Iceland basin off the south coast, most likely to be jökulhlaup deposits. Similarly, studies of sediments in the Budi moraine complex and a core from Lake Hestavatn in southern Iceland indicate that multiple jökulhlaups issued from the calving tidewater margin of the Younger Dryas glacier on the south coast of Iceland (Geirsdottir et al 2000). These events have been dated using radiocarbon dating to between 10,300 and 9800 14C BP and also around 9000 14C BP. Triggers for these events are postulated to be subglacial volcanic eruptions and

the drainage of ice dammed lakes. Geirsdottir et al relate a high number of jökulhlaup events to possible higher eruption rate of volcanoes associated with glacial unloading during deglaciation. Lakes existed in the Hreppar area to the west of Hekla (Kjartansson 1939, Eiriksdottir 1996), in Ofaerugil near Hekla (Johannesson et al 1995, Geirsdottir et al 1998) and north of Mýrdalsjökull (Kaldal and Vilmundardottir 1989, Vilmundardottir and Kaldal 2001). Drainage of these lakes may be either an alternative explanation for the triggering of these floods events or possibly a dual cause.

Lacustrine deposits found to the north-west of Mýrdalsjökull (Kaldal and Vilmundardottir 1989, Vilmundardottir and Kaldal 2001) are associated with lakes dammed by glacier ice during deglaciation and during the Holocene. These lakes began to form around 9500-9000 years ago. Around 25m of lacustrine sediment are exposed in valleys north-west of Mýrdalsjökull (Figure 2.10A and B). These laminated sediments are related to the past ice marginal lagoons of Launfitarlon, Torfalon, Grashagalon and Emstrurlon (Vilmundardottir and Kaldal 2001. These deposits mainly consist of laminated silt and clay, with interbedded tephra layers. Some gravelly or pebbly beds are found, particularly in the lower inclined foreset beds. The lacustrine sediments are overlain by gravel, soil and tephra layers. Launfitarlon, Torfalon and Grashagalon were fed by meltwater streams which drained the rapidly melting retreating Younger Dryas ice in the region. They were dammed by rock obstacles, which have since been breached at Fljotsgil and Torfahlaup. The drainage of these lakes is not envisaged to have generated any large floods since they became infilled by 6000-5000 years ago. Emstrurlon was the southernmost lake c.25km^2 in size. The lake sediments are dominated by black, basaltic tephra from Katla and also record several jökulhlaup events that entered the lake. The eastern areas of the lake sediments have been covered by a lava flow and jökulhlaups have variously eroded lacustrine layers or buried then in flood deposits. A section exposed near the Markarfljótbru clearly shows some of the Emstrurlon lake sediments and overlying lava and jökulhlaup deposits. A rock threshold that has since been breached and is now Markarfljótsgljufur dammed Emstrurlon.

These jökulhlaups associated with deglaciation and also those in to Emstrurlon are the earliest jökulhlaups known about from Mýrdalsjökull. Their origin and impact downstream into the Markarfljót outside of the lake system is as yet unknown, as is whether or not these lakes themselves drained catastrophically.

Past work in the Markarfljót valley has suggested that at least one flood event has occurred in prehistoric time (Haraldsson 1981, Sigurdsson 1988). However the timing, extent and effects of this / these event(s) have not been securely constrained. Haraldsson (1981:39) suggests that one or more jökulhlaups may have flowed down the Markarfljót, probably associated with a volcano-glacial flood from Entujökull although he states that it is more likely to be related to the drainage of an ice-dammed lake north of this canyon. A date of 1485+65 yr 14C BP on tree remains buried in 1-3 metres of sand south of Fljótshlið (Haraldsson 1981) is discussed in Haraldsson (1993). He suggests that these tree remains were rapidly buried by sand in a flood, possibly caused by a subglacial eruption. Although the

field evidence cannot allow an unambiguous interpretation of the genesis of this flood, Haraldsson (pers. comm. 2002) states that that a 'huge flood' is a likely explanation for the 'sandy, sub-soil sediments in the area' and the buried tree remains. Sigurdsson (1988) notes from geomorphological observations that prehistoric jökulhlaups have flowed to the west of the ice cap down the Markarfljót valley. He refers to a large jökulhlaup in the Markarfljót 1600 years ago that he associates with the erosion of Markarfljótsgljufur and deposition of sedimentary terraces from Einhyrningur to Fauskheiði and in northern Þórsmörk. This jökulhlaup may have drained beneath Entujökull. However, it is possible that a fissure eruption occurred on the flanks of the volcano Katla and meltwater drained from Sléttjökull into the Markarfljót valley (Johannesson et al 1990).

The records of prehistoric floods are summarised in Figure 2.11. It can be noted from this comparison that in the main the known flood events that entered the Emstrur Lake do not seem to show any clear synchrony with the record of Holocene floods from Sólheimajökull. The one possible similarity between the known Markarfljót stratigraphy and the Sólheimajökull record is the timing of the Skógasandur hlaup (1480+75 14C BP) and the proposed flood in the Markarfljót dated from a tree surrounded by sand deposits (1485+65 14C BP). In the early Holocene Geirsdottir et al (2000) suggest that there was a period of jökulhlaup activity around 9000 14C BP which coincides with the approximate age of the oldest flood deposit found in Emstrurlon by Vilmundardottir and Kaldal (2001).

Jökulhlaup routing

It is clear that jökulhlaups associated with volcanic or geothermal activity or drainage of a subglacial lake can flow to the south-east or south from Kötlujökull or Sólheimajökull. Sedimentary evidence, particularly that from Emstrurlon (Vilmundardottir and Kaldal 2001) suggests that the north-west (Sléttjökull and/or Entujökull) could also be a jökulhlaup routeway, however, as yet there is no definitive account of this occurring. To determine if this north-west route is glaciologically viable for jökulhlaup drainage a simplified hydraulic potential map was constructed (Figure 2.12). This is based on the principles of water flow beneath a glacier proposed in the seminal works of Shreve (1972) and Rothlisberger (1972), summarised in boxes 1.3.1 and 1.3.2 respectively.

Subglacial equipotential contours calculated from the present ice surface and subglacial topography show the likely direction of flow of full, pressurised conduits. This simplified map of hydraulic potential suggests that water will flow beneath any of the main outlet glaciers from the main caldera region. No obvious sites for subglacial lakes are clear despite distinct depressions within the subglacial topography, confirming the observations of Björnsson et al (1993). The exact route which water will take is very sensitive to small changes either in the source of water generation or ice surface topography. An eruptions or release of water to the east of the caldera will be most likely to generate a

jökulhlaup beneath Kötlujökull and across Mýrdalssandur. Eruptions to the south are more likely to causes floods to the south and those to the north or north west may flow beneath Entujökull.

Should there be ice divide migration as suggested by Dugmore and Sugden (1991), this pattern of water routing would be likely to change, due to the dominant influence of the ice surface topography on water flow. However, the present pattern of equipotentials effectively allows for past patterns of flood from both Sólheimajökull and Kötlujökull with distinct channels in the contours, assuming different locations of volcanic activity within the caldera. However, if volcanic activity were to remain in the same place ice divide migration would be necessary to explain the series of floods from Sólheimajökull, with a movement towards the NE to allow this to occur.

The accuracy of this map is limited by the accuracy of the basal topography data used, which is less up-to-date than the most recent ice radar survey data (Björnsson et al. 2000). However, the similarity between images of the subglacial topography produced from this new data (Figure 2.13 & 2.14) and the data used are close enough to produce meaningful results. Additionally, the use of Shreve's equation for pressurised flow in a conduit means that this map cannot predict the behaviour of water when it is at atmospheric pressure due to low overburden pressure beneath thin ice as is likely at the margin of the ice cap, nor cannot it illustrate the flow of supraglacial water. Flows under these conditions will follow the dominant subglacial slope or the ice surface slope respectively. However, the behaviour of flows originating in the central caldera is the most relevant query for this paper and since this deals with ice up to 700m thick this problem of modelling the behaviour of water at atmospheric pressure is less relevant. It might be noted however, that if there is any relevant effect this might actually concentrate flow of water in the deepest breaches of the caldera thus reducing flow over the caldera rim and exiting the system through the smaller side glaciers. Ice is likely to be considerably thinner at the lip of the caldera and therefore water flow may be concentrated to either side of the ridge and not directly over the ridge and out of the caldera.

It is possible that water may be routed over the glacier surface, either may flow directly from an eruption site or through hydraulic fracturing of the ice along the routeway, both of which would allow a dominant role for ice surface slope. Studies of a large number of jökulhlaups suggests that surface flow over ice due to an eruption is less common than subglacial drainage (Mayor and Newhall 1989), however, glaciohydraulic fracturing of ice has been observed during two recent glacier bursts in Iceland where subglacial tunnels could not expand in line with increasing discharge, resulting in englacial and supraglacial routing of flood waters. (Roberts et al. 2000).

Future jökulhlaups from Katla/Mýrdalsjökull

It seems likely that future eruptions of Katla will cause flooding from Mýrdalsjökull. Since there is no known stored subglacial water the likelihood of very large subglacial lakes to drain is low. However,

variations in the geothermal heat flux are likely to cause small accumulations of water at the glacier bed, resulting in small floods as have occurred at various intervals since 1918. Drainage of marginal ice-dammed lakes are less likely to happen under present patterns of deglaciation with reduced ice dam thickness' possible (Björnsson 1992), as is believed to be the likely pattern for marginal lake formation and drainage around Iceland. Future volcanic eruptions may be like the most recent basaltic eruptions that have caused known floods. However, they may also be silicic in nature. There have been no known silicic floods but this does no mean that there have been no floods associated with silicic activity.

It is also possible that the location of the eruptive activity may move within the caldera, as is believed to be occurring in the Grímsvötn area, which may cause routing of the flood water beneath different glaciers. Patterns of tephra distribution from the Katla eruptions, both silicic and basaltic, show differing centres of activity which adds weight to the variable volcanic centre theory (Larsen 2000).

The Sólheimajökull 1999 flood, increased seismic activity to the west of the ice cap and persistent sulphurous smells from rivers draining the ice cap have increased concern over activity from Katla and resultant flood hazards. Figure 2.15 shows recent earthquake activity concentrated near the western margins of Katla. An eruption in this location may trigger a flood to the west of the ice cap from Entujökull, or if on the caldera rim, from one of the Þórsmörk glaciers into the Krossa, or southwards beneath Sólheimajökull. Volcanological studies suggest that there may be links between the behaviour of Eyjafjallajökull and Katla, which are linked by the Fimmvorduhal ridge. Eyjafjallajökull has also been exhibiting increased activity, with rises in the elevation of the southern slopes of the mountain, probably associated with rising magma beneath the surface.

2.2 Research questions

There are three key questions:

1. Little is known about the flood history to the west. What, if any, is the history of jökulhlaups to the west of the ice cap?
2. How do floods relate to glacier activity? (extent and ice cap morphology). What is the pattern of glacier activity?
3. Are patterns of jökulhlaups and glacier fluctuations related to patterns of volcanic activity?

Chapter 3: Approach and Methods

This chapter introduces the study area and outlines the methodology used to answer the questions posed in Chapter 2.

3.1 The Markarfljót valley

The Markarfljót valley, located around 100km south east of Reykjavík, extends approximately 30 miles (50 km) inland from the North Atlantic coast of south-central Iceland into the Highlands and upland grazing areas of Emstrur. It is bordered by the ice caps of Mýrdalsjökull to the east, Eyjafjallajökull to the south and Tindfjallajökull to the north Figure 3.1.1. The river Markarfljót drains these ice caps and the northern inland area of Torfajökull. Expanses of black sands and conical mountains with little vegetation and small areas of exposed eroded soils dominate the upper valley. As you travel down-valley the narrow valley is in-filled with lava flows, cut through by a gorge >100m deep in places. The valley widens downstream becoming 2-6km wide to the west of Þórsmörk and consists of an active sandur (glacial outwash plain) with shifting braided river channels confined by steep valley walls, before spreading out into a 2km wide stretch on the coastal sandur plain of Landeyjar. The lower part of the valley mainly consists of stable, vegetated areas and inactive sandur with rich farmland in Fljótshlið and Storamörk Figure 3.1.2. Þórsmörk (Þór's Forest) and Goðaland (the Land of the Gods) are protected areas of the valley where sheep no longer graze and are popular with walkers and tourists. This area is characterised by birch woodland and small glacial lobes, which cascade over the rim of the Katla caldera into the lowland valleys. For ease of discussion throughout this thesis, the area has been sub-divided into lower valley (Þórsmörk to Landeyjar), middle valley (Þórsmörk to Einhyrningur) and upper valley (ice-marginal areas and highland watersheds) regions.

The Markarfljót valley lies in the eastern volcanic zone, mainly within the Moberg Formation. The lower part of the valley lies within the late Pliocene and early Pleistocene Grey Basalt formation. Thus, the geology of the Markarfljót area (Figure 3.1.3) is dominated by subglacially erupted 'moberg' or palagonite formed when the area was covered in ice in the Pleistocene. Acid extrusive formations (e.g. The Enta nunatak which appears through the Entujökull ice surface) and more recent post-glacial basaltic lava are also found across the area. Postglacial fissures are found in the northern part of the drainage area. NE-SW trending ridges run from Hattafell in Emstrur towards the northern outwash plain of Mýrdalsjökull, Maelifellsandur. Other fissures are found in northern Þórsmörk. These features are characterised by basic and intermediate hyaloclastites and tuffaceous sediment and tend to be noticeable in the landscape by a distinct reddish tinge associated with the scoraceous pyroclastic material around the vent. Lavas from these fissures are found in the foreland of Entujökull,

in Emstrur and in the north of Þórsmörk. These basic and intermediate lavas are postglacial and older than 4000BP (Johannesson et al 1990).

The source region of the valley, Torfajökull is mainly rhyolitic in composition with Tertiary and Pleistocene acid extrusive, giving the landscape to the north a distinctive yellow-green colouring. The high lands of Tindfjöll and Eyjafjöll are ice-capped stratovolcanoes, predominantly composed of interglacial and supraglacial basic and intermediate lavas as well as basic and intermediate hyaloclastites and tuffaceous sediment. Tindfjallajökull has not been active in postglacial times. It is the source of the Þórsmörk ignimbrite erupted during the Pleistocene (Roberts 2001). This formation outcrops mainly in the Þórsmörk lowlands and the southern flanks of Tindfjallajökull and has been extensively eroded by more recent glacial and fluvial activity.

The volcano Eyjafjöll forms the southern edge of the Markarfljót valley and consists of a central crater about 2.5km in diameter and the elongated Eyjafjöll massif which runs west to east in association with the predominant orientation of the eruptive fissures (Strachan 2001). Overlying the volcano is the glacier Eyjafjallajökull that has two main northern outlets, Gigjökull and Steinsholtsjokull, which descend in to the Markarfljót valley. The last eruption of Eyjafjallajökull was in 1821-23 (Loughlin 1995) producing both tephra and a flood that emanated from Gigjökull into the Markarfljót. A non-volcanic flood from Steinsholtsjokull occurred in 1967 (Kjartansson 1967). This was triggered by a rockfall onto the glacier and into the proglacial lake, producing both the unusual semi-chaotic terrain found in the glacial foreland and the spread of boulders which fans out into the lower land beyond.

The superficial geology of south-central Iceland is primarily of glacial and fluvioglacial origin. In particular the south coast is characterised by expansive glacial outwash plains such as Mýrdalssandur and Sólheimasandur, which are dominated by jökulhlaup activity. However, the confined nature of the majority of the Markarfljót, gives it a more classical glacial appearance. Much of the area is covered by the braided sandur system of the Markarfljót and its tributaries. Haraldsson (1981) has studied the sedimentology and petrological characteristics of the lower sandur area in great detail. From seismic profiles taken across the area Haraldsson (1981;29-31) discusses a series of stages of glacial erosion and infilling by lava, moberg or later marine, glacial and fluvioglacial material.

At the Last Glacial Maximum the Markarfljót area was completely covered by ice which reached as far as the edge of the continental shelf (Kjartansson 1970). As the Markarfljót ice retreated the sea flooded the valley both during the LGM deglaciation and after the Younger Dryas (Budi) advance. The sea may have reached the proximal margin of the recent valley sandur west of Þórsmörk (ie. filled entire lower valley). Haraldsson (1981) attributes terraces at 80 metres above sea level in Fljótshlið to marine inundation after the retreat of the Budi glacier. Seismic profiles recorded by Haraldsson (1981) suggest that an arcuate terminal moraine lies between 23 and 73 metres below the present sandur surface. This ridge is 40 – 60 metres high at its crest. The Budi glacier terminated in the sea. Morainic

material is also found in the lee of Stóra Dímon (Haraldsson 1981), on the upper slopes of Fljótshlið and northern slopes of Eyjafjallajökull (Dugmore, personal communication 2000).

The Holocene environment of the Markarfljót has been dominated by glaciofluvial activity forming the sandur and slope processes. Krigstrom 1962 and Hararldsson 1981 have studied the morphology and sedimentology of the sandur. Langanes, along the northern slopes of Eyjafjallajökull between Storamörk and Gigjökull is dominated by numerous alluvial fans. These fans are mainly composed of interbedded soils, tephras and fluvial deposits.

Þórsmörk is characterised by very highly dissected palagonite hills with very steep slopes covered in active scree and rockfall material. The largest rockfalls are probably caused by spring melt of interstitial ice and disruption by earthquakes, as occurred in the large earthquakes in July 2000 (centred on Hella, a town to the west of the Markarfljót. ~6.5 on Richter scale) and smaller local earthquakes during July 2002.

Late Holocene patterns of environmental change in the Markarfljót were significant, particularly around the time of Norse settlement. The period of Norse colonisation (Landnam) in Iceland is generally accepted to be between AD 870 – 930 AD (Figure 3.1.4). Archaeological investigations in the south of Iceland suggest that settlement began early in this period (Haraldsson 1981, Sveinbjarnardottir et al 1982, Sveinbjarnardottir 1992). Fluctuations in climate resulted in changes in glacial extent, aeolian activity and vegetation cover (Dugmore 1989, Dugmore and Kirkbride submitted). Expansion, decline and re-expansion of birch occurred in the 500 years (approximately) prior to AD 870 (Haraldsson 1981, Pahlsson 1981). Specifically in the Markarfljót area, Haraldsson (1981) has described large-scale changes to river patterns around the time of Landnam. Before and throughout the Landnam period the Markarfljót flowed in a number of channels across the sandur plain. This changed around AD 1200 when the river suddenly shifted, concentrating into one single channel (Figure3.1.5). Haraldsson (1981) suggests that these changes may be associated with glacial meltwater fluctuations in relation to changes in regional climate. Since Haraldsson's work it has been found that climate change, reflected in major glacial changes, did occur in the centuries before settlement (Dugmore 1989, Guðmundsson 1997). Maizels (1991) however, has suggested that infrequent, catastrophic jökulhlaup events rather than systematic changes in glacial outwash dominate the morphology of those sandur surfaces exposed to jökulhlaup activity.

In the Landeyjar and Eyjafjallasveit districts, early occupation sites are found in three main types of location: mid-sandur sites, escarpment sites on the sandur edge and the inland valleys of Þórsmörk (Figure 3.1.5). The sandur sites were generally on low ridges, small hills or partly stabilised dunes on the mainly flat sandur plains (Haraldsson 1981:3, Sveinbjarnardottir et al. 1982:81). These sites are very similar to the locations of present-day farms. Some sites have been lost to coastal and river inundation and others have been abandoned possibly due to factors such as erosion, economic change,

plagues and climatic change. Inland sites in the Þórsmörk area and further north at Einhyrningsflatir were raised above the valley floors in prominent positions (Sveinbjarnardottir 1992:41). Early abandonment of these farms may represent an over-optimistic pioneer fringe as suggested by Thorarinsson (1970), where climatic or other environmental factors were (or became) marginal for successful farming.

3.2 Methodology

The field and laboratory work draws on techniques from geomorphology, sedimentology and geochemistry. The necessity of inter-linking findings from geomorphological research with an assessment of the sedimentological history of an area is now widely accepted. As Bryant (1991;42) states *'contrary to interpretation based purely on morphological criteria, sedimentological analyses often indicate deposition in a number of complexly inter-related sub-environments'*. The key methods used to carry out this research reflect this view that where possible geomorphological studies should be thoroughly backed up by an understanding of the local sediment history.

Geomorphological mapping

Geomorphological mapping has been used to allow consideration of the role of flood and ice moulding of the landscape and thus the spatial distribution of areas affected by these factors. A combination of geomorphological data and sedimentary evidence has been used to assess landform genesis.

The landforms of the Markarfljót valley were mapped from stereoscopically viewed 1990 and 1994 aerial photographs obtained from Landmaelingar Islands (Icelandic Geodetic Survey). Photographs were enlarged to 1:10,000 scale and morphological maps were made on acetate overlays. The compiled map was not corrected for photographic distortion. Topographic maps at 1:10,000 and 1:20,000 (Vegagerdin 2000 and Orkustofnun 1999) were used as base maps for elevation details.

Interpretative maps were produced from the original morphological maps and in particular highlight features likely to be indicative of glacial or large-scale fluvial activity. Areas of particular relevance to the research were mapped in detail in the field. Field mapping at high resolution focussed on the area between the Entujökull foreland and Húsadalur in Þórsmörk. Key landforms were surveyed with an altimeter, Magellan GPS, 30 metre tape and Abney level or Silva compass-clinometer to characterise shape for genetic interpretation.

Sedimentology and stratigraphy

Sediments were analysed for three main purposes:

- Determination of landform genesis through consideration of exposed and surficial deposits, as part of the geomorphological mapping procedure. The results from these observations are included in Chapter 4.
- Development of a regional tephra stratigraphy for correlating environmental evidence from throughout the field area and to provide a datable chronology in which to place events such as floods and glacier fluctuations.
- Identification and interpretation of flood and glacial events within this stratigraphy.

Sub-surface stratigraphic and sedimentary analyses were carried out by studying exposed sediments in gullies and riverbanks and by digging vertically into unconsolidated sediments or traversing slopes in steps where no such exposures were available. Once exposed, sections were sketched and photographed and their location recorded with a GPS point or a grid reference. Vertical sedimentary logs record the details of each section, using procedures advised by Jones et al (1999). Each log was measured to an accuracy of < 5mm and show details of layer thickness, colour, grain size and shape, sorting, texture and sedimentary structures. Characteristics of surface lags were recorded noting the possibility of winnowing of much thicker units. Possible flood units and airfall tephras were traced along horizontally continuous sections and between different localities to ensure that they were indeed regional time markers/events and not associated with purely local conditions of deposition.

Grain size analysis employed the Udden-Wentworth (1922) scale (Figure 3.2.1). Grain shape (Figure 3.2.2) is characterised by comparison with a chart of standardized images of particle roundness adapted from Krumbein (1941) and measurements of the three clast axes (after Zingg 1935). Ternary diagrams illustrating particle shape based on the method recommended by Benn and Ballantyne (1993) and first proposed by Sneed and Folk (1958) were plotted using the 'TRI-PLOT' spreadsheet developed by Graham and Midgley (2000). Detailed measurements of clast shape are presented of those deposits with a large lithic content and with a high percentage of clast >5cm long, selecting at least 25 clasts at each appropriate location. Fabric data was collected where clasts were >5 cm in length and had an elongation ratio of at least 1.5:1 (from Jones et al 1999). Fabric was determined by measuring the orientation and dip of a clast; orientation with a compass and dip (the angle between horizontal and the plane the clast lies in) with a clinometer.

Units were classified into broad bands of aeolian soil, tephra or lithic-rich units. Samples were collected of pumice, tephra layers (particularly those which were visually distinctive and thus useful marker horizons), lithic-rich layers (possible flood units) and organic-rich units for radiocarbon dating. Further samples were collected of deposits of known origin (modern sandur deposits, glacial

deposits and known jökulhlaup deposits) for comparison with those sediments of unknown origin in later analyses.

Grain size distributions of sediments are frequently used as methods of characterising a deposit (Lindholm 1987) and have frequently been used to infer different origins. Maizels (1997) used cumulative grain size curves to show differences between floods of different origin from samples collected along the south coast of Iceland. However, the links between cumulative grain size curve shapes and origin of a deposit can be unclear. Care must be taken not to infer too much from the study of one sedimentary characteristic. Studies of the nature of diamictons show that very similar deposits may result from significantly different transport regimes.

Grain size analysis was carried out on samples of possible flood deposit and on samples of known origin (Markarfljót fluvial sand, Skogassandur and Sólheimasandur jökulhlaup deposits). Samples of approximately 500 grams were dry-sieved for grain size analysis. This size of sample is suitable for material with clasts no greater than1cm in size. The parent deposits from which these samples were collected tend to contain clasts up to boulder size. Samples were limited to size ranges below 3cm clasts, and only material which passed through a 16mm sieve was included in the size analysis calculations. This curtailment of the deposit for the purposes of grain size analysis is common practice in studies of diamicts, particularly glacial till and river gravels for purposes of practicality (Jones et al 1999, Haraldsson 1981). Approximately 500 grams (dry weight) of each sample was oven dried and then sieved for 15 minutes using an automated shaker. Sieves at 1 phi intervals were used (16mm, 8mm, 4mm, 2mm, 1mm, 500 microns, 250 microns, 125 microns). The remaining sediment in each sieve was weighed. The resultant figures were used to construct cumulative grain size curves. The results from analysis of samples of unknown origin were then compared with the known origin samples and published data.

Attempts were made to see if geochemical tracing of deposits other than tephra layers were possible. Key points investigated were whether a deposit could be related to another deposit elsewhere in the region based on similar geochemical properties, and whether a deposit had predominantly basaltic or silicic material within its matrix, and if so, to which volcanic complex it was most related. Geochemical analysis was carried out on the matrix material from massive and diamicton deposits both of known origin (Skogassandur, Sólheimasandur and Markarfljót sandur) and unknown origin. These analyses used an Electron Microprobe.

Tephrochronology

The main dating and chronological tool used in this study is tephrochronology, a technique that uses tephra layers within the sedimentary record as time-parallel marker horizons. Such horizontally continuous units represent an instance in time within the sedimentary record of a region. By tracing

these tephra layers across an area, a regional chronology can be developed. Using historical records, ice core data and radiometric dating techniques, independent ages can be obtained for these layers. This stratified sequence of dated tephra layers can then provide a chronological framework within which events recorded in the sedimentary record can be placed.

Tephrochronology was developed in the 1940s, predominantly by Thorarinsson (e.g.1970, 1975), and has since become an important dating tool in palaeoenvironmental and archaeological studies throughout areas of proximal and distal tephra deposition. Icelandic tephra deposits have been identified in northwest Europe, in the Greenland ice cores and sediments in the North Atlantic, allowing connections to be made across the North Atlantic region with activity in Iceland (Hammer 1984, Gronvold et al 1995, Dugmore 1987). Iceland in general, and specifically the Markarfljót region, is well suited to the application of tephrochronology due to the very detailed and well-constrained record of tephra layers for the region (Thorarinsson 1967, 1975, Larsen 1978, 2000, Larsen and Thorarinsson 1977, Larsen et al 1999, 2001 Dugmore 1987, 1989b). Throughout the Holocene (approximately the last 10,000 years), a number of very active volcanic systems in close proximity to the Markarfljót (mainly Hekla, Katla, Eyjafjallajökull and Veiðivötn) have produced many visually and geochemically distinctive tephra layers. These layers are particularly suitable for stratigraphy-based tephrochronology, (eg. Dugmore 1989a, Dugmore et al 1995), and are used here to date the main sedimentary events and landforms in the study area.

Tephra sequences were recorded above the valley bottom with the aim of recording undisturbed sequences of layers, unaffected by flooding, river or glacial action or mass movements. Sequences were also recorded across the valley floor and on lower slopes to allow dating and correlation of sediments and landforms throughout the valley. In total 173 sedimentary profiles were recorded. Reference profiles composed of tephras and aeolian soil at Langanes, Fljótshlið, Kanastaðir, Einhyrningur and at the western edge of the Entujökull foreland add to the regional tephra stratigraphy developed by other researchers throughout the valley. The early Holocene tephra sequence upvalley required expansion since little has published on this subject. These main reference profiles were augmented with shorter profiles throughout the valley.

Tephra sequences were logged at a <5mm scale precision noting layer thickness, colour, grain size, grain shape and the nature of contacts between adjacent layers. Black layers tend to be basaltic tephras from the Katla Volcanic System in this area and are not normally chemically distinctive enough to allow differentiation between different black layers. Samples were taken from pale tephra layers. Sampling was carried out with a clean knife, where possible from the base of the tephra layer to avoid mixed material.

Geochemical analysis of tephras can allow a layer to be attributed to a particular volcanic system and sometimes to a particular eruption based on major element composition (Figure 3.2.3) (e.g. Larsen et

al 2001, Larsen et al 2002). Samples of tephra were mounted on slides using araldite for major element geochemical analysis a Cambridge Instruments Microscan V electron microprobe and a Cameca Camebax Microbeam electron microprobe. Carbon coated samples were analysed using the wavelength dispersive method, an accelerating voltage of 20 kV and a beam current of 10nA. Corrections were made for counter dead-time, atomic number effects, fluorescence and absorption using a ZAF correction programme based on Sweatman and Long (1969). A piece of homogeneous andradite was analysed at regular intervals between samples to establish the stability of the instrument. Only analyses of pure glass with totals above 95% were accepted. To minimise the differences between analyses carried out on the two instruments the same samples were analysed on both instruments under a variety of conditions. The results of these analyses are listed in appendix 1. Optimum conditions for analysing different glass types for both instruments are those which give highest totals and the least loss of sodium during the analysis. Tests were carried out on the Microscan V instrument looking at the homogeneity of glass grains by analysing glass grains along transects and for variations in instrument calibration by analysing a homogeneous grain a number of times over a restricted area. The results of these are included in appendix 1.

Stratigraphical techniques have been used to correlate between closely spaced sediment / tephra profiles. The stratigraphical framework and historical and radiometric dates constrain the ages of individual tephra layers. These are discussed in chapters on the tephra stratigraphy (5) and on the chronology (7).

Chapter 4: Results

Geomorphology

4.1 Introduction

This chapter describes the results of the geomorphological investigations. The approach to this overall study has been to integrate geomorphological and sedimentary data and therefore this chapter describes the relevant landforms in the Markarfljót, and also the composition of the features.

The main features considered in this study are those formed through glacial or large-scale fluvial action, identified in comparison with classic examples discussed in the literature. Glacial and fluvioglacial landforms are thoroughly reviewed by Benn and Evans (1998) while section 1.3 summarises flood landforms. The majority of these features are most clearly genetically identifiable as assemblages. To aid clear discussion of these features individual landforms (and groups of similar landforms) have been described in Tables 4.1-4.3, while particular features and related assemblages of features are considered in the text.

Apart from these types of landform, steep slopes and active glacial outwash streams heavily dominate the area's landscape. These features reflect the highly active and changeable nature of much of this region, particular in ice-proximal areas, along the valley axes and in areas of highly erodable moberg geology. This results in selective preservation of evidence for Holocene environmental events and needs to be born in mind when the distribution of both landforms and sediments are discussed.

Figure 4.1.1 shows an overview of the geomorphology of the Markarfljót. Maps at 1:10,000 scale have been made of the upper and middle Markarfljót valley (Figures 4.1.2-4.1.3: loose geomorphological maps). The content of these detailed geomorphological maps will now be described.

4.2 Glacial and fluvioglacial landforms in the Upper Markarfljót

Table 4.1 lists the main ice-marginal landforms recorded from aerial photograph interpretation and field investigations.

The Entujökull foreland

Entujökull descends from the main ice cap of Mýrdalsjökull, through a breach in the Katla caldera rim into the lower glacial foreland. Two pinnacle-shaped hills at grid references 830 697 and 833 702,

TABLE 4.1A: UPPER VALLEY – TABLE OF GLACIAL FEATURES

Feature	ID no.	Location	Description	Dimensions	Sediment notes	Related features
Ridges 4A-D	AS01-2	Entujökull foreland. Orientated N-S across valley approximately parallel to the present-day ice margin.	Grey boulder-strewn ridges picked out by intervening green vegetation. Ridges grouped into two main zones (1+2 furthest from ice, 3+4 closer to ice)	1-3m high, up to 1350m long.		Trimlines, sandur, relation to gorge feature.
Dissected ridge 3A	S2001-3	Entujökull foreland, western lava surface and step up to lava (by path).	Fragments of ridges and hummocks. Larger mounds along lava edge. Others elsewhere on eastern side of lava surface.			Trimlines?, Sandur, hummocky zone (ice-contact), cataracts.
Hummocky zone	S2001-3	Entujökull foreland, against western lava surface	Semi-chaotic mounds and terraces dissected by gullying. At least 3 levels of surface stacked up against lava edge. Upper surfaces / mounds may be associated with debris flows/landslide from cliff.		Composed of black tephra-rich sands and gravels. Selected mounds / ridges are more diamict-like in composition (moraine?).	Possibly from ice contact/moraine, flood then landslide: see notes S2001-3.
Ridge	S01-3	Western-most moraine of Entujökull foreland.	Clear asymmetric ridge (steeper on ice proximal side). Most distinct to S/SE. Ridge becomes diminished and discontinuous. Dissected to south by later gully. Possibly washed (thus explaining boulder distribution downstream).	Up to ~3m high.	Contains gravel and boulders with black-tephra rich sand matrix. Some large boulders.	Possible ice-contact feature (terrace / mound) on opposite side of gorge. Associated with flat surface to west with a surface scatter of boulders.
Ridge and channels	S01?-3, A01-2	On cliff above Botn and Entujökull	Channels run from cliff cutting cliff-side ridges.		Pumice here..	Potholes,
Ridge	A/S00-1 31/8/00	Botn basin, crossed by walking trail and exposed by dissection of active stream.	Ridge with large boulders scattered on surface.		Shattered palagonite boulders (frost-shattering?)	
Boulder sheet	S02-3	On hill above Botn				
Ice-cored debris	A01-2	South valley side between LLIA moraines and ice front, below trimline.				Very active frost heave and stone sorting. Kettles, esker(s).
Boulder sheet	J02-1	W of gorge and Entujökull foreland (by road)	Large boulders 1.5-2m.			

TABLE 4.1B: UPPER VALLEY – TABLE OF FLUVIOGLACIAL FEATURES

Feature	ID no.	Location	Description	Proportions	Sediment notes	Related features
Sinuous ridge	A01-2	From LLIA ridge 2 towards Entujökull.	Bifurcating ridge orientated approx. along valley axis. Depressions in the bends of the ridge and between ridge divisions. Upglacier end of esker truncated by channel.			Kettles
Sinuous ridge	A01-2	From LLIA ridge 3 (or 4?) towards ice.	Orientated ~SE-NW. Very sinuous ridge.	~2m high.		Kettles to SE of esker.
Depressions	A01-2	To south of ridges 3 +4 and south of esker 2.	Semi-chaotic hummocky region. Channel drains to ~N from hummocky zone. Possibly some E-W linearity. Larger kettles nearer moraine ridges.			

TABLE 4.1C: UPPER VALLEY – TABLE OF FLOOD FEATURES

Feature	ID no.	Location	Description	Proportions	Sediment notes	Related features
Sandur		Entujökull foreland, west of LLIA moraines.	Smoothed, slightly hummocky sandur surfaces composed of black tephra on top of lava surface. Little vegetation.			Channels, fans.
Sandur		Entujökull foreland, western lava surface	Smoothed, slightly hummocky sandur surfaces composed of black tephra on top of lava surface. Little vegetation.			Channels, …
Cataract	S01-3	Cataract at end of channel on western lava surface, where channel meets main gorge.	Overhang with plunge pool. Concave channel sides approaching cataract and steep high cliffs below into main gorge.			Polished smoothed bedrock with elongated depressions.
Dissected basin-infill	S02-3	Botn	Various levels of terraces and mounds composed of bkt/s and with gravel lags.			
Dissected sandur	A01-2	From LLIA moraines to W.	Poorly vegetated, steep sided, liner ridge. Appears to continue up onto moraine.		Bk sands and gravel	Sandur
Channel	A01-2	Sandur surface below LLIA moraines	Dendritic channel extending from moraine ridges to edge of sandur surface. Bars and terraces. Lag on surface. End of channel has smoothed bedrock at base and ends in dry cataract. As channel narrows downstream boulders become clustered on channel base.		Channel bases composed of crudely bedded bkt and gravels – fcs.	
Dissected sandur / flood deposit??	A01-2	By gorge from Entujökull, upstream of western lava surface.	Dissected basin with dry channels and bars. Rock-cored ridge between dissected deposits and gorge.			
Potholes	S02-3	On hill above Botn. One at 27 58 2297E, 7 07 1599N (elevn. 673m)	Pothole, with lip at top. Base infilled with gravel and fine t coarse sands.	Up to 25cm deep. Base infill up to 5cm.		
Scoured palagonite	S02-3	On hill above Botn / Entujökull cliff				
Low ridges and terraces	A01-2	By gorge from Entujökull, upstream of western lava surface.	River terraces not flat (slope towards gorge) and ridge. Ridge steeper on gorge side, infilled behind. Outwash?			
Lava flow surface	J02-1	Emstrur, road to Slettjökull / Botn	Surface covered in cbkt, palagonite, lava fragments and scoria. … therefore washed.			
Outwash area in	A01-2	Between N. Entujökull	Channel from Slettjokul (?), onto palaeo-			

Feature	ID no.	Location	Description	Proportions	Sediment notes	Related features
front of N. Entujökull.		and cliffs	outwash surface, raised on lava plateau. Channel runs along Entujökull ice front, with waterfall. Cliff has steep slopes down to channel on west side of outwash area. Terraces stacked against northern cliffs.			
Slettjökull channels	A01-2		Terraces and channel. Gorge through lava.		Terraces composed of crudely bedded black sand inc. bkt and lithics. No visible soils.	
Ripples	A/S00-1	On surface of large tephra-rich bar.	Asymmetrical ripples. (less distinct than Skogassandur) Measurements taken of cross-sections and orientations.		Coarser material on crests.	
Ripples	J02-1	Botn (W side of basin)				
Terraces	J02-1	Fauskheiði (Emstrur (790 760)), NW of Hattafell and W side of Hattafell, on side of lava flow to SE of Hattafellsgill	Terraces. Poss all same height. Fauskheiði (Emstrur) terrace slopes of \E, more horizontal to W. All terraces slope very gently (maybe 1°) to SW. Large-scale fan?			
Terraces	J02-1	N edge of Utigonguhofdar (mordor)				

TABLE 4.2: MIDDLE VALLEY LANDFORMS

Feature	ID no.	Location and grid references	Description	Proportions	Sediment notes	Related features
Moraine	JJ01 -2	Einhyrningur			Dated with 24/6/2001 profile EIN REF	
Moraines?	JJ01 -2	By junction in path to Husadalur / Langidalur.				
Ridges (moraines)	A01 -1	SE side Ljosa near campsite	3 ridges. Cross-section through one ridge by river.			
Lava flow and vent			Lava flow which extends into the big channel from vent area. Depositional terrace on top of lava flow at channel margin. Lava surface above terrace is uneven, below terrace, lava surface is smoothed.			
Markarfljotglufur	G1	Valley axial	Valley-central gorge draining Emstrur and Entujokull foreland.	Up to 100m deep.		Bars, channels, terraces, active river features. Cataract features in clifftops (some dry, others associated with tributary streams).
Markarfljotglufur rock terraces	A01 -1		At least 2 levels within gorge. Steps in rock walls, some with bars and deposits on top of them.		Northern side tend to be less associated with deposition than southern (N. thorsmork side)	
Markarfljot	A01	South side	Depositional terraces with channels		Terraces	

depositional terraces	-1	channel on rock terraces.	(dewatering or later event).		composed of crudely bedded black tephra / vesicular basalt. Lag on surface inc. rhyolite, BS, scoria, palagonite. Matrix: f-csbkt, lithic-rich.	
Trollagja (*'Ravine of the trolls'*) (*photos / sketches / annotations..sketch in JJ00/2*)	G2	Runs along north-western margin of valley downstream of Einhyrningur, joining with Markarfljotgluf ur at …	Base of channel polished lava / smoothed. Within channel there are fans and terraces / mounds.		Gravel pit at uptream end of gorge.	Cataracts (inc. C1 and C2), fans and terraces.
Fans	July 200 2-2	Trollagja channel	Fans in lee of eastern channel margin (upstream). Later channel between fan deposits coincides with channel on lava surface.		Fans composed of cobbles-boulders up to 1m, with sand and gravelly black matrix. Windblown fines on surface.	
Terraces	July 200 2-2	Trollagja, downstream of road towards Markarfljot.	2 levels of terraces. Upper terraces mainly deposited against gorge side (although one mound noticeably disconnected). Lower terraces dissected by later (possibly snowmelt) channel.		Upper terraces composed of boulders, cobbles and gravels. Top 60cm of terraces has brown-black tephra-rich	

					matrix. Material finer on downstream side of terraces / mounds (f/cs compared to cobbles and gravel). Lower terraces bedded f/cs – cobbles/gravel. Reworking of this material.	
Streamlined erosional hill(s) in lava *(sketch of moat)*	JJ01 -2	Klappir, on Fauskheidi lava, opp. Thorsmork	Streamlined palagonite hill, with 'moat' – selective erosion and deposition. 'Moat' similar to catarct feature with in-channels and associated gouges on lava surface. Depositonal mounds upstream and downstream of hill with lag on surface.		Lag on upstream mound includes boulders 6-3-2m dimensions – smaller clasrs up to 1m longest axis. Channels infilled with cobbles and gravels.	Cataracts, smoothed lava, 'moat'. Small crescentic 'potholes'.
Streamlined erosional hill	A01 -1	North Thosmork	Streamlined palagonite hill with 'moat'-like channels either side. Found within very large horseshoe feature (like cataract) with upstream channels and downstream channel feature(s). Deposition in bar a downstream of hill.			Channels, bars, terraces, cataracts along upstram edges of channels with overhangs.
Cataract 1 *(Relate to pit Trollagja 1*	C1	Trollagja (upstream)	Small cataract at upstream end of Trollagja gorge with channel running downstream if cataract to Trollagja.	~2m from infilled pool to lava	Lag in channel leading up to cataract with	

26/6/2001 at 63 43 15N 019 30 00W (6 sats))				surface.	36cm fbkt below.	
Cataract 2	C2 J/J0 1 -2	Trollagja (upstream)	Cataract with distinct plunge pool. Cliffs overhand plunge pool.	~8.5m deep from partially infilled plunge pool to lava surface. 3.5m deep channel leads into cataract.	Gravel and SR-WR clasts between 0.5m and >1m in plunge pool. Some clasts show cavitation / p-form type marks on surface.	
Cataract 3	C3	North Thorsmork, SW of streamlined hill and large cataract (not decsribed??)	Horseshoe shaped break in lava (cataract) with channels upstream and downstream. Upstream surface polished and covered in gravel – boulder lag. Cliff at cataract edge has overhang. Base of feature infilled with fs-fgravel.		Sedimentary channels / bars upstream and downstream. Potholes and fluted erosion marks in upper surface.	
Cataract 4	C4, J02-1	Fauskheidi lava, west side of Klappir	Orientated NE-SW. Infilled horeshoe-shaped depression in lava with cliff sides. Edges mapped with GPS.			Channels into and out of cataract. Scratches and flutes on lava surface.
Cataract 5	C5, J02-1	East side of Klappir.	Infilled cataract with polished channel system inside outer horeshoe-shaped margins.			Polished channel system.
Smoothed lava	J02-	Fauskheidi lava	Surface ropey, smoothed in places. Some			Cataracts (some infilled with

	1		elongated scratches and flutings.			soil and tephra), scratches, flutings, polished channels.
Polished channel system	J02-1	East side of Klappir, within margins if cataract 5.		Orientation and dimensions of channels mapped in detail		
East Einhyrningur terraces	S02-3	Along north-eastern margin of valley extending from Markarfljotgluf ur towards Einhyrningur.	2 levels of terrace above washed lava.			
Terraces	JJ01-3	Fauskheidi	3 terraces		See sketches of layers and tephra profiles	
Thronga terraces *(sequence of sediments described in detail)*	A01-1, J02-1	Mouth of Thronga, north Thorsmork	2 terraces on top of lava at mouth of Thronga. Equivalent to terraces at Fauskheidi?			
Big channel *(sketches, locations and orientations of channels / cataracts and imbricated clasts mapped and measured.*	A01-1	North thorsmork	Main channel composed of washed lava. Terraces either side, particularly clear on northern margin. Large boulders and gravel lag across surface if channel. Downstream end of channel marked by cataracts and fans along shallow lava cliff. 3 heights of terrace. Channele xtends from more confined channel upstream.		Imbricated boulders. Some clast >3m. Others frost-shattered. Uphill limits of tephra-rich lag on low hills.	Lava from crater on southern margin of channel. Terraces. Imbricated boulders. Cataracts. Smoothed / polished lava. Potholes. Chutes / flutes.
Boulder bars		Big channel, north Thorsmork.				

Ljosa terraces						
Bar and channel	A01 -1	North Thorsmork, SW of streamlined hill	Bar dissected by channel with terrace to north of channel.		Boulders on bed of channel. Boulders (BS, scoria, palagonite) on upper surfaces of bars. Terrace composed mostly of sand to gravel.	Cataract upstream. Boulder cluster at head of channel. Clasts within boulder cluster include Bs and palagonite up to 1.5m. some are very polished SR clasts.
Channels and terraces downstream of streamlined hill. *(cross-section heights measured)*	A01 -1	North Thorsmork	Downstream of erosional hill. Series of channels and associated terraces with very smoothed lava bases, at edge of higher exposed lava flow. 2 Terraces to east of channel are covered with a gravelly lag forming a frost-shattered pavement. Gravel and sand lag on surface of lava at edges of channel. Higher exposed lava: to N smoothed, to S (Ljosa) less smoothed.		Lag (<10cm - >3m long) includes basalt and palagonite. Largest clast 'erratic' boulder 6/4/1.5m (orientated long axis 311N). Matrix includes f-cbk sand inc. vesicular BS up to 1cm, lithics inc palagonite and red scoria and BS. Laregst boulders on lower terrace 1.	
Úthólmar/Ljosa channels	A01 -1	???	Channels. Wash limits			
Ljosa terraces	A01 -1	Ljosa, north thorsmork	Terraces on opposite sides of valley at different heights.			
Streamlined hill by Ljosa *(sequence of*	A01 -1		High point of hill has low basin and abandoned channels surrounded by low		Gravel and cobble lag	

sediments described in detail)			hills. Gullies on hill towards Ljosa have old tephras exposed in channel sides (no lag).		(Flood = unit 8B?) on top of old tephras and soils.	
Pronga terraces	JJ01 -2/3	Along Pronga river / Kapurani				

TABLE 4.3: LOWER VALLEY – TABLE OF FEATURES

Feature	ID no.	Location and grid references	Description	Sediment notes
Moraines	JJ0 1-3/1	Fljotsdalsheidi	Min. 5 ridges trending downslope between 340m and 210m contours.	
Palaeochannels/ surfaces	JJ0 1-3	N Aurasel		
Terraces		Fljotshlid (Barkarstadir)		
Terraces	AS 00-2	Terraces along northern margins of Markarfljót channel.		Soft sediment banks, sometimes with hardpans and surface gravely lag.
Halli's island *Is this a previous limit of Markarfljót glacier, since washed and dissected by floods?*	JJ0 1-2, A0 1-2	Bet. Markarfljót and Gilsa.	Streamlined island, linked to northern river bank by short causeway. Divided up by channels and elongated ridges overlain by soft sediments.	Extensive flood deposit evidence and tephra records. Ridges palagonite / diamict?
Stora Dimon		Sandur	Bedrock 'island' in sandur. Teraces around lower slopes.	

divide Entujökull into two tongues (Figure 4.2.1) The northernmost tongue, a low lobe of ice around 3200m across, has a small foreland area, confined by a wall of cliffs. The 1994 aerial photographs of this foreland show that the ice front stood back ~800m southeast from these ~120m high cliffs. The southern tongue is smaller (~800m wide) and flows from east to west into the ~4km long Entujökull valley. The valley floor is composed of two raised lava plateau areas separated by a small valley with uneven topography. The Fremri-Emstruá drains both the northern and southern tongues of Entujökull and runs in a gorge along the northern and western valley sides. This valley has steep ~120m high scree-covered walls to the south. To the north the valley walls are lower with a number of small cols separating the main valley from the Botn basin. Soil cover throughout this area is sparse with much of the foreland covered in a very thin (0-5cm) soil. Depressions and areas in the lee of landforms which shelter them from the prevailing down-valley katabatic wind are the few places where deeper soils may be found.

There are six zones of ice-marginal landforms that have been preserved in the Entujökull forelands, which have been numbered starting with the most distant from the present-day ice margin. S/E and N/E refer to positions in the southern and northern Entujökull forelands.

Limit S/E1: The outermost evidence of ice limits in the Entujökull foreland is located on the slopes to the west of the Markarfljót gorge, ~4 km from the present-day ice margin. A sheet of bouldery material marks this limit, with clasts up to 2m in diameter covering the hillside. This sheet stops abruptly just west of the Fjallabakki road (F261). This margin is indistinct in places due to variable soil cover in the area. On the slopes between the road and the gorge, >5m deep soils and tephra deposits occur stratigraphically above this bouldery sheet.

Limit S/E2: ~3.9km from the ice front at the westernmost extent of the western plateau there is an asymmetrical ridge, steepest on the ice-distal side and up to 3m high. It is most distinct to the southeast, though cut by a gully, becoming more discontinuous and diminishing to the northwest. This ridge is composed of gravel and boulders with a black tephra-rich sandy matrix. The up-valley plateau is characterised by bedrock mounds and a covering of black tephra-rich sands. A spread of boulders extends downvalley from this ridge across the flat surface of the lava plateau towards the Markarfljót gorge. A terrace on the opposite side of the gorge correlates with this feature. Further ridges are located on a terrace above this plateau.

Limit S/E3A, 3B, 3C and 3D: The western plateau is covered by a variety of ridges, mounds and channels. Most of these ridges are orientated downvalley or are non-distinct mounds. However, three clusters of ridge fragments and aligned mounds are identifiable on the plateau (3A-3C). Ridge section 3A is assymetrical with a gentle extended slope to the west, and is orientated approximately cross-valley, bending round to follow the plateau edge to the north. A line of boulders marks the crest of the ridge. The southern end peters out but is cut through by a now dry channel (Channel 1).

Approximately 2.9 km from the ice front there is a dissected ridge (3B) that is preserved as a series of ridge fragments and mounds aligned along the eastern edge of the westernmost lava. Many of these ridges are aligned at 90 degrees to the plateau edge, are streamlined, with gentle slopes extending to the west, and reaching heights in the order of 5m. The largest mounds are found closest to the up-valley edge of the plateau. These larger ridges and mounds are predominantly composed of grey cobbly diamict with heavily frost shattered boulders on their surfaces, contrasting significantly with the surrounding features which are mostly made up of black tephra-rich sands (eg. Ridges A-C are cobbly, ridge D is sandy). The matrix of this material tends to be black sand, with cobbles up to 10cm in diameter.

Two small semi-arcuate ridges, less than 2m in height, mark limit 3C. These ridges are located partway up the side of the lava plateau on a rock-cut terrace and are composed of diamict and boulders. Black tephra-rich sands on top of a shallow soil cover are found on the intervening surface between the ridges.

Stacked up against the edge of the lava surface is a zone of hummocky topography (3D) composed of semi-chaotic mounds and terraces, dissected by gullies. These mounds can be divided up into 3 sub-groups with similar height, as illustrated in Figure 4.2.2. The lava cliff, which marks the edge of the western plateau, has unvegetated areas with loose material, leading into large gullies that cut through the uneven topography below. The upper mounds are composed of boulder-rich material and are slightly fan-shaped, having upslope margins that peter out against the lava cliff behind. These features are all at slightly different elevations and do not appear to be part of a dissected surface. The lower mounds are more predominantly composed of black tephra-rich sand with fine gravel lithics. The lowest features are heavily dissected by gullies draining the surrounding slopes and the main channel through the valley bottom. Southern mounds in this complex (no.70 and 74 particularly, see figure 4.2.2) are composed of bouldery diamicton, with heavily frost-shattered clasts on their surfaces. Mounds 70 and 71 are continued as a line of boulders along the southern valley side towards the east.

Limit S/E4A, 4B and 4C: Within 1900m of the ice front there is a zone of well-preserved glacial landforms. Winsborrow (2002) has described this area, and also that close to the ice, in detail, as part of a study into the processes of glacial moraine formation. Fragments of ridges are found through much of this near-ice area, particularly following the edges of cross-valley channels.

The most conspicuous glacial landforms in the Entujökull foreland are two clusters of ridges that run parallel to each other, orientated north-south across the foreland. These two clusters are made up of two 1350m long ridges and several shorter ridge fragments. These are clearly identifiable from their grey, poorly vegetated appearance against the bright green moss growing in the adjacent channels. These ridges are 1-3m high and are predominantly composed of sub-angular to sub-rounded cobbles.

The down-valley ridge (4A) is mostly continuous, while the second ridge (4B) is non-continuous, dissected by channels. Winsborrow (2002) observes that ridge 4A has a widespread distribution of clast shapes and that there are relatively few angular and sub-angular clasts. A third, lower ridge (4C), 1600m from the ice front is similar in orientation to ridges 4A and 4B. Between these ridges, mostly in depressions and abandoned channels there are shallow soils up to 25-34 cm depth with few tephra layers and bands of black tephra mixed with gravel to sand-sized lithic grains. Below these soils there is consistently a cobble and gravel rich unit with a sandy matrix.

Subdued disconnected linear ridges and mounds are stacked against the southern valley side, forming a series of linear features extending from ridges 4A and 4B, sloping upslope at angles of ~10-20 degrees. Two parallel minor ridges are clear. These features are composed of gravel and cobbles with a finer matrix and are mostly covered in a layer of moss.

Below these linear features on the southern valley side there is a low region of chaotic, poorly vegetated topography. The surfaces of these mounds are covered with sand, gravel and well-rounded cobbles. Silt-rich water drains from chaotic mounds, suggesting that they are ice-cored. A high ridge of debris marks the downvalley end of this depression. A small braided channel drains this ice-cored debris and runs along the southern valley side into the low valley between the two lava plateaux.

In addition to features representing ice margins there are numerous fluvioglacial features in the Entujökull foreland. Two sinuous ridges lie east of Entujökull ridges 2A and 2B. The first sinuous ridge is low (up to 2 metres high), sharp-crested and bifurcates in places, branching into four sections with intervening hollows close to ridge 2B. The upvalley end of this sinuous ridge terminates where it is cut by a cross-valley channel. This feature is composed of rounded cobbles and gravel with a sandy matrix. A second sinuous ridge up-valley extends towards the present-day ice margin from ridges 2C and 2D.

Two regions of enclosed depressions with low surrounding rims are located along the southern side of the valley. Region A is located up-valley of ridge 2B and region B is located to the south-east of sinuous ridge 2. These features vary in size, between 1 and 3 metres in diameter and up to 2m in depth. The base of these depressions is in-filled with sediment. A basal gravel and cobble rich unit is overlain by shallow soils containing layers of mixed tephra and lithics. Some E-W linearity in the orientation of intervening mounds exists in region A. Larger depressions in this region are located closer to ridge 2B. These depressions, in association with the sinuous ridges, are mapped as kettle holes.

Two deep (>5m) channels run approximately south to north across the southern Entujökull foreland between ice limit 2 and the present glacier snout. Small discontinuous ridge sections and mounds are located along the up-valley margins of both these channels. At present the southern valley sides are

drained by gullies which are channelled into these main cross-valley drainage routes, into the main gorge system along the northern edge of the valley. However, when investigated in the summer of 2001 small misfit streams occupied these channels. The western channel (Channel 1) truncates sinuous ridge 1. Terraces with abandoned channel patterns on their surface are found within the channel. This channel drains the southern valley sides and a region of chaotic topography with numerous depressions (Region A).

Limit S/E5: The youngest glacial features are found at the present-day ice margin. In front of the ice margin (October 1999-August 2002) there is a region dominated by active meltwater streams which have formed a small area of confined sandur. These streams dissect small metre-scale ridges that run approximately parallel to the ice front. The ridges are predominantly composed of sub-angular clasts, trace the edge of the ice and are unvegetated. A zone of debris-covered ice extends along the ice front and along the southern lateral ice margin. In places glacier ice is clearly visible beneath the debris, which varies in thickness dependant upon topography. This heavily debris mantled zone may be related to the plentiful supply of supraglacial material from the southern cliffs.

Limit N/E1: Figure 4.2.3 shows a panorama of the northern Entujökull foreland. There are no clear moraine-like ridge formations obvious from the aerial photographs of this area, or from the vantage-point from which the photograph in Figure 4.2.3was taken. Access to this area during field seasons 1999-2002 was not possible due to the active outwash streams in the valley floor. Two terraces are visible stacked against the northern cliff and channels extending to the north from the top of this cliff (now with no viable water source) suggest that the margin of the ice was once positioned against this obstacle.

The Botn basin and Stora-Mofell

The Botn basin is largely characterised by low-level mounds and channels composed of black vesicular tephra and sands, which fill the lower parts of the basin, extending to ~500m up the basin sides, particularly to the west. The northern and southern basin margins are characterised by steep cliffs with fans and gullies. These mounds vary in colour between grey-brown and black, depending on the proportion of tephra in the surface sediments (higher the amount of basaltic tephra, darker the colour). Two discontinuous arcuate ridges in the northeastern sector of the basin are visible when exposed in gullies and where the overlying material is thin. These often partially buried ridges are composed of palagonite boulders with a finer pale matrix and contrast greatly in colour with the predominantly black landscape.

Making your way up the eastern side of the basin you cross a distinct boundary between palagonite-rich deposits and predominantly basaltic surface sediments. These two sheets of material contrast in colour and in nature. The palagonite-rich sheet is more compact and orangey in colour. The basaltic

material is grey, includes glassy clasts and has a black tephra and sandy matrix, forming a very thin veneer over exposed bedrock. The palagonite material is very similar to that which composed the exhumed ridges in Botn. The grey material is less well compacted and becomes slightly thicker to the east.

On the low southern slopes of Stora-Mofell an extensive complex of ridges and channels are located . Three clear, continuous ridges are identifiable. Two of these follow the edge of the ice-facing cliff. These ridges are >3m in height, discontinous and separated by channels. The third forms a zig-zag outline, clearly visible on the 1994 aerial photographs, approximately 800 m from the cliff edge. This ridge is continued along the southern foot of Stora-Mofell. Between these ridges there is a more complex arrangement of small ridges, mounds, channels and intervening basins. The general trend of these channels is from the eastern cliff margin, following the line of the long ridges down hill NE-SW to the southern Entujökull foreland. A larger channel extends SE-NW away from the cliffs that face the present ice margin, cutting through the cliff-side ridges. The zig-zag moraine extends down into this channel and is dissected by later use of the channel at 27582344E 7071869N (629m GPS elevation).

The Sléttjökull foreland

The foreland of Slettjökull has been mapped from aerial photographs with limited investigation in the field. The main feature of this region is a very wide, extensive sandur area which reaches from the ice margin as far as the highlands around the Hvanngil / Torfajökull area. The F261 mountain road approximately follows the northern edge of the Slettjökull foreland. Conical hills and narrow ridges, marked on the geological map (Johanneson et al 1990) as fissures stand as isolated peaks in the expanse of relatively flat sandur. The main glacial features of this foreland are two parallel ridges that approximately parallel the ice margin, now 2.5 km from the snout of the Slettjökull ice lobe. These ridges are similar in size and in relative position to the present ice margin and each other to Entujökull ridges 2A and 2B.

4.3 Glacial landforms in the Middle Markarfljót

The middle valley extends from the westward end of the Entujökull foreland to the eastward extension of the Markarfljót sandur by Húsadalur in Þórsmörk. The geomorphology of the central valley area, around the axis of the valley, is illustrated in Figure 4.1.3. The Markarfljót flows down the axis of the valley. This section of the valley is 1.5 km wide at the northeastern end widening downvalley to ~3 km by Húsadalur, where the river opens out into a ~3-4 km wide sandur plain. Individual features or clusters of features are listed in Table 4.2.

No clear ridges, as were found in the upper valley, are visible in this region. Less distinct ridges however were identified around Einhyrningur, in Þórsmörk and on the southeast bank of the Ljósá.

The Einhyrningur ridges are composed of apparently unsorted compacted sediments with up to >2 metres of soil on top of them. Boulder lags are also found on the hillsides on the lower slopes below Einhyrningur. Similar exposed ridges rich in palagonite and with eroded soils on top are found in Þórsmörk and along the Ljósá.

4.4 Glacial landforms in the Lower Markarfljót

The main landforms of the lower valley are listed in Table 4.3. The lower valley downstream of Húsadalur in Þórsmörk is dominated by the Markarfljótsaurar sandur, which is characterised by braided glacial outwash streams and intervening bar systems. The southern margin of the valley, along the margin of the Eyjafjallajökull massif, is lined with large fan systems formed by streams draining from the ice cap above, and the glacial forelands of Steinsholtsjokull and Gigjökull. Evidence for Mýrdalsjökull glacial activity in the lower Markarfljót valley is limited due to the presence of deep soils throughout much of this area and poor preservation through the activity of slope processes and outwash streams.

A series of ridges is stacked on the hillside above the Fljótsdalur farm. These landforms are partially covered by >4 m deep soils and in places are best revealed due to exhumation by recent streams and soil erosion which has resulted in extensive roftbard formation. Five ridges were identified in the field from around 2 to 5 metres in height, all of which are characterised by their orientation which strikes across the hillside approximately ENE to WSW. The ridges are primarily composed of massive cobbles and gravels with a finer sand and granule matrix. The lowermost ridge has a more complex composition combining massive diamict-like deposits, similar to those that make up the other ridges, with sorted sands and gravels.

Further glacial landforms are found along Langanes and where Gigjökull and Steinsholtsjokull extend towards the valley floor from Eyjafjallajökull (Dugmore 1989) and in Þórsmörk where caldera rim outlets of Mýrdalsjökull descend to lower altitudes. Haraldsson (1981) described gently dipping terraces in Fljótshlið that he interpreted as ice marginal and marine terraces.

4.5 Classification of glacial and fluvioglacial landforms

Glacial and fluvioglacial features in the Markarfljót valley have been identified and have been mapped as such in Figures 4.1.2 and 4.1.3.

Within the Upper valley limits S/E1-5 are similar in form and composition to terminal moraines, being ridge-like, un-branching relatively linear features composed of diamicton and orientated across valley. Limits SM and B are similar in their shape but their positioning may be more controlled by local topography, representing terminal or semi-lateral ice positions on Stóra-Mófell and in the Botn basin. Lateral ridges in the upper valley are similar to these limits but are located on valley sides and thus are lateral ice-marginal features including morainic and fluvioglacial deposits. The ridges identified in the middle and lower valleys are less distinct, but again are linear ridges composed of diamict, predominantly located on valley sides and thus are older lateral moraines.

The fluvioglacial features most resemble a combination of eskers, kettle and kame topography (ice-stagnation topography) and ice-marginal meltwater channels. The sinuous ridges are more like eskers than moraines, despite their ridge-like form, since they are sinuous, branching and are orientated approximately in line with ice-flow direction rather than cross-valley. The depressions with intervening ridges resemble kettle and kame topography, the chaotic landscape left from the melt-out of ice blocks. Channels draining from these regions emphasise the possibility of drainage from ice block melting. The much larger cross-valley channels are associated with small-scale glacial limits and are disproportionately large in comparison to their present-day streams and thus are considered to be past ice-marginal drainage channels.

4.6 Large-scale fluvial landforms in the Upper Markarfljót

Overlain and cross-cutting these glacial and glaciofluvial features are a suite of landforms which cannot easily be explained by glacial processes.

Entujökull foreland

The Entujökull 'Sandar' *(Icelandic for 'sand')* areas on the two plateaux are characterised by a covering of black tephra and sand-rich material, frequently with a frost-shattered lithic lag. Abandoned networks of channels cover these surfaces. Where channels meet the margins of these plateaux the channel bed tends to be eroded down in to the underlying lava with polishing of this base rock, pothole formation terminating in cataract features at the plateaux margins.

The eastern plateau surface extends for approximately 1000m down-valley of ridge 2A and covers an area of ~0.75km2. Sections dug through this surface show that the overlying deposit is primarily composed of crudely bedded vesicular black tephra with some sand to gravel sized lithics. No soil was found beneath this material, although this may be because the poorly consolidated nature of the deposit prevented deep pits being dug through infilling.

A dry, broad, dendritic channel extends from ridge 2A across this eastern plateau surface. Streamlined mounds are located within the channel composed of vesicular black tephra, sands and gravels and with a surface scatter of boulders which reach up to 1.2m in diameter. At the eastern end of the channel a broad smooth, gently sloping terrace extends from ridge 2A, dividing the upper channel into two. Downstream of ridge 2Aand this terrace the channel narrows and becomes braided. The channel floor at this point becomes unevenly covered in sediment, with clusters of boulders and sections where the underlying lava is exposed. This exposed lava is smooth and has small-scale step-like cataract features. Where the channel meets the margin of the plateau it is eroded into the underlying lava with rock-cut walls, terminating in a dry cataract and cliff.

Associated with this eastern surface is a southern linear ridge that extends westwards from ridge 2A along the line of the southern channel. This ridge is sharp-crested and unvegetated, with slopes of ~45 degrees. The ridge crest extends eastwards and overlies the western face of ridge 2A. It is composed of black sand and gravel material similar in nature to the deposit that overlies the eastern lava surface. Frost-shattered boulders and cobbles litter the surface of the ridge but are not extensively found within the deposit.

To the north west of this eastern 'Sandar' area is another, topographically more uneven area composed of similar tephra-rich black sands with a surface bouldery lag. This area is composed of a horseshoe-shaped, rock-cored ridge with overlying unconsolidated material, which approximately follows the line of the more northerly gorge.

A similar sandur deposit also overlies the western lava surface. As well as the characteristics already noted above, this surface is more uneven in topography having occasional mounds and depressions between distinct channels. Close to the eastern edge of the sandur area there is a string of disconnected smaller ridges and mounds. Three main channels cross the main plateau, each having anabranching forms and terminating in cataracts at the plateau edge. The downstream sections of these channels all erode down in to the underlying lava, with sections of polished bedrock on the channel floors and rock-cut channel sides close to the cataracts. Channel 3 shows particularly tall rock-cut channel floor up to 12m in height and with a concave shape (Figure 4.6.1) and large palagonite and basalt boulders in the channel bottom (Figure 4.6.2). Between these channels and the intervening mounds there are small areas of polished and striated outcrops of lava. These features tend to be more smoothed on the

southeastern edges and craggy to the northwest, some with diamict emplaced around them forming streamlined mounds.

Botn basin

The Botn basin is effectively described by Townsend (1987):

'A truly blasted, inhospitable landscape surrounds this haven (the Botn hut), *a scene wild and inhumane more lifeless and totally 'other worldish' than any place in any mountains I have ever passed through... The black mounds .. are the only natural phenomena I've ever encountered that rival in desolation the emptiness of abandoned industrial landscapes' (p.220)*

This quote stunningly emphasises how black mounds of basaltic tephra-rich sands dominate this basin, although it may somewhat over-emphasise the barrenness, an aspect as much controlled by the variable mountain weather as the landscape. These black mounds fill the basin up to an elevation of 500m and appear to have been dissected by later channels.

The thickness of these deposits varies, reaching just a thin (<2 m) spread of material at the edges, to at least 23 m in the centre of the basin (profile 115). In places this sandy material appears to be homogeneous and massive. However, throughout the basin the upper sections of the unit show cross bedding and where the deposit is thinner towards the western edge of the basin further bedding and sub-divisions of the unit are identifiable. Diamicts, gravels, finely laminated silts and sands, and soils with tephra layers have been found beneath this black sandy material.

A particularly dark black streamlined hill is located within the centre of the basin. This landform is very similar in form to the other black or dark grey mounds surrounding it in the basin. However, it seems that it is composed of a higher percentage of basaltic tephra than the other features (hence the colour) and is characterised by distinct metre-scale ripples across its surface. These asymmetrical ripples are orientated with crests running approximately downslope although they are mostly sinuous. These large surface ripples have an average wavelength of ~8 m and height of 50cm. The coarsest material is concentrated along the crests of the ripples and they are stabilised by grass and moss growth along their westward slopes. When dug into, the ripples show no interior structure. Further ripples are located along the western edge of the basin. Again they are orientated with crest approximately downslope and reach <1 m in height.

Stora-Mofell

Stóra-Mófell flood topography mainly consists of channels between moraine ridges. These channels are filled with tephra-rich sands with lithic lags on the surfaces. The largest channel dissects the outer

'zigzag' ridge and originates close to the cliff edge to the south. Potholes up to 12cm in diameter and up to 15cm deep are found over much of the exposed bedrock area to the north of the zigzag moraine (Figure 4.6.3). Small, rounded pebbles and gravel are found at the base of many of these potholes.

Sléttjökull foreland

Channels with >5m high terraces, feeding in to gorges and channel areas with polished bedrock are found downstream of the Sléttjökull foreland. These terraces are composed of crudely bedded black sands including black tephra and lithics. There are no visible soils below these deposits or fine-scale structures within them.

4.7 Large-scale fluvial landforms in the Middle Markarfljót

The Middle Markarfljót is dominated by channel landforms, either sedimentary or carved into the underlying lava flows that fill the valley bottom. Many features associated with the channels resemble those of scabland topography made famous by Bretz (1932) and Baker (1973).

Overlain and eroded into these postglacial lavas are assemblages of landforms indicative of large-scale fluvial erosion. These can sub-divided into the following categories:

- Gorges
- Streamlined erosional hills
- Scabland features – cataracts, polished and scoured lava surfaces, potholes,
- Other channels on different scales including abandoned channels with associated terraces, bars, and boulder deposits.
- Streamlined loess mounds

Gorges

The Markarfljótglufur is a gorge up to 100m deep in places extending from both the Emstrur and Entujökull areas, joining to form a single valley-central gorge, and reaching as far as the valley sandur near Húsadalur in Þórsmörk. The gorge from Emstrur to Markarfljótsaurar is ~13 km long and is cut through at least two layers of lava with more complex geology, including breccias, red iron-rich scoria, moberg often overlying lake deposits. Rock-cut benches on two levels are found within the gorge. Bars and sedimentary channels overlie some of these benches.

A smaller gorge, Tröllagjá, runs from Einhyrningsflatir along Fauskheiði, meeting with the main Markarfljót gorge just upstream of Húsadalur. The gorge is mainly dry now, with recent snowmelt

channels in the base. Tröllagjá reaches ~3 km in length and has walls cut through the postglacial lavas of up to ~10m in height. Deposited within and at the start of the gorge are bars and terraces composed primarily of black tephra-rich sands. These gorges are associated with cataracts, potholes and tributary channels. Sand deposits are in places draped over the margins of these features, similar in nature to sand deposits on the lava through which they are cut.

Streamlined erosional hills

Two large erosional hills, streamlined with' moats' or channels running either side of them are found in the middle valley. The first, Klappir, is 15m high with a low channel in the lava which runs to the north and south of the hill. The 'moat' has tributary channels in the surrounding lava. There are bars at both the upstream and downstream ends of the hill.

The second hill in northern Þórsmörk is mainly composed of palagonite and is surrounded by scabland lava flow topography. The channels around this hill are much deeper than at Klappir (Figure 4.7.1) reaching up to 15-20m in depth along the northern margin. Channel sides are vertical with overhangs and collapsed faces. Tributary channels upstream lead into the major channels resembling the margins of a large cataract. The channel floors are covered with swathes of black vesicular tephra and lithic sand. In particular streamlined sandbars are located on the floors of the channels and in the lee of the hill. There is little soil in the channels although there is some preserved beneath the black sands close to the cliffs and also on the higher vegetated margins of the central streamlined hill.

Scabland features

Cataracts are associated with many of the smaller-scale channels found on and around the lava surfaces. These features forms steps in the channel ranging from <10cm to >2m in size. Upstream of the cataracts there tend to be polished channels within the lava with small-scale over-deepened gouges and potholes in places. Table 4.2 describes the main cataract features recorded. Clear examples of these cataract features were surveyed and field-mapped in detail to show the orientation and relationships between the main landform and related small-scale structures. Figure 4.7.2 (A and B) illustrates the appearance and key features of this landform. Unlike the large Tröllagjá cataract, which has an impressive pothole with overhanging walls the Fauskheiði feature is wider and probably significantly infilled with water- and wind-transported material. In particular this example shows how gouges and scratches on the lava surface are orientated radiating from the axis of the cataract. This points to formation by a large-scale flow with erosion by clasts in transport and cataract formation at points of flow concentration.

Potholes are found throughout the area on different scales (from centimetres to metres). Mainly they are small-scale and apparently independent of other features. Large potholes are found at the base of

cataracts. Whatever scales the features are found on they tend to be infilled with debris. The size of clasts within the bases of potholes varies depending on the scale of the pothole although they tend to be rounded.

Lava surfaces within the limits of the valley-scale flood channel show evidence of post-depositional erosion and deposition. Less modified parts of the lava surface show a ropy texture. However, where erosion has occurred surfaces are smoothed, sometimes with gouges and scratches. Polished channels are also found on these modified surfaces. The dendritic polished channel system south of Klappir (Figure 4.7.3) is clearly indicative of erosion from a large-scale flow. It closely resembles in appearance Nye channels that are formed by pressurised flows of water beneath glaciers. However, the lava into which it is carved is postglacial (Johannesson 1990) and therefore another high-pressure flow must be evoked to explain its formation.

On top of the valley-central lava flows there is an uneven covering of vesicular black tephra up to granule size. The thickness of this layer varies and in places the black sand forms drifts or mounds several metres thick, particularly when found in the lee of cliffs and uneven terrain. This material has been deposited on top of the lava after it was formed, probably either through flood or wind action.

Channels

The extent of all this flood geomorphology is confined within a large valley-scale channel, bounded by eroded terraces of soil and stratified deposits between the foot of Einhyrningur and the northern edge of the Markarfljót gorge. Continuation of these northern valley-side terraces is found at Fauskheiði. These terraces are approximately 2 km in length and 1-5m high, forming three levels of terrace gently stacked on the low valley side. The deposits within these terraces are discussed in detail in chapters 5 and 6. The eastern / southern margin of the flood geomorphology is less distinct, and is marked more by the extent of related deposits rather than distinct landforms.

Within this valley-scale channel there are multiple abandoned channels that run beside and over the lava flows. Many of these connect up with the much large gorge system. The biggest channel by far runs (approximately E-W) and is ~900 m wide and ~2 km long. This large abandoned channel can be traced upstream along much narrower valleys to the top of the cliff that borders the southern margin of the Entujökull foreland. Terraces composed of sands and gravels mark the margins of this big channel. Within the channel there are widespread bars, some composed of large boulders, and a lag of gravel, sand and boulders across the entire feature. Imbricated boulders are common, particularly towards the western end of the channel (downstream). These deposits are composed of two boulders stacked against one another, and are indicative of deposition from a flow. The western edge of this channel is marked by scabland topography with typical polished channels, cataracts and gouges.

Elsewhere, particularly in association with smaller-scale abandoned channels and terraces, 'erratic' boulder deposits were identified. These may be orientated with long-axis parallel or perpendicular to the valley axis. It should be noted that although these types of deposit are most commonly associated with glacial action these boulders are found in locations stratigraphically above postglacial lavas.

Streamlined loess mound

Úthólmar is a streamlined ridge-shaped hill, reaching ~20-25m in elevation above the surrounding lava flows and abandoned channel systems. This hill is mainly composed of palagonite with overlying soil and tephra deposits. The surface is mainly covered by a gravely, black tephra-rich lag. The ridge is higher in elevation to the northeast and has a low basin halfway along corresponding to a col into the Ljósá river valley.

4.8 Large-scale fluvial landforms in the Lower Markarfljót

Despite the dominance of the sandur and river action, which tends to remove or bury palaeo-environmental evidence, valley side terraces and streamlined islands have been preserved. These have primarily provided sedimentary evidence for flood activity, being composed of bedded soils, tephra layers and diamicts. However, their present form is consistently streamlined and all these features are covered by a surface gravely lag with a black tephra-rich matrix.

Terraces are found along the northern valley margin and are particularly clear around the Kanastaðir area and east of Gilsá to where the valley central lava flows meet the sandur plain north of Húsadalur. Two streamlined islands are found in the sandur between Gilsá and Þórsmörk. The largest is linked to the northern valley margin by a small causeway and is easily accessible. The smaller 'island' is located in the middle of the sandur is completely surrounded by outwash streams.

The larger 'island', unnamed on the map and referred to as Halli-Island because of sown-grass graffiti found on it in the summer of 2002 (Figure 4.8.1) has two elongated ridges that run NE-SW and a low basin in between. A core of diamict is evident in a section cut by the present Markarfljót. This diamict is overlain by soils, tephra, diamicts and gravels, which are discussed in chapters 5 and 6. This 'island' may be associated with 10-15m high mounds and small ridges that are similarly aligned towards the northern valley margin to the NE. These aligned mounds and the diamict core may represent an old ice limit ridge that has long since been dissected and buried by more recent deposits. The streamlined form of these features and their surface lag suggests that they may have been shaped by a large-scale flow event.

4.9 Classification of large-scale fluvial landforms

Large-scale fluvial features in the Markarfljót valley have been identified in comparison with documented examples described in Chapter 1.3. The features found in the middle valley are most similar to the classic features discussed by researchers of flood erosion and deposition in bedrock valleys such as the Channelled Scablands. The range of landforms closer to the ice in the Upper Valley are less distinctive. However, their forms are similar to features found along the south coast at Skógasandur and Mýrdalssandur. The assemblage of landforms here and their association with glacial features leads to the interpretation as flood forms, set in a complex landscape representing the action of volcanic, glacial, periglacial and large-scale fluvial activity.

Chapter 5: Results

Tephras

5.1 Introduction

Analysis of the Markarfljót sequence of tephra layers and intervening soil horizons has allowed the development of an extended Markarfljót tephra stratigraphy, developing from the work of Larsen (1978), Dugmore (1987) and others (Thorarinsson 1967, Larsen et al 2001). This provides a chronological context in which to place other events recorded in the sedimentary sequence, such as flood and glacial activity and allows connections to be made between the 173 profiles recorded in this thesis. The development of this tephra stratigraphy is important, both as a tool for understanding the chronology of events in the area and as a method of linking the various strands of environmental evidence obtained from sedimentary logs throughout the valley.

173 profiles were recorded, the locations of which are illustrated in Figure 5.1. Full details are in Appendix 3. Altogether a maximum of 98 tephra layers have been recorded in the deepest sections in the sediments of the Markarfljót valley. Most of these layers are coarse-grained blue black, brown black or coal-black, basaltic layers from the nearby volcano Katla. Prehistoric black tephras may be bedded and tend to be coarser than the historic black tephras which tend to be predominantly silty. Unique identification of these layers based on colour, grain size or chemical characteristics obtained by major element analysis, is difficult (Larsen 2000). However, the relationships between these black layers and other visually or chemically distinctive layers can sometimes allow accurate identification to be carried out. Pale layers range in colour through various hues of white, yellow, olive, and greyish blue. Most layers have very fine grains in the size ranges silt to very fine sand. Certain layers reach coarse sand size. At least four of the yellow/olive layers have elongated 'needle' grains ranging in size from less than 1mm to around 1cm in length and up to 2mm in thickness.

In order to differentiate between these pale layers and to confirm visual identification and field correlations geochemical analyses of key layers was carried out. 87 tephra and tephra-rich samples were analysed, a total of ~1400 analyses. The chemical composition of the analysed tephras show medium to high potassium and silica / alkali ratios that vary from basalt (~44-48% silica) through basaltic andesites, andesites, dacites to silica rich rhyolites (up to ~73% silica) (Figure 5.1.1). Within this spread of data two main components can be visually picked out. Figure 5.1.1a shows a tight cluster of basaltic analyses, which have around 45-54% silica and approximately 4% alkalis. The second cluster is less compact but centres in the dacitic field. A spread of data lies between these clusters and extends into the rhyolitic field

with up to 73% silica and 10% alkalis. Many of the samples analysed were bimodal with some shards characterised by basaltic and others by dacitic or rhyolitic compositions. The correlation of profiles is primarily based upon field identifications of the distinctive pale, higher silica, tephra layers, and is backed up by geochemical analyses.

5.2 Reference profiles and key layers

Reference profiles provide data on the tephra stratigraphy of the area. These profiles are all from soil above the level of the channels and flood-type geomorphology in the valley bottom, providing a reference tephra stratigraphy undisturbed by any potential flood or other fluvial activity. From this stratigraphic framework, correlations can be made between more fragmentary profiles throughout the valley. A composite stratigraphy for the Markarfljót has been compiled from the longest stratigraphic sections in the area on hillsides above the valley bottom, and is illustrated in Figure 5.2.1. The thicknesses shown here are not to scale since this figure is purely intended as a schematic guide to the tephra stratigraphy of the area. Specific profiles used as references for this composite diagram are shown in loose-leaf tephrochronology diagrams appended. Other profiles discussed in the text will be illustrated as referred to. Each set of distinctive layers is described below, starting with the youngest, uppermost historic layers.

Historic sequence

The stratigraphy presented here is based upon reference profiles recorded at Seljaland (171), Smjörgíl and Langanes (12, 14, 23, 31), Fljótshlið (152), Kanastaðir (55) and shallow reference profiles in Emstrur (122). Comparisons have been drawn between stratigraphic relationships identified between these new profiles and those recorded by Dugmore (1987) and Larsen et al (2001). Table 5.1A summarises the key layers.

Hekla 1947, Seljaland A and B. The highest set of key tephra layers is composed of two thin, fine-grained upper tephras and a lower very coarse dark pumice layer. This lower coarse dark pumice is usually the uppermost layer in the stratigraphy of the Markarfljót and is often incorporated in to the root mat very close to the surface. The two highest tephras were found only at Seljaland (profile 171).

Hekla 1947: Over the majority of the area, the uppermost key tephra layer found throughout the region is highly distinctive. A very coarse to coarse, dark pumice with blue-black to dark grey and pale brown grains, usually with red scoria fragments, is found within the first 10 cm of soil across the area. The grain size varies and reaches a maximum of 2.5cm, in Fljótshlið. The tephra layer also varies considerably in thickness. Areas to the east, in Emstrur and northern Þórsmörk, only tend to have a single grain thickness,

TABLE 5.2A: HISTORIC KEY TEPHRA LAYERS

Tephra layer	Colour	Grain size	Comments	References
V-E 1973 or H		fine	Eldfell, Heimey? Very thin trace of tephra, only found at Seljaland and along Langaness[1]	
V-E 1963 or H		fine	Surtsey? Only found at Seljaland and along Langaness[1]	
H 1947	Pale pumice, mainly brown with red and black grains.	coarse		Thorarinsson (1967), Murray (2002)
K1918	Black	fine		
E1821-3	White/grey	fine		
K1755	Black	fine	Not recorded at Seljaland	
K1721	Black	fine	Not recorded at Seljaland	
H1597	Brown pumice, includes red scoria grains.	coarse		
H1510 Mixed into in soil	Pale pumice, mainly Brown with red and black grains.	coarse		
K1500	Black	Fine		
H1341	Blue/grey	Very fine		
H1300	Pale pumice, mainly Brown with red and black grains.	coarse		
E934	Blue/black	fine	3	Larsen 1979, Hammer et al 1980, Zielinski et al 1995.
KR920	Black	coarse	R refers to Reykjavik	
V870 Landnám or Settlement layer	Upper (VII) olive green/brown with white plagioclase crystals. Lower (VI) is coarser and white/yellow	fine	Often the two parts of the tephra are mixed together particularly around Gigjökull although they tend to be separated further west in Landeyjar and up-valley, closer to the source.	

whereas to the west, in Fljótshlið, thicknesses within soil sections reach 10 cm. It is also noticeable here that thick drifts of this tephra are found across the hillsides and particularly at the foot of slopes.

This layer is from the large-scale eruption of Hekla in 1947. Murray (2002) found that thickness measurements of this tephra within the Markarfljót in the summer of 2001 showed considerable variation from the original measurements collected by Thorarinsson (1967) within the first two weeks after the eruption. Extensive clearing of farmland as well as natural reworking of the layer has significantly altered the pattern of deposition and preservation.

Seljaland A and B: These are both thin fine-grained tephras. The uppermost layer is dark grey / black and the one below is more bluish in hue. These colour characteristics suggest an origin from Hekla, however no similar layers have been found in the more northerly profiles in the Markarfljót, closer to the Hekla volcano. By calculating and extrapolating a soil accumulation rate of x cm per year since 1947 it appears that these thin layers were deposited in the early 1960s and 1970s. It is therefore possible that these tephras are associated with the eruptions of Surtsey and Heimaey in the nearby Vestmanneyjar in 1963 and 1973 respectively. Earlier work by Larsen (personal communication 2002) identified a thin fine dark tephra at Seljaland further suggesting that these two recorded in profile 171 are likely to be primary fall out layers and not reworked material from earlier eruptions. Geochemical analysis and further mapping of the distribution of these layers is necessary to confirm these identifications.

Eyjafjallajökull 1821-3. Below these most recent tephras there is a distinctive fine-grained white to grey tephra layer separated from H 1947 by one black tephra. This pale layer is around 0.5cm thick closest to Eyjafjallajökull at Gigjökull, Seljaland and Lambafellsheiði (profile numbers 12, 26, 31, 146 and 171) and thins to the north and east. Due to its distinctive colour it is clearly visible even as a trace in Fljótshlið, Kanastaðir and in northern Þórsmörk (profiles 55, 77, 82 and 152). The distribution and colour characteristics of this layer indicate that it is from the eruption of Eyjafjallajökull in 1821 – 1823.

Hekla 1510, Katla 1500. The next marker pair is composed of a fine to coarse-grained black tephra layer with a coarse, dark pumaceous layer mixed into the soil almost immediately above. This black layer tends to be thicker and coarser than the other black layers above. The pumaceous layer includes dark grey, pale brown and red scoria grains, similar but finer than H 1947. These two tephra layers are interpreted as the K 1500 and H 1510 couplet, a distinct pairing recorded by previous researchers in southern Iceland. Thorarinsson (1967; 58-63) discussed the characteristics and extent of the H1510 tephra and both Haraldsson (1981) and Dugmore (1987) used these two layers to correlate stratigraphic profiles throughout the Markarfljót area. The dominance of these layers in the youngest soils varies considerably over the area, as do the numbers and nature of intervening layers between Layer B and Sequence C.

Where there are a larger number of black tephra layers this pair does not stand out as being quite so distinctive. This couplet is particularly visible at Seljaland (profile 171, and Dugmore 1987) and across Landeyjar (Duncan 2000).

Historic SILK tephra, Hekla 1341, Hekla 1300, Hekla 1206. A triplet of tephras is found in the northern part of the Markarfljót area below K1500. In a few profiles this triplet is overlain by a pale yellow tephra, which will be discussed below. The uppermost layer is a fine blue-grey tephra layer and is probably from the eruption of Hekla in 1341. In profiles 83 – 85, 89 and 94 this layer is bedded with fine blue-grey tephra above and below a very fine pale blue-grey tephra. Geochemical analyses of samples from this bedded tephra confirm that is from Hekla (Table 5.2.1). Underlying this layer is a coarser blue-grey tephra with characteristic Hekla geochemistry (Table 5.2.2), probably Hekla 1300.

	SiO_2	TiO_2	Al_2O_3	FeO	MnO	MgO	CaO	Na_2O	K_2O	Total
Max (a)	59.36	1.80	16.65	11.87	0.31	2.49	5.73	4.77	1.86	98.89
Min (a)	56.80	1.14	13.05	8.53	0.19	1.32	4.93	3.39	1.37	96.36
Mean(a)	58.36	1.50	14.25	10.69	0.27	1.85	5.29	3.85	1.60	97.72
s.d. (a)	0.78	0.18	1.05	0.91	0.04	0.30	0.24	0.44	0.16	0.82
Max (b)	48.35	4.93	15.63	15.45	0.26	7.80	11.53	3.54	0.91	99.75
Min (b)	45.49	2.24	11.76	11.06	0.11	4.33	8.68	2.24	0.40	96.38
Mean(b)	46.55	3.71	13.56	14.00	0.19	5.80	9.85	2.91	0.61	97.18
s.d. (b)	0.72	0.98	1.28	1.27	0.04	1.14	0.73	0.35	0.17	0.83

TABLE 5.2.1: Summary of geochemical characteristics of possible H1341. From analyses 84-1 and 84-2.

	SiO_2	TiO_2	Al_2O_3	FeO	MnO	MgO	CaO	Na_2O	K_2O	Total
(a)	**58.76**	**1.34**	**14.85**	**9.89**	**0.23**	**1.88**	**5.26**	**3.50**	**1.63**	**97.34**
	58.67	**2.05**	**13.04**	**11.45**	**0.31**	**1.92**	**5.28**	**3.76**	**1.89**	**98.37**
	58.31	**1.48**	**14.61**	**9.93**	**0.25**	**1.98**	**5.31**	**4.07**	**1.44**	**97.36**
	57.70	**1.63**	**14.45**	**10.03**	**0.27**	**1.91**	**5.52**	**4.04**	**1.59**	**97.15**
mean	***58.36***	***1.62***	***14.24***	***10.32***	***0.26***	***1.92***	***5.34***	***3.84***	***1.64***	***97.56***
s.d.	***0.48***	***0.30***	***0.81***	***0.75***	***0.04***	***0.04***	***0.12***	***0.26***	***0.18***	***0.55***
(b)	47.41	4.75	12.22	14.77	0.28	4.81	9.33	3.19	0.74	97.50
	46.96	4.41	12.55	14.58	0.24	4.77	9.42	3.21	0.85	97.00
	46.76	4.78	12.55	14.53	0.24	4.77	9.39	3.14	0.79	96.95
	46.45	4.25	12.44	14.60	0.22	4.97	9.47	3.38	0.67	96.44
	46.44	2.25	15.29	11.02	0.20	7.82	11.75	2.36	0.34	97.46
	46.28	4.24	12.65	14.33	0.23	4.83	9.39	3.21	0.74	95.90
	46.06	2.90	14.85	13.46	0.20	6.63	10.19	2.80	0.45	97.54
	45.96	4.69	12.43	14.69	0.26	4.95	9.49	3.29	0.72	96.47
	45.76	4.61	12.51	14.49	0.29	5.25	9.74	3.04	0.67	96.35
	45.60	3.13	14.53	14.84	0.23	6.52	9.84	2.38	0.45	97.53
	45.60	3.00	13.97	13.79	0.21	6.35	9.97	2.86	0.48	96.24
	45.42	3.33	13.82	14.93	0.30	5.78	9.85	2.90	0.51	96.84
	45.23	3.28	13.99	14.46	0.23	5.81	10.11	2.87	0.47	96.46
mean	*46.15*	*3.82*	*13.37*	*14.19*	*0.24*	*5.64*	*9.84*	*2.97*	*0.61*	*96.82*
s.d.	*0.64*	*0.86*	*1.07*	*1.04*	*0.03*	*0.96*	*0.64*	*0.32*	*0.16*	*0.56*

TABLE 5.2.2: Analysis 94-2. Possible H1300. Data in bold type is similar to Hekla-S type chemistry, suggesting an origin in the Hekla system.

In sections near the Markarfljót bridge (160, 161), in northern Þórsmörk and in the Entujökull foreland there is a layer that underlies H1341 and H1300. This lowermost layer is coarse grained, with both pale grey-yellow grains and dark grey/black grains. Sometimes the layer is mixed and appears dark greyish, but mostly it is divided up into layers of different colours. Thickness reaches around 3cm at the most. This layer is not found near Einhyrningur or further down-valley. The colour characteristics and grainy nature of this layer suggest that it is from Hekla. It is most similar to the prehistoric Hekla tephra H-M, although with somewhat more subdue colours (slightly less yellow-orange). Stratigraphic relationships with the overlying blue-grey tephras and in relatively shallow soils (mostly <1 m) indicate, however, that this is a historic tephra layer. The eruption of Hekla in 1206 AD deposited tephra to the east of Hekla (Larsen et al 1999). H-1206 may be grainy in this area, with lighter grains with a greyish-yellow to brownish-grey colour and dark upper fraction where present, and thus is a likely candidate for this layer (Larsen, pers. comm. 2003).

The pale yellow tephra above the Hekla 1341-1300-1206 triplet is found as a trace in soils in North Þórsmörk. In profile 89 located on a terrace within the Markarfljót gorge in North Þórsmörk a trace of pale yellow tephra overlies a fine dark tephra (H1341) above the E935-KR920-V871 triplet. Geochemical analyses of this trace of pale tephra above the bedded grey tephra (H1341) in profiles 83 and 94 shows more similarity with silicic Katla tephra than any documented historic layer (Table 5.2.3). Analyses of the traces of tephra in 83 and 94 have different silicic Katla type characteristics. 83-2 has higher silica values similar to older SILK tephras while 94-1 is closest to SILK YN in chemical composition. This does not necessarily indicate that they are from two different eruptions since Larsen et al (2001) indicate that the composition of tephra produced in silicic eruptions of Katla varies during the eruption with the most silicic (>70% SiO_2) material produced at the start of eruptions. In fact they also note that the most silicic material does not usually get incorporated in to tephra layers in nearby soil since this material is erupted prior to the eruption breaking through the overlying ice cover. Casely's (2001) geochemical data from analysis of the H1341 tephra includes SILK-type shards (Larsen pers comm., Table 5.2.4). Re-logging of this profile indicates that a trace of pale tephra overlies the grey tephra analysed by Casley (profile 170). There is no clear erosional unconformity within this section and these layers lie above the E935-KR920-V871 triplet placing them in the historical sequence. These profiles indicate that a historical silicic eruption of Katla may have occurred soon after the eruption of Hekla in 1341, possibly c.1357. This layer is only found close to the ice margin in Þórsmörk as a trace within soil, suggesting that the eruption was only small and that tephra distribution was limited.

83-2: 885C

	SiO_2	TiO_2	Al_2O_3	FeO	MnO	MgO	CaO	Na_2O	K_2O	Total
	69.93	**0.23**	**12.98**	**3.43**	**0.13**	**0.15**	**1.05**	**4.34**	**3.92**	**96.15**
	49.65	1.76	13.44	12.36	0.21	6.75	11.56	2.39	0.20	98.30
	49.64	1.89	13.24	12.63	0.27	6.65	11.03	2.46	0.27	98.08
	49.38	1.88	13.14	12.54	0.20	6.54	10.91	2.48	0.23	97.30
	47.62	4.53	12.40	14.46	0.24	4.68	9.04	3.22	0.84	97.03
	47.24	4.41	12.54	13.67	0.28	4.91	9.50	2.97	0.81	96.32
	47.04	4.57	12.36	14.85	0.27	4.87	9.32	3.15	0.76	97.18
	46.98	4.58	12.64	14.45	0.24	4.97	9.37	3.17	0.77	97.16
	46.78	4.63	12.17	14.35	0.27	4.77	9.16	3.29	0.82	96.23
	46.75	4.62	12.36	14.28	0.27	4.89	9.21	3.14	0.78	96.30
	46.74	4.83	12.28	14.83	0.26	4.76	9.08	3.17	0.75	96.70
	46.35	4.11	12.75	14.24	0.26	5.01	9.37	3.20	0.75	96.03
	46.06	4.61	12.32	14.94	0.22	4.93	9.58	3.06	0.70	96.41
	45.98	4.13	12.61	14.68	0.22	5.01	9.39	3.38	0.72	96.12
mean	*47.40*	*3.89*	*12.63*	*14.02*	*0.25*	*5.29*	*9.73*	*3.01*	*0.65*	*96.86*
s.d.	*1.31*	*1.18*	*0.40*	*0.92*	*0.03*	*0.78*	*0.84*	*0.34*	*0.24*	*0.73*

94-1: SLIDE 1: North Þórsmörk H4? 13/8/2001-3

	SiO_2	TiO_2	Al_2O_3	FeO	MnO	MgO	CaO	Na_2O	K_2O	Total
	68.99	**0.95**	**13.83**	**5.17**	**0.14**	**0.76**	**2.32**	**4.39**	**3.10**	**99.65**
	68.52	**0.87**	**13.74**	**5.44**	**0.12**	**0.79**	**2.20**	**3.90**	**3.33**	**98.90**
	67.99	**1.03**	**13.90**	**5.08**	**0.13**	**0.80**	**2.57**	**4.05**	**3.08**	**98.62**
	66.39	**1.06**	**13.99**	**6.46**	**0.14**	**1.10**	**2.95**	**4.56**	**2.78**	**99.44**
	66.38	**1.05**	**13.98**	**5.99**	**0.14**	**0.99**	**2.71**	**4.40**	**2.73**	**98.38**
	66.26	**1.12**	**13.92**	**5.93**	**0.13**	**1.13**	**2.85**	**4.51**	**2.69**	**98.55**
	66.13	**1.16**	**13.90**	**5.93**	**0.13**	**1.14**	**2.92**	**4.53**	**2.73**	**98.56**
	66.04	**1.21**	**14.01**	**6.03**	**0.21**	**1.05**	**3.11**	**4.52**	**2.87**	**99.05**
	66.00	**1.23**	**14.10**	**6.07**	**0.15**	**1.10**	**3.08**	**4.48**	**3.03**	**99.24**
	65.97	**1.24**	**14.02**	**6.22**	**0.23**	**1.16**	**3.00**	**4.39**	**2.73**	**98.97**
	65.86	**1.14**	**13.79**	**6.50**	**0.22**	**1.10**	**3.07**	**4.05**	**2.74**	**98.46**
	65.79	**1.10**	**13.72**	**6.04**	**0.20**	**1.05**	**2.89**	**4.51**	**2.83**	**98.14**
	65.75	**1.27**	**13.93**	**6.11**	**0.21**	**1.09**	**2.86**	**4.45**	**2.65**	**98.32**
mean	***66.62***	***1.11***	***13.91***	***5.92***	***0.17***	***1.02***	***2.81***	***4.36***	***2.87***	***98.79***
s.d.	***1.11***	***0.12***	***0.11***	***0.44***	***0.04***	***0.14***	***0.29***	***0.22***	***0.20***	***0.46***
	49.87	3.85	12.80	13.05	0.24	4.32	8.57	3.39	1.12	97.21
	48.50	4.12	12.69	13.59	0.24	4.56	9.05	3.21	1.02	96.97
	46.51	4.45	12.62	14.47	0.27	5.20	10.04	3.02	0.73	97.33
	46.43	4.54	12.60	14.43	0.19	5.15	10.22	2.88	0.71	97.15
	46.28	4.57	12.43	14.09	0.23	5.06	9.88	2.94	0.76	96.24
	46.08	4.51	12.55	14.65	0.25	5.18	9.83	3.14	0.70	96.89
mean	*47.28*	*4.34*	*12.61*	*14.05*	*0.24*	*4.91*	*9.60*	*3.10*	*0.84*	*96.96*
s.d.	*1.55*	*0.29*	*0.13*	*0.62*	*0.03*	*0.38*	*0.64*	*0.19*	*0.18*	*0.39*

TABLE 5.2.3: Geochemical data for samples 83-2 and 94-1. Data in bold indicates a similarity with silicic Katla tephras.

Ref.	Field ID*	SiO_2	TiO_2	Al_2O_3	FeO	MnO	MgO	CaO	Na_2O	K_2O	Total	Interp made here
AS_K R2/D	H1341 ?	72.96	0.17	*11.32*	2.65	*0.02*	*0.02*	0.42	*4.25*	4.16	95.97	bit like A1
AS_K R2/B	H1341 ?	70.49	*0.29*	13.03	4.13	0.16	0.22	1.24	4.75	3.54	97.85	like A1 mostly
AS_K R2/J	**H1341 ?**	**65.55**	**1.26**	**13.9**	**6.44**	**0.16**	**1.13**	**3.26**	**4.61**	**2.85**	**99.16**	**like SILK YN**
AS_K R2/H	H1341 ?	58.7	1.25	14.85	9.59	0.32	1.82	5.47	4.1	1.53	97.63	like HS
AS_K R2/C	H1341 ?	58.25	1.36	14.31	10.48	0.28	2.04	5.54	3.88	1.62	97.76	like HS
AS_K R2/K	H1341 ?	57.96	1.69	13.94	10.04	0.29	1.89	5.35	4.35	1.65	97.16	like HS
AS_K R2/A	H1341 ?	57.47	1.76	12.73	11.51	0.28	2.07	5.4	3.71	1.75	96.68	like HS
AS_K R3/B	H1300 ?	68.08	0.89	12.97	5.7	0.17	0.59	2.09	4.11	3.32	97.92	Hekla or Katla?
AS_K R3/E	H1300 ?	67.44	0.82	13.06	5.78	0.17	0.57	2.31	4.26	3.05	97.46	Hekla or Katla?
AS_K R3/D	**H1300 ?**	**67.36**	**0.88**	**13.14**	**4.78**	**0.16**	**0.6**	**2.03**	**4.66**	**3.06**	**96.67**	**like SILK YN**
AS_K R3/C	**H1300 ?**	**65.35**	**0.97**	**13.83**	**6.25**	**0.2**	**0.79**	**2.76**	**4.52**	**3**	**97.67**	**like SILK YN**
AS_K R3/A	H1300 ?	47.65	4.24	12.25	14.61	0.32	4.52	9.11	3.32	0.98	97	Katla Basalt

TABLE 5.2.4: KROSSÁRJÖKULL DATA FROM CASELY (2001). Possible reinterpretation.

* indicates field identifications made and interpretation from Casely (2001). Bold text indicates analyses of glass shards similar in chemical composition to SILK YN silicic Katla tephra.

Eldgjá 935, Katla R 920, Veiðivötn 871. A highly distinctive triplet of tephras is found across most of the area, up to 2 layers below possible H1206. The uppermost tephra is a fine-grained and blue to dark grey in colour and is from the Eldgjá eruption of ~AD935. It is found throughout most of the area, although it was noticeably lacking in the profile at Seljaland (no.171). This tephra was erupted from the fissure swarm to the north of Mýrdalsjökull / Katla , perhaps explaining the lack of deposition at Seljaland, the area farthest from its source. Almost immediately below this is a thick (5-15 cm) coarse black tephra, Katla 'R' (Reykjavík: so called because ash fell in Reykjavík) dating from c.920AD (Dugmore 1987). The lowermost layer, called the Landnám layer, is unique throughout the entire Holocene sequence in this area, although lacking at Lambafellsheiði (no.146). It is greenish brown in colour with white plagioclase feldspar crystals mixed into it. In Landeyjar and in northern areas of the middle valley (152, 165 and Duncan 2000) a thin fine yellow to orange fraction is found immediately below this upper greenish brown tephra. This pale layer is not visible in Northern Þórsmörk (77, 82) or in Langanes. As well as being very easy to distinguish in the local stratigraphy and thus being a useful correlative horizon, the Landnám

layers conveniently mark the recognised arrival of Norse settlers in Iceland. The Norse settlement of Iceland or land-taking (Landnám) has been dated from historical accounts to AD 870 (ÍF 1 1968:4). The Veiðivötn layers have been dated to 871±2AD from studies of the Greenland ice cores (Gronvold et al 1995). This triplet is highly recognisable in the field as well as geochemically and marks the boundary between prehistoric and historic environmental events.

Prehistoric sequence

The prehistoric stratigraphy is based upon new profiles recorded in the Markarfljót and is defined as being those layers found below the distinctive Landnám layer. This record is more fragmentary and variable but particularly important for the correlation of Holocene sedimentary records. In this case, identification has been backed up by geochemical analyses of distinctive layers. See Table 5.2B for a summary of stratigraphic characteristics.

Layer 'H' and SILK YN. The uppermost prehistoric marker layers are two pale tephras separated by one to two coarse black tephras. Most often there is only one black layer between them. However, in Northern Þórsmörk (profiles 81, 82, 91, 100) two to three black tephras are found. Casely (2001) also found two black layers at the same stratigraphic location in Goðaland, around Tungnakvíslarjökull and Krossárjökull.

The upper pale layer is a fine pale yellow to white tephra and tends to include both coarser (coarse sand sized) pale pumice grains and dark basaltic grains. This layer is thickest (2 cm) around Eyjafjallajökull, particularly in the soils that make up the fans near Gigjökull and also at Lambafellsheiði. Northwards and to the northeast, upvalley and in Fljótshlið this layer is still visible in the soil although in places is only very thin (less than 0.5cm thick). Around Gigjökull there are two visible and chemically identical layers (profiles 10, 21, 31 and 32, analyses 31-3, 32-2) separated by up to 2 cm of soil in the same stratigraphic position as this upper pale tephra elsewhere. The upper layer of this 'split' tephra is not mixed, is very continuous over stretches of greater than 100m and thus appears to be a primary airfall layer.

The chemistry of this upper pale tephra is bimodal, with a basaltic element with SiO_2 between 45.67% and 52.24% and a rhyolitic element with 68.54 to 71.49% silica (Table 5.2.5, Figure 5.2.2). The basaltic component is compositionally homogeneous (transitional alkaline, medium K calc-alkaline series) and the silicic is a little more variable (transitional alkaline to alkaline, medium to high K). The silicic component of this tephra layer is similar in composition to tephra produced by Eyjafjallajökull in 1821 (Dugmore et al 2000), though somewhat less homogeneous. Dugmore (1987) refers to a pale tephra he terms 'Layer H' (the "Hoftorfa" tephra) from Gigjökull to Þórsmörk and on Lambafellsheiði stratigraphically below the E935-KR920-V871 complex (Sequence D). Layer H has been attributed to Eyjafjallajökull, based on

TABLE 5.2B: PREHISTORIC KEY TEPHRA LAYERS

Tephra layer	Age	Source	Colour	Grain size/ shape	Comments	References
Layer H	c.600 AD	Eyjafjallajökull	pale yellow/white tephra with pale pumice and dark grains	Fine Pumice inclusions coarser	Divides into two horizons near Gigjökull.	Dugmore (1987)
SILK YN[4]	c. 420AD	Katla	Pale olive/yellow	Fine includes small needles	Subdivides into a lower needle-rich layer ~x cm thick with larger yellow/brown fine pale layer immediately above, in Northern Þórsmörk area.	Larsen et al (2001)
SILK UN	c.2660B P	Katla	Pale olive/grey	needle grains visible to the naked eye	Very distinctive needles, more so than other needle layers.	Larsen et al (2001)
Layer St (H-M, grainy layer)		Hekla	Yellow / orange / brown to base. Darker, black to top, possibly separate black layer above	Coarse		Dugmore (1987)
K-E		Katla	black	Bedded, coarse to fine.	Thickness increases downslope.	Larsen et al (2002)
H-S		Hekla	Blue grey, includes yellow layer or grains	Fine	Can look blotchy and mixed.	Larsen and Thorarinsson (1967)
SILK N4		Katla	Pale	Mainly fine		Larsen et al (2001)
K-N		Katla	black	Bedded, coarse to fine.	Thickness increases downslope.	Larsen et al (2002)
H4		Hekla	Blue grey upper, yellow layer below.	Fine to coarse	Mainly subdivided and thus rarely mixed.	Larsen and Thorarinsson (1967)

Ages of prehistoric layers are in 14C years BP. Prehistoric layers are referred to by names either given by other workers or referring to the localities in which they have been found in the study area. The SILK prefix refers to silicic tephra layers from Katla (Larsen et al. 2001).

thickness distributions. Analysis and distribution of this tephra layer suggests that it also originates from Eyjafjallajökull and is most likely 'Layer H'.

	SiO_2	TiO_2	Al_2O_3	FeO	MnO	MgO	CaO	Na_2O	K_2O	Total
max (a)	71.49	0.40	14.34	5.36	0.33	0.28	1.78	6.92	4.00	99.69
min (a)	68.54	0.19	13.29	2.89	0.10	0.05	0.68	4.09	3.02	97.27
mean (a)	69.46	0.30	13.87	4.42	0.15	0.14	1.10	5.40	3.53	98.36
s.d. (b)	0.53	0.05	0.22	0.40	0.05	0.04	0.21	0.69	0.21	0.64
max (b)	52.24	4.97	13.92	14.97	0.36	5.19	10.21	4.11	2.04	98.34
min (b)	45.67	2.87	12.00	11.86	0.15	3.54	7.07	2.97	0.73	95.89
mean (b)	48.18	4.11	12.68	13.83	0.22	4.50	8.84	3.31	1.06	96.75
s.d. (b)	1.96	0.55	0.52	0.82	0.05	0.57	0.93	0.31	0.35	0.53

TABLE 5.2.5: Summary of Layer 'H' reference profile data presented in this thesis. For data tables see appendix 1

	SiO_2	TiO_2	Al_2O_3	FeO	MnO	MgO	CaO	Na_2O	K_2O	Total
max	70.49	0.45	14.67	4.81	0.21	0.21	1.36	7.06	3.93	99.94
min	68.31	0.30	13.64	3.75	0.09	0.05	0.77	3.53	3.15	96.54
mean	69.13	0.36	14.10	4.29	0.15	0.13	1.10	6.14	3.50	98.88
s.d.	0.61	0.05	0.28	0.27	0.03	0.04	0.17	0.71	0.17	0.78

TABLE 5.2.6: Summary of E1821-3 reference profile data summarised from Larsen et al 1999.

The lower pale layer of the marker set is olive to yellow in colour and fine-grained. Thickness varies across the valley from less than 0.5cm at one profile on Fljótsdalsheiði (profile 59) to around 2cm farther south and east, in Langanes and Þórsmörk (91). In Northern Þórsmörk (profiles 81) this layer subdivides into a lower needle-rich layer 1.5 cm thick with a thicker yellow-brown pale layer immediately above. Profiles near Einhyrningur (profiles 163 and 165) in the middle valley show alternate bedding of a very fine pale yellow fraction and darker olive / brown tephra, sometimes with small (<1mm long) needles. In places the non-differentiated layer has small needles mixed into it. This layer is the uppermost pale tephra layer with characteristic needle-shaped grains found in this study in the Markarfljót valley.

This layer has a bimodal chemical composition. The silicic component is dacitic with silica content ranging from 65.07% to 72.63%(Table 5.2.7). Figure 5.2.3 shows that this dacitic component plots on the subalkaline to transitional alkaline field with medium to high K_2O. Although sometimes similar in appearance to Layer 'H' above (both being pale tephras) chemical analyses of the silicic components of both tephra layers show that this lower layer has reduced levels of SiO_2, Na_2O and K_2O and considerably higher levels of TiO_2, FeO, MgO and CaO. The chemical composition of this component is very similar to silicic Katla tephra analysed by Newton (1999) in the subdivision SILK A(1) which includes layers YN, MN, LN, N4, N1, A1 and A9 in order of increasing age(Table 5.2.8). SILK YN is the youngest recorded silicic tephra layer from Katla and has been radiometrically dated to 1660±12 BP (Larsen et al 2001).

The basic component of the tephra is basaltic, transitional alkaline with medium K calc-alkaline series characteristics. These characteristics are similar to basaltic tephra from intracaldera eruptions of Katla such as K1625 (Larsen 2000).

	SiO_2	TiO_2	Al_2O_3	FeO	MnO	MgO	CaO	Na_2O	K_2O	Total
max (a)	72.63	1.37	14.30	6.54	0.46	1.22	3.45	5.92	3.95	99.13
min (a)	65.07	0.15	12.76	3.39	0.08	0.14	0.89	3.76	1.73	96.52
mean (a)	66.15	1.08	13.80	5.88	0.19	1.01	2.87	4.37	2.82	98.17
s.d. (b)	1.35	0.19	0.26	0.56	0.07	0.20	0.42	0.32	0.34	0.60
max (b)	49.81	4.70	12.97	14.74	0.28	5.31	10.14	3.41	1.12	97.76
min (b)	45.92	4.02	12.35	12.83	0.14	4.30	8.66	2.86	0.63	95.70
mean (b)	46.63	4.47	12.58	14.07	0.20	5.07	9.78	3.05	0.76	96.62
s.d. (b)	0.88	0.14	0.15	0.49	0.04	0.24	0.37	0.15	0.11	0.52

TABLE 5.2.7: Summary of SILK YN reference profile single shard major element analysis data presented in this thesis (for data tables see appendix 1).

	SiO_2	TiO_2	Al_2O_3	FeO	MnO	MgO	CaO	Na_2O	K_2O	P_2O_5	Total
a											
Mean	46.28	4.56	12.62	14.75	0.23	4.89	9.97	2.72	0.71	0.72	97.44
S.d.	0.46	0.22	0.33	0.30	0.03	0.08	0.24	0.12	0.05	0.12	0.69
b											
Max	67.53	1.27	14.20	6.28	0.23	1.19	3.26	4.60	3.17	-	99.00
Min	63.76	0.95	13.37	5.10	0.14	0.54	2.03	3.92	2.48	-	96.10
Mean	65.55	1.12	13.93	5.85	0.18	1.02	2.98	4.20	2.76	-	97.60
S.d.	1.03	0.10	0.20	0.32	0.03	0.15	0.29	0.23	0.15	-	0.82

TABLE 5.2.8: **a:** Chemical composition of basaltic material from the intracaldera eruption of the Katla system in 1625. From Larsen (2000; Table 2) **b:** Chemical composition of SILK YN, data summarised from Dugmore et al (2000).

SILK UN and Layer St (H-M). Below this first prehistoric marker set there are a number of thick coarse black tephra layers, probably from Katla and then a further pair of distinctive pale layers. The number of black layers between SILK YN and the sequence below varies but is generally around 9-11, with a greater number closer to the Mýrdalsjökull massif. Along the southern edge of the valley at Langanes (profiles 27/6/2000-1, 3/7/2000) there are 9 layers separating these marker layers and 11 to the north at Kanastaðir . This second prehistoric sequence is a set of 2 pale layers separated by one to three (Kanastaðir (2), Fauskheiði (3)) black coarse tephras.

The upper pale layer is pale olive grey with needle shaped grains visible to the naked eye and up to x cm in length. The length of the needles increases towards the east. Similar, to SILK YN, this upper needle-rich layer is bimodal with basaltic and dacitic components(Figure 5.2.4; Table 5.2.9). Plotted on TAS plots these two layers seem very similar having a basic, transitional alkaline component with medium K and a

dacitic subalkaline component with medium to high K. However, this needle tephra has lower SiO_2 content (63.21-65.83% compared to 65.07-72.63) and slightly higher TiO_2, FeO, MgO and CaO. This layer is most similar to group A(2) of Newton's (1999) analyses of silicic Katla tephras, which comprises layers UN, N3, N2 and A5 (Table 5.2.10). The very obvious 'needle' shaped grains and the similarity to group A(2) silicic Katla material indicate that layer Fa is SILK UN, the largest of the Holocene silicic layers from Katla.

	SiO_2	TiO_2	Al_2O_3	FeO	MnO	MgO	CaO	Na_2O	K_2O	Total
max (a)	65.83	1.45	14.10	6.39	0.28	1.45	4.02	5.58	4.19	99.36
min (a)	63.21	1.11	12.74	5.54	0.14	1.22	2.42	4.00	1.14	96.40
mean (a)	64.59	1.31	13.73	5.99	0.21	1.32	3.41	4.47	2.63	97.66
s.d. (b)	0.61	0.08	0.25	0.19	0.04	0.06	0.27	0.35	0.45	0.74
max (b)	47.21	4.83	12.66	15.84	0.30	5.03	9.72	3.44	1.14	96.93
min (b)	46.30	4.29	11.29	13.83	0.19	4.22	9.04	3.03	0.76	95.90
mean (b)	46.79	4.49	12.27	14.44	0.23	4.77	9.42	3.20	0.87	96.49
s.d. (b)	0.24	0.16	0.46	0.50	0.04	0.23	0.22	0.12	0.12	0.34

TABLE 5.2.9: Summary of SILK UN reference profile single shard major element analysis data presented in this thesis (for data tables see appendix 1).

	SiO_2	TiO_2	Al_2O_3	FeO	MnO	MgO	CaO	Na_2O	K_2O	Total
max (a)	64.97	1.43	14.36	6.25	0.25	1.47	3.62	4.64	2.70	97.95
min (a)	63.59	1.26	13.43	5.24	0.16	1.19	3.17	4.10	2.30	96.31
mean (a)	64.16	1.33	13.95	5.94	0.20	1.36	3.40	4.37	2.59	97.30
s.d. (b)	0.41	0.06	0.24	0.31	0.03	0.08	0.13	0.20	0.11	0.54

TABLE 5.2.10: Chemical composition of SILK UN, summarised from Larsen et al 2001.

The lower pale layer is unusual in the Markarfljót tephra stratigraphy, being coarse with grains up to x mm and yellow – orange or brown in colour. The upper part of the layer is darker, almost black. There is no visible soil between the paler brown base and the black upper suggesting that this tephra is from one eruption characterised by the production of increasingly basaltic (dark) tephra during the course of the eruption

Analyses of this grainy layer show that it has quite a varied chemistry, with individual grains with silica content ranging from 45.59-72.5%. These sub-divide into four main clusters of analyses; basalts, andesites, dacites and rhyolites. The basalts and rhyolites are trans-alkaline while the andesites and dacites are sub-alkaline. This variation in chemistry, associated with variation in tephra colour and the production of more basic material over the course of an eruption is typical of the products of Hekla eruptions (Larsen and Thorarinsson 1977). Larsen and Thorarinsson state that most historical Hekla tephras ranging in silica content, starting with tephra with ~70% silica and eventually producing lava with 53-54% silica.

Prehistoric Hekla layers produced material with up to 74% silica at the start of the eruption. This variation is similar to the clusters of data from this lower grainy tephra a, b and c (Table 5.2.11, Figure 5.2.5). However, sub-sample d is more basaltic with silica reaching as low as 45.59%. In fact though the sub-samples b and c show some similarity with Hekla tephras H3 and H-S (data from Dugmore and Newton 1997, Dugmore et al 1992 and Wastegård et al 2001) and a, is similar to the historical material from Hekla discussed by Larsen and Thorarinsson (1977), fraction d is far more characteristic of basaltic Katla material. Comparing with Larsen's summary of the Katla 1625 material, it is clear that fraction d of this tephra and typical basaltic Katla material cannot be differentiated by major element chemistry alone. It may be in fact that a-c represents material from airfall of a Hekla tephra, and fraction d is composed of contaminant material from Katla.

	SiO_2	TiO_2	Al_2O_3	FeO	MnO	MgO	CaO	Na_2O	K_2O	Total
Max (a)	72.50	1.64	14.33	4.79	0.22	0.21	1.48	6.90	4.44	99.71
Min (a)	68.06	0.22	11.80	3.46	0.02	0.05	0.93	4.07	2.85	97.08
Mean (a)	69.36	0.38	13.62	4.32	0.14	0.15	1.18	5.61	3.44	98.19
s.d. (a)	1.21	0.42	0.68	0.41	0.06	0.05	0.19	0.84	0.41	0.76
Max (b)	64.91	1.36	16.67	6.74	0.26	1.36	5.05	5.35	2.58	99.13
Min (b)	62.31	0.74	13.70	5.19	0.02	0.90	3.44	3.86	1.32	95.02
Mean (b)	63.39	0.89	15.20	6.20	0.16	1.20	4.43	4.28	1.62	97.36
s.d. (b)	0.78	0.15	0.71	0.47	0.06	0.15	0.43	0.41	0.29	1.07
Max (c)	58.05	2.43	16.86	14.52	0.32	3.09	6.99	4.74	1.81	99.18
Min (c)	54.44	1.47	12.84	7.79	0.18	1.63	4.68	2.86	0.94	96.54
Mean (c)	56.29	1.93	14.54	10.80	0.24	2.36	6.04	3.97	1.40	97.57
s.d (c)	1.14	0.23	1.23	1.71	0.05	0.46	0.58	0.54	0.22	0.90
Max (d)	47.45	5.17	12.60	16.48	0.27	5.11	10.04	3.24	1.04	96.86
Min (d)	45.59	4.31	11.28	13.07	0.18	4.00	9.00	2.79	0.70	95.92
Mean (d)	46.47	4.55	12.29	14.54	0.22	4.83	9.65	3.08	0.78	96.43
s.d. (d)	0.56	0.29	0.36	0.82	0.03	0.32	0.29	0.12	0.10	0.33

TABLE 5.2.11: Summary of chemical composition of single shard major element analysis of Layer 'St' (H-M), presented in this thesis (see Appendix 1 for data sets).

This lower coarser Hekla layer found below SILK UN is variously called Layer St ("Steinholts" tephra) by Dugmore (1987) and H-M by Larsen et al 2002. Analyses of Layer St have not previously been recorded. These two layers are highly distinctive through appearance alone and make a very clear stratigraphic marker in the late Holocene tephra stratigraphy in this region.

Katla-E. Immediately below Sequence F is the upper of two very thick well-bedded coarse black tephra layers.Coarseness of the grains ranges from ~2cm to silt. Although in places this layer is massive, it is

usually horizontally bedded. Geochemical analysis of a sample from Western Kanastaðir clearly identifies this as a basaltic Katla tephra layer. Larsen et al 2002 refer to a thick black layer in this stratigraphic location, which they call K-E.

*Hekla-S and SILK N4.*Below K-E there is another clear pair of marker layers. Again, these are separated by a single black tephra up to 30cm thick.

The upper marker layer is a fine blue-grey tephra, which in places is mottled with a fine yellow / orange tephra or is subdivided into a lower yellow base and grey-blue upper fraction. This layer is characterised by colour variations across the area, ranging from dark blue-grey to paler grey and to a bright orange/yellow tephra. This means that the same layer may not look the same in every locality. However, it most often appears blue-grey, and in association with a pale layer below. Thickness of this upper blue-grey tephra varies across the area, from a trace at Fljótsdalsheiði (138), thickening to the east and north to 1-1.5cm at Kanastaðir (129) and West Kanastaðir (144).

This blue-grey layer varies in chemistry, as would be expected from the range of colours. The analyses from the Fljótsdalur (59-1) reference section and two samples collected at West Kanastaðir (35-1 and 41-2) all plot on a TAS diagram as a gradation of composition from andesite to dacite, with a few basaltic grains (Table 5.2.12). The majority of these analyses are subalkaline with medium K, apart from the most basaltic component with normalised silica less than 50% which are transitional alkaline.

	SiO_2	TiO_2	Al_2O_3	FeO	MnO	MgO	CaO	Na_2O	K_2O	Total
a										
max	69.59	1.42	16.67	11.99	0.99	2.84	5.39	5.26	2.66	99.74
min	58.79	0.30	12.69	4.65	0.08	0.27	2.69	2.80	1.10	95.04
mean	63.55	0.82	14.37	8.11	0.27	0.88	4.07	4.39	1.94	98.38
s.d.	2.15	0.26	0.92	1.76	0.14	0.44	0.64	0.48	0.30	0.82
b										
	56.27	*2.38*	*13.68*	*11.51*	*0.25*	*2.23*	*6.33*	*2.93*	*1.61*	*97.19*
	54.46	*2.66*	*13.64*	*12.37*	*0.29*	*3.33*	*7.02*	*3.17*	*1.22*	*98.16*
c										
max	48.87	5.07	12.79	14.79	0.28	5.19	10.21	3.38	1.16	97.07
min	45.03	4.00	12.23	13.45	0.17	4.12	8.78	2.34	0.69	96.09
mean	47.96	4.31	12.52	13.94	0.22	4.48	9.08	3.12	0.96	96.60
s.d.	1.24	0.33	0.19	0.49	0.03	0.32	0.47	0.35	0.15	0.36

Table 5.2.12: Summary of chemical composition of H-S, presented in this thesis. See Appendix 1 for full data sets.

Fractions a and b are similar to prehistoric Hekla tephras such as H3, H4 and H-S (Figure 5.2.6), material typical of Plinian eruptions from Hekla as described by Larsen and Thorarinsson (1977) and data presented in http://www.tephrabase.ed.ac.uk. None of these tephra layers can easily be distinguished purely on major element chemistry alone, since it should be born in mind that the difference distributions of each of the layers may be an artefact of different sampling rather than real differences in the composition of the products of each eruption. Certainly each of these three layers, in all of the diagrams, plot on a continuous trend. If comparing the analyses for these three prehistoric Hekla layers in the silica ranges which are similar to the blue-grey tephra (54.46-69.59%) they cannot be separated using TAS plots or bi-variate plots of FeO, CaO, MgO, K_2O and TiO_2. Assuming that the different spread of each layer on the TAS plot does reflect real differences it can be noted than HS is less variable in SiO_2 and alkalis than either H3 or H4. H4 has a more silicic tendency than H3 and considerably more so than H-S which plots throughout the andesite and dacite fields without any rhyolitic material analysed in the published data. This blue tephra has a mainly dacitic component and less spread out than the H3 or H4 reference data sets. These trends however, should be considered with caution.

The basaltic component c of this upper blue-grey layer is less typical of Hekla material than the other two components. It has some similarities with basaltic Katla material, with somewhat higher SiO_2, lower FeO and slightly elevated values for NaO2 and K_2O. All of these basaltic shards were from one sample from West Kanastaðir and may not be part of the primary airfall layer.

This upper blue tephra can be interpreted as a Hekla tephra layer based on the colour variations of the layer and on the range of chemical composition associated (a and b) with this. However, it is not possible to say purely from chemistry which Hekla tephra this may be. The clustering of analyses in the dacitic field show some similarity with the distribution of analyses from H-S, but overlaps also with the H3 and H4 reference data sets.

The lower pale layer is fine grained and olive-grey to yellow in colour. Thickness varies across the valley, reaching a maximum thickness in North Þórsmörk and in the terraces to the south east of Einhyrningur (5-10cm. Profiles 92, 124, 126 and 127). This thickness decreases with distance downstream (3cm at Halli Island, profile 117 and 2cm at Kanastaðir, profile 129). Needles were noted in the profile 117 and not elsewhere.

This lower pale layer is very similar, in fact undifferentiable, in chemistry from the silicic component of SILK YN, falling into the same group of silicic Katla material. SILK layers YN, MN, LN, N4, N1, A1, and A9 belong to this group. Chemistry alone cannot specify which of these tephras this pale layer

actually is. However, its position somewhat midway through the stratigraphic record and association with the upper blue-grey tephra can suggest a likely identification.

This blue/pale tephra couplet is distinctive throughout the Markarfljót valley. While neither layer can be identified purely on major element geochemistry, their positioning together, and stratigraphic location beneath the SILK layers YN and UN, suggests that they are tephra layers Hekla-S and SILK N4. Larsen et al (2001) note that SILK N4, with an overlying black layer and two-coloured Hekla-S tephra form a distinct stratigraphic marker to the NE, N and NW of Mýrdalsjökull. This is the same pattern found in the Markarfljót valley in this thesis.

Katla-N. This tephra is the lower of the two horizontally bedded coarse black tephra layers. Analysis of this layer also confirms that it is a basaltic tephra from Katla.

Hekla-4. This key layer is a fine-grained to coarse-grained (silt-sized through to 2mm grains) blue-grey tephra with a yellow basal layer. Throughout most of the prehistoric section logged along the northern margin of the Markarfljót and up-valley towards Einhyrningur and North Þórsmörk this layer can be found. However, it was not identified in the reference profile on Fljótsdalsheiði (59). The yellow layer is very thin throughout the region, often less than 0.5cm thick and is sometimes barely visible at all, possibly mixed into the rest of the tephra layer. Thickness of the upper dark layer varies, being thinnest farthest west (Kanastaðir (129, 144) and Halli Island (117): 2cm) and thickening to up to between 4 and 8cm in the middle valley in North Þórsmörk and to the south east of Einhyrningur (124, 215, 127). These low valley-side terraces near Einhyrningur show bedding of the blue-grey upper section, with sorting of the tephra in to alternating fine-coarse-fine beds.

Samples of both the darker layer and the yellow layer were analysed from the Kanastaðir reference profile (129-1 and 129-2) Figure 5.2.6 and Figure 5.2.7. These show very different chemical compositions, with a small number of shards overlapping in their characteristics. The darker layer (129-1) is andesitic, subalkaline with medium K_2O. One shard analysed was classified as basaltic and transitional alkaline and another single shard as rhyolitic. The yellow layer (129-2) on the other hand was predominantly rhyolitic with SiO_2 between 73.88 and 71.27%, subalkaline with medium K_2O. Other elements.. Analysis of the same stratigraphic layer from the West Kanastaðir site (75-4) showed much similarity with the andesitic shards within the darker layer (129-1) from Kanastaðir. The layer appeared grey-blue in the soil without such a distinct pale yellow base thick enough to sample effectively.

It is possible that the two components of this tephra are associated with two separate eruptions and possibly from two different volcanic sources. However, the rhyolitic analyses are more silicic than any material documented from silicic eruptions of Katla (63-67%, Larsen et al silk paper) or Eyjafjallajökull

(68.31-71.49%, Larsen et al 1999, Layer H/'Hoftorfa' tephra this thesis). Al_2O_3 and FeO are both a bit low for the silicic component to be from Veiðivötn, although this layer is otherwise very similar, particularly in high silica content, to the Landnám layer. The greatest similarity occurs between the rhyolitic shards of this tephra and the pale pumice produced in the Hekla 4 eruption. The andesitic component is also comparable with material from eruptions of Hekla 4 and Hekla-S, and similar to the material with ~57% silica which was deposited in North Britain and further afield from the eruption of Hekla 4.

Isopach maps of the distribution of Hekla 4 (Larsen and Thorarinsson 1977) show that although much of the tephra fallout occurred to the north of Hekla, the darker layer spread farther to the south than the light lower part. The highly silicic component of this key layer, identified below an andesitic upper layer, and stratigraphically located beneath the Hekla-S/SILK N4 couplet suggests that this layer is most likely to be Hekla 4. Although the rhyolitic component is most distinguishable the andesitic component is most prevalent in this area, and alone can really only indicate that the layer originates from Hekla. Stratigraphy is necessary combined with geochemistry for this layer to be identified in the Markarfljót area.

The sequence throughout the valley becomes less distinct and less continuous in the layers below Hekla 4. This is partly because the sediments are heavily indurated making much of the soil and tephra layers very hard. This alteration also means that the colour of layers is not clear and cleaning a section using a knife, trowel or spade actually polishes the surface rather than creating a fresh surface to study. Those layers that could be recorded were often not clear and in places it was only possible to record colour as dark or pale in the sedimentary logs. This makes interpretation of the sequence below Hekla 4 somewhat difficult and correlation even between the reference profiles is not as simple as in the more recent sediments.

Bedded grey tephra. A bedded grey tephra layer is found beneath Hekla-4 in the Kanastaðir reference profile (129) and in the East Einhyrningur terraces, separated from H-4 by up to 12 black tephras. This tephra usually consists of three horizons, an upper fine dark blue-grey tephra, a middle very fine pale blue-grey tephra and a lower fine dark blue-grey layer. This tephra is similar in colour to the historic Hekla layer H1341 and the blue-grey parts of the Hekla-4 and H-S layers, suggesting a possible origin in the Hekla Volcanic System.

Below H4 there are numerous pale tephra layers intercalated with highly indurated black tephra layers probably from Katla. In West Kanastadir (144), at Halli Island (117) and in North Þórsmörk (91) these layers cluster into two main sets. The first is most commonly a set of two layers, one pale blue/grey , the other olive/yellow with intervening black tephras are called the *'Twins'* here for correlative purposes. The lower pale layers include three or more olive/grey layers, sometimes with one blueish layer in the upper sequences. This lower sequence of layers is highly variable between different locations and is called the

'Triplets'. Analyses of these layers have been carried out where possible but the lack of stratigraphic correlation makes definite identifications difficult. It is likely that some of these layers are the oldest SILK layers A5-A9.

5.3 Correlation of tephra stratigraphic logs using key tephras

Valley-side profiles have been used to construct a reference tephra stratigraphy, from which valley-wide, more fragmentary profiles can be correlated. These correlated logs are illustrated in looseleaf diagram of profiles. Analysed tephras are indicated on these figures and the associated data sets are presented in Appendix 1. Profiles from each main area of the valley will be summarised here and particular profiles or analyses of note mentioned in the discussion. Otherwise, identifications are indicated on the profile logs and also in association with the data sets in Appendix 1.

Lower Valley

The tephra stratigraphy in the lower valley is the most complete in the study area particularly in the Langanes and Fljótshlið - Kanastaðir areas. The Langanes profiles recorded in this thesis, along the southern margin of the valley, extend from the present day surface through the entire historical tephra sequence to a little below SILK UN/Layer St (H-M). This represents the base level of most of the streams and rivers that dissect the alluvial fans spreading across Langanes from the high land of Eyjafjallajökull to meet the Markarfljót. However, much deeper soils were noted in western Langanes profiles indicating that the entire Holocene sequence is probably preserved in this area. The sections recorded in Langanes were tied together from analyses of Layers H, SILK YN, SILK UN and St.

The profiles along the northern margin of the Markarfljót between Fljótshlið and Kanastaðir / Halli's Island showed that the soils close to the river in this region are mainly prehistoric in age, with little younger than SILK UN / Layer St (H-M). However, the soils extend further back in time than any other exposed soils in the valley, including the triplet sequence and older highly indurated layers. Younger soils are found on the higher slopes with the full tephra sequence from present day through the historical layers to at least Hekla 4 being found at Fljótsdalsheiði and Kanastaðir. Analyses of distinctive pale layers from SILK UN down were used to correlate these profiles.

Isolated profiles were recorded farther afield to the west and south at Fljótshlið and Seljaland. The Seljaland profile purely covers the historic sequence, being recorded as part of an archaeological investigation in the area (Smith and Ahronson, 2003), and is very similar to those from Langanes and records collected by Dugmore (1987). The Fljótshlið profiles were also late Holocene in age, the ones

closest to the valley margin, being dominated by aeolian soil and containing distinct blue-grey tephras, probably from eruptions of Hekla. The profiles recorded across the Markarfljót sands south of Fljótshlið, close to Aurasel and Drumbabót were dominated by tephra-rich black sands and silts. These Aurasel and Drumbabót profiles cannot easily be tied in with the profiles elsewhere in the valley based on visual identifications alone since they are so heavily dominated by thick bedded black sands. However, the age of these sand layers is important and analysis of pale layers in profiles 68 have suggested some correlation.

North Aurasel layer 68-1 'upper pale tephra' is a 4cm mixed yellow-olive fine tephra, immediately underlain by a trace of fine black tephra. This layer appears to be reworked and may be the lower layers of a brown pumice-rich bedded deposit that lies at the top of this profile. Layer 68-2 'bottom pale tephra' is a 2cm thick patchy pale olive very fine tephra underlain by 0.5cm thick patchy brown fine tephra. Although patchy, this layer is more distinct, less mixed than 68-1 and is more likely to be an airfall tephra. These two layers are separated by 5 dark (black and blue) tephras and 7cm of soil (see profile 68). Layer 68-2 can be traced over several metres along the Aurasel river bank.

Both 68 1 and 68 2 show similarities with both the Landnám tephra and material from basaltic eruptions of either Katla. Both layers are bimodal with basaltic and rhyolitic components. The rhyolitic shards most closely resemble Landnám, particularly in the case of 68-1. Analyses for 68-2 have slightly higher NaO2 levels. The basaltic component may also be associated with a Veiðivötn source, although in both cases Al_2O_3 is somewhat lower and FeO slightly higher than analyses of the Landnám tephra. The basaltic component is very similar (eg elements) to basaltic material produced in eruptions of Katla.

It may be from these analyses that these layers include tephra from the Landnám eruption. The appearance of 68-1 suggests some re-working and the geochemical analyses are not entirely conclusive.

Middle Valley

The tephra record in the middle valley is patchy, with very shallow soils in the central area flanking the Markarfljót gorge and with better preservation of soils on higher ground (eg. Einhyrningur and N.Þórsmörk). The Þórsmörk area near Húsadalur has extensive historical soils, which were not logged in this study.

The soils of North Þórsmörk, where they are well preserved on valley-sides and in tributary valleys, are deep, recording as full a Holocene sequence as anywhere else in the valley. Sections 91 and 92 (big hill) are mainly above the height of flood activity and act as good reference profiles. Other sections in this area

have been tied together by recognition of the Layer H-SILK YN sequence and the H4-bedded grey tephra sequence, with analyses of Layer H, SILK YN, SILK N4 and bedded grey tephra). Silicic Katla layers were all thicker in these profiles than elsewhere in the valley and where needles were present they are more easily distinguishable (both longer and wider). Other profiles were recorded to determine the age of landforms and possible flood deposits.

Upper Valley

The tephra stratigraphy in the Entujökull / Emstrur area is less clear than other parts of the valley, being dominated by many coarse-grained brown and grey-blue layers. Soil cover is limited in the Entujökull foreland and thus the tephra stratigraphy developed for this area is fragmentary. The most distinctive layers in the historic sequences are blue-grey and are probably therefore from Hekla. The distinctive pale olive-grey silicic tephras from Katla are highly visible in the prehistoric sequences.

Reference profiles were recorded at the just beyond the westernmost end of the Entujökull foreland (122), opposite the foreland (162) and in shallower sections near the Markarfljót bridge (160, 161). These profiles all show only historic tephra sequences. Other profiles were measured to give an indication of the ages of landforms and sediments. However, overlying, thick, unconsolidated sandy deposits in many parts of the foreland reduced the depths to which sections could be dug prior to infilling.

Profile 162 opposite the Entujökull foreland is measured from below multiple metres of soil at the foot of a gully exposure. Tephras in this profile are prehistoric and are interpreted form stratigraphy and chemistry to possibly represent H-S and SILK N4. This means that soil accumulation in this area has continued without glacial activity since the deposition of SILK N4 and probably far earlier than this.

5.4 Summary

Stratigraphic correlation and geochemical analyses have been used to link 173 profiles in the Markarfljót. Those most relevant to the aims of this thesis are enclosed separately. Geochemical data is in Appendix 1. Key layers have been identified through the historic and prehistoric sequences across the valley. Pale layers from silicic eruptions of Katla, Eyjafjallajökull and Hekla provide the most distinctive marker horizons. New, tentative identifications of Hekla 1206 and a putative historic silicic tephra layer from Katla in Emstrur may aid interpretation of the sedimentary record.

Chapter 6: Results

Flood deposits

6.1 Introduction

The history of flood activity in this region is of particular interest to this study. However, as indicated in Chapter 1, flood deposits are difficult to identify based on sedimentary characteristics alone, being very similar in nature to deposits formed by glacial activity, other flow events or normal river flow. One of the main criteria pinpointed as crucial to the identification of a flood deposit was the recognition of the horizontal continuity of a unit over a wide area and particularly within the topographic lows of a region. This important criterion allows deposits associated with local events such as slope activity to be discounted as possible large-scale flood deposits.

7 horizontally continuous deposits are intercalated with tephras and soils in those profiles located close to the valley floor. Two (Units 2 and 8A-B) of these are particularly extensive. A further 4 (Units 1, 9,10 and 11) somewhat less extensive but very similar deposits have been recorded. These deposits tend to be diamicts with lithic clasts in the size ranges sand to boulder with a tephra-rich matrix and few structures. A further two historic units are identified. Figure 6.1.1 summarises the stratigraphic relationships identified. Each deposit will be discussed individually, making reference to key sites and the sedimentary characteristics. Table 6.1.1 summarises the characteristics of each unit where found in multiple locations. Where carried out, geochemical analyses of sediment matrices and pumice clasts and cumulative grain size analyses will be discussed.

6.2 Historic flood units (Units A and B)

Two historic flood units have been identified in the Entujökull foreland and North Þórsmörk. The older one (B) lies beneath a bedded grey tephra, possibly H1341. It is characterised by bedded tephra-rich sands and gravels and in places (eg. 94) is composed of diamict. Scouring of lava in profiles 83 and 84 occurs at the same stratigraphic location. Profile 94 indicates that flow travelled along the big channel in North Þórsmörk. The younger unit (A) is lies above K1500 and is composed of bedded tephra-rich sands and gravels. It does not have a diamict component evident in any of the sections. Though stratigraphic evidence for these events is good the sedimentary information about the nature of these events is fragmentary since in numerous profiles they are represented by scouring rather than deposition.

Lithofacies scheme used in this thesis, adapted from Miall (1979) and Graham (1988)

Lithofacies code	Lithofacies	Sedimentary structures
Dmm - (rs)	Diamict, matrix-supported, massive. - showing evidence of resedimentation	Structureless admixture. - Initially appears structureless, but on closer inspection shows subtle textural variability and fine structures.
Dmg - (cu) - (fu)	Diamict, matrix supported, graded - coarsening upwards - fining upwards	Diamict showing variable vertical grading in matrix or clast content.
Dms - (rs)	Diamict, matrix supported, stratified - showing evidence of resedimentation.	Obvious textural variation or structures within diamict, more so than Dmm (r). -
Gmm	Gravel, matrix-supported, massive.	None
Gh	Gravel, horizontally bedded.	Horizontal bedding. May be imbrication.
Grh	Granules	Horizontal bedding.
Grt	Granules	Trough cross bedding
Sh	Sands	Horizontal bedding.
St	Sands	Trough cross bedding
Fm	Fines (clay, silt, may include very fine sands), massive.	None

TABLE 6.1.1

Drumbabot Unit: Unit 2

SEDIMENT SITES (Profile numbers)	SITE MORPHOLOGY	DESCRIPTION	LITHOFACIES CODES	STRATIGRAPHY
DRUMBABOT (64, 76)	Braided sandur.	Bedded coarse black tephra including lithics from fine sand-0.8cm clasts, olive brown silt at base, lenses of fine sand, fine black tephra at base. SILK pumice[1] in surface lag. Deposit surrounds mature well-preserved macrofossil trees.	**Sh/Grh**	Below: SILK YN[1], exact stratigraphic relationship unclear. Trees have radiocarbon date ~1200±BP
SMJÖRGIL (17. 26. 28)	South margin of valley. Bench-like surface in terrace extends for >200 metres along valley side.	Bedded unit. Lower section dominated by very coarse sand to granules. Upper layers matrix-supported cobble unit with clasts up to 25cm. Pockets of finer, sorted material.	Upper: **Gmm (rs)** Lower: **Sh/Grh**	Below: Layer H and one black tephra. Above: V870 and 3-4 black tephras. Some may be reworked layers.
EINHYRNINGSFLATIR (48, 49)	Roftbard in soil terraces above postglacial lavas.	Bedded. Lower layers gravel-rich with clasts up to 0.8-1cm. Upper layers mainly fine to coarse black tephra and lithic sand. Some silt drapes.	Upper: **Sh** Lower: **Gh**	Above: V870 and 2 black tephras.
NORTH AURASEL (67)	Braided sandur. Riverbank exposure.	Horizontally bedded granules overlaying structured fine sands (coarse black tephra and coarse sand lithics) with cross bedding (foresets?), ripple laminations and silt drapes. Deltaic structures.	Upper: **Grh** Lower: **Ft (r)**	Above: V870 and 4+ black tephra layers. Some may be reworked.

[1] SILK pumice and SILK YN geochemical analyses in Appendix 1.

Smjörgil Unit: Unit 3

SEDIMENT SITES (Profile numbers)	SITE MORPHOLOGY	DESCRIPTION	LITHOFACIES CODES	STRATIGRAPHY
SMJÖRGIL (8-12, 16-18, 27, 28?, 31, 45, 63) and LANGANES (30)	South margin of valley. Bench-like surface in terrace extends for >200 metres along valley side.	Thickness 71-107cm, increasing towards the axis of the valley. Matrix supported diamict initially appears massive. On closer inspection shows pockets of sorting and cross-bedding. Matrix contains black basaltic Katla tephra[1] and undisturbed pockets of SILK YN[1] tephra. Lithic clasts up to 15cm (intermediate axis). Clast orientation generally NNE-SSW.	**Dmm (rs/c)**	Above: One black tephra, Layer H[1] and complete historic tephra sequence. Below: SILK YN[1].
ÞRÖNGÁ (100A-C)	Terraces at the mouth of the river Þröngá. Only found on Markarfljót side of the terraces.	Thickness 10-29cm. Matrix supported massive diamict. Matrix includes fine sand – silt and black tephra. Lithic clasts up to 10cm (intermediate axis). Lower boundary erosive and tephra layers folded and faulted below unit.	**Dmm**	Above: One black tephra and Layer H[1]. Below: SILK YN[1], and SILK UN[1].
NORTH ÞÓRSMÖRK (79, 81, 82. 89)	Margin of valley, exposed in gullies at base of hill. Above Markarfljótsglúfur.	Thickness 22cm. Matrix supported predominantly massive diamict. Cross-bedding. Matrix includes dark brown tephra 1-2mm, fine-coarse sands and pockets of undisturbed SILK YN[1] tephra and soil lenses. Lithic clasts ~5cm. Uneven lower surface.	**Dmm (rs/c)**	Above: Two black tephras (one reworked) and Layer H[1]. Below: SILK YN[1].
EINHYRNINGUR TERRACES (136)	Low terraces at northern margin of valley.	Cobble and tephra-rich lag on surface. Lower erosional boundary. Disturbed tephra layers below with some blocks of soil and tephra at 90° from horizontal.	**Dmm (rs)**	Below: SILK YN[1].

TRÖLLAGJÁ (60, 156-159)	~20m deep gorge through lava surface. Tributary of Markarfljót.	Bedded 4 unit deposit, with channels, ripples, cross-bedding, inclusions of tephra and soil, c black tephra mainly. **Lower Unit 1:** Crudely bedded silt to cobbles. Mainly granules black tephra. Some lithics. Some cross-bedding, most layers are crudely horizontally bedded. Silt pockets between coarser beds show fine bedding and ripples. **2:** Greater than 2.4m thick. Dark brown matrix supported diamict. Appears massive though in places shows crude bedding and discontinous black tephra-rich beds. Boulders up to 50cm. Upper 60cm includes pockets of orange silt and pale olive yellow tephra with dark brown tephra grains and 1mm long needle grains like SILK YN[1]. **3:** Bedded sands to cobbles. Massive units. Some coarsening upwards sequences. Erosional lower boundary. **Upper Unit 4:** Channel. 10m wide, 3m deep. Channel infilled with mainly horizontally bedded fine sands to gravel. Mainly black tephra. Some lithic clasts especially in gravelly and diamict bands. Channel eroded into bedded sands and diamict below.	1. **Grms (c)** 2. Upper 60cm: **Dmm (rs),** rest **Dms** 3. **Smg – Gmg (cu)** 4. **Fh - Gh**	Unsure. Probably above SILK YN based on incorporation of SILK YN like tephra within the deposit.

Unit 4

SEDIMENT SITES (Profile numbers)	SITE MORPHOLOGY	DESCRIPTION	LITHOFACIES CODES	STRATIGRAPHY
SMJÖRGIL (10, 16, 17..)	South margin of valley. Bench-like surface in terrace extends for >200 metres along valley side.	1. At 10: clast-supported cobbley unit with clasts up to 20cm. 2. Otherwise, massive, matrix-supported diamict. SA-SR clasts with b-axis 5-13cm. No sorting. Matrix dark brown.	1. **Gmc** 2. **Dmm**	Above: SILK YN and 1 black tephra. Also one fluvial gravelly reworked tephra layer in sections 16 and 17.
LANGANES (14, 30)	South margin of valley. Dissected alluvial fans west of Smjörgil.	14: Gravel /cobble layer at base, with horizontally bedded cbkt above 30: Bedded, cross bedding, maybe fluvial	?	Above: SILK YN and 1 (14)-2 (30) black tephras.
EINHYRNINGUR TERRACES (130)	Low terraces along northern margin of valley.	Lag including clasts up to 50cm VA-SR. Dark brown tephra-rich matrix. f-cs lithic rich layer below	**Dmm**	Below: Layer St (H-M) and 1 black tephra.
KANASTAÐIR (34, 144)	Low terraces along northern margin of valley.	Composed of two units. **1:** Upper unit. Dark brown mixed gravelly soil. Surface lag with clasts up to 15cm. May represent a more recent event and disturbed soil below. **2:** Lower unit. Dark brown matrix-supported diamict. Fines upwards, SA-R clasts up to 5cm in upper sections, up to 15cm towards base.	1. **Gmm** 2. **Dmg (fu)**	Below: SILK UN and 3 (34) – 6 (144) black tephras.

FAUSKHEIÐI (138, 141, 142), HALLI ISLAND,	Low terraces along northern margin of valley.	Mostly a matrix supported diamict. Clasts up to 3cm. Matrix includes black tephra and f-cs lithics. Surface lag includes clasts up to 10-35cm. To the east (142) the unit is more variable, being mainly bedded cbkt in places or gravelly. A channel infilled with bedded gravel and fines has eroded into surface of unit 4 at section 142.	**Dmm** To the east (margin of valley) **Grh - Gh**	Below: SILK UN and 5-9 black tephras.

Unit 5

SEDIMENT SITES (Profile numbers)	SITE MORPHOLOGY	DESCRIPTION	LITHOFACIES CODES	STRATIGRAPHY
EINHYRNINGUR TERRACES (126, 132)	Low terraces along northern margin of valley.	126: Lag of fine gravel up to 1cm. Possibly erosional lower boundary. 132: Bedded black tephra and fine to coarse sand lithics.	**Grh**	Below: 126: H-S, 4 dark tephras, 1 pale tephra, 1 diamict (unit 6) and four more dark tephras. 132: H-S and 12 dark tephras.
ÞÓRSMÖRK (61)	River bank section to west of Husadalur.	Bedded fine to coarse black tephra including mixed lithic grains in coarse layers especially towards the top. Large v vesicular dark brown / black tephra (pumice?). Upper half more mixed.	**Fh - Grh**	Above: Layer St (H-M)
KANASTAÐIR (40), HALLI ISLAND (44)	Low terraces along northern margin of valley. Streamlined island in braided river, east of Gilsa, northern margin of valley.	Bedded coarse black tephra, grains up to 5mm. Few lithics. Dark grey silt drapes. Some mixed layers with clay and silt and iron rich inclusions. Very hard near Halli Island. Analysis of matrix shows mainly basaltic Katla tephra and 1 shard was similar to Eyjafjallajokull silicic tephra.	**Grh**	Above Layer St (H-M). May also be up to 4 black layers between St and Unit 5, at section 44. Unclear due to a lot of mixing of sediments.

Unit 6

SEDIMENT SITES (Profile numbers)	SITE MORPHOLOGY	DESCRIPTION	LITHOFACIES CODES	STRATIGRAPHY
KANASTAÐIR (41, 144)	Low terraces along northern margin of valley.	Thickness? Bedded coarse black tephra. Lithics up to 2cm in lowest beds. Upper beds only contain tephra. Silt drapes.	**Grh**	Below: H-S and 5 black tephras
HALLI ISLAND (43, 74, 117)	Streamlined island in braided river, east of Gilsa, northern margin of valley.	Massive matrix supported diamict. Little or no bedding. Tephra-rich matrix up to 1.5cm. SR/SA clasts up to 6cm. Lithic lag with clasts up to 20cm. Fining upwards sequence in places (74) with cobbles up to 25cm near base. Erosional lower boundary at profile 117.	**Dmm – Dmg (fu)**	Below: H-S and 5-6 black tephras
FAUSKHEIÐI (72, 142)	Low terraces along northern margin of valley.	Bedded coarse black tephra including lithics. Very finely bedded in places. Thins out to a black tephra layer in places along gully (142) and has an erosive lower boundary on the terrace surface (72), marked by a lithic lag with clasts up to 80cm.	**Grh**	Below: H-S and 1 (72) to 7 (142) dark tephras
EINHYRNINGUR TERRACES (126, 131)	Low terraces along northern margin of valley.	Dark brown diamict equivalent to the lithic lags on other terrace surfaces. Clasts up to 11cm matrix mainly fine black tephra with inclusions of soil.	**Dmm (rs)**	Below: H-S and 4 black tephras. One pale tephra immediately below unit 6 in section 126. Above: UN/St (H-M) and 13 dark tephras including one very thick bedded layer (131).

ÞRONGÁ, NORTH ÞÓRSMÖRK	Riverbank exposure. Terraces along Þrongá valley side.		?	

Unit 7

SEDIMENT SITES (Profile numbers)	SITE MORPHOLOGY	DESCRIPTION	LITHOFACIES CODES	STRATIGRAPHY
ÞRONGÁ, NORTH ÞÓRSMÖRK (101)	Riverbank exposure. Terraces along Þrongá valley side.	Upper: Matrix-supported diamict. Appears massive but shows horizontal and cross-bedding at base. Very hard. Clasts up to 10cm. Dark brown tephra and fine sand lithics in matrix, very mixed layers. Lower: bedded black tephra silt to coarse sand size.	Upper: **Dmm**, **Dmm (rs)** towards base. Lower: **Sh** (f-cbkt)	Above: SILK N4 and 2 dark tephras Below: 3 black tephras, 1 grey-blue tephra.
ÞÓRSMÖRK (61)	River bank section to west of Husadalur.	Coarse black tephra-rich massive, matrix-supported diamict including sub rounded to angular clasts ranging in size from greater than 10cm to fine sand.	**Dmm**	Above: SILK N4 and 1 black tephra?
FAUSKHEIÐI (138)	Low terraces along northern margin of valley.	Gravel mixed with soil and fine dark brown tephra.	**Grmm**	Above: SILK N4 and 2 black tephras.

Kanastaðir unit: Unit 8A and 8B

SEDIMENT SITES (Profile numbers)	SITE MORPHOLOGY	DESCRIPTION	LITHOFACIES CODES	STRATIGRAPHY
EINHYRNINGUR TERRACES (124, 125, 128, 133) Best represented in profile 124.	Low terraces along northern margin of valley.	Thickness varies across terraces, (x-x) decreasing away from valley axis. There are 2 units divided by up to 1.5cm soil. Upper 11.5cm thick coarse – fine gravel with clasts up to 3cm. Matrix included black tephra. Lower (total thickness x) divides into 4 subunits (124). **1**: ~6cm. Fine black tephra 1mm within pockets in top of flood. **2**: 16-23cm. Hard brown diamict. Massive. Clasts up to 5cm. Very angular clasts (133). Possible trace of soil between 2 and 3. **3**: 25m. Black coarse gravel diamict with fine to coarse black tephra in matrix. Coarsening upwards with 5cm clasts at top. Loosely packed. **4**: Fine to coarse black trough-cross bedded tephra interbedded with traces of orange-brown silt or soil (silt drapes).	Upper: **Gmm** Lower: 1. **Fm** (fbkt) 2. **Dmm** 3. **Dmg (cu)** 4. **St** (f-cbkt)	Above: H4, 1 very coarse (1.5cm max.) black tephra and 1 finer (2mm) black tephra. Below: 4 black tephras, 1 fine blue/grey tephra, and 2 black tephras….
NORTH ÞÓRSMÖRK (78, 84, 92, 98, 99)	Margin of valley, exposed in gullies on side of hill (alt. 341m?) and on top of streamlined hill in middle of valley (alt. 310m?). Above Markarfljótsglúfur.	26 – 12cm thick matrix-supported diamict. SR-A lithic clasts up to 21cm (long axis). Matrix mainly silt-coarse sand with isolated grains up to 1cm including brown/black vesicular tephra. Lithic lag on west side of Ljosa hill (99) and scouring of cataract headwall (84).	**Dmm**	Above: H4, 1 coarse loose black tephra, 1 fine hard black tephra. Below: 4 black tephras, 1 fine grey/blue tephra, 7 black tephras, fine olive/yellow tephra with needles, 1 black tephra, very fine bl/ olive layer.

FAUSKHEIÐI (72, 139, 140)	Low terraces along northern margin of valley.	Three units (deposit thins upslope; up to 2.5m at 140, 8cm at 139 and thins to a surface lag overlying palagonite upslope): **1.** Upper bedded sands, including lithics and black tephra. **2.** Lithic and tephra-rich diamict. Dark brown to black. Clasts up to cobble and gravel size. Coarsens upwards. Fine to coarse black tephra-rich matrix. **3.** Bedded coarse dark tephra separated by thin layers of silt. Underlain in section 140 by a 0.5cm thick organic-rich layer with compressed leaves. Surface lag with sub-rounded to angular clasts up to 25cm in section 139.	1. **Sh** 2. **Dmg (cu)** 3. **Grh**	Above: H4 and two black tephras. Below: 8-10 dark tephras including 1 coarse grey tephra, 2 pale tephras.
HALLI ISLAND (43, 74, 117)	Streamlined island in braided river, east of Gilsa, northern margin of valley.	Augen-lenses of diamict connected with black tephra at slightly higher elevations between lenses in 117. Tephra: coarse black tephra with grains up to 3mm. Mainly silt. Diamict: subdivided into three units: **1.** Upper. Dark brown diamict, matrix-supported. Crudely bedded in places. Fining upwards in 43 and 73. Coarsening upwards in 117. Clasts up to 10cm. Matrix black tephra 1-3mm and fine to coarse sand lithics. **2.** Middle. Crudely bedded gravels and coarse black tephra. (74) **3.** Lower. Sands and gravels including fine to coarse black tephra. Trough cross bedded. Silt layers.	'Diamict unit': 1. **Dmg (cu/fu)** 2. **Gh** 3. **St**	Above: H4 coarse black tephra (2mm), coarse black tephra (1mm). Below: 10 black tephras (some coarse, some finer), 1 trace fine grey tephra (may be black), 1 black tephra, pale ol/grey tephra silty, 1 coarse black tephra (2mm), 1 pale olive tephra….
KANASTAÐIR (42, 75, 144)	Low terraces along northern margin of valley.	2 main units separated by 5.5cm soil including black tephra and gravel. **Upper**: 9cm gravelly diamict. Clasts up to 1cm. Black tephra-rich matrix. **Lower:** 39cm. Massive diamict. Clasts up to 6cm and lenses of black tephra and soil. Crudely bedded to base.	Upper: **Gmm** Lower: **Dmm (r)**, to **Dms (r)** at base.	Above: H4, coarse dark brown tephra (1mm), fine black tephra (<1mm). Below: up to 12 (including 4 traces

				tephra) black/grey tephras varying degrees coarseness. Fine light grey tephra, possible trace coarse black tephra, coarse black tephra, pale silty olive/grey tephra….

6.3 Aurasel pumice unit (1)

A pale yellow-olive to brown colour and the inclusion of very rounded pieces of white pumice distinguishes the Aurasel pumice unit. The pumice clasts distributed across the sandur surface along the riverbank north of Aurasel have intermediate axes up to 3cm and float when placed in a basin of water. The main unit is composed of brown bedded silts to very fine sands, with paler olive to yellow layers. Some layers are very mixed and incorporate olive-yellow tephra and white pumice. Similar very pale pumice was found within the surface lag on Halli Island.

The olive-yellow colour of the bedded deposit and the very pale yellow colour of the pumice suggest that this deposit is mainly composed of silicic tephra, similar to the pale part of the Landnám tephra layer or the pale layers from Katla and Eyjafjallajökull. The colour of the pumice is most similar to the colour of pumice analysed and recorded by Newton (1999) being considerably paler than the silicic Katla pumice. Electron Microprobe Analysis of the pumice from north of Aurasel (section 68, analyses 68-P1 and 68-P2) showed that this material was highly silicic with a SiO2 content between 70-71%, with high K2O around 4.6%. This chemical composition is very similar to the silicic component of the Landnám tephra layer, characterised by high levels of K_2O, typically greater than 4% where SiO_2 content is greater than 70% (Larsen et al. 1999). This suggests that this pumice was produced in an eruption of Veidivotn, possibly the Landnám eruption of c.871AD.

The Aurasel pumice unit is stratigraphically located above the V870 tephra (68-1, 68-2). In sections 67 and 68, 5-6 dark tephra layers separate the pumice unit and V870. In section 68 one of these layers is a fine blue-grey tephra, but otherwise they are all fine black tephra layers, some of which are mixed along both upper and lower surfaces. Some of these layers may be reworked, indicated by repeated thin bands of pale olive reworked Landnám tephra (like 68-1). The location of pumice unit above a possible blue-grey layer suggests that it may have been deposited well in to the historic period.

The bedded nature of the North Aurasel unit suggests transportation by water, as does the presence of the pumice, which is far larger than any airfall material from the Landnám eruption found in this area. The slightly mixed nature of the sub-units, lack of fine-scale fluvial structures and consistent yellow-brown colouring of the unit that is so distinctly different from the predominantly black Katla-sourced sands making up the sandur, suggests deposition in a single medium-energy flood. Each separate bed may be associated with separate pulses of flow within a single event. The pumice included in the deposit suggests a link with the Landnám Veiðivötn eruption c.871AD. However, the separation of the pumice unit from the Landnám tephra by numerous tephra and soil layers indicates some delay between the Landnám eruption and the timing of the pumice unit event. This may reflect storage of water and pumice material close to the eruption site and later (lake) drainage, or may reflect the incorporation of the Veiðivötn pumice and tephra into an unrelated flood. The source of such an

unrelated flood however, must have been close to the eruption site to account for the size of the pumice pieces entrained in the flow and deposited at Aurasel.

6.4 Drumbabót Unit (2)

The Drumbabót Unit is a horizontally bedded tephra-rich sand to gravel deposit found at Drumbabót south of Fljótshlið in the braided sandur plain. This deposit surrounds an expansive once forested area, with macrofossil tree trunks with diameters of up to 25cm entombed by the sands (Figure 6.4.1). These trees show no sign of damage or scouring and are coated in a fine layer of pale silt between their bark and the surrounding sands. The thickness of this bedded deposit varies but was once several metres deeper, this overlying material having been eroded in strong winds (Haraldsson, personal communcation 2000). The means that as well as once being a much deeper deposit, the structure and nature of the uppermost sections of this deposit can no longer be known. The surface of this deposit is littered with occasional dark brown pumice clasts up to 10 cm in diameter.

The trees are very well preserved birch trees and one sample has been dated using AMS radiocarbon dating to 1230 + 35BP (Appendix 4). Calibration of this date places the death of the sample tree to be some time shortly before the eruption of the Landnám tephra. Soils found above the bedded sand and gravel deposit include dipping beds of tephra. Pale tephra layer (76-1) from this profile has a geochemical composition very similar to SILK YN with 67% SiO2. The orientation of the tephra beds suggests that this layer dips below the bedded deposit thus providing a indicating that Unit 2 overlies SILK YN.

Similar bedded fines, sands and granules have been identified in similar stratigraphic locations nearby at Aurasel (67), at Smjörgíl on the southern margin of the valley and in the middle valley at Einhyrningsflatir (48, 49). These deposits are all found beneath the V870 tephra and/or above Layer H, although the exact number of black tephras separating them from these key horizons varies. The deposits at Aurasel and Smjörgíl are characterised by bedded relatively finer material overlain by coarser gravel or granules. The Smjörgíl facies are generally coarser and less well bedded than the similar facies at north Aurasel downstream. Geochemical analysis of tephra within the matrix of the Smjörgíl Unit 2 diamict showed similarities with both basaltic Katla tephra and the silicic Layer H from Eyjafjallajökull (appendix 1). The Einhyrningsflatir deposits, the base of which is not visible, shows an upper horizontally bedded sand unit, underlain by gravel-rich beds with clasts up to 1cm.

If these deposits are indeed the products of a single event it may be that a progression from finer horizontally bedded units can be interpreted to be followed by deposition of coarser material and then later finer sands towards the end of the event. Bedding of these sands suggests wind of water transport. Cross bedding and ripple laminations in the deposit at Aurasel suggest water transport. The pumice found on the surface of the deposit while being relatively light in mass compared to its volume

is most unlikely to have been transported by wind. It does however float on water and could have been transported from further upvalley by water. The lack of bands of lithics or extensive low-flow facies with fine ripples and laminations, combined with the extremely good preservation of the trees suggests rapid emplacement of the sands within one flow event.

6.5 Smjörgil Unit (3)

Unit 3 overlies SILK YN, with 1 black tephra and Layer H above. This unit was first identified at a >200-m long section cut by the Smjörgil stream and at this location is best represented in profiles 16-18 .(Figure 6.5.1) This unit was then traced throughout the mid- to lower valley as far northeast as profiles 79-82 in Northern Þórsmörk (Figure 6.5.2). Thickness varies, with purely a surface lag above an erosional unconformity along the northern and north-western margins of the channel in the middle valley, extended to deposits up to 29cm thick on the south-eastern channel margin. Downstream, in the lower valley at Smjörgil the deposit is thickest reaching 107cm in places, with a non-erosional lower boundary.

Throughout this area the unit is a matrix-supported diamict with a tephra-rich matrix. Analysis of tephra from the matrix of this layer shows that it includes basaltic material from Katla. In some locations pockets of sorted sands with cross-bedding have been observed within Unit 3, as have pockets of the SILK YN tephra. Coherent blocks of soil and tephra re-orientated through at least 90 degrees were found in the surface deposits at Einhyrningur.

Clast shape and roundness at the Smjörgíl section (16) indicate that most clasts have compact, blocky shapes and are primarily sub-rounded to sub-angular (Figure 6.5.3). Comparison with published data for till and scree (actively and passively transported material) suggests a relatively high degree of alteration during transport caused by abrasion and fracture. Unusually for actively transported material the samples have 28% very angular to angular clasts. The mix of particle roundness characteristics however, may reflect the original shape of clasts rather than shaping during transport, with more rounded clasts originating from fluvial deposits and angular material having been eroded from the lava surfaces upstream with little subsequent alteration. Although analysis of shape and inferences about transport pathways works well for glacial material the greater range of likely source material for flow deposits must be taken in to account in interpreting this data. Despite this, comparisons between different flow deposits may prove useful in comparing factors such as water-sediment ratios (nature of flow) and transport distance.

The most complete facies assemblage is found in the exposures within the gravel pit at the up-valley end of Tröllagjá (156-159). Crudely horizontally bedded granules with some cross bedding and silt pockets with ripples are overlain by a main diamict facies. The diamict is predominantly massive and matrix-supported, with some crude bedding. The upper 60cm however includes pockets of silt and

pale olive tephra with needle-shaped shards up to 1mm long. Electron microprobe analysis of samples of this pale tephra show that it is a silicic tephra from Katla, like SILK YN. This diamict is similar to the Smjörgíl exposure diamict. This unit at Smjörgíl is crudely bedded but on closer inspection shows finer structures such as pockets of well sorted, cross bedded sands. Eroded into this diamict at Tröllagjá are overlying black tephra-rich sands and gravels. The uppermost facies in deposited within a 10 metre wide 3 metre deep channel eroded into the sands and diamict below. Infilling this channel are predominantly horizontally bedded silts, black tephra-rich sands and granules.

Orientation of clasts was assessed at a number of locations along the Smjörgíl section and also at the Tröllagjá gravel pit (156) (Figure 6.5.4). Directional data for Unit 3 in profile 16 and 45 shows a considerable variation within a small ($<2m^2$) sample area. However, although no strongly consistent pattern exists for the deposit there is a general trend of clasts orientated between E-W and N-S, indicating possible preferential orientation along a flow direction from between north and east. Variation within this pattern may suggest rapid deposition or non-laminar flow. Towards the centre of the valley (profile 63) clast fabric is stronger with a dominant orientation towards WSW, possibly associated with stronger flow with increased distance from the valley margin. Within the Tröllagjá diamict (profile 156-9) clasts are orientated at odds with this downstream pattern. Clast strikes range over little more than 180 degrees, with a dominance of orientation between east to south. If associated with flow down the Markarfljót valley this suggests that many clasts were deposited at right angles to the main valley axis NE-SW. However, topographic situation of this deposit at the head of the Tröllagjá channel where the channel narrows may suggest that flow direction would be inconsistent with the main pattern in eddies directing flow at odds with the main flow direction.

This sequence shows extensive evidence of water transport, in the bedding structures, ripples and grading structures, even within the main diamict unit. The assemblage progresses from bedded granules deposited in a relatively low-energy flow through to diamicts indicating a higher energy environment of deposition and higher sediment to water ratio. The final bedded sands and gravels and uppermost channel infill indicate a return to lower energy and water-dominated flow conditions. This pattern of deposition is characteristic of hyperconcentrated flow events with a rising limb, main flow stage with associated bulking by incorporation of eroded material and a final water dominated falling stage associated with lower flow competence and sometimes with dewatering from previously deposited sediments. The dominance of black tephra within the lower and upper, bedded facies suggests a volcanic origin for this event. The diamict deposits at Smjörgil and throughout the valley are highly typical of lahar or hyperconcentrated flow deposits.

6.6 Unit (4)

Unit 4 is stratigraphically located between SILK YN and UN. The numbers of black tephras between these key layers and Unit 4 varies. Consistently however, this unit comprises a lower dark brown

diamict and upper granules to gravels. Mainly the diamict is massive and matrix supported with clasts with b-axis between 3cm and 15cm. The matrix is generally tephra-rich. Analysis of tephra from the matrix of Unit 4 at Smjörgíl shows that it contains material similar to basaltic Katla material and silicic material from Eyjafjallajökull (appendix 1). In North Þórsmörk it is crudely bedded and at Kanastaðir it fines upwards. Profiles at terraces east of Einhyrningur, Fauskheiði and Halli's Island all have surface lags above this unit with larger clasts (up to 13-50cm) than within the deposit (mainly 3-5cm), possibly suggesting a coarsening upwards sequence with winnowing of the uppermost layer or later deposition of only the largest clasts. Bedding within the finer layers and crude bedding within the diamicts suggests the action of water in the transport and deposition of these units. The lack of fine structures such as laminations, ripples and current reworked cross bedding indicates that deposition occurred rapidly and that the sediment to water ratio was high.

Clast shape, roundness and orientation were assessed in profile 16 (Figure 6.6.1). Clast shape and roundness show that most clasts have an intermediate shape between blocky and elongate, with a slight lean towards elongation. Primarily clasts were sub-angular or slightly less so, sub-rounded. These characteristics suggest some alteration during transport, though either with a more passive transport path than Unit 3 (Smjörgíl Unit) or with a shorter transport distance. Orientation of clasts in Unit 4 in profile 16 is variable, with a general trending strike between W and SSE. The most northerly sample had a stronger fabric orientated towards the SSE, whereas samples progressively farther from the valley centre had progressively more variation in orientation. This may suggest waning flow power towards the valley margin, as also appears to occur in Unit 3. Generally the orientation data suggests flow from the north to east and the variation within this suggests rapid deposition from a non-laminar flow.

6.7 Unit (5)

Unit 5 is a bedded tephra-rich deposit between SILK UN/H-M and H-S. Exact location in the stratigraphy may vary with different numbers of intervening black tephras between Unit 5 and the key pale tephra layers above and below. Consequently, this may represent one or more different events. Despite this, the characteristics of this layer (or layers) are consistent across the valley. Fine sand to granules sized lithics are mixed within the predominantly bedded black tephra deposit. Very few lithic grains are found in the deposit at West Kanastaðir. Lithic content and silt and clay laminations within the deposit indicate likely deposition from a flow event. In reference profiles at Kanastaðir a thick, bedded, black tephra layer (K-E) is found in a similar stratigraphic location.

6.8 Unit (6)

Unit 6 is a further bedded tephra-rich deposit between SILK UN/H-M and H-S, found lower in the stratigraphy than Unit 5. Generally this unit overlies H-S and is separated by up to 7 black tephra

layers. However, the number of black tephra layers between Unit 6 and H-S varies between 4 and 7. In profile 72 a lithic lag is separated by only one black tephra from H-S, with an erosive lower boundary. Characteristics of this unit vary. At valley marginal positions at West Kanastaðir and Fauskheiði (41. 144, 142) this unit is primarily a bedded black tephra deposit. At W Kanastaðir the lower layers contain lithics with a axis up to 2cm. At Fauskheiði however lithics are found throughout the deposit. At Halli Island and Einhyrningur (43, 74, 117, 126, 131), somewhat closer to the valley axis, Unit 6 is a massive matrix-supported diamict with a tephra-rich matrix. At profile 74 larger lithics are found closer to the base of the deposit. Variable stratigraphic position and variable characteristics may suggest that this unit actually represents at least two events, however they may also reflect variation in the nature and erosivity of a single flow at different locations within the valley.

6.9 Unit (7)

Unit 7 is found below SILK N4 and 1 to 2 black tephra layers, and above the H4 layer. This deposit has only been found in sections in Þórsmörk, Fauskheiði and in the Þröngá riverbank. The unit is composed primarily of massive, matrix-supported, tephra-rich diamict. Horizontally and cross-bedded facies are found towards the base of the unit, most clearly in the Þröngá river section. Like unit 3, unit 7 represents transitions in flow over the period of deposition, being typical of hyperconcentrated flow deposits.

6.10 Kanastaðir Unit (8A and 8B)

The Kanastaðir unit is so-called because it was first identified at the riverbank exposure west of Kanastaðir where stratigraphic relationships are most clearly represented (section 144). Consistently this unit is found stratigraphically below H4, one coarse black tephra layer and one fine black tephra layer. Below the Kanastaðir unit there are 8-12 dark tephra layers and then the characteristic 'twin' pale layer sequence.

The structural details of the whole deposit are best preserved at the terraces east of Einhyrningur (124). At both Kanastaðir and the Einhyrningur terraces (124 and 144) the unit is divided into two main units. The upper unit (8A) is a massive, matrix-supported gravel, separated from 8B by a thin soil layer. The lower unit (8B) is in most locations sub-divided into up to four facies, with lowered bedded sands and granules, diamict facies (2 different diamict facies at Einhyrningur terraces) with tephra-rich matrices as the main body of the unit and upper bedded silts and sands. Tephra within the West Kanastaðir diamict prove to be from basaltic eruptions of Katla (geochemical analyses, appendix 1). The detail of this facies assemblage is clearest in the terraces east of Einhyrningur along Fauskheiði to Halli's Island. The upper and lower bedded units are less clear at Kanastaðir and the exposures in North Þórsmörk show a much thinner, single facies matrix supported massive diamict.

Profile 84 in North Þórsmörk, in the base of an eroded channel with cataract shows sediments which have accumulated since the Kanastaðir event, suggesting scouring of previously deposited soils and tephras when elsewhere, particularly nearer the valley sides, deposition occurred.

The horizontal and cross bedding identified in the upper and lower facies suggests transport by water in relatively low energy environments. The middle facies however are interpreted as being related to higher energy environments and more rapid deposition, particularly where there are few sedimentary structures identified. These diamict deposits and the related bedded facies above and below are most similar to hyperconcentrated flow deposits described by Scott (1988), being too poorly sorted and lacking suitable structures to suggest deposition from an entirely water-dominated flood. The different facies are characteristic deposits representing a flow rising limb, main flow stage and later falling limb with related changes in flow rheology over time.

At Halli's Island, Fauskheiði and the terraces near Einhyrningur, the bedded lower sands and gravels are followed by the deposition of graded diamicts. Both fining upwards and coarsening upwards sequences are found at different locations, suggesting possible fluctuations in the direction of main flow and thus different routing of pulses of flow and sediment over time. The fining upwards sequences face directly upstream and reflect a reduction in energy over the time in which the unit was deposited, whereas the coarsening upwards sequences are found on the lee side of the Island and along the northern valley margins where flow competence gradually increased. The Island lee side deposit (117) transforms horizontally from a pure airfall tephra layer to a diamict indicating that these location was not entirely inundated by the event that deposited the graded diamict deposit. Despite apparently low flow here however, the Ljósá hill, further upvalley is covered by a thin deposit of the Kanastaðir Unit, indicating that at this point in the valley the flow was constrained by valley walls and covered the valley-central lava surface. Similarly the same deposit is found within soils in reference pit 91 in North Þórsmörk at ~340 m a.s.l.

Within the upper predominantly massive diamict at Kanastaðir there are rip-up clast lenses of soil and tephra. Despite the lack of erosional lower boundaries found associated with Unit 8B, these rip-clasts indicate that the underlying soil and tephra deposits in some parts of the valley must have been eroded and entrained within the flow. Scouring to the underlying postglacial lava within the channel (84) in North Þórsmörk confirms this, possibly indicating prevalence of erosion upstream and along the axis of the valley and deposition downstream and along the valley margins.

6.11 Units 9, 10 and 11.

Units 9, 10 and 11 are only exposed within the lower valley at the riverbank section west of Kanastaðir and at Halli's Island. At these locations units 9 and 11 are continuous over several hundred

metres, but it is not clear due to lack of mid to early Holocene exposures whether these layers are continuous throughout the valley.

Unit 9 has only been identified at Halli's Island (74) below the twin pale tephras below H4. This deposit is mainly composed of bedded black tephra with five coarse layers intercalated with finer layers. Lithic clasts range in size between fine sand and gravel with a axes less than 1cm. Unit 10 lies beneath the lower 'triplet' of pale tephras in the West Kanastaðir section (143) and is recorded as a non-continuous, orange, gravely diamict with gravel-sized lithic clasts. The oldest layer (11) identified in the West Kanastaðir profile below Unit 10 is a dark grey to black diamict, with sub rounded to angular clasts up to 50cm and a black tephra-rich matrix. Tephras and soils are not visible beneath this layer due to thickness of this unit and induration of sediment. This layer may be equivalent to diamicts at the base of profiles at Einhyrningur and in North Þórsmörk (91, big hill), above the geomorphological limits of flood extent, and interpreted as glacial till.

6.12 Emstrur deposits

Similar deposits to those recorded downstream have been identified within the Botn basin, on the plateau surfaces in the Entujökull foreland, on the lower slopes of Stóra-Mófell and north of Sléttjökull. Correlation of these deposits with those downstream has proven difficult due to the lack of exposed soils and difference in the tephra stratigraphy between the upper, middle and lower valley. Where possible, correlations are suggested here. Further links will be considered during reconstruction of the relationships between past glacier margins and flood routes in Chapter 7.

The Botn deposits predominantly consist of very thick (>15m) bedded black tephra-rich sands. Sections in the basin show differences in the structure of the main units and in the nature of the underlying material compared to sections at the margins of the basin and will thus be considered separately. The central exposures are found in the channels that separate the black mounds that characterise the geomorphology of the whole basin. Marginal sites are located in the gullies that cut through the edge of these mounds from the bedrock knolls along the western basin margin.

The central exposure within the base of the basin shows bedded black tephra-rich sands overlying finely laminated pale silts (Figure 6.12.1b). The bedded coarse sands are 23m thick and sub-divided into three units with upper horizontally bedded sands, intermediate gently dipping cross beds and lower more steeply dipping cross beds. Section 114 through the uppermost layers of these sands shows that they are mainly crudely bedded coarse black tephra and lithic sand grains with pale silt drapes, lenses of fine to coarse sands and inclusions of pale silty tephra. The surface layers are eroded into by bedded gravel up to 5cm. The surface is covered with a lag of large boulders and cobbles.

Underlying the black sands at section 113 are pale horizontal, rhythmically laminated silts with ripples on the surface at the contact between the black sands and the silts. The laminated silts at this location have not been eroded by the event that deposited the overlying sands. However, the silts are not continuous along the base of the section suggesting that in places they had been eroded or are covered with a thick layer of scree from the unconsolidated sands above. Within other gullies in the mounds filling the Botn basin the black sands are dissected by vertical 'vein' structures infilled with pale grey streaky silts very similar in colour to the laminated silts in the main section. These veins sometimes have a pale thin layer of silt coating the vertical edges and then massive silts and fine sands infilling the main body of the vein. The presence of this silt at ~100m from the laminated silts indicates that the same laminated silt deposits may underlie much of the basin sands.

The laminated silts and vein structures suggest that prior to the deposition of the sands the Botn basin was filled with a lake. The overlying sands exhibit delta like cross-bedding grading to horizontal bedding in the upper layers, similar to a 'Gilbert-type' delta sequence with foresets overlain by planar topsets. This indicates that the sands were probably deposited into a lake environment. The vein structures are typical pipe dewatering structures indicating the upward displacement of sediment by escaping fluid. This means that the sands were deposited on top of waterlogged fine sediments, which deformed under the loading of the denser sands.

The marginal Botn basin sections (115, 150 and 151; Figure 6.12.1a) expose bedded sands and diamicts overlying soil and tephra layers. Characteristics of these sand and diamict deposits are very similar to Units 3 and 8 and the Tröllagjá gravel pit sections (156). Bedded sands and gravels form the uppermost and lowermost beds with intervening diamicts. These represent rising, peak and waning stage deposits similar to hyperconcentrated flow sequences.

Geochemical analyses of the matrix of marginal deposits near to the Botnar hut show a mix of chemical compositions. Most of the tephra is basaltic material from Katla. However, a small fraction is rhyolitic and is most similar to the high silica fraction of the SILK tephra, A1, with SiO2 between 69-71%, low FeO (3.9-4.3%) and high K2O (3.3-3.9%) (Tables 6.12.1 and 6.12.2: show A1 analyses from Larsen et al (2001) and N/A-4 analyses). This comparison does not necessary suggest that this flow event is associated with the A1 eruption, rather that similar silicic material was incorporated within the deposits either from erosion of A1 tephra or from juvenile material produced in associated eruption. Basaltic eruptions of Katla may produce a small amount of silicic tephra. Silicic eruptions may also have produced a greater range of tephra compositions, with initial eruption products which do not fall as tephra since they are confined beneath the ice being incorporated into flood deposits.

The direction of the cross beds in profile 113, indicates the building up of the deposits with a flow direction and supply of sediment from the west of the basin. This is commensurate with a glacial source. Clasts within the lower diamict in profile 151 are preferentially orientated towards the SW.

	SiO2	TiO2	Al2O3	FeO	MnO	MgO	CaO	Na2O	K2O	Total
(a)	70.87	0.27	13.27	3.99	0.17	0.25	1.40	4.20	3.90	98.32
	70.37	0.33	13.08	3.93	0.17	0.20	1.46	4.96	3.50	98.00
	70.12	0.34	12.42	4.31	0.17	0.23	1.11	4.38	3.85	96.93
	69.60	0.37	13.10	3.95	0.15	0.17	1.14	4.57	3.39	96.44
mean	*70.24*	*0.33*	*12.97*	*4.05*	*0.17*	*0.21*	*1.28*	*4.53*	*3.66*	*97.42*
s.d.	*0.53*	*0.04*	*0.37*	*0.18*	*0.01*	*0.03*	*0.18*	*0.33*	*0.25*	*0.88*
(b)	47.07	4.28	12.15	14.01	0.24	4.55	9.33	3.21	0.77	95.61
	46.19	4.44	12.51	14.94	0.29	5.32	10.03	2.90	0.60	97.22
	46.18	4.39	12.35	14.24	0.23	4.72	9.72	3.09	0.69	95.61
	46.15	4.36	12.36	14.15	0.22	4.81	9.92	3.15	0.73	95.85
	46.13	4.33	12.44	14.13	0.22	4.89	9.71	3.04	0.68	95.57
	46.10	4.46	12.31	14.80	0.23	5.12	10.02	2.95	0.63	96.62
	46.03	4.43	12.46	14.44	0.25	4.90	9.67	3.07	0.66	95.91
	45.96	4.34	12.46	14.23	0.22	5.16	10.02	2.97	0.61	95.97
	45.92	4.57	12.35	14.39	0.27	5.09	9.97	3.05	0.64	96.25
	45.67	4.42	12.46	13.90	0.23	5.03	9.70	3.07	0.61	95.09
	45.60	4.62	12.41	13.94	0.17	5.25	9.97	3.01	0.65	95.62
mean	*46.09*	*4.42*	*12.39*	*14.29*	*0.23*	*4.99*	*9.82*	*3.05*	*0.66*	*95.94*
s.d.	*0.38*	*0.10*	*0.10*	*0.33*	*0.03*	*0.23*	*0.22*	*0.09*	*0.05*	*0.58*

TABLE 6.12.1: N/A-4 sample from Emstrur, close to the Botnar hut. Note fraction (a) is highly silicic.

	SiO2	TiO2	Al2O3	FeO	MnO	MgO	CaO	Na2O	K2O	Total
(a)	72.46	0.12	13.34	2.24	0.07	0.10	0.38	5.08	4.64	98.43
	72.15	0.12	13.30	2.32	0.06	0.08	0.40	4.93	4.88	98.24
	69.48	0.26	13.33	3.93	0.16	0.23	1.33	4.80	3.57	97.09
Mean	*71.36*	*0.17*	*13.32*	*2.83*	*0.10*	*0.14*	*0.70*	*4.94*	*4.36*	*97.92*
s.d.	*1.64*	*0.08*	*0.02*	*0.95*	*0.06*	*0.08*	*0.54*	*0.14*	*0.70*	*0.73*
(b)	67.55	1.14	14.01	5.28	0.16	1.14	2.69	4.50	2.89	99.63
	66.07	1.16	14.20	5.30	0.19	1.12	3.16	4.51	2.83	98.54
	65.73	1.12	14.26	5.44	0.17	1.21	3.01	4.36	2.78	98.08
	65.59	1.25	13.92	5.82	0.19	1.18	3.05	4.53	2.86	98.39
	65.55	1.22	14.09	5.64	0.15	1.21	3.15	4.24	2.69	97.94
	65.24	1.28	14.60	5.64	0.17	1.18	3.13	4.26	2.83	98.33
	65.23	1.27	14.07	5.55	0.21	1.11	3.19	4.49	2.75	97.87
	64.69	1.24	14.03	5.49	0.17	1.06	3.16	4.37	2.75	96.96
Mean	*65.71*	*1.21*	*14.15*	*5.52*	*0.18*	*1.15*	*3.07*	*4.41*	*2.80*	*98.22*
s.d.	*0.85*	*0.06*	*0.21*	*0.18*	*0.02*	*0.05*	*0.16*	*0.12*	*0.07*	*0.75*
©	49.87	3.81	12.95	12.17	0.26	3.82	8.00	3.54	1.22	95.64
	48.24	4.12	12.40	13.91	0.24	4.49	8.80	3.37	0.93	96.50
	47.25	4.51	12.66	14.18	0.22	5.10	9.15	3.22	0.85	97.14
	47.24	4.72	12.40	14.96	0.23	4.76	9.35	3.11	0.76	97.53
Mean	*48.15*	*4.29*	*12.60*	*13.81*	*0.24*	*4.54*	*8.83*	*3.31*	*0.94*	*96.70*
s.d.	*1.24*	*0.41*	*0.26*	*1.18*	*0.02*	*0.54*	*0.60*	*0.19*	*0.20*	*0.83*

TABLE 6.12.2: Geochemical data on SILK A1 from Larsen et al (2001). Compare fraction (a) with fraction (a) of sample N/A-4 in Table 6.12.1, above.

These orientated clasts suggest either flow from the NE as the topography directed flow direction around the basin or orientation of clasts at an angle to the main flow direction.

Similar, though shallower, deposits are found on both of the plateau surfaces in the Entujökull foreland. Each of these are characterised by spreads of bedded black tephra-rich sand overlying lava. Geochemical analysis of tephra from these deposits shows that they are primarily composed of basaltic Katla tephra (appendix 1). One of nineteen analyses was silicic in composition with SiO2 of 67.76%. This analysis is similar to SILK tephras SILK YN and N4. However the value for Al2O3 is somewhat lower at 12.98% than Larsen et al (2001)'s analyses around 14%. This individual analysis statistically can not have much significance.

The Stóra-Mófell moraines and channels are coated with a lag of tephra-rich sands, incorporating pumice and lithic clasts. The depth of these deposits is higher (at least 1m) within the channels and in enclosed basins. This material forms a grey-coloured lag on the surface with a limited extent to the north and west, overlying a more compact, brown till sheet.

The Sléttjökull deposits cover an extensive sandur plain to the north of Sléttjökull and Entujökull. Channels within these sediments are clear in the western section of the sandur, connected with bedrock-cut channels and cataracts. Gullies are exposed within these sediment terraces at the margins of these channels. These sections expose crudely bedded black tephra-rich sands up to 15 m high, similar to the Botn deposits and the jökulhlaup deposits on Skogassandur and Sólheimasandur.

6.13 Comparison with known origin deposits

These bedded sands of Emstrur are very similar to the jökulhlaup-dominated sandur facies found along the south coast, particularly those from Sólheimajökull. Sólheimajökull deposits are characterised by bedded units in the basal and upper sequences, with massive sand beds in the middle.The diamicts of the Botn basin deposits are less typical of ice-proximal jökulhlaup deposits. However, the roundness characteristics and fine-scale bedding suggest that in part at least they have experienced transport by water. Incorporation of morainic material and higher energy transport regimes allowing further erosion of the flow bed would make these deposits coarser than those at Sólheimajökull. The valley-confined nature of a Markarfljót flood would result in bulking to hyperconcentrated flows like lahars (eg. Mount St Helens.. Scott 1988)

Geochemical analyses of tephra from known flood deposits at Skogassandur and Sólheimasandur show a narrow range of chemical composition all indicating a dominance of basaltic Katla tephra (Appendix 1). No SILK tephra was found in the southern flood deposit tephra analyses. Some variation in chemical composition is clear between the tephra from different events, however this variation is only very small and probably not significant enough to chemically differentiate between

different events. Analyses were also carried out on tephra from samples of Markarfljót fluvial sand (Appendix 1). This material showed a far greater variation in chemical composition than any of the known flood deposits or any of the unknown deposits analysed. This reflects incorporation of tephras from the main local volcanic systems by rivers in the basin. The great range in chemical composition, not duplicated in analyses of unknown layers discussed here indicates that they are unlikely to have a normal fluvial origin, showing greater similarity to the southern flood deposits than the normal fluvial sands.

Cumulative grain size analyses carried out on known flood and normal fluvial deposits give comparison for analysis of grain size characteristics of unknown deposits (Figure 6.13.1, Appendix 3). Flood deposits from Sólheimajökull have 'S' shaped cumulative grain size curves, generally coarser than the fluvial sands which have much straighter shaped curves. The fluvial sands are finer, depleted in the size ranges –2 to –1 phi and rich in size ranges 1 to 5 in comparison to flood deposits. The biggest difference actually probably reflects distance from the ice margin, since the flood deposits were sampled within 2 –3 km of the ice margin, whereas the fluvial sands were sampled much farther downstream. This same pattern is evident in the unknown samples analysed and thus it seems that cumulative grain size analyses are not especially useful for determining flood origin unless samples are selected at set distances from the ice margin. Downstream samples show much more 'straight-line' graphs than the ice proximal deposits. The downstream samples were all diamict deposits, and thus the largest grain sizes are not represented in the graphs. The upstream samples were tephra-rich sands and granules primarily. Differences in the ice proximal deposits are apparent and can usefully be compared with each other and the southern flood deposits, since they are all from approximately the same distance downstream from previous ice margins. The Botn (113) sub horizontal deposits have grain size distributions like the southern flood deposits, with greatest concentration between –1 to 1 phi. Similar but finer distributions are apparent in the Botn (113) upper cross-bedded unit, Stóra-Mófell channel deposits and Entujökull eastern plateau channel deposits. These may represent lower flow waning stage flood flows. Two samples from the Entujökull western plateau are quite different with relatively uniform size distributions, similar to the Thrasi's cliff southern flood unit which is more like the Markarfljót sands than the Sólheimajökull tephra-rich flood units. The Thrasi's cliff deposit is located very close to an ice margin and extends downstream from a moraine ridge. The Entujökull western plateau flood is similarly found close to a dissected moraine and incorporation of this material may explain this different grain size distribution. Although the Stóra-Mófell and Entujökull eastern plateau samples are found close to moraines they are both taken from channels and thus may reflect later deposition than wider spread material. The Entujökull deposit may also be somewhat older than the moraine ridge found along the eastern margin of the sands.

6.14 Silicic Katla Pumice in the Markarfljót

Pumice deposits have been found at ice marginal positions near Entujökull and on the sandur south of Fljótshlið. All of these deposits have been surface lags incorporating pumice clasts. Other than the highly silicic material found at Aurasel that has been attributed to Veiðivötn and was discussed above, the pumice is dark brown to black, sub-rounded to sub-angular (Figure 6.14.1). Pumice clasts range in size from 1 - 10 cm and float. Similar mid to dark brown pumice clasts were also recorded on the western plateau in the Entujökull foreland and on the terraces east of Einhyrningur. Geochemical analyses of the brown pumice indicate that all this pumice is silicic in nature with 59-69% SiO2, and shows similarities with silicic tephra from Katla (appendix 1). The geochemical analyses allow the samples to be grouped in to two categories.

Group A includes the majority of the samples analysed. Pumice in this group was found within channels and on the surface of moraine ridges on the lower slopes of Stóra-Mófell and on within the surface lag at Drumbabót. These pumice pieces have a silicic content of between ~60-70% SiO.

Group B actually only includes one analysed pumice clast from a surface lag overlying lithified tuff incorporating palagonite and basalt clasts, outside the limits of the Stóra-Mófell moraine ridges. This pumice was described as very dark in the field. However, electron microprobe analysis of one clast indicates that it is silicic in composition with 68-68.8% SiO2 content (appendix 1). It has slightly lower levels of Ti, Fe, Mg and Ca than the other pumice pieces analysed from the Entujökull area (Group A) and higher levels of Na, K and Si.

The chemical composition of clast B is similar to pumice analysed by Newton (1999, Staosnaig report and Camas Daraich report) and also to the Vedde ash found in Norway (Birks et al 1996, Lacasse et al 1995 and Magerund et al 1984). Newton (1999) analysed pumice from archaeological sites and identified four groups based on major element chemistry. Clast B analysed in this research corresponds most closely to Group B. Pumice from Vikurholl, on the southern flanks of Katla, also has similar chemical characteristics (Newton 1999). Recently analysed ocean-rafted pumice found at archaeological sites in Britain (dark brown pumice at Camas Daraich, Skye and light brown pumice at Staosnaig, Colonsay) also has a similar composition. The Vedde tephra deposited in the Late Glacial is found throughout North West Europe and has been linked to one or more eruptions of Katla. The chemistry of this tephra is very similar to the pumice clast B, Vikurholl pumice and the archaeological pumice analysed by Newton (1999). Although chemically similar these pumice clasts may not all be associated with the same eruption.

These analyses and finds of silicic Katla pumice in the Markarfljót are important because they add to the limited data available about Katla pumice from terrestrial sites in Iceland. Pumice piece B may be the product of the same activity that produced the pumice deposits at Vikurholl in the Late Glacial or

from similar activity around that time. Group A pumice is the only dacitic Katla pumice which has been found in Iceland, previously having only been identified in ocean-rafted pumice deposits around the North Atlantic.

6.15 Summary

164 possible flood units identified in a total of ~90 sections. Of these 11-15 units are identifiable. Two historic floods units are found in the north of the area. The Smjörgíl Unit and the Kanastaðir Unit are the most continuous facies assemblages recognised within this study, with the most consistent stratigraphic relationships. These deposits are the most extensive of all the flood-like deposits identified are were most likely the largest of the Holocene events recognised here. The other deposits have not been recognised in so many exposures. This may reflect a lack of extensive distribution, lack of conditions favouring deposition or purely a lack of suitable exposures.

Chapter 7: Reconstruction and Chronology

This chapter aims to:

- Assess whether the Markarfljót has been a Holocene flood route
- Reconstruct the routes of past jökulhlaups and relate to past positions of Entujökull.
- Determine the timing, frequency and nature of these floods.
- Assess whether floods are associated with volcanic activity or lake drainage
- And if associated with volcanic activity, whether this is basaltic or silicic.
- Evaluate any evidence for the Markarfljót as a route for the terrestrial transport of the North Atlantic ocean-rafted pumice.

7.1 Introduction

Geomorphological and sedimentary evidence presented in this thesis shows that the Markarfljót valley has indeed been a route for large-scale 'floods' during the Holocene. Large, valley-scale floods occurred within the Markarfljót valley on at least eight, and possibly up to fifteen, occasions within the last ~4/5000 years. Floods probably also occurred prior to this time as suggested by Vilmundardóttir and Kaldal (2001). However, the valley-side sedimentary record of the Markarfljót is limited to the last 7000-8000 years and the oldest sediments are highly indurated and poorly exposed. This chapter brings together the evidence for 'flood' events during the mid to late Holocene, their timing, nature and extent, and relates them to fluctuations of Entujökull.

7.2 Middle and Lower Valley Chronology

Figure 7.2.1 shows the chronology of flow events. Dating is multi-proxy. Where possible, interpolated sediment accumulation rates have been calculated to further refine the chronology based on tephra layers and radiocarbon analyses (appendix 4), an approach justified by Dugmore (1987). Dating shows that the identified flows have not occurred at regular intervals but it is likely that only the largest and most extensive events are represented in the sedimentary records, some smaller events were constrained within the Markarfljót gorge. The larger floods have left depositional evidence along the valley margins where preservation potential is higher. Similarly, floods associated with advanced positions of Entujökull have flowed across Langháls in to Northern Þórsmörk where preservation is better than along the main valley

axis. Floods from periods when Entujökull has been less extensive (like today, for example) would need to have filled and over-topped the Markarfljót gorge before any sedimentary evidence would have been well preserved. Thus it is likely that there have been many more floods than represented in the sedimentary record.

The two largest and most extensive flows occurred ~4500 and ~1600 years ago (Units 8 (A and B) and 3). Event 8, the Kanastaðir flow, occurred shortly before the deposition of the Hekla-4 tephra (3826+12 BP), about 4,000 to 4,500 years B.P. This flow was a classic laharic flow, with rising and waning stages dominated by water flow and higher sediment concentrations within the main hyperconcentrated peak flow. The main event was followed by a later and smaller hyperconcentrated flow (Unit 8A at Einhyrningur Terraces and West Kanastaðir).

This 8B event was far more extensive than any flow event that has since occurred in the Markarfljót. In North Þórsmörk the limit of deposition reaches 341m a.s.l. up the valley sides (profile 91) and flow width was ~1.5 km. The flood washed through a col between the Ljósá valley and the Markarfljót valley across the Úthólmar hill (profile 98). The peaks of this hill are not covered by flood deposit, giving an upper limit to flood depth in this location of ~20m. Downstream where the valley widens onto the Markarfljót sandur the flow spread out to leave ~90cm thick deposits in West Kanastaðir, washing over Halli's Island. Thickness variations in Unit 8B around this Island show that the flow was deepest towards the valley axis. On the northern Island margin Unit 8B is much thinner (>10cm) and in places grades into a basaltic Katla airfall tephra layer. This indicates that the flow merely washed over the Island and passed around the Island. This limits flow depth estimates here to >4m. The transition to an airfall tephra layer suggests that this flow event was a volcanigenic flow associated with an eruption of Katla. This is confirmed by a tephra layer in the reference profile at Kanastaðir at the same stratigraphic location as the flow deposit in the riverbank at West Kanastaðir.

Event 3, the 'Smjörgil' flow occurred about 20 radiocarbon years after the SILK YN silicic eruption of Katla. Towards the northern end of the middle valley the flow was approximately 1km wide, eroding along the line of the Markarfljót (profile 79-82 and terraces) and depositing sediment along the eastern margin of the channel. The flow washed the valley central lava, although flow depth was probably no more than 1-2 metres, the main flow being channelled along the main Markarfljót gorge and the channel through the lava between the Ljósá and the Markarfljót. Downstream the valley narrows a little, reducing the flow width to ~900m and focussing flow within the channels of Tröllagjá and the Markarfljót. Further downvalley, the flow spread out across the sandur plain up to 6 km wide near Gigjökull.

The exposure in the gravel pit at Tröllagjá shows clearly how the flow nature changed over the duration of the event from water-dominated flow to a sediment laden hyperconcentrated flow and back to waning stage water floods, similar to the Kanastaðir event (8B). The uppermost channel deposits at Tröllagjá may represent a later flood or the final stages of the Unit 3 event. Deformation of underlying deposits and incorporation of intact rip up clasts of tephra and soils within the peak flow deposit suggest that the underlying ground may have been deeply frozen and that the event occurred in the winter.

These two floods (8 and 3, 'Kanastaðir' and 'Smjörgíl') probably have had the biggest geomorphological impact of all of the recorded flow events in the Markarfljót valley. They both produced extensive deposits rich with lithics along the entire middle to lower valley. This material was undoubtedly entrained en route downvalley from unconsolidated fluvial and glacial deposits and from erosion of the main channels and lava flow margins. Multiple small-scale erosional features such as scratches, cataracts and potholes were formed and later polished and smoothed by the repeated action of these events. At a large scale, the Markarfljót gorge may predate these floods, it being possible that drainage of the Emstrur lakes is responsible for the original gorge incision. The ages of the lava flows through which the gorge is cut have not been dated in detail. The geological map of the area shows them as postglacial, prehistoric lavas older than c.4000 BP. It may be likely that they were erupted at around the same time as the three lava flows from Maelifellssandur that cap the Emstrurlon sediments, some time before 2,500 BP (Vilmundardóttir and Kaldal, 2001). The gorge has two rock-cut terrace levels above the present river level. This indicates that it has been incised in stages and thus it is suggested that the 'Kanastaðir' and 'Smjörgíl' flow events c.4-4,500 and 1,600 BP significantly deepened the gorge.

Similar flow events formed mixed lithic and tephra-rich deposits Units 2, 4, 6 and 7, around 1230 BP, c.2000 BP, c.3200 BP and c.3600 BP. Units 2 and 4 both incorporate Eyjafjallajökull silicic tephra which may suggest an element of flow from Eyjafjoll as well as a main flow down the Markarfljót valley. Unit 2 at Smjörgil decreases in thickness towards the main valley axis, possibly indicating a source from Eyjafjöll. Dugmore (2003) suggests that volcanic and thus jökulhlaup activity from Katla and Eyjafjallajökull may be linked. In particular he suggests that in the 10th Century AD floods occurred across Langanes from eruptions of subglacial fissures, which radiate to the east from the main crater area. It may be that this has also occurred at least twice in prehistory c. 1230 BP and c.3200 BP. Unit 2, may actually represent two different flows (or periods of flows), one from Eyjafjallajökull leaving deposits at Smjörgil, North Aurasel and swamping a mature wood at Drumbabót south of Fljótshlið, and a later flow from Katla leaving deposits on Einhyrningsflatir. This later flow incorporated silicic Katla pumice transported from beneath or close to the margin of Mýrdalsjökull and left a pumice lag on the surface of the Drumbabót tephra-rich sands.

Event 7 (c.3600 BP) is different from the others in that deposits are not found further upstream than Fauskheiði in the lower section of the middle valley. A diamict unit is however, found within the Þröngá riverbank exposure, suggesting flow down the Thornga valley rather than the main Markarfljót valley. Þröngá drains small outlet which extent downvalley from Merkurjokull, a relatively thin lobe of ice extending over the caldera rim into Northern Þórsmörk. A gentle plateau area extends eastwards between Merkurjökull and Krossárjökull. This area, like the plateau area Lakar between Merkurjökull and Entujökull is gullied and on aerial photographs has a smoothed appearance possibly indicating that floods have passed over the area into Þröngá. Floods from Merkurjökull may have also passed over Lakar into the Ljósá valley at the same time, associated with eruptions of Katla along fissures near the caldera rim.

These various examples of hyperconcentrated flow events, possibly caused by volcanic melting of ice, show some similarity with other documented jökulhlaup and lahar sediment assemblages. Maizels' catastrophic volcanic type III sandur model, developed along the southern coast of Iceland, has the same low flow basal and upper facies, with a main flow unit in the middle with less structural features. However, in Maizels' model these main flow units tend to be composed primarily of pumice granules, unlike the mixed lithic and tephra-rich diamicts in the Markarfljót. The diamict facies of the Markarfljót floods noted here are most similar to the main flow units of valley constrained lahar deposits from Mount St. Helens and Nevado del Ruiz (Harrison and Fritz 1982, Scott 1988, Lowe et al 1986, Naranjo et al 1986). These lahar events travelled a long distance from the ice margins in confined channels before spreading out and depositing their sediment downstream and thus their deposits are dominated by sediment derived from the local valleys rather than primary eruptive material. The low flow stages representing the start and end of the flows are common to both Maizels' jökulhlaup facies and valley-confined lahar deposits. Thus, the deposits formed in hyperconcentrated flow type events in the Markarfljót are interpreted as lahar-like events similar to those documented at other volcanoes where flows are channelled along valleys radiating from the volcano. Despite the Markarfljót lahars and the south-coast jökulhlaups both being caused by volcanic eruptions beneath the ice their different proglacial routes have dominated their downstream legacy more so than their original cause.

Tephra-rich granular deposits represent the other main type of flow event in the Markarfljót. The clearest examples of these events are Units 5 and 6. There are two main characteristics of these units, namely variable stratigraphic location and the dominance of tephra in the material within the deposit. Variable stratigraphic location is taken to indicate variable timing of flows at different localities, suggesting that deposits were formed in a number of different events rather than a single, main valley-scale flow. This dominance of tephra over lithic content is very similar to the south coast volcanigenic jökulhlaup deposits. However, the variable stratigraphic position suggests short travel distances, rather than a volcanic jökulhlaup origin. Instead, these deposits are formed from a number of different, though similar events

occurring over a period of several years. Around the same time as these events very thick basaltic Katla tephra layers, K-E and K-N were deposited. In many volcanic regions such thick unconsolidated tephra deposits form lahars when exposed to heavy rainfall and snowmelt, often some years after the original eruption. These deposits are therefore interpreted here as tephra remobilisation flows which occurred at different times in the valley shortly after the deposition of K-E and K-N. The volume of these flows was probably significantly lower than the events that formed valley-wide diamict deposits. Event 6 shows characteristics of both types of flow and may represent one flow with different characteristics at different stages or perhaps different types of flow.

As well as these prehistoric events, two historic floods are proposed. Units A and B are found in Northern Þórsmörk uppermost in sedimentary sections and above tephra layers which are probably historical in age. These flood events occurred in the 10th century and sometime after 1510 AD. These deposits are the only dateable flood type deposits found in the large channel and across the scablands in North Þórsmörk. They are also found above the erosional unconformity associated with Unit 3 on the terraces within the Markarfljót gorge. The 10th Century flood passed along the big channel in the North of Þórsmörk, depositing diamict in the lee of the scabland cliffs at the western margin of the channel. The flow then scoured the lava surface and cataract of the scabland and streamlined hill/cataract between Stóraland and Fauskatorfur. The flood washed the upstream side of the streamlined hill here although the summit of the hill remained above the maximum water level. The upstream side was also still above the general maximum water level but the flow patterns around this obstacle would have elevated the flow at this point and reduced flow velocities in the lee of the hill, resulting in the deposition of a pendant bar. This flood did not cover the higher lava surfaces between the cataract and the Markarfljót channel, with a separate flow travelling along the Markarfljót gorge. The deposits from the 10th Century flood are similar to those left by events such as 3 and 8. However, the 10th Century flood was considerably smaller in extent. Thus, it is possible that this also was a volcanically generated flow event, linked to either the 920 or 935 AD eruption of Katla.

Sediments from the most recent event (sometime post 1510 AD) are far more rich in tephra than the 10th Century flood, showing similarities to the south-coast type deposits, with crudely bedded tephra granules, capped by a lithic lag. Only a very thin lag covers the top of the profile (94) although the tephra sequence is beheaded suggesting possibly that this area was washed by the flood eroding the soil above the 10th Century deposit, but not that the flood necessarily passed over the area from the western big channel since flow in this direction would probably have left a deposit in the lee of the lava cliff here. Rather, it is suggested that flow may have been primarily directed along the Markarfljót channel, spreading out in to North Þórsmörk.

These recent historical age floods have eroded away any clearly dateable evidence of previous floods across the big North Þórsmörk channel. However, boulders 2-3m, some imbricated, within this channel, are probably far too large for these small-scale historical floods to have transported. Any time Entujökull has been more extended than c.2km from it's present location (1994) then volcanigenic and glacial floods routed to the NW of the ice cap would have flowed along this channel.

7.3 Upper Valley Chronology

The linkages between these middle and lower valley records and the pattern of flood deposition upstream is somewhat fragmentary. This reflects the fragmentary tephra record in Emstrur, the different characteristics of flood deposits close to the ice margin compared to downstream, and the complex topography of the Entujökull foreland formed by the actions of volcanic, glacial, fluvioglacial, slope and jökulhlaup processes during the Holocene. Within the Entujökull foreland and in the Botn area there are areas of flood topography and deposition that are related to different glacier margins. Two other flood regions have been identified from Sléttjökull northwards and from NE Entujökull. (Figure 7.3.1)

Basaltic-tephra rich deposits dominate all these areas. Closest to the ice margins the flood deposits form thin covers over the underlying morainic or lava topography, sometimes having washed over old moraine forms and altered their shapes. In the Botn basin the deposits are thicker and concentrated within the basin. Bedded deposits are low flow sediments associated with early and final flows and the diamict deposits between these upper and lower bedded layers are like the laharic flows downstream.

The flood topography represents four different stages of glacial extent and associated flood deposition; the Sandur stage (floods across the eastern plateau), the Valley stage (flood deposits in the valley between the two plateaux), the Botn stage (deposition in the Botn basin) and the Stóra-Mófell stage (pumice flood covering the lower slopes of Stóra-Mófell and the western plateau). Floods from the Stóra-Mófell and Botn stages probably also flowed northwards from the NE lobe of Entujökull. Timing of these stages of flood activity can be carried out with reference to tephra sequences in the Entujökull area, pumice ages and flood records downstream. These records, combined with theoretical ice surface profile calculations also constrain estimates for past positions of Entujökull. The positions of glacier margins associated with particular flood routes are estimated using procedures for determining ice surface profiles as described by Paterson (1994; Appendix 5).

The youngest, Sandur stage, is characterised by a flood across the eastern plateau and has not been overridden by a glacier. Distinctive moraine ridges border the eastern margin of the Sandur flood deposit. East of these ridges, pits dug in surface deposits show that only one to two black tephras (possibly K1918

and K1755) lie above glaciofluvial or glacial deposits. This suggests that these ridges were formed some time before 1755, and possibly also after the eruption of Katla in 1721, indicating a Little Ice Age advance to this position in the early 1700s. The age of the flood deposit must therefore be the same as this or earlier. Profile 116 north-west of the Little Ice Age moraines has a basal till overlain by historical tephras including the putative Hekla 1206 and bedded grey Hekla 1341 tephras. Overlying these layers there is a dark diamict deposit associated with possible glacial or jökulhlaup activity. This profile suggests that the Sandur stage flood occurred after the basal till and Hekla tephras were deposited, giving bracketing ages of c.1400s to early 1700s AD. This may tie in with the c.1600s flood deposit (Unit A) identified in the North Þórsmörk profiles. Calculations of ice surface profiles for all the flood routes north and south out of the foreland indicate that, with an ice position at the LIA limit, floodwaters are unlikely to be routed any other way than along the present drainage route towards the Markarfljót.

The Valley Stage refers to a time when Entujökull occupied a frontal position in between the two plateau lava flows. Within this area of the foreland there are numerous fragments of moraine ridges, some of which have since been covered and dissected by jökulhlaup activity and normal glaciofluvial stream action. Profile 116 (referred to above) suggests that some time shortly before the deposition of Hekla 1206 Entujökull extended westward of the Sandur stage. It is also known from North Þórsmörk that a flood was routed along the big channel in North Þórsmörk around the 10th Century. For flood waters to have been routed this way the glacier margin must have been located between the Little Ice Age moraines (minimum distance downvalley with 100kPa shear stress) and the western end of the foreland (maximum distance downvalley with 50kPa shear stress) (Figure 7.3.2). A position mid-way between these extremes using a value of 50kPa for shear stress and basal topography at the elevation of the lava surfaces places the ice front in the middle of the valley, tying in with fragmentary moraine evidence. Thus, it is suggested that around the 10th to early 13th Centuries Entujökull lay in the valley between the two lava plateaux and a flood issued from this margin into North Þórsmörk and the Markarfljót valley. An ice front in this location may also have sent water and sediment in to the Botn basin and northwards in to Emstrur.

There are two floods with similar glacier positions. The Stóra-Mófell stage (Figure 7.3.3) is represented by a more extensive ice position sending floods into two areas, the western plateau and across the cliffs near Stóra-Mófell. Both areas have SILK pumice lags. There are also multiple moraine ridges in both locations, some of which have been overridden by flood flows. The pumice suggests that the two areas and thus two regions of flood and morainal topography are contemporary. The SILK-YN-type pumice in the lags floats, so must have been deposited in the last flood over these areas and the chemical composition indicates that the flood events occurred around the same time or after a SILK-YN type eruption. The preservation of this pumice suggests that its origin was most likely to be the last prehistoric silicic Katla eruption (SILK YN).

However it can't be ruled out on geochemical grounds that some of the pumice relates to earlier eruptions, such as those that produced the MN, LN, N4, N1, A1 and A9 tephra layers.

The Botn Stage refers to deposits overlying finely laminated lake sediments within the Botn basin (Figure 7.3.4). These lake deposits are extruded upwards through the flood deposits in pipe-like dewatering structures. The lower deltaic flood structures, the lake sediments and dewatering structures indicate that the flood deposits were deposited into a proglacial lake environment. A lake could only have existed in the Botn basin if the Botnaá channel was blocked by ice filling the Entujökull foreland. No pumice is found on the surface of the Botn deposits suggesting that these sediments were deposited in a different episode of flooding from the Stóra-Mófell and western plateau areas. Tephra layers below these Botn deposits in profiles 115, 150 and 151 include at least one silicic Katla tephra layer like SILK YN.

The timing and nature of the Botn and Stóra-Mófell Stages can be interpreted in two main ways.

1. The first interpretation suggests that the Botn stage came first, with an ice front along the edge of the Botn/Entujökull cliff and a flood occurring through the cols in to the basin. Floodwaters may have covered the lower slopes of Stóra-Mófell. This flood occurred after the deposition of a SILK-YN type tephra. This may be coincident with event '3 (Smjörgil)' downvalley or an older flood. The later Stóra-Mófell stage reflects an advance of Entujökull from this position, with Entujökull reaching the cliff-edge Stóra-Mófell moraines and possibly advancing in to Botn basin. A flood incorporating silicic pumice (though not necessarily a silicic volcanic flood) then occurred across Stóra-Mófell and was routed across the Botn deposits dissecting the earlier Botn Stage flood sediments. This pumice flood may tie in with the Drumbabót event, although this assumes that silicic pumice was trapped close to the ice margin or within the glacial system after the SILK eruption and not washed away by normal seasonal glaciofluvial activity. This reconstruction gives approximate dates for the Stóra-Mófell and Botn stages as c. 1600 (or earlier) and c.1200 BP respectively.

2. The second interpretation requires that the Stóra-Mófell stage occurred first with the formation of the cliff-edge moraines and a flow including silicic pumice, possibly associated with the eruption of SILK YN. Water (and pumice) from this ice limit would have been trapped in the Botn basin, which contained an ice-dammed lake. Retreat of the ice from the Stóra-Mófell position to a lower position along the Botn/Entujökull foreland cliff and below the Stóra-Mófell cliff edge then occurred, to form the Botn Stage. A basaltic flood then was routed over the col in the Botn lake basin, later draining along the Markarfljót (Possibly Event 3). Further retreat of the ice in to the Entujökull foreland would have allowed normal glaciofluvial drainage and a later flood (tying in

with Drumbabót (2) downstream and producing the pendant bars on the Botn/Entujökull cliff) to dissect the earlier flood deposits and entrain both basaltic tephra and silicic pumice. This would give dates of c.1676 BP and c.1600-c.1200BP for the Stóra-Mófell and Botn stages respectively.

Both scenarios are based on limited evidence and thus the details of reconstruction are debatable. Scenario one would involve the blockage of the Botnaá channel after the deposition of the Botn flood layers (based on reconstructed ice front, Appendix 5) and thus may have caused a second lake to form in which the Stóra-Mófell pumice flood would be deposited. The alternative is that an open conduit existed beneath the ice from the Botnaá channel allowing drainage from Botn to be re-routed beneath Entujökull. No evidence has been found for a lake in the Botn basin after the Botn flood sediments were deposited. Scenario 2 does not have this problem because, with the Botn floods occurring after the Stóra-Mófell Stage, the drainage of the Botn flood could have left a large enough to channel for continual drainage of normal glacial melt waters to occur beneath the Botn Stage ice prior to retreat in to the Entujökull foreland. Additionally, scenario 2 allows for the possibility of silicic flooding being responsible for the pumice on Stóra-Mófell and the western plateau, without resorting to more complex requirements of erosion of interglacial pumice deposits in a later flood. Were scenario 2 to be the case floodwaters from the Stóra Mófell stage, probably carrying pumice, would have emanated from the north and south flood routes in to Emstrur, North Þórsmörk and also down the main Markarfljót gorge. However, such water and pumice from the SILK (possibly SILK YN) eruption would not necessarily need to be represented in sedimentary sequences downstream. Thermodynamic research in to subglacial silicic activity (Hoskuldsson and Sparks 1997) indicates that much less water is produced in these types of eruptions than in basaltic eruptions. Even some of the basaltic floods are only barely represented in valley-side sequences. Smaller volume floods, such as silicic floods would possibly be focussed along the Markarfljót gorge and flow straight out to sea leaving little erosional or depositional evidence in valley-side sequences. Thus, scenario two is favoured.

The Emstrur Stage, in the mid to early Holocene occurred when ice was more expanded. Entujökull was advanced enough to block the Markarfljót channel. Moraine limits are found beneath the Botn flood deposits, on Stóra-Mófell and in lobes extending northwards over the cliffs from the Northern outlet of Entujökull. Terraces and spreads of till represent extended positions of Entujökull on the western side of the Markarfljót gorge. Tephra layers in profile 162, are interpreted as Hekla-S and SILK N4, and suggest that ice has not covered the hillside opposite Entujökull here since some time before 3515+55BP.

Further constraints of ice extent and flood history can be inferred from the history of adjacent lakes. Emsturlón existed until c.6-5000BP, dammed by a rock barrier at Markarfljótsglufur (Vilmundardóttir and Kaldal 2001). Drainage of this lake (and the other lakes north of Emstrur) did not occur catastrophically (Vilmundardóttir and Kaldal, pers comm 2003) and no large floods are recorded in the

upper lake sediments. Overlying the lake sediments are three lava flows (probably from before 4000 BP, Johanneson et al 1990) and flood sediments attributed to flooding between 2500 and 2000 BP (Vilmundardóttir and Kaldal 2000). However, the Kanastaðir flood (8B, c.4500-4000BP) must have occurred after Emstrurlón was infilled. Thus, this flow must have occurred either prior to (or between) the episodes of lava flow emplacement or after the eruption of the lavas. This might mean that the flood deposits overlying both the Emstrurlón sediments and the lava flows represent numerous flood events rather than one single flow as proposed by Vilmundardóttir and Kaldal.

7.4 Summary

This thesis shows that the Markarfljót has indeed been a route for Holocene jökulhlaups/lahars on at least eleven occasions and probably more. One of these flood events was probably associated with activity from Veiðivötn. The rest have all been routed along the Markarfljót from the Entujökull/Emstrur area except possibly event 7, which may have flowed along the Þröngá valley. Two very large flows occurred c.1660 and c.4000-4500 BP. These were probably caused by subglacial volcanic activity beneath Katla. A further six floods were similar to hyperconcentrated laharic flows like those produced in the 1980 Mount St. Helens eruption and the 1985 Nevado del Ruiz disaster. Two further flows were formed by remobilisation of the very thick K-E and K-N tephra deposits.

Silicic Katla pumice has been transported in floods from the Entujökull foreland area. Possibly this is associated with a jökulhlaup from Entujökull triggered by a silicic eruption of Katla although equally this pumice may have been transported in another type of flood event, possibly associated with basaltic activity. This pumice is the first Icelandic terrestrial evidence of pumice from a SILK-YN-type eruption of Katla and is evidence for the Markarfljót as a route for silicic pumice transport between Mýrdalsjökull and the North Atlantic.

Sedimentary and geomorphological evidence points to numerous advances of Entujökull in the mid Holocene. Morainal patterns and constructed ice extents from flood routes indicate that Entujökull extended across the foreland during the mid-Holocene, far exceeding the Little Ice Age position reached in the early 18th to 19th Centuries. For the first time five stages of Holocene flood activity from Entujökull and related glacier extent are proposed.

Chapter 8: Implications

Jökulhlaups, glacier fluctuations and palaeoenvironment.

This research has provided new data on Holocene flooding and glacier fluctuations in the Markarfljót valley, narrowing the gaps in knowledge about the interaction of Mýrdalsjökull and its underlying volcano, Katla. This chapter presents these results and their direct implications in the context of regional and wider knowledge and identifies some important issues for future research.

8.1 Mýrdalsjökull glacier fluctuations

Comparisons of reconstructed fluctuation patterns of Entujökull with the rest of Mýrdalsjökull suggest that there are two types of behaviour displayed by the outlets of the ice cap. Entujökull's fluctuations are most similar to those of Sólheimajökull. This is particularly the case with the Sandur (early 18thC), Valley (10thC) and Botn Stages (1660-1200 BP) at Entujökull in relation to the Little Ice Age (c.1700-1900), 10th Century and Ytzagil stages (1400-1200 BP) at Sólheimajökull. Further, the older Emstrur stage (c.7000-3500 BP) at Entujökull may be similar to the Holsargil and Drangagil stages (>3100 BP and 7000-4500 BP) at Solheimajökull. This pattern of glacial advances in the mid-Holocene is different from the behaviour of the smaller caldera rim glaciers, also probably the northern lobe of Slettjökull (Kruger and Humlum 1981), which experience a Holocene maximum during the Little Ice Age (Dugmore and Casely, in review).

Macintosh (2000) modelled the behaviour of Sólheimajökull and determined that glacial sensitivity to climatic forcing was the main factor influencing variation in glacial extent. Topographic pinning points put a local twist on glacial extent, independent of wider climatic patterns. Other explanations such as enhanced or limited glacial expansion through the action of subglacial volcanism or varying ice catchment sizes through ice divide migration (Dugmore and Sugden 1991) were not deemed necessary to explain Sólheimajökull's fluctuations.

The similarity of fluctuations at Entujökull and Sólheimajökull suggests a common cause that is most likely climatic. Ice-divide migration scenarios are unlikely, since expansion of Sólheimajökull's catchment area with changing ice surface topography would result in a reduction in Entujökull's catchment size and cause asymmetric fluctuations: expansion of Sólheimajökull would be associated with retreat or reduced expansion of Entujökull. Similarly, volcanic activity is an insufficient explanation for fluctuations that are in phase in both the north-western and southern flanks of the ice cap. One eruption is more likely to affect one glacier outlet rather than the whole ice cap.

Mackintosh's conclusions that climate is the dominant factor in controlling the behaviour of Sólheimajökull seems the simplest, most likely explanation for the behaviour of Entujökull as well.

The differing topographic locations of Entujökull and Sólheimajökull help explain past patterns of glacier behaviour. The southern lobe of Entujökull confined within a narrow valley is similar in topographic situation to Sólheimajökull and thus would be expected to respond in a similar way to regional climatic change. However, during times of greatest Holocene glacier expansion (Emstrur stage at Entujökull and Drangagil stage at Sólheimajökull), the behaviour of both glaciers is likely to vary, since their topographic situations downvalley are quite different. Sólheimajökull's valley extends southwards onto a flat, open sandur plain, and expansion of the ice can occur as a thin broad lobe. The foreland at Entujökull however is confined by higher land, which rises up from the Markarfljót gorge towards the Tindfjallajökull massif. Expansion of ice to the west at this location cannot occur without extensive ice thickening. Rather, the glacier thickened and spread northwards into the Botn basin. At times of more limited ice extent, topographic controls such as the high cliffs of Stóra-Mófell and the upglacier edge of the western lava plateau may have influencing the lateral extent of Entujökull in addition to wider climatic controls.

8.2 Mýrdalsjökull jökulhlaup history

Floods have flowed through all the main outlet glaciers that breach the Katla caldera. During the last c.4500 years the Markarfljót has been a route for volcanic jökulhlaups as well as other flow events. Two historical floods have been identified, both of which are probably volcanic in origin. Some similarities exist between the Markarfljót and Sólheimajökull records (Dugmore 1987). Dugmore (1987) refers to an early 10th Century flood issuing from Sólheimajökull that is perhaps associated with the Katla (KR) 920 AD eruption. The 10th Century flood from Entujökull may be related to the same event. Dugmore (2003) has identified flood activity in Langanes associated with 10th Century fissure eruptions on the flanks of Eyjafjöll. Prehistoric Markarfljót floods 2 and 4 may be contemporary with Sólheimajökull Eystriheiði and Layer L events (Dugmore 1987 and Figure 2.9).

Stratigraphic correlations in prehistoric sequences between the Markarfljót and Sólheimar regions can be made based on some distinctive key tephras such as the SILK layers, the Landnam tephra, distinctive Hekla layers and radiocarbon dated deposits. However, the number and thickness of black, basaltic tephra layers (probably produced locally within Katla) varies dependent on wind direction at the time of eruption, making direct correlations difficult between some closely spaced events. The Eystriheiði flood was different from other floods to the south in that its sediments are dominated by lithics rather than pumice (Dugmore 1987). The timing of this flood is similar to the Layer H tephra from Eyjafjallajökull but these events cannot as yet be correlated. Possibly, parts of the Drumbabót event recorded in the soils at Langanes and downstream and the Eystriheiði flood are also associated with activity in Eyjafjallajökull (or on fissures nearby) and Fimmvorðuhal between the two ice caps.

Historical activity in the main Eyjafjallajökull crater has typically lasted for a number of years (such as in 1821 to 1823), in association with shorter-term activity in Katla (1823). Flooding associated with Eyjafjallajökull activity may occur on more than one occasion such that floods may be routed from Eyjafjöll, Katla and from Fimmvorðuhal southwards over a period of years. These relationships present specific chronological challenges that are difficult, even with an excellent tephrochronology.

Layer L (c.2300 BP, between YN and UN with two black tephras above and three black tephras below) may correlate with Markarfljót flood 4 (between YN and UN with 1-2 black tephras above and 2-9 black tephras below), although stratigraphies are difficult to compare without detailed mapping of all of the minor black tephras. As it stands, Event 4 is interpreted to have an Eyjafjallajökull component, possible like the Drumbabót event, again reflecting linked activity in Katla and Eyjafjallajökull.

No other links between the overall flood sequences of Sólheimajökull and Entujökull are apparent. Layer K (3480+60 BP), though similarly placed in the stratigraphy is probably a few hundred years older than Event 6 which lies up to 6 black tephra layers above H-S (3515+12 BP). Crucially, this may indicate that flooding in the Markarfljót and from Sólheimajökull is coincident only when activity is spread or shared between the two volcanic systems of Katla and Eyjafjallajökull. Katla activity causing flooding to the west and south of the Mýrdalsjökull does not appear to route floods in both of these directions at the same time. Historical evidence from flooding to the south and southeast suggests that most floods are routed only in one direction. Only in 1860, when volcanic activity is thought to have occurred in both western and eastern parts of the caldera, have floodwaters emanated from both Kötlujökull and Sólheimajökull (Björnsson et al 2000). The evidence of Katla floods from Entujökull not necessarily being associated with Sólheimajökull floods would therefore fit the historical pattern of single outlet Kötluhlaups.

The addition of data about Katla jökulhlaups along the Markarfljót to previous records of flooding around the ice cap indicates that prehistoric floods have occurred to the south and west. Most probably prehistoric floods also flowed from Kotlujokull although any evidence for this has probably been washed away by subsequent flooding. Post 10th Century events have predominately flowed from Kotlujokull although one flood each from Solheimajökull (1860) and Entujökull (after 1510) have also occurred. Larsen (2000) refers to post-'Eldgjá Fires' (c.935AD) re-routing of jökulhlaups towards the Kotlujokull gap. This she suggests may be associated with ice divide migration, changes to caldera topography or shifting intra-caldera eruption sites citing the latter as the most probable. This thesis confirms Mackintosh's proposal that significant ice divide migration has not occurred at Mýrdalsjökull. Subglacial topographic changes, though quite likely in association with the Eldgjá eruption, would need to be quite considerable to alter water drainage patterns in the caldera where ice thickness is greatest and ice surface topography dominates patterns of hydraulic potential and thus water flow directions. Shifting intra-caldera eruption sites may best explain why occasional historical

floods have been routed to the west and south. As Larsen states, the most straight-forward explanation for this shift from western and southern pre- Eldgjá floods to eastern post- Eldgjá flood routes is a eastward shift in eruption sites during this major volcanic event.

8.3 Silicic Katla jökulhlaups and terrestrial silicic pumice transport to the North Atlantic

There are previously unknown silicic pumice deposits to the west of Mýrdalsjökull close to past ice margins of Entujökull. Two types of silicic Katla pumice, one similar to the SILK YN eruptives and another similar to the Vedde tephra (c.10,600 BP) indicate multiple periods of pumice deposition in this area. The younger deposits form a loose lag within flood channels and may have been transported to the coast in a jökulhlaup event. The older material is found within a compact layer, similar to the Sólheimar ignimbrite deposit (Newton 1999) and bedded units to south of Mýrdalsjökull at Rjúpnagil (Newton and Smith, unpublished data). These deposits may be formed by pyroclastic flows and emplaced either subaerially or subglacially.

This new data on silicic Katla pumice adds to previous knowledge of Vedde-type pumice found at Vikurhol, south of Mýrdalsjökull (Newton 1999), suggesting that Katla silicic pumice has been transported along a number of routes to the North Atlantic. Finds to date indicate possible pumice transport routes to the south and west of the ice cap. Thus, flood routes from Kotlujokull across Mýrdalssandur seem likely, although the active nature of the proglacial environment in this area may mean that no evidence exists to the south east. The landscape where silicic pumice has been found to date is favourable for preservation of such evidence unlike the sandur plains to the southeast or the active glaciofluvial areas in front of present ice margins. This may mean that although further investigation will reveal silicic pumice along past ice marginal positions suitable for preservation of evidence the resultant pattern of pumice finds may represent preservation potential as much as actual patterns of pumice transport. Similarly records of Holocene glacial extent and jökulhlaup activity to the southeast are constrained by poor preservation potential.

8.4 Markarfljót hazard issues

Future jökulhlaups and related lahars in the Markarfljót valley are likely, associated with either basaltic or silicic activity, or related to remobilisation of thick freshly deposited tephra layers. No clear relationships have been identified between jökulhlaup routing and ice extent. This may suggest that routing to the west is simply associated with volcanic activity in western or northern areas of the caldera that lie within the contemporaneous ice and water divides of Entujökull. This means that potential flood routes could be predicted by the locations of earthquake epicentres, ice surface depressions and changes in solute contents of glacial rivers indicate changing positions of active

geothermal and subsurface volcanic/magmatic activity. Intense monitoring of these factors is coordinated by the Icelandic Meteorological Office and thus forms the basis of an effective strategy.

Present farm sites located on raised ground such as terraces or on gentle lower slopes in Fljótshlið and Stóramörk are most likely safe from all but the very largest floods from the main Markarfljót valley. Artificial barriers, which protect farmland and buildings on the sandur plain from normal river action, most probably will provide little protection from large floods. The campsite and hut at Húsadalur and the Laugarvegur walking trail through Northern Þórsmörk, in particular, lie directly in the path of virtually all of the flow events recorded over the Holocene and in historic time. This could create a potentially difficult situation during the summer tourist season in general and a 'party weekend' in particular when there may be up to 3,000 people in Þórsmörk (and possibly up to 1,000 vehicles) with just one track as a potential escape route.

Activity along the Katla caldera rim could be responsible for floods in the Ljósá, Þröngá and Krossá rivers in Þórsmörk, although evidence for past activity and flooding in these areas is limited. Main crater and fissure eruptions on Eyjafjoll may be responsible for Holocene floods in Langanes (this thesis) and early 10th Century flooding in the Smjorgil channel (Dugmore 2003). Future activity in this region could destroy sections of the road between Stóramörk and Þórsmörk. As discussed in the previous section, there is some indication in the timing of Eyjafjallajökull floods and stratigraphic relationships that volcanic and flood activity from Katla and Eyjafjallajökull may be linked, which has crucial implications for hazard assessment. Further investigation of flood patterns from Eyjafjöll and possible linkages between Katla and Eyjafjallajökull is necessary from both volcanological and hazard assessment perspectives and is crucial to determine the likely extent of these combined events.

Katla silicic floods, although probable on millennial timescales, are less likely to be reflected in the sedimentary records of the area, or to present considerable future hazards. Silicic eruptions are known to be 'cooler', thus melting less ice and producing smaller scale floods. Additionally, Holocene silicic eruptions of Katla have been smaller than their basaltic counterparts. Silicic floods may well be water-dominated events, with smaller discharges and less environmental, geomorphological and hazardous impact. In the main Markarfljót such events would most probably been constrained within the gorge system. Most probably, only if such events occurred along the caldera rim and flows travelled into Þórsmörk or across the southern flank of Mýrdalsjökull would impact be particularly significant. It has been suggested that silicic activity could occur along the caldera rim (Larsen 2000), making flows across these areas a possibility.

Additional, localised hazards may be presented by remobilisation of thick tephra-fall deposits as lahars triggered by intense rainstorm events. As these phenomena would follow an eruption and could occur a significant time afterwards, they present a further, lower order problem to planners.

8.5 Environmental change and landscapes of settlement

This thesis has shown that jökulhlaups have had a major role in shaping the landscape of the Markarfljót valley. The glacial foreland has been variously infilled, washed and dissected by the action of jökulhlaups, leaving a complex palimpsest of landforms that represent the interplay of glacial, volcanic, fluvial, slope and jökulhlaup activity. The middle valley is most clearly shaped by the action of jökulhlaups and subsequently transformed lahar-like flows with erosional and depositional landforms reminiscent, though smaller in scale, of the channelled scablands of eastern Washington (Baker 1973) and jökulhlaup areas east of Vatnajökull (Björnsson 1992, Russell et al 2002). The largest events at c.4500 and c.1600 BP would have had considerable impacts on the geomorphology of the valley, increasing deposition along channel margins and eroding both sediments and bedrock from the valley axis. These flow events, particularly the largest events would have reset trajectories of environmental change during the Holocene. The most recent events (c.1600 BP, c.1200 BP, c.871AD, c.10th C and c.16-17thC) have had major roles in shaped the terraces and surface sediments found along the valley margins. These late prehistoric and early historical events would have set trajectories of environmental change in the middle and lower valleys over the following decades or centuries.

The environmental effects of such jökulhlaups would have been extensive. Haraldsson (1981, 1993) associated the c.1200 BP flood with burial and sudden destruction of forest south of Fljótshlið. Deposition of tephra-rich diamict across the sandur surface will have initially resulted in a wasteland landscape devoid of vegetation, especially inland from Fljótshlið where the valley is more confined. Lava surfaces in the middle valley between Einhyningur and Husadalur have been stripped of soil with subsequent floods washing the same areas and preventing long-term sediment accumulation. It seems likely that flows would have spread out and become channelled in the Landeyjar, leaving a mosaic of slightly higher vegetated land and lower non-vegetated land. Those regions covered in flood deposits in the lower valley may have had clast-pavement surfaces similar to the eroded flood surfaces in the middle valley, and to the sandur plains of Skógasandur and Sólheimasandur to the south. These thick flood deposits lack fines and are well drained. Upper layers may have been further depleted of fines and sands by wind-erosion making them unsuitable for rapid colonisation by vegetation.

Dugmore et al (2000) suggest that patterns of early settlement and possibly later abandonment were significantly influenced by environmental conditions at the time of occupation and pre-Landnam trajectories of landscape change. Environmental studies based on pollen and tephra analyses indicate that the Markarfljót in late pre-history and during initial settlement was a changing and dynamic landscape (Påhlsson 1981, Dugmore and Buckland 1991, Hallsdóttir 1995). The direction of this change, retreat and advance of vegetative margins, could be crucial in determining initial settlement success. Settlement of a landscape that is in the process of natural destabilisation rather than in a state of equilibrium could create unforeseen and thus potentially unmanageable problems.

Settlement of Landeyjar and the Markarfljót valley occurred a few hundred years after the last prehistoric flood (c.1200 BP). During the Landnám (settlement) period two floods (one from Veidivotn, another from Katla) flowed down the Markarfljót valley. These events over-topped the Markarfljót gorge in the middle valley, inundating areas of Einhyrningsflatir and leaving deposits along the lower slopes west of Húsadalur close to early inland farm sites. Downvalley flows were more spread out, probably washing over parts of Langanes and diverging into numerous channels on the sandur plain. Such flows would have had a crucially bad impact on the sandur-edge farm site of Kanastaðir. This farm was abandoned early and the site is now lost. It may have been devastated by one of these historical age floods. The earlier landscape changes and selective destruction of vegetation of the Drumbabót (c.1200 BP) flood would have influenced the distribution of different vegetation types throughout the valley. The floods from Veiðivötn and Katla in the 9th and 10th Centuries would have further stunted vegetation recovery in their flow paths, resulting in a landscape composed of elements of bare or thinly veiled rock and grasslands and woodlands in different stages of maturity. Additionally, these coarser tephra-rich deposits will have only had relatively thin soil cover in contrast to areas untouched by flooding where deep soils have been retained. This legacy of prehistoric flood activity and repeated early historical deluges could make some areas of the sandur more susceptible to erosion when cleared of vegetation by settlers for pastoral farming and subsequently exposed to grazing pressures. These increased environmental pressures and early exposure of settlers to Markarfljót flood risks would have been greatest in the middle valley at marginal farm sites and may have contributed to their early abandonment.

In common with the Sólheimajökull floods (Dugmore et al 2000), the Markarfljót floods would have added large pulses of sediment to the coastal environment, initially causing sandur aggradation and extension of the Landeyjar districts towards the sea. However, as the sediment supply was not continuous, this land would have been subsequently eroded causing local coastal retreat, but probably resulting in sediment transport to the west and related coastal extension of land.

8.6 Eruptive history and tephrochronology

A substantial body of data on the tephra stratigraphy of the Markarfljót has been collected within the chronological framework of this thesis. This contributes to the work carried out around Mýrdalsjökull and Eyjafjallajökull in southern Iceland, predominantly by Thorarinsson, Larsen and Dugmore. Stratigraphic records have been extended into key areas of North Þórsmörk and the foreland of Entujökull where little work had previously been carried out. Historic tephra sequences in the North of the Markarfljót valley differ significantly from those downstream around Kanastaðir and on the northern flanks of Eyjafjallajokull. A greater range of historical Hekla layers appear to be deposited in this area, producing a sequence as much dominated by blue-grey layers as black Katla tephras. For example, a highly distinctive grained layer with both pale and dark grains is found in recently formed

soils less than 2 metres deep around Entujökull. This may be the airfall from the eruption of Hekla in 1206. This intercalation of fallout from the Hekla and Katla systems may also extend in to the prehistoric sequences providing novel combinations of layers with particularly useful dating implications. Geochemical analyses and detailed recording of these layers may usefully produce a detailed tephrochronological record with a large number of key distinctive layers suitable for precise dating of environmental and geomorphological reconstructions. Further expansion of this tephra stratigraphy is necessary in these areas and in Emstrur to separate out and/or correlate closely spaced events and so gain a fuller understanding of the nature of environmental change, volcanic, glacial and jökulhlaup history in this region.

Original data collected from Northern Þórsmörk indicates that a historical silicic Katla eruption may have occurred shortly after the Hekla 1341 eruption. All published records of silicic Katla activity have thus far only identified prehistoric events. The youngest SILK tephra (YN) identified to date was erupted around 410 AD (Larsen et al. 2001). Younger silicic Katla eruptions are not known and an apparent ending of Holocene silicic activity has been linked to possible reorganisation or disruption of the magma system below Katla due to the large Eldgjá c.935 eruption (Larsen 2000). However, single shard electron microprobe analyses of a thin yellow tephra above a bedded grey tephra within a putative historic-age sequence in North Þórsmörk indicate a SILK origin. Analyses range in composition, with most similar to the SILK YN tephra, though some have silica levels up to >70% (Appendix 1). No needles have been found in this layer. The bedded grey tephra is geochemically linked to Hekla and may be the 1341 airfall layer. It is underlain by a coarse, grey, Hekla tephra, possibly from Hekla 1300. This places the SILK layer around the mid 14th Century AD. Assuming major change had not occurred in Katla after the Eldgja eruption, the occurrence of a small silicic eruption in the mid 14th C is not difficult to envisage. The ice cap over Katla was probably relatively small during this time, as data from GISP2 and GRIP and proxy drift ice records in Iceland indicate warm (glacier minimum) conditions (Dugmore 1987). Reduction in ice cover and resultant deloading of subglacial magma chambers is widely recognised as a trigger for volcanic activity, particularly having been linked to episodes of volcanism towards the end of the last glaciation (Hall 1982). Reduction in ice cover prior to the 14th C may have triggered activity in the relatively quiescent silicic centre. The limited volumes of the Holocene silicic Katla layers suggest that these eruptions were smaller in magnitude than basaltic Katla activity, and possibly only the largest of the silicic eruptions break through the ice cover to disperse tephra over the surrounding landscape (Larsen 2000). This evidence of a putative 14th Century Katla silicic tephra from close to the western margin of the ice cap may indicate that small eruptions have occurred more frequently and more recently than previously thought.

8.7 Implications for jökulhlaup sedimentology

Sedimentological study of jökulhlaup and lahar-like deposits in the Markarfljót has emphasised the varied nature of possible deposits produced by floods and mudflows associated with ice/volcano interaction in Iceland. Most jökulhlaup flows witnessed or studied in Iceland have been tephra-rich granular flows or water dominated flows, which in historical time have flowed across the sandur plains of the south coast. The diamicts and lithic-rich units identified in the Markarfljót bear greater resemblance to lahar deposits recognised in North and South America and New Zealand where flows are, like in the Markarfljót, focussed along valleys for much of their route.

Russell and Marren (1999) note that discrimination between jökulhlaup deposits and normal glaciofluvial outwash can be difficult. This opinion is supported by the findings of this thesis which also show that the differentiation of jökulhlaup flows in valley-confined settings from other diamict-producing events such as glacial deposition and mass movement or localised debris flow activity can be difficult. Key features of the Markarfljót flows which allowed identification as probable jökulhlaups are stratigraphic continuity across considerable reaches of the valley and sequences of rising flow, peak flow and waning stage flow facies. Transformation of flows between ice margins and downstream depositional settings and selective erosion can make identification of deposits and routes of a single event difficult unless a sound spatially extensive stratigraphic framework is in place. Further laboratory-based analyses could be carried out in studies of jökulhlaup and flow events to provide further information on transport history, erosivity and provenance.

Identification of tephra-remobilisation flows was based upon semi-continuous distributions and the presence of small lithics within some beds of otherwise crudely bedded thick black tephra deposits. In some locations differentiation between flow events and airfall layers prove difficult and the true distribution of these flow events may indeed be underestimated due to the lack of lithics within exposed sediments. Grain shape studies (possibly using a scanning electron microscope) may be a useful tool in differentiating between airfall layers and those that have been transported by water because the rather fragile forms of vesicular glass grains can be rapidly modified. This technique was originally used in studies of the transport histories of quartz grains but has been extended to look at surface patterns and grain shapes of airfall tephra (Heinken and Wohletz 1984). Certainly, large-scale shape patterns in jökulhlaup deposits (generally SR-SA) suggest a degree of rounding of larger particles in transport. Similar may be the case with tephra matrix particle shapes. This technique may help differentiate between low lithic content tephra remobilisation flows that have travelled some distance and thick, bedded airfall tephra layers that have travelled little or no distance following primary deposition.

The largest flood events in the Markarfljót are characterised by high lithic content and a paler, brown to dark brown coloured matrix, compared to smaller events. Similarly localised tephra remobilisation

flows have far lower lithic contents than farther-travelled jökulhlaup flows. Quantification of lithic to tephra content, particularly in the matrix of a deposit, may be a useful determinant of erosivity or distance travelled of an event. Conclusions built upon palaeohydrological reconstructions using simple equations are probably much less than realistic, particularly when flows are more dominated by sediment than water. The ratio of lithic to tephra content in a standard grain size fraction of a possible flood deposit (in comparison with known-origin deposits in the same locality) may be a useful indicator of either erosive power or distance travelled based on sedimentary rather than theoretical principles.

Provenance of flow deposits in the Markarfljót has been based on distributions of deposits and on the geochemical composition of tephra within flood deposit matrices. Fluvial sands had the greatest range of chemical compositions while known flood deposits tended to be dominated by basaltic Katla glass. Those floods containing tephra from Eyjafjallajökull were interpreted as possibly having been routed from the Eyjafjöll. Development of this approach could provide useful data on the nature and variability of glass composition within non-airfall layers possibly allowing more precise provenance relationships to be determined. Jónsson (1982) and Tómasson (1996) discuss the jökulhlaup-transported tephra from the Katla 1918 flood and assume that much of this material originated in the 1918 eruption. However, analysis of tephra transported in the Vatnajökull 1996 jökulhlaup has been carried out to determine whether the floods (Maria et al 2000) transported primary eruptive material from the Gjálp fissure suggests that this is not always the case. Maria et al's (2000) study showed that in the case of the Gjálp eruption most of the material transported by the floods were from older eruptions and that little or no primary eruptives were incorporated into the jökulhlaup deposits. This may reflect the complex route that this flood took beneath the Vatnajökull ice cap via the Grímsvötn Lake prior to reaching the sandur plain. The valley-confined Markarfljót events most probably have different characteristics associated with distance from the ice margin. Entujökull ice marginal deposits are very similar to those of the Katla 1918 flood while those downstream may also reflect the range of soils and tephras over which the flow has passed.

8.8 Summary

This thesis has answered the three key questions proposed in section 2.2:

1. **Little is known about the flood history to the west. What, if any, is the history of jökulhlaups to the west of the ice cap?**

This thesis has produced a new chronology of 11 to 15 Holocene flood events in the Markarfljót valley and related them to past positions of Entujökull. Most of these were hyperconcentrated flow events originating from or close to, the northwest area of the ice cap and are associated with subglacial volcanism. One flood originated in the Veiðivötn area and on three occasions Katla-related floods may have been contemporaneous with sediment flows from Eyjafjallajökull. The two largest flows

date from c.1600 B.P. and c.4500 B.P. A further two phases of 'flood' activity relate to rainfall triggered re-mobilisation of thick tephra deposits

Similarities exist between the timing of some floods in the Markarfljót valley and Sólheimajökull and may reflect a volcanological link between Katla and Eyjafjallajökull. Prehistoric floods have occurred from both these western and southern outlets but only two post 10th Century floods have been recorded. One of these floods may have been associated with a silicic eruption of Katla. Since the 10th Century most floods have issued from Kötlujökull to the south east, possibly reflecting changes in intra-caldera eruption sites or subglacial topographic change associated with the Eldgjá eruption in c.935 AD.

2. What is the pattern of glacier activity? How do floods relate to glacier activity? (extent and ice cap morphology).

Geomorphological evidence of flood events and glacial activity indicate that Entujökull reached a Holocene maximum in the mid-Holocene, far exceeding the Little Ice Age glacier position in the early 18th to 19th Centuries. The patterns of glacier fluctuations at Entujökull are similar to those of Solheimajökull and probably indicate that the three major outlet glaciers of the ice cap respond to climatic forcing in similar ways. This fits in closely with wider patterns of Holocene glacial fluctuations in Iceland identified in recent studies (Guðmundsson 1997, Kirkbride and Dugmore 2001a, Bradwell 2001).

Floods have issued from Entujökull when the ice was filling the entire foreland and at various stages between maximum and present ice extent. Within the range of glacial extent possible to study there is no distinct relationship between ice extent and jökulhlaup triggering or frequency. However, ice extent has a major role in determining the proglacial route taken by a flow and thus which parts of the valley are subject to its impacts.

Changes to ice divide positions would alter the hydraulic pressure patterns beneath the ice and could alter the preferential routing of jökulhlaup water generated within the crater to different outlet glaciers.

3. Are patterns of jökulhlaups and glacier fluctuations related to patterns of volcanic activity?

Climatic forcing and local topographic constraints are most likely to be the dominant controls on the patterns of glacier fluctuations at Entujökull and the other outlets of Mýrdalsjökull. The timing of apparent flood route switching from mainly prehistoric activity to the south and west to historical activity to the southeast appears to indicate a transition around the time of the Eldgjá Fires c.934 AD. This eruption was a major event in the Katla Volcanic System and since this time eruptions have

mostly occurred around Kötlugjá on the eastern side of the caldera. If this were indeed the case then it would suggest that the positioning of volcanic activity within the Katla caldera has a dominant effect on the route taken by jökulhlaups. This has been confirmed by equipotential modelling in this thesis. Lack of evidence of prehistoric events from Kötlujökull does not mean that prehistoric floods did not occur here. The high flood frequencies characteristic of Kötlujökull today may extend into prehistory. Burial of deposits and lack of documented accounts leaves us without sufficient evidence to confirm this.

This research raised further issues which were not part of the original aims of the thesis but have important implications for future research into glacier-volcano interaction and practical hazard planning. The environmental impact of these floods would have been extensive and future flooding could prove to be a significant hazard in the Markarfljót valley. The middle and upper valleys are dominated by scabland and sandur topography formed by the repeated action of large-scale floods. Late prehistoric and early historic flood events would have had a major role in shaping the landscape and vegetation patterns at the time of Norse colonisation and may have influenced initial decisions regarding farm site locations. Unfavourably thin soils and extensive flood deposit distribution may have resulted in environmental conditions unsuitable for successful farming leading to early abandonment of inland sites along or close to past flood paths.

Further tephrochronological studies in the Emstrur and Entujökull areas would be useful for forming clearer links between the upper and middle Markarfljót valley chronologies. Additionally, investigation of possible flood routes and a small-scale historic SILK tephra along the western margin of the Mýrdalsjökull and in Þórsmörk may prove fruitful. Detailed studies of volcanic glass shapes, chemistry and lithic to glass ratios could possibly provide more detailed pictures of the transport histories and sources of flow deposits, particularly when found in valley-confined localities.

References

A

Andrews, J. 1979. The present ice age: Cenozoic. *In* B. S. John (ed.) *The Winters of the World.* 173-219. David and Charles, Vermont 256pp.

B

Ballantyne, C.K. 1990. The Holocene glacial history of Lyngshalvoya, northern Norway: chronology and climatic implications. *Boreas,* 19, 93-117.

Baker, V.R. 1973. Erosional forms and processes for the catastrophic Pleistocene Missoula Floods in Eastern Washington. *In,* Mourisawa, M. (ed), *Fluvial Geomorphology,* Allen and Unwin, London, p.123-148.

Baker, V.K., Greeley, R., Komar, P.D., Swanson, D.A. and Waitt, R.B. Jr. 1987. *Columbia and Snake River Plains,* Geological Society of America, Centennial Special Volume 2, Chapter 11, 403-468.

Barnes, H.L. 1956 Cavitation as a geological agent. *American Journal of Science,* 254, 493-505.

Beget, J.E. and Nye, C.J. 1994. Postglacial eruption history of Redoubt Volcano, Alaska. *Journal of Volcanological and Geothermal Research.* 62 (1-4): 31-54.

Benn, D.I. 1992. The genesis and significance of 'hummocky moraine': evidence from the Isle of Skye, Scotland. *Quaternary Science Reviews.* 11, 781-799.

Benn, D.I, Ballantyne, C.K. 1993. The description and representation of particle shape. *Earth Surface Processes and Landforms,* 18, 7, 665-672.

Benn, D.I and Evans, D.J.A 1998. Glaciers and Glaciation. Arnold. London. 734pp.

Benn D.I., Wiseman S., Hands K.A. 2001. Growth and drainage of supraglacial lakes on debris-mantled Ngozumpa Glacier, Khumbu Himal, Nepal. *Journal of Glaciology.* 47 (159): 626-638.

Bennett, M.R. and Boulton, G.S. 1993. The deglaciation of the Younger Dryas or Loch Lomond Stadial ice-field in the Northern Highlands, Scotland. *Journal of Quaternary Science,* 8, 133-146.

Bennett, M.R. and Glasser, N.F. (1996). *Glacial Geology: Ice Sheets and Landforms.* John Wiley, London. 364 pp.

Bickerton, R.W. and Matthews, J.A. 1992. On the accuracy of lichenometric dates: an assessment based on the 'Little Ice Age' moraine sequence of Nigardsbreen, southern Norway. *The Holocene,* 2, 227-237.

Birks, H.H., Guliiksen, S., Haflidason, H., Mangerud, J. and Possnert, G. 1996. New radiocarbon dates for the Vedde Ash and the Saksunarvatn Ash from Norway. *Quaternary Research,* 45, 119-127.

Björnsson, H. 1974 Explanation of jökulhlaups from Grímsvötn, Vatnajökull, Iceland, *Jökull,* v.24, p.

Björnsson, H. 1975 Subglacial water reservoirs, jökulhlaups and volcanic eruptions, *Jökull,* v.25, p.1-11.

Björnsson, H. 1977 The cause of jökulhlaups in the Skaftá River, Vatnajökull. *Jökull,* v.27, p.71-77.

Björnsson, H. 1979. Glaciers in Iceland. *Jökull.* 29, 74-80.

Björnsson, H. 1988 *Hydrology of Ice Caps in Volcanic Regions.* Reykjavík

Björnsson, H. 1992. Jökulhlaups in Iceland: prediction, characteristics and simulation. *Annals of Glaciology.* 16, 95-106.

Björnsson, H. 1998. Hydrological characteristics of the drainage system beneath a surging glacier. *Nature,* 395 (6704): 771-774.

Björnsson, H., Palsson, F. and Guðmundsson, M.T. 1993. Mýrdalsjökull, yfirbord, botn og rennslisleidir Kotluhlaupa. Kotlustefna, RH 03-93, 14-16.

Björnsson, H., Palsson, F, and Guðmundsson, M.T 2000. Surface and bedrock topography of Mýrdalsjökull, Iceland: The Katla caldera, recent eruption sites and routes of jökulhlaups. *Jökull,* 49, 29-46.

Björnsson H., Rott H., Guðmundsson S., Fischer A., Siegel A., Guðmundsson M.T. 2001. Glacier-volcano interactions deduced by SAR interferometry. *Journal of Glaciology.* 47 (156): 58-70.

Boygle 1994. *Tephra in Lake Sediments: An unambiguous geochronological marker?* Unpublished PhD thesis, University of Edinburgh.

Bradwell, T. 2001. *Glacier Fluctuations, Lichenometry and Climate Change in Iceland.* Unpublished PhD Thesis, Department of Geography, University of Edinburgh.

Brazier, V., Owens, I.F., Soons, J.M. and Sturman, A.P. 1992. Report on the Franz Josef Glacier. *Zeitschrift fur Geomorphologie,* Supp. 86, 35-49.

Brazier V., Kirkbride M.P., Gordon J.E. 1998. Active ice-sheet deglaciation and ice-dammed lakes in the northern Cairngorm Mountains, Scotland. *Boreas,* 27 (4): 297-310.

Bretz, J.H. 1932. The Grand Coulee. *American Geographical Society, Special Publication* 15, p.1-89.

Bretz, J.H. 1969. The Lake Missoula floods and the Channeled Scabland. *Journal of Geology.* 77, 505-543.

Brown, I.M. 1993. Pattern of deglaciation of the last (Late Devensian) Scottish ice-sheet – evidence from ice-marginal deposits in the Dee Valley, northeast Scotland. *Journal of Quaternary Science,* 8 (3): 235-250.

Brugman, M.M. 1986. Mapping recent fluctuations of Shoestring Glacier, Mount St. Helens. *Annals of Glaciology,* 8, p.203.

Brugman, M. and Meier, M. 1981. Response of glaciers to the eruptions of Mt. St. Helens, *In:* Lipman, P.W. and Mullineaux, D. (eds.) *The 1980 eruptions of Mt. St. Helens, Washington,* U.S. Geological Survey Professional Paper, 1250, pp.743-756.

Bryant, I.D. 1991. Sedimentology of Glaciofluvial Deposits. *In* Ehlers, J., Gibbard, P.L. and Rose, J. *Glacial Deposits in Great Britain and Ireland,* Rotterdam, 437-442.

C

Calkin, P.E. 1988. Holocene glaciation of Alaska (and adjoining Yukon Territory, Canada). *Quaternary Science Reviews,* 7 (2): 159-184.

Caseldine, C.J. 1991. Lichenometric dating, lichen population studies and Holocene glacial history of the Tröllaskagi, Northern Iceland. *In,* Maizels, J.K and Caseldine, C.J. (eds) *Environmental Change in Iceland, Past and Present,* pp213-223. Dordrecht.

Caseldine, C.J. and Matthews, J.A. 1987. Podzol development, vegetation change and glacier variations at Haugabreen, southern Norway. *Boreas* 16, 3, 215-230.

Caseldine, C. and Stotter, J. 1993. 'Little Ice Age' glaciation of Tröllaskagi peninsula, northern Iceland: Climatic implications fore reconstructed equilibrium-line altitudes (ELAs). *The Holocene,* 3, 357-366.

Casely, A.F. 2001. *'Little Ice Age' glacier fluctuations and climatic change in Iceland – A multidisciplinary approach.* Unpublished MRes thesis. University of Edinburgh. 113pp.

Casely, A.F. & Dugmore, A.J. (in press) 'Climate change and constraining 'anomalous' glacier fluctuations: the southwest outlets of Mýrdalsjökull'. *Boreas.*

Chapman, M. G., Allen, C. C., Guðmundsson, M. T., Gulick, V. C., Jakobsson, S. P., Lucchitta, B. K., Skilling, I. P.and Waitt, R. B. 2000. Volcanism and ice interactions on Earth and Mars. *In* Gregg, T.K.P. and Zimbelman, J.R. (Eds.), *Deep Oceans to Deep Space: Environmental Effects on Volcanic Eruptions*, Plenum Press, New York. 39-74.

Chen, J. and Funk, M. 1990. Mass balance of Rhonegletscher during 1881/83-1986/87. *Journal of Glaciology.* 36, 199-209.

Clague, J. J. and S. G. Evans 1997 The 1994 jökulhlaup at Farrow Creek, British Columbia, Canada. *Geomorphology,* v.19, p.77-87.

Clague, J. J., S. G. Evans and I. G. Brown 1985. A debris flow triggered by the breaching of a moraine-dammed lake, Klattasine Creek, British Columbia. *Canadian Journal of Earth Sciences,* v.22, p.1492-1502.

Clarke, G. K. C. 1982 Glacier outburst floods from "Hazard Lake", Yukon Territory, and the problem of flood magnitude prediction, *Journal of Glaciology,* v.28, no.98, p.3-21.

Cooke, R. U. and J. C. Doornkamp 1990 *Geomorphology in Environmental Management: An Introduction,* 2nd edition, Clarendon Press, Oxford.

Costa, J.E. 1988. Floods from dam failures. *In:* Baker, V.R., Kochel, R.C. and Patton, P.C. (eds). *Flood Geomorphology.* 439-463. John Wiley, New York.

Cunha, S.F. 1998. Maps, Remote Sensing and Natural Hazards in the Eastern Pamirs, Tajikistan. *Proceedings, 5th International Symposium on Remote Sensing Cartography.* (1998). Arcata, California.

Cutler, Paul, Clayton, L., Mickelson, D.M., Colgan, P.M., & Attig, J.W. 2000 Tunnel Channels and associated fan deposits in Wisconsin, U.S.A.: insights into the plumbing of the Southern Laurentide Ice Sheet. *Modern & Ancient Ice-Marginal Landsystems Meeting, Keele University, April 29th -31st, 2000*

D

Dahl, S.O., Nesje, A., 1994. Holocene glacier fluctuations at Hardangerjøkulen, central-southern Norway: a high-resolution composite chronology from lacustrine and terrestrial deposits. *The Holocene,* 4, 269-277.

Dahl, S.O., Nesje, A., 1996. A new approach to calculating Holocene winter precipitation by combining glacier equilibrium-line altitudes and pine-tree limits: a case study from Hardangerjøkulen, central southern Norway. *The Holocene,* 6, 381-398.

Denton, G.H. and Karlen, W. 1973. Holocene climatic variations: their pattern and possible cause. *Quaternary Research.* 3, 155-205.

Desloges, J. R. and M. Church 1992 Geomorphic implications of glacier outburst flooding: Noeick River valley, British Columbia. *Canadian Journal of Earth Sciences,* v.29, p.551-564.

Drewry, D. 1986. *Glacial Geologic Processes.* Edward Arnold Publishers.

Driedger, C. L. 1981 Effect of ash thickness on snow ablation *In* Lipman, P. W. and D. R. Mullineaux (eds.)*The 1980 Eruption of Mount St.. Helens, Washington*, U.S. Geological Survey Professional Paper no.1250.

Dugmore, A.J. 1987. *Holocene glacier fluctuations around Eyjafjallajökull, south Iceland: A tephrochronological study.* Unpublished PhD thesis, Department of Geography, University of Aberdeen.

Dugmore, A. J. 1989a. Tephrochronological studies of Holocene glacier fluctuations in south Iceland *In,* Oerlemans (ed.), *Glacier Fluctuations and Climate Change,* pp.37-55, Kluwer, Dordrecht.

Dugmore, A.J. 1989b Icelandic volcanic ash in Scotland, *Scottish Geographical Magazine,* 105, 3, 168-172.

Dugmore, A.J. 2003. 10th Century floods from Eyjafjöll. *Report to Vegagerdin.* University of Edinburgh.

Dugmore, A.J. and Buckland, P.C. 1991. Tephrochronology and late Holocene soil erosion in South Iceland. *Environmental Change in Iceland.* Eds. Maizels, J. and Caseldine, C. 147-159. Kluwer Academic Publishers, Dordrecht.

Dugmore, A.J. and Newton, A.J. 1997. Holocene tephra layers in the Faroe Islands. *Frodskaparrit (The Faroese Journal of Natural and Medical Sciences),* 4, 141-154.

Dugmore, A. J. and D. E. Sugden 1991 Do the anomalous fluctuations of Sólheimajökull reflect ice-divide migration? *Boreas,* v.20, pp.105-113.

Dugmore, A.J. and Kirkbride, M.P. Tephrochronological dating of glacier advances AD 410-1947 in southern Iceland. Submitted to *Quaternary Research.*

Dugmore, A.J., Larsen,G., Newton, A.J. and Sugden, D.E. 1992. Geochemical stability of fine-grained silicic tephra layers in Iceland and Scotland. *Journal of Quaternary Science.* 7, 173-183.

Dugmore, A.J., Larsen, G. and Newton, A.J. 1995. Seven Tephra Isochrones in Scotland, *Holocene* 5(3) p.257-266

Dugmore, A.J., Newton, A.J., Larsen, G. & Cook, G.T. 2000. Tephrochronology, Environmental Change and the Norse Settlement of Iceland. *Environmental Archaeology.* 5, 21-34

Duncan, A. 2000 Unpublished Undergraduate Dissertation, University of Iceland.

Dyke, A.S. and Prest, V.K. 1987. Late Wisconsin and Holocene history of the Laurentide Ice Sheet. *Geographie Physique et Quaternaire,* 41, 237-263.

E

Eiriksdottir, E.S. 1996. Skaldabudalon. Lysing og tulkan a jardlogum. Unpublished BSc thesis, University of Iceland.

England, J., Smith, I.R., Evans, D.J.A. 2000. The last glaciation of east-central Ellesmere Island, Nunavut: ice dynamics, deglacial chronology, and sea level change. *Canadian Journal of Earth Sciences,* 37 (10): 1355-1371.

Eronen, M. 1983. Late Weichselian and Holocene shore displacement in Finland. *In* Smith, D.E. and Dawson, A.G. (eds) *Shorelines and Isostacy.* Academic Press. London. 183-208.

Evans, D.J.A., Archer, S. and Wilson, D.J.H. 1999. A comparison of the lichenometric and Schmidt hammer dating techniques based on data from the proglacial areas of some Icelandic glaciers. *Quaternary Science reviews,* 18, 13-41.

Everest, J.D. 2003. *The Deglacial Behaviour of Small Plateau Icecaps: examples from Scotland and Iceland.* Unpublished PhD Thesis, Department of Geography, University of Edinburgh.

Eythorsson, J. 1935. On the variations of glaciers in Iceland I. Drangajökull. *Geografiska Annaler,* 17.

F

Falconer, G., Ives, J.D., Loken, I.H. and Andrews, J.T. 1965. Major end moraines in eastern and central Arctic Canada. *Geogrphical Bulletin.* 7, 137-153.

Fay, H. 2002. Formation of ice block obstacle marks during the November 1996 glacier-outburst flood (jökulhlaup), Skeiðárarsandur, southern Iceland. *Flood and Megaflood processes and deposits.* IAS Special Publication no.32.

Fisher, D. 1969 Subglacial drainage of Summit Lake, British Columbia, by dye determinations *In, Symposium of the Hydrology of Glaciers,* International Association of Scientific Hydrology, no.95, Cambridge, p.111-116.

Fountain A.G. and Walder, J.S. 1998. Water flow through temperate glaciers. *Reviews of Geophysics.* 36 (3): 299-328.

Fowler, A.C. 1987. A theory of glacier surges. *Journal of Geophysical Research,* 92, 9111-9120.

G

Geirsdóttir, A., Hardardóttir, J. and Sveinbjornsdóttir, A.E. 1998. Late glacial/Holocene transition in south central Iceland as evaluated from lacustrine and terrestrial sediment sections. *In:* 28th Arctic Workshop, Abstract volume. Institute of Arctic and Alpine Research, Boulder, 60-61.

Geirsdóttir, A., Hardardóttir, J. and Sveinbjornsdóttir, A.E 2000. Glacial extent and catastrophic meltwater events during the deglaciation of Southern Iceland. *Quaternary Science Reviews.* 19, 1749-1761.

Glen, J. W. 1954 The stability of ice-dammed lakes and other water-filled holes in glaciers, *Journal of Glaciology,* v.2, no.15, p.316-318.

Goepfert, Y. 1993. *Chamonix: Mont Blanc.* Editions AIO, Le Cannet, France.

Gordon S., Sharp M., Hubbard B., Smart C., Ketterling B. and Willis I. 1998. Seasonal reorganization of subglacial drainage inferred from measurements in boreholes. *Hydrological Processes.* 12 (1): 105-133.

Graham, D.J. and Midgley, N.G. 2000. Graphical representation of particle shape using triangular diagrams: an Excel spreadsheet method. *Earth Surface Processes and Landforms*, 25, 13, 1473-1477.

Grönvold, K, Óskarsson, N., Johnsen, S.J., Clausen, H.B., Hammer, C.U., Bond, G. & Bard, E. 1995. Tephra layers from Iceland in the Greenland GRIP ice core correlated with oceanic and land based sediments. *Earth and Planetary Science Letters.* 135, 149-155.

Grove, J.M. 1988. *The Little Ice Age.* Routledge. London and New York.

Grove, J.M. and Switzur, R. 1994. Glacial geological evidence for the Medieval warm period. *Climate Change,* 26, 143-169.

Guðmundsson, H.J. 1997. 'Review of the Holocene Environmental History of Iceland' *Quaternary Science Reviews.* 16, 81-92.

Guðmundsson, H.J. 1998. *Holocene Glacier fluctuations and Tephrochronology of the Öræfi district, Iceland.* Unpublished PhD thesis, University of Edinburgh. 238pp.

Guðmundsson, M., H. Björnsson and F. Pálsson 1995 Changes in jökulhlaup sizes in Grímsvötn, Vatnajökull, Iceland, 1934-91, deduced from in-situ measurements of subglacial lake volume. *Journal of Glaciology,* v.41, no.138, p.263-272.

Guðmundsson, M., F. Sigmundsson and H. Björnsson 1997 Ice-volcano interaction of the 1996 Gjálp subglacial eruption, Vatnajökull, Iceland, *Nature,* v.389, p.

H

Haeberli, W. 1983 Frequency and characteristics of glacier floods in the Swiss Alps. *Annals of Glaciology,* v.4, p.85-90.

Hafliðason, H., Larsen, G. & Ólafsson, G. 1992. The recent sedimentation history of Thingvallavatn, Iceland. *Oikos.* 64, 80-95.

Hajdas I, Bonani G, Moreno PI, Ariztegui D 2003. Precise radiocarbon dating of late-glacial cooling in mid-latitude South America. *Quaternary Research.* 59 (1): 70-78.

Hall, K. 1982. Rapid deglaciation as an initiator of volcanic activity: an hypothesis. *Earth Surface Processes and Landforms,* 7, 45-51.

Halldorsson, M.M. 1998. 'The Dec. 18 - Dec. 28, 1998 Grímsvötn eruption' http://www.hi.is/~mmh/gos/

Hallsdóttir, M. 1995. On the pre-settlement history of Icelandic vegetation. *Icelandic Agricultural Science.* 9, 17-29.

Hammer, C. V. 1984. Traces of Icelandic eruptions in the Greenland Ice Sheet. *Jökull.* 34, 51-65.

Hammer, C.V., Clausen, H.B. & Dansgaard, W. 1980. Greenland ice sheet evidence for postglacial volcanism and its climatic impact. *Nature.* 288, 230-235

Haraldsson, H. 1981. The Markarfljót sandur area, southern Iceland. Sedimentological, petrological and stratigraphical studies. *Striae.* 15, 1-60.

Haraldsson, H. 1993. Eyðings lands af völdum vatn. *Goðasteinn*, 28-29, 76-84.

Harrison, S. and W. J. Fritz 1982 Depositional features of March 1982 Mount St. Helens sediment flows. *Nature,* v.299, p.720-722.

Hastenrath, S. and Kruss, P.D. 1992. The dramatic retreat of Mount Kenya's glaciers between 1963 and 1987, greenhouse forcing. *Annals of Glaciology,* 16, 127-133.

Heiken, G. and Wohletz, K.H. 1984. *Volcanic ash.* Univeristy of California Press, Berkeley.

Heim, D. 1983. Glaziare Entwasserung und Sanderbildung am kotlujokull, Sudisland. *Polarforschung* 53, 17-29.

Hjartarson, Á. and Ingólfsson, Ó. 1988. Preboreal Glaciation of Southern Iceland. *Jökull* 38, 1-16.

Hjulstrom, F. 1935. Studies of the morphological activity of rivers as illustrated by the River Fyris. *Bulletin of the Geological Institution,* 25, 221-455.

Hoblitt, R.P., Walder, J.S., Driedger, C.L., Scott, K.M., Pringle, P.T. and Vallance, J.W. 1995. Volcano Hazards from Mount Rainier, Washington*: USGS Open-File Report* 95-273

Hoinkes, H. C. 1969 Surges of the Vernagtferner in the Ötztal Alps since 1599. *Canadian Journal of Earth Sciences,* v.6, p.853-861.

Hooke, R. LeB. 1984. On the role of mechanical energy in maintaining subglacial water conduits at atmospheric pressure. *Journal of Glaciology,* 30 (105): 180-187.

Hooke, R. LeB. 1989. Englacial and subglacial hydrology – a qualitative review. *Arctic and Alpine Research,* 21 (3): 221-233.

Hooke, R. LeB., Laumann, T., Kohler, J. 1990. Subglacial water pressures and the shape of subglacial conduits. *Journal of Glaciology,* 36 (122): 67-71.

Hooke, R. LeB. 1998. *Principles of Glacier Mechanics*, Prentice Hall, Upper Saddle River, NJ, 248pp.

Höskuldsson, A. and Sparks, RSJ. 1997. Thermodynamics and fluid dynamics of effusive subglacial eruptions. *Bulletin of Volcanology*, 59(3), 219-230.

I

Ingólfsson, O., Björck, S., Haflidason, H. & Rundgren, M. 1997 Glacial and climatic events in Iceland reflecting regional North Atlantic climatic shifts during the Pleistocene-Holocene transition. *Quaternary Science Reviews* 16, 1135-1144.

Ingólfsson, Ó. & Norðdahl, H. 1994. A review of the environmental history of Iceland, 13,000-9,000 yr BP. *Journal of Quaternary Science* 9, 147-150.

Irvine, T.N. and Baragar, W.R.A. 1971. .A guide to the chemical classification of the common volcanic rocks. *Canadian Journal of Earth Sciences,* 8, 523-548.

Ives, J.D. 1986. *Jökulhlaup disasters in the Himalaya and their identification, a case study: The Langmoche Jökulhlaup of 4th August 1985, Khumbu Himal, Nepal.* ICIMOD: Kathmandu.

Ivy-Ochs S., Schluchter, C., Kubik, P.W., Denton, G.H. 1999. Moraine exposure dates imply synchronous Younger Dryas glacier advances in the European Alps and in the Southern Alps of New Zealand. *Geograqfiska Annaler Series A – Physical Geography.* 81A (2): 313-323.

J

Jakobsson, S. P. 1979. Petrology of recent basalts of the Eastern Volcanic Zone, Iceland. *Acta Naturalia Islandia* **26**: 1-103.

Jinshi, L. 1992 Jökulhlaups in the Kunmalike River, southern Tien Shan mountains, China, *Annals of Glaciology,* v.16, p.85-88.

Johannesson, H., Geirsdottir, A., Einarsson, P. and Gronvold, K. 1995. Vitnisburdur um jardskjalfta fra sidjokultima I settlogum I grennd Heklu. *In:* Abstract volume, Geoscience Society of Iceland, Spring Meeting. Geoscience Society of Iceland, Reykjavik, 12.

Jóhannesson, H., Jakobsson, S.P. & Sæmundsson, K. 1990. *Geological map of Iceland,* sheet 6, South-Iceland, third edition. Icelandic Museum of Natural History and Iceland Geodetic Survey, Reykjavík.

Johannesson, T. and Sigurdsson, O. 1998. Interpretation of glacier variations. *Jökull,* 45, 27-34.

Jones, A.P., Tucker, M.E., & Hart, J.K. 1999. Guidelines and recommendations. *The Description and Analysis of Quaternary Stratigraphic Field Sections. Technical Guide 7.* Eds. Jones, A.P., Tucker, M.E., & Hart, J.K. 27-62. Quaternary Research Association, London.

Jonsson, J. 1982. Notes on the Katla volcanoglacial debris flows. *Jökull,* 32, 61-68.

K

Kaldal, I. and Vikingsson, S. 1991. Early Holocene deglaciation in central Iceland. *Jökull.* 40, 51-66.

Kaldal, I. and Vilmundardóttir, E.G. 1989. Dating of plant remains in lacustrine sediments in southern Iceland. *In:* Ed. Eiriksson, J and Geirsdóttir, A. *Physics-Geophysics-Geology. An interdisciplinary Field of Research,* Nordic Symposium, Skalholt, Iceland. 24/6-1/7 1989: 78-79.

Kaldal, I. and Vilmundardóttir, E.G. 2001. Forn Ión ad Fjallabakki. *Orkustofnun Internal Report OS-2001/072,* Orkustofnun, Rannsoknasvið, Reykjavík. 44p.

Kamb, B. 1987. Glacier surge mechanism based on linked cavity configuration of the basal water conduit system. *Journal of Geophysical Research,* 92, 9083-9100.

Kapista, A.P., Ridley, J.K., Robin, G. de Q., Siegert, M.J. and Zotikov, I.A. 1996. A large deep freshwater lake beneath the ice of central East Antarctica. *Nature,* 381, 684-686.

Karlen, W. 1988. Scandinavian glacial and climatic fluctuations during the Holocene. *Quaternary Science Reviews.* 7, 199-209.

Kirkbride, M.P. and Dugmore, A.J. 2001a. Timing and significance of mid-Holocene glacier advances in northern and central Iceland. *Journal of Quaternary Science.* 16 (2): 145-153.

Kirkbride, M.P. and Dugmore, A.J. 2001b. Can lichenometry be used to date the "Little Ice Age" glacial, maximum in Iceland? *Climate Change.* 48 (1): 151-167.

Kirkbride, M.P. and Dugmore, A.J. (accepted subject to revision). Glaciological responses to the 1947 eruption of Hekla, Iceland. *Journal of Glaciology.*

Kjartansson, G. 1939. Stadier i isens tilbagerykning fra det sydvestislandske lavland. *Meddelelser fra dansk Geologisk Forening*, 9, 426-458.

Kjartansson, G. 1970. Ur sogu berggrunns og landslags a Midsudurlandi. *Sudri,* 2, 12-100.

Kjartansson, G. 1967 The Steinsholtshlaup, Central-south Iceland on January 15th, 1967. *Jökull,* v.17, p.249-262.

Knight, P.G. 1999. *Glaciers.* Nelson Thomas, Cheltenham, 261pp.

Kohlbeck, F, Mojica, J, Scheidegger, AE 1994. Clast orientations of the 1985 lahars of the Nevado-del-Ruiz, Columbia and implications for depositional processes. *Sedimentary Geology.* 88, 3-4.

Kor, P.S.G., Shaw, J., and Sharpe, D.R., 1991. Erosion of bedrock by subglacial meltwater, Georgian Bay, Ontario: a regional view; *Canadian Journal of Earth Sciences*, 28: 623-642.

Krigstrom, A. 1962. Geomorphological studies of sandur plains and their braided rivers in Iceland. *Geografiska Annaler,* 44, 328-346.

Kruger, J. and Humlum, O. 1981. The proglacial area of Mýrdalsjökull with particular reference to Slettjökull and Hofðabrekkujökull. General report on the Danish Geomorphological Expedition to Iceland, 1977. ***Folia Geographica Danica,*** XV, 1-58

Krumbein, W.C. 1941. Measurement and geological significance of shape and roundness of sedimentary particles. *Journal of Sedimentary Petrology,* 11, 64-72.

Kuno, H. 1966. Lateral variation of basalt magma types across continental margins and island arcs. *Bulletin of Volcanology,* 29, 195-222.

L

Lacasse, C., H. Sigurdsson, H. Johannesson, M. Paterne and S. Carey 1995. Source of Ash Zone 1 in the North Atlantic. *Bulletin of Volcanology,* 57, 18-32.

Lacasse, C., Sigurdsson, H., Carey, S., Paterne, M. and Guichard, F. 1996. North Atlantic deep-sea sedimentation of Late Quaternary tephra from the Iceland hotspot. *Marine Geology,* 129, 207-235.

Lamb, H. 1979. Climatic variation and changes in the wind and ocean circulation: The Little Ice Age in the northeast Atlantic. *Quaternary Research,* 11, 1-20.

Larsen, G. 1978. *Gjoskulog I nagrenni Kötlu.* BSc Hons thesis, University of Iceland. 57 pp.

Larsen, G. 1979. Um aldur Eldgjárhrauna. *Náttúrufræðingurinn.* 49, 1-26.

Larsen, G. 2000. Holocene eruptions within the Katla Volcanic System, south Iceland: Characteristics and environemtnal impact. *Jökull,* 49, 1-28.

Larsen, G., Dugmore, A.J. and Newton, A.J. 1999. Geochemistry of historical-age silicic tephras in Iceland. *The Holocene,* 9, 4, 463-471.

Larsen, G., Newton, A. J., Dugmore, A. J. Vilmundardóttir, E. G. 2001. Geochemistry, dispersal, volumes and chronology of Holocene silicic tephra layers from the Katla volcanic system. *Journal of Quaternary Science.,* **16**: 119-132.

Larsen, G. and Thorarinsson, S. 1977.H4 and other Acid Hekla tephra layers, *Jökull,* 28-46.

Larsen, G., Vilmundardóttir, E.G. & Róbertsdóttir, B.G. 2002. SE-trending Hekla tephra sectors erupted between 2660 and 2880 ^{14}C yrs BP: Characteristics of potential marker horizons outside Iceland. Abstract only. *The 25th Nordic Geological Winter Meeting. January 6-9th 2002.* Ed. Jónsson, S.S. 121. Reykjavík.

Lavigne, F. and Thouret, J.C. 2003. Sediment transportation and deposition by rain-triggered lahars at Merapi Volcano, Central Java, Indonesia. *Geomorphology.* 49 (1-2): 45-69.

Le Maitre, R.W. (ed.) 1989. A Classification of Igneous Rocks and Glossary of Terms: Recommendations of the International Union of Geological Sciences Subcommission on the Systematics of Igneous Rocks. Blackwell Scientific Publications Ltd, Oxford, 193pp.

Lindholm, R. C. 1987. *A practical approach to sedimentology.* Allen and Unwin, London, 276pp.

Lliboutry, L. 1971. Permeability, brine content and temperature of temperate ice. *Journal of Glaciology,* 10 (58), 15-29.

Lliboutry, L., B. M. Arnao, A. Pautre and B. Schneider 1977 Glaciological problems set by the control of dangerous lakes in Cordillera Blanca, Peru. I. Historical failures of morainic dams, their causes and prevention. *Journal of Glaciology,* v.18, no.79, p.239-254.

Loughlin, S. 1995. *The evolution of the Eyjafjöll volcanic system, southern Iceland,* Unpublished PhD thesis, Durham University.

Lowe, D.R., Williams, S.N., Leigh, H., Connor, C.B., Gemmell, J.B. & Stoiber, R.E. 1986. Lahars initiated by the 13 November 1985 eruption of Nevado del Ruiz, Columbia. *Nature.* 324, 51-53.

Luckman, B.H. and Osborn, G.D. 1979. Holocene glacier fluctuations in the middle Canadian Rocky Mountains. *Quaternary Research,* 11, 52-77.

Lundquvist, J. 1986. Late Weichselian glaciation and deglaciation in Scandinavia. *Quaternary Science Reviews,* 5, 269-292.

M

McCarroll, D., Matthews, J.A., and Shakesby, R.A. 1989. Striations produced by catastrophic subglacial drainage of a glacier-dammed lake, Mjolkedalsbreen, southern Norway. *Journal of Glaciology,* 35 (120): 193-196.

Mackintosh, A.N. 2000. Glacier Fluctuations and Climatic Change in Iceland. Unpublished PhD thesis, Department of Geography, University of Edinburgh. 134 pp.

Maag, Hans, 1969. Ice-dammed lakes and marginal glacial drainage on Axel Heiberg Island, Canadian Arctic Archipelago. *Axel Heiberg Island Research Reports*, McGill University, Montreal, Quebec, 147 p.

Mangerund, J., Lie, S.E., Furnes, H., Kristiansen, I.L., and Lomo, L. 1984. A Younger Dryas ash bed in western Norway and its possible correlations with tephra in cores from the Norwegian Sea and the North Atlantic, *Quaternary Research,* 21, 85-104.

Maizels, J. K. 1989 Sedimentology, palaeoflow dynamics and flood history of jökulhlaup deposits: palaeohydrology of Holocene sediment sequences in southern Iceland sandur deposits. *Journal of Sedimentary Petrology,* v.59, no.2, p.204-223.

Maizels, J. K. 1991. The origin and evolution of Holocene sandur deposits in areas of jökulhlaup drainage, Iceland *In* Maizels, J. K. and Caseldine, C. (eds.) *Environmental Change in Iceland: Past and Present,* pp.267-302, Kluwer Academic Publishers, Dordrecht.

Maizels, J. K. 1992 Boulder ring structures produced during jökulhlaup flows – origin and hydraulic significance, *Geografiska Annaler,* v.74A, no.1, p.21-33.

Maizels, J. K. 1993. Lithofacies variations within sandur deposits: the role of runoff regime, flow dynamics and sediment supply characteristics, *Sedimentary Geology,* v.85, pp.299-325.

Maizels, J.K. 1997. Jökulhlaup deposits in proglacial areas. *Quaternary Science Reviews*, 16, 793-819.

Maizels, J. K. and A. J. Russell 1992 Quaternary perspectives on jökulhlaup prediction, *Quaternary Proceedings,* v.2, p.133-152.

Major, J. J. and C. G. Newhall 1989 Snow and ice perturbation during historical volcanic eruptions and the formation of lahars and floods, *Bulletin of Volcanology,* v.52, pp.1-27.

Manley, G. 1971. The mountain snows of Britain. *Weather* 26: 192-200.

Manville V, Hodgson KA, Houghton BF, Keys JRH, White JDL 2000. Tephra, snow and water: complex sedimentary responses at an active snow-capped stratovolcano, Ruapehu, New Zealand. *Bulletin of Volcanology,* 62 (4-5): 278-293.

Maria, A., Carey , S., Sigurdsson, H. and Kincaid, C. 2000. The source and dispersal of jökulhlaup sediments discharged to the sea following the 1996 Vatnajökull eruption. *Geological Society of America Bulletin*, 112, 1507-1521.

Matthews, J.A., 1991. The late Neoglacial (Little Ice Age) glacier maximum in southern Norway: new 14C-dating evidence and climatic implications. *The Holocene* 1, 219-233.

Meier, M.F. and Post, A.S. 1969. What are glacier surges? *Canadian journal of Earth Sciences,* 6, 807-819.

Morisawa, M. 1985. Chapters 3 and 4 *In* Clayton, K.M. (ed) *River: Form and Process.* New York, Longman, 25-53.

Murray, F. 2002. Unpublished BSc Hons dissertation, University of Edinburgh.

N

Naranjo, J. L., H. Sigurdsson, S. N. Carey and W. J. Fritz 1986 Eruption of the Nevado del Ruiz Volcano, Columbia, on 13 November 1985: tephra fall and lahars. *Science,* v.233, p.961-963.

Nesje, A. 1989. Glacier-front variations of outlet glaciers from Jostedalsbreen and climate in the Jostedalsbre region of western Norway in the period 1901-80. *Norsk Geografisk Tidsskrift,* 43, 3-17.

Nesje, A. and Kvamme, M. 1991. Holocene glacier and climate variations in western Norway: evidence for early Holocene glacier demise and multiple Neoglacial events. *Geology.* 19, 610-612.

Newton, A. J. 1999. *Ocean-transported pumice in the North Atlantic.* Unpublished PhD thesis, University of Edinburgh, 394 p.

Newton, A.J. and Dugmore, A.J. 1995. Pumice: Analytical Report. *In,* Branigan, K. and Foster, P. (eds) *Barra:Archaeological Research on Ben Tangaval,* Sheffield Academic Press, Sheffield, 145-148.

Nienow P., Sharp M. and Willis I. 1998. Seasonal changes in the morphology of the subglacial drainage system, Haut Glacier d'Arolla, Switzerland. *Earth Surface Processes and Landforms.* 23 (9): 825-843.

Norðdahl, H. 1991. Late Weichselian and early Holocene deglaciation history of Iceland. *Jökull,* 40, 27-50.

Nye, J. F. 1976 Water flow in glaciers: jökulhlaups, tunnels and veins, *Journal of Glaciology,* Vol.17, p.181-207.

Nye, J.F. and Frank, F.C. 1973. Hydrology of the intergranular veins in a temperate glacier. *Proceedings of the Symposium 'Hydrology of Glaciers'* IAHS – IASH, 95, 157-161.

O

Olszewski, A. and Wiśniewski, E. 2000. Relief of the Höfðabrekkujökull forefield, South Iceland, in light of geomorphological mapping, *Jökull*, No. 47, 2000, 59-70.

Orkustofnun 1999 Maps of Entujökull and Emstrur

Owen, L.A., Finkel, R.C., Minnich, R.A., Perez, A.E. 2003. Extreme southwestern margin of late Quaternary glaciation in North America: Timing and controls. *Geology,* 732 AUG 2003

P

Påhlsson, I. 1981. A pollen study on a peat deposit at Lágafell, Southern Iceland. *Striae.* 15, 60-64.

Palmer, S.P., Pringle, P.T. and Shulene, J.A. 1991. Analysis of liquefiable soils in Puyallup, Washington, *In,* Borcherd, and Shah (Eds.), *Proceedings of the Fourth International Conference on Seismic Zonation,* Stanford, California, Earthquake Engineering Research Institute, 2, 621-628.

Paterson, W.S.B. 1994. *The Physics of Glaciers,* Pergamon Press, Oxford, 380p.

Pierson, T.C. and Costa, J.E. 1987. A rheological classification of subaerial sediment-water flows, *Geological Society of America, Reviews in Engineering Geology,* V11, 1-12.

Pierson, T.C. and Scott, K.M. 1985. Downstream dilution of a lahar: transition from debris flow to hyperconcentrated streamflow. *Water Resources Research.* 21, 1511-1524.

Pringle, P.T. and Palmer, S.P. 1992. Liquefiable volcanic sands in Puyallup, Washington, correlate with Holocene pyroclastic flow and lahar deposits in upper reaches of the Puyallup River Valley (abstract), *Geological Society of America Abstracts with Programs,* 24, 5, p.76.

R

Rampino, Self and Fairbridge, 1979. Can rapid climatic change cause volcanic eruptions?, *Science,* 206: 826-829

Raymond, C.F. and Harrison, W.D. 1975. Some observations of the behaviour of the liquid and gas phases in temperate glacier ice. *Journal of Glaciology,* 14(71), 213-233.

Rickwood, P.C. 1989. Boundary lines within petrologic diagrams which use oxides of major and minor elements. *Lithos,* No. 22, p. 247-263.

Rist, S. 1967 Jökulhlaups from the ice cover of Mýrdalssandur on June 25, 1955 and January 20, 1956. *Jökull,* v. 17, p.243-248.

Rist, S. 1983 Floods and flood danger in Iceland. *Jökull*, v.33, p.119-132.

Roberts, M.J., Russell, A.J., Tweed, F.S. & Knudsen, Ó. 2000. Ice fracturing during jökulhlaups: implications for englacial floodwater routing and outlet development. *Earth Surface Processes & Landforms*, 25, 1429-1446.

Roberts, M.J., Russell, A.J., Tweed, F.S. & Knudsen, Ó. 2001. Controls on englacial sediment deposition during the November 1996 jökulhlaup, Skeiðarárjökull, Iceland. *Earth Surface Processes & Landforms*, 26, 935-952.

Roberts. S. J. 2002. Quaternary tephrochronology in Iceland dating principles & applications *Unpublished PhD thesis,* University of Edinburgh.

Rossbacher, L. A. and D. D. Rhodes 1987 Planetary analogues for geomorphic features produced by catastrophic flooding. *In,* Mayer, l. and D. Nash (eds.) *Catastrophic Flooding,* The Binghampton Symposia in Geomorphology, International Series, no.18, Allen and Unwin, Boston.

Röthlisberger, H. 1972. Water pressure in intra- and subglacial channels. *Journal of Glaciology,* 11(62): 177-203.

Röthlisberger, F. 1986. *10,000 Jahre Gletschergeschichte der Ende.* Verlag Sauerlander, Aarau.

Röthlisberger, H. and H. Lang 1987 Glacier Hydrology *In* Gurnell, A. M. and M. J. Clark (eds.) *Glacio-fluvial Sediment Transfer*, John Wiley and Sons, ? p.207-284.

Russell, A.J. 1989. A comparison of two recent jökulhlaups from an ice-dammed lake, Sondre Stromfjord, West Greenland. *Journal of Glaciology.* 120, 157-162.

Russell, A. J. 1991 *The geomorphological and sedimentological effects of jökulhlaups,* Unpublished Ph.D. thesis, University of Aberdeen.

Russell, A. J. and Knudsen, Ó. 1999 Controls on the sedimentology of the November 1996 jökulhlaup deposits, Skeiðarársandur, Iceland. *In* Smith, N. D. and J. Rogers (eds.) *Fluvial Sedimentology VI,* International Association of Sedimentologists, Blackwell Science, Oxford, p.315-329.

Russell, A.J., Knudsen, Ó, Fay, H., Marren, J.K., Heinz, P.M. and Tronicke, J. 2001. Morphology and sedimentology of a giant supraglacial, ice-walled, jökulhlaup channel, Skeiðarárjökull, Iceland: implications for esker genesis. *Global and Planetary Change*,28,193-216.

Russell, A.J., Knudsen, Ó., Tweed, F.S., Marren, P.M., Roberts, M.J., Waitt, R.B., Rice, J.W. Jr. & Rushmer, L. 2002. Volcanically generated jökulhlaup from the northern margin of Vatnajökull ice cap, Iceland. Abstract only. *The 25th Nordic Geological Winter Meeting. January 6-9th 2002.* Ed. Jónsson, S.S. 180. Reykjavík.

Russell, A. J. and Marren, P. M. 1998. A Younger Dryas (Loch Lomond Stadial) jökulhlaup deposit, Fort Augustus, Scotland. *Boreas,* v.27, p.231-242.

Russell, A. J. and Marren, P. M. 1999 Proglacial fluvial sedimentary sequences in Greenland and Iceland: a case study from active proglacial environments subject to jökulhlaups, *In,* Jones, A. P., M. E. Tucker and K. Hart (eds.) *The Description and analysis of Quaternary stratigraphic field sections,* Technical Guide no.7, pp.171-208, Quaternary Research Association, London.

S

Scarth, A. and Tanguy, J-C. 2001. *Volcanoes of Europe.* Terra Publishing, Harpenden, England. 243 pp.

Scott, K.M. 1988. Origins, Behaviour and Sedimentology of Lahars and Lahar-Runout Flows in the Toutle-Cowlitz River System, Mount ST. Helens, Washington. *U.S. Geological Survey Professional Paper.* 1447-A, 74p.

Scott, K.M. 1989. Magnitude and frequency of lahars and lahar-runout flows in the Toutle-Cowlitz river system, Mount St. Helens, Washington, *U.S. Geological Survey Professional Paper,* 1447-B, 33 pp.

Scott, K.M., and Vallance, J.W., 1995. Debris Flow, Debris Avalanche, and Flood Hazards At and Downstream from Mount Rainier, Washington *USGS Hydrologic Investigations Atlas HA-729*

Selby, M.J. 1993. *Hillslope Materials and Processes,* Oxford. Chapter 14, p.299-319.

Shoemaker, E.M., 1991. Water sheet outburst floods from the Laurentide Ice Sheet. *Canadian Journal of Earth Science*, 29:1250-1264.

Shoemaker, E.M. 1992. Subglacial floods and the origin of low-relief ice-sheet lobes. *Journal of Glaciology*, 38, 105-12.

Schomacker, A., Krüger, J. and Larsen, G. 2003. *'An extensive late Holocene glacier advance of Kötlujökull, central south Iceland'*. Quaternary Science Reviews, 14, 1427-1434.

Sejrup, H., Sjøholm, J., Furnes, H., Beyer, I., Eide, L., Jansen, E. & Mangerud, J. 1989. Quaternary tephrachronology on the Iceland Plateau, north of Iceland. *Journal of Quaternary Science,* 4, 109-114.

Shakesby, R. A. 1985 Geomorphological effects of jökulhlaups and ice-dammed lakes, Jotunheimen, Norway, *Norsk Geografisk Tidsskrift,* v.39, p.1-16.

Shaw, J. 1988. Subglacial erosion marks, Wilton Creek, Ontario. *Canadian Journal of Earth Sciences,* 25, 1256-1267.

Shaw, J. 1994. Meltwater erosional marks, Marysville. *In,* Gilbert, R. (compiler) A field guide to the glacial and post-glacial landscape of southeastern Ontario and part of Quebec. *Geological Survey of Canada Bulletin,* 453, 44-45.

Shreve, R. L. 1972 Movement of water in glaciers, *Journal of Glaciology,* v.11, no.62, p.

Sigbjarnasson, G. 1973. Katla and Askja, *Jökull,* v.23, p.45-51.

Sigurðsson, F. 1988. Fold og vötn að Fjallabaki. *Árbók Ferðafélags Íslands.* 1988, 181-202.

Smellie J.L. 1999. Subglacial eruptions. *In:* Sigurdsson H. (Ed.) *Encyclopaedia of volcanoes.* Academic Press, pp 403-418.

Smith, K.T. and Ahronson, K. 2003. 'Dating the cave? The preliminary tephra stratigraphy at Kverkin, Seljaland'. *Northern Studies*, 37, 71-80.

Sneed ED, Folk RL. 1958. Pebbles in the lower Colorado River, Texas, a study in particle morphogenesis, *Journal of Geology*, 66(2): 114-150.

Spring, U. and K. Hutter 1981 Numerical studies of jökulhlaups, *Cold Regions Science and Technology*, 4, 221-244.

Stoiber, R.E. and Williams, S.N. 1990. Monitoring active volcanoes and mitigating volcanic hazards – the case for including simple approaches. *Journal of Volcanological and Geothermal Research.* 42 (1-2): 129-149.

Stone, K. H. 1963 The annual emptying of Lake George, Alaska, *Arctic,* v.16, no.1, p.27-39.

Strachan, S. 2001. *A geophysical investigation of the Eyjafjallajökull glaciovolcanic system, South Iceland, using radio echo sounding.* Unpublished PhD thesis, University of Edinburgh.

Sturm, M, Benson, C. and MacKeith P. 1986. Effects of the 1966-1968 eruptions of Mount Redoubt on the flow of Drift Glacier, Alaska, USA. *Journal of Glaciology,* 32, 355-362.

Sturm, M., Hall, D., Benson, C. and Field, O. 1991. Non-climatic control of glacier terminus fluctuations in the Wrangell and Chugach Mountains, Alaska. *Journal of Glaciology,* 37, 348-356.

Sveinbjarnardóttir, G. 1992. *Farm Abandonment in Medieval and post-Medieval Iceland: a Multidisciplinary Study.* Oxbow Monograph 17. Oxford Books, Oxford.

Sveinbjarnardóttir, G., Buckland, P.C., & Gerrard, A.J. 1982. Landscape change in Eyjafjallasveit, Iceland. *Norsk Geografiska Tidskrift.* 36, 75-88.

Swanson, Cameron, Evarts, Pringle, and Vance, 1989. AGU Field Trip T106: Cenozoic Volcanism in the Cascade Range and Columbia Plateau, Southern Washington and Northernmost Oregon: *American Geophysical Union Field Trip Guidebook* T106.

Sweatman, T.R. and Long, J.V.P. 1969. Quantitative electron microprobe analysis of rock-forming minerals, *Journal of Petrology,* 7, 332-279.

T

Thorarinsson, S. 1936. Vatnajökull. Chapter III. *Geografiska Annaler.* 18, 189-195.

Thorarinsson, S. 1944. Tefrokronologiska studier paa Island. *Geografiska Annaler.* 26A, 1-217.

Thorarinsson, S. 1954. The tephra fall from Hekla on March 29 1947. *The eruption of Hekla 1947-1948.* II. 3. Ed. Þórarinsson, S. Visindafélag Íslendinga. 1-68. Societas Scientiarum Islandica, Reykjavík.

Thorarinsson, S. 1953. Some new aspects of the Grímsvötn problem. *J. Glaciology*, 4, 267-274.

Thorarinsson, S. 1956. On the variations of Svinafellsjökull, Skaftafellsjökull and Kvíarjökull in Öræfi. *Jökull,* 6, 1-15.

Thorarinsson, S. 1957. The jökulhlaup from the Katla area in 1955 compared with other jökulhlaups in Iceland. *Jökull,* 7, 21-25.

Thorarinsson, S 1964. On the age of the terminal moraines of Bruarjökull and Halsajökull. *Jökull,* 14, 67-75.

Thorarinsson, S. 1967. The eruptions of Hekla in historical times. *The eruption of Hekla 1947-48,* I, 1-170. Soc. Sci. Isl., Reykjavík.

Thorarinsson, S. 1970. Tephrochronology and Medieval Iceland. *Scientific Methods in Medieval Archaeology.* Ed. Berger, R. 295-328.

Thórarinsson, S. 1975. Katla og Kotlugosa (Katla and its historical eruptions). *Arbok Ferdafelags Islands* 1975: 125-149.

Tómasson, H. 1996. The jökulhlaup from Katla in 1918, *Annals of Glaciology,* v.22, pp.249-254.

Townsend, C. 1987. *The Great Backpacking Adventure*, Oxford Illustrated Press, Oxford.

Trabant, D. C. and D. F. Meyer 1992 Flood generation and destruction of 'Drift' glacier by the 1989-90 eruption of Redoubt Volcano, Alaska, *Annals of Glaciology,* v.16, p.33-38.

Tryggvasson, E. 1960 Earthquakes, jökulhlaups and subglacial eruptions, *Jökull,* 10, p.18-20.

Tuffen H., Gilbert J.S., McGarvie D.W. 2001. Products of an effusive subglacial rhyolite eruption: Bláhnúkur, Torfajökull, Iceland. *Bulletin of Volcanology* 63, 179-190.

Tufnell, L. 1984 *Topics in Applied Geography, Glacier Hazards.* Longman Group, London. P.44-55.

Turney, C.S.M., McGlone, M.S., Wilmshurst, J.M. 2003. Asynchronous climate change between New Zealand and the North Atlantic during the last deglaciation. *Geology,* 31 (3): 223-226.

Tweed, F.S. 2000. Jökulhlaup Initiation by Ice-Dam Flotation: The Significance of Glacier Debris-Content. *Earth Surface Processes and Landforms*, 25, 105-108.

U

United States Geological Survey (USGS) 1998. http://volcanoes.usgs.gov.html

V

Vegagerdin 2000 Maps of Markarfljót valley

Vilmundardottir, E.G. and Kaldal, I. 2001. *Forn lon ad Fjallabaki.* Unnid fyrir Audlindadeild Orkustofnunar og landsvirkjun. OS-2001/072. Orkustofnun, Rannsoknasvið, Reykjavik. (*Old lagoons*

in Fjallabaki, an internal report for the Natural Resources Department of the Icelandic Energy Authority).

W

Walder, J. S. and C. L. Driedger 1993. Glacier-generated debris flows at Mount Rainier, *USGS Open-File Report,* 93-124

Walder, J. S. and C. L. Driedger 1995 Frequent outburst floods from South Tahoma Glacier, Mount Rainer, USA: relation to debris flows, meteorological origin and implications from subglacial hydrology. *Journal of Glaciology,* v.41, p.1-10.

Wastegård, S., Björck, S., Grauert, M. and Hannon, G.E. 2001. The Mjáuvøtn Tephra and the other Holocene tephra horizons from the Faroe Islands: a potential link between the Icelandic source region, the Nordic Seas, and the European continent. *The Holocene,* 11, 101-109.

Watnabe, T., Ives, J. and Hammond, J.E. 1992. Rapid growth of a glacial lake in the Khumbu Himal, Nepal: prospects for a catastrophic flood. *Journal of Mountain Research and Development,* 14, 4.

Waythomas, CF, Miller, TP and Begét, JE 2000. Record of late Holocene debris avalanches and lahars at Iliamna volcano, Alaska. *Journal of Volcanological and Geothermal Research*, 104, 97-130.

Wentworth, C.K. 1922. A scale of grade and class terms for clastic sediments. *Journal of Geology,* 30, 377-392.

Whalley, W. B. 1971 Observations of the drainage of an ice-dammed lake – Strupvatnet, Troms, Norway, *Norsk Geografisk Tidsskrift,* v.25, p.165-174.

Whipple, K., Anderson, R., and Hancock G., 2000. River incision into bedrock: mechanics and relative efficacy of plucking, abrasion, and cavitation. *Geological Society America Bulletin*, v. 112, no. 3, p. 490-503.

Winsborrow, M. 2002. Unpublished BSc Hons dissertation, University of Edinburgh.

E.Wiśniewski, A.Olszewski, M.Karasiewicz, P.Weckwerth 2000. Geomorphological map of the forefield of Höfðabrekkujökull, *Jökull*, No.47.

X

Xiangsang, Z. 1992 Investigation of glacier bursts of the Yarkant River in Xinjiang, China. *Annals of Glaciology,* v.16, p.135-139.

Y

Yongjian, D. and L. Jingshi 1992 Glacier lake outburst flood disasters in China, *Annals of Glaciology,* v.16, p.180-184.

Z

Zielinski, G.A., Germani, M.S., Larsen, G., Baille, M.G.L., Whitlow, S., Twickler, M.S. & Taylor, K. 1995. Evidence of the Eldgjá (Iceland) eruption in the GISP2 Greenland ice core: relationship to eruption processes and climatic conditions in the tenth century. *The Holocene.* 5, 2, 129-140.

Zielinski, G.A., Mayewski, P.A., Meeker, L.D., Grönvold, K., Germani, M.S., Whitlow, S., Twickler, M.S. & Taylor, K. 1998. Volcanic aerosol records and tephrochronology of the Summit Greenland ice cores. *Journal of Geophysical Research.* 102, 26625-26640.

Zingg, T. 1935 Beitrag zur Schotteranalyse, *Schweizerische Mineralogische und Petrologische* Mitteilungen, Bd.15, 39-140.